Influence of enzyme location and culture rheology on glucose oxidase production and recovery by *Aspergillus niger* NRRL-3 and *Penicillium* sp. CBS120262

Madelyn Johnstone-Robertson

Submitted in total fulfilment of the requirements of the degree of Doctor of Philosophy

July 2012

Department of Chemical Engineering
UNIVERSITY OF CAPE TOWN

Acknowledgements

I would like to thank the following people:

My supervisor Prof Sue Harrison for her insight, wisdom, support, encouragement and financial assistance throughout this study. In allowing me to spend some time away to explore other avenues in the enzyme field (BBI Enzymes SA (Pty) Ltd and the University of Stellenbosch).

My co-supervisor Prof Kim Clarke (Process Engineering, University of Stellenbosch) for her continued interest and assistance.

To Sue Jobson for looking after all the admin, finance, and housekeeping matters, Fran Pocock as CeBER's very resourceful and knowledgeable lab manager, Joe Macke for maintenance of the babies (Chemaps) and Bill Randall and Granville le Cruz for all the electronic maintenance of the ancillary equipment. To Helen Divey and Stephanie Snoek for assistance in the analytical laboratory. To all the Chemeng and CeBER people (past and present) that has assisted me in various ways.

To the late Prof. George Lindsey at the Molecular and Cell biology department of UCT and Dr. Brendon Price at the Electron Microscope Unit at UCT for their assistance with the immunocytochemical studies.

To Dr. Michael Graz at BBI Enzymes SA (Pty Ltd) for valuable lessons learnt. Prof Johann Gorgons (Process Engineering, University of Stellenbosch) for the opportunity to do research in Stellenbosch.

National Research Foundation (NRF), Department of Chemical Engineering, Technology Innovation Agency (TIA) and Centre of Bioprocess Engineering Research (CeBER) for funding.

To all my friends for their friendship, interest and encouragement.

To my Johnstone-Robertson family (Mom, Mel & Lorette) thank you for always believing in me and for providing me the opportunity to reach for anything.

To my partner Paul Esselaar, thank you for your commitment, patience, love and support throughout this period. And above all thank you for Mark and Katherine – a new adventure! To the rest of the Esselaar family, thank you for your all your love and care.

Publication declaration

Johnstone-Robertson M, Clarke KG, Harrison STL (2008). Characterisation of the distribution of glucose oxidase in *Penicillium sp*. CBS 120262 and *Aspergillus niger* NRRL-3 cultures and its effect on integrated product recovery. Biotechnology and Bioengineering. 99(4), 910-918.

Clarke KG, Johnstone-Robertson M, Price B, Harrison STL (2006). Location of glucose oxidase during production by *Aspergillus niger*. Applied Microbiology and Biotechnology, 70, 72 – 77.

Johnstone-Robertson, M., Clarke, K. and Harrison, S.T.L. 2006. Comparison of the location of glucose oxidase in *Penicillium Canescens* tT42 and *Aspergillus Niger* NRRL-3 cultures. Proceedings of the South African Chemical Engineering Congress 2006, 20-22 September 2006, Durban, South Africa. ISBN 1-86840-616-4.

Synopsis

The production of enzymes from micro-organisms has many applications in the food, beverage, medical, technology and pharmaceutical industries. In order for the production and optimisation of these enzymes to be economically feasible, an understanding of both the production and the recovery process from their host organisms, as well as their integration, is required. Many enzymes are secreted from their host organism while others are located intracellularly within their host. While extracellular location precludes the need for cell disruption and reduces the number of contaminating proteins from which purification is needed, intracellular production enables pre-concentration of the biomass and thereby protein product, albeit a more challenging separation results. In those cases where the enzymes are located in multiple locations the recovery process becomes increasingly challenging and needs to be modified in order to maximize enzyme yield and purity while minimizing the number of process recovery steps. Alternatively the simplified recovery processes tailored for recovery of intracellular or extracellular products only may result in reduced enzyme yields.

The aim of this thesis is to establish and understand the location of glucose oxidase (GO) in fungi *Aspergillus niger* NRRL-3 and *Penicillium* sp. CBS120262 to inform the enzyme recovery. GO was chosen to be a model system and the outcomes obtained in this study could then be applied to other enzyme and microbial systems in which product location has been shown to be influenced by operating conditions. For the model GO system chosen, its distribution within fungal cultures is not well defined and controversy exists in the literature regarding its cellular location. GO from *A. niger* has been reported to be predominantly an intracellular enzyme (Pazur, 1966; Van Dijken and Veenhuis, 1980; Witteveen *et al*., 1992) although some studies indicate its distribution across multiple locations (Mischak *et al*., 1985; Hatzinikolaou and Macris, 1995). GO from *Penicillium* sp. has, contrarily, generally been reported as an extracellular enzyme (Kusai *et al*., 1960; Nakamatsu *et al*., 1975; Petruccioli *et al*., 1993) although intracellular predominance has also been reported (Rando *et al*., 1997).

The controversy in the literature with respect to GO location may, in part, be attributable to the difference in species and in the growth conditions of the fungus, including the growth phase in which the cells were harvested for analysis. The effect of growth phase and physiological culture conditions, changing a process condition such as the pH control agent used, on the location of GO and the fungal morphology was investigated.

The information available on the secretion of enzymes from filamentous fungi is limited compared to that of yeast and higher eukaryotes. To contribute to this body of knowledge, the location of GO was

studied in *A. niger* NRRL-3 and *Penicillium* sp. CBS 120262 across a range of operating conditions. The enzyme secretion in fungi has been postulated to occur at the hyphal tips (Wessels 1990; Worsten *et al*., 1991); hence the interaction of hyphal morphology and secretion was investigated. Further, the mass transfer approach based on Fick's law of diffusion was used to describe the transport of GO out of the hyphal cell on a macro scale, where the GO concentration gradient from the intracellular region to the extracellular environment was used as the driving force for secretion. This cell-based mass transfer analysis of experimental data is to provide an understanding and new insights of the changing relative location of GO.

In submerged culture, *Penicillium* exhibits a filamentous morphology, which tends to result in non-Newtonian behaviour and, consequently, mass transfer limitations in the bulk suspension at high mycelia concentrations. *Aspergillus*, on the other hand, grows with a pelleted morphology which results in a less viscous culture suspension with potential for mass transfer limitation within the pellets. The culture rheology significantly influences the yields and productivities through their influence on physical transport processes, such as mixing, and heat and mass transfer processes (Olsvik and Kristiansen, 1994). This, in turn, influences the operating conditions, and thus affects the growth, morphology and product formation (Olsvik and Kristiansen, 1994). The rheological properties of microbial cultures are affected by the biomass concentration, the growth rate and morphology (Metz and Kossen, 1977; Charles, 1978; Metz *et al*., 1979; Olsvik and Kristiansen, 1994; Doran, 1999).

The production and location of GO as well as the changes in fungal morphology was investigated using batch cultures of *A. niger* NRRL-3 and *Penicillium* sp. CBS 120262. It was found that, in both cultures, GO was growth-associated. *A. niger* and *Penicillium* sp. showed similar specific growth rates of 0.15 h^{-1} and 0.16 h^{-1} respectively. *Penicillium* sp. supported higher biomass concentration (2.20 g l^{-1} vs. 1.56 g l^{-1}), higher total volumetric GO concentration (8.1 U ml^{-1} vs. 4.7 U ml^{-1}) and higher specific GO activity (3598 U g^{-1} vs. 2838 U g^{-1}) on reaching stationary phase than *A. niger*. *A. niger* had equivalent volumetric biomass (0.04 g l^{-1} h^{-1}) and volumetric total GO productivity (0.19 U $l^{-1}h^{-1}$) compared to *Penicillium* sp while the extracellular GO productivity from *Penicillium* was double than that of *A. niger* . These observations, and the coincident occurrence of the maximal specific GO activity, maximal cell concentration and maximal extracellular location, makes *Penicillium* sp. CBS 120262 a preferred choice over *A. niger* NRRL-3 for GO production, hence it was used to study the effect of changing the pH control agent from NaOH to $Ca(OH)_2$. The production of GO from *Penicillium* sp. was favourably influenced with a 2.4- and 2.5- fold increase in GO and biomass productivity when $Ca(OH)_2$was used as pH control agent.

To determine the location of GO, the amounts associated with the supernatant, the cell wall and membrane , the cytoplasm and the slime mucilage were determined quantitatively by fractionating the culture and determining the activity of GO in each fraction. The fraction of GO associated with the cell wall of *A. niger* NRRL-3 was also assessed qualitatively using immunocytochemical labelling. To investigate the effect of growth phase on GO location, and its implication with respect to the time of harvest, *A. niger* and *Penicillium* sp. cultures were harvested in mid-exponential phase and stationary phase. GO activity was shown to be located in multiple sites in both *Penicillium* sp. and *A. niger* cultures. The distribution between the extracellular fluid, slime mucilage, cytoplasm, cell wall and membrane fractions depended on the micro-organism used and on the growth stage in which it was harvested. The results showed that as the cultures moved from active growth to the stationary phase, the fraction of GO activity in the cytoplasm decreased 1.6- and 1.3-fold in *Penicillium* sp. and *A.niger* respectively. In *Penicillium* sp., there was a 1.7- and 1.9- fold decrease in the fraction of GO activity in the cell wall and membrane fraction and in the slime mucilage respectively. This translated into a 2.0- fold increase in the extracellular fluid. In *A. niger*, a decrease in the cytoplasmic GO activity was accompanied by a 1.3- fold increase in the cell wall and membrane fraction and the slime mucilage with a 1.3-fold decrease in the extracellular fluid. While the extracellular activity increased with increasing total activity in the stationary phase, its fraction decreased.

In addition, the effect of changing the pH control agent from NaOH to $Ca(OH)_2$ on the location of GO in a stationary phase *Penicillium* sp. CBS 120262 culture was studied. The fraction of GO in the extracellular medium in the presence of $Ca(OH)_2$ compared to that of NaOH increased by 1.6-fold. The fraction of GO trapped in the cell wall and membrane fragments was 3.3-fold lower than for NaOH, indicating that $Ca(OH)_2$ might assist in increasing the permeability of the cell wall. Similarly, the fraction of GO trapped in the slime mucilage after progression through the cell wall was 9-fold lower than for NaOH.

A novel method to quantify the morphology of *Penicillium* sp. CBS 120262 was developed using manual and semi-automatic procedures. Semi-automated image analysis routines were developed to determine morphological indices through empirical correlations for freely dispersed *Penicillium* sp. hyphae. Image analysis experiments were undertaken to view the changes of the hyphae in terms of the morphological indices during growth and changing growth conditions for *Penicillium* sp. CBS 120262. During batch cultivation of *Penicillium* sp. the number of tips N_t, longest hyphal length, L_e and total hyphal length, L_t indices increased during the active growth phase while the hyphal growth unit, L_{hgu} index decreased and the hyphal diameter, L_d index remained constant, indicating a higher degree of branching and greater number of tips. During growth, the morphological indices for $Ca(OH)_2$ showed marked differences from those obtained for NaOH with higher values for all the

morphological indices except for a lower L_{hgu} index which indicated that the hyphae were more branched. At the end of the *Penicillium* sp. cultivation there were 19 tips per hyphal body using $Ca(OH)_2$ compared to the 8 tips per hyphal body for NaOH. Both the predominantly extracellular location of GO (93%) and the increased abundance of hyphal tips illustrates that GO secretion was improved when $Ca(OH)_2$ was used as pH control agent.

Viscosity measurement of *A. niger* and *Penicillium* sp. cultures were performed and the effect of biomass concentration, growth rate and morphology on culture rheology were studied and compared with literature. Results indicated that with an increase in biomass concentration (0 to 14 g l^{-1}) the apparent viscosity of the culture for *A. niger* and *Peniciilium* sp. increased and that the rheological correlations obtained compared favourably with that of literature.

It has been previously postulated that enzyme secretion occurs dominantly through the apical tips and that the enzyme becomes trapped in the lateral cell wall as the porous apical wall is transformed into the non-porous lateral wall. To further investigate this, the secretion of GO and its subsequent location in the fungi was further expanded by investigating the morphology of *Penicillium* sp. and the relative rates of enzyme formation and secretion. The secretion of GO was investigated using the GO activity as a function of growth phase and location together with a mass transfer approach based on Fick's law of diffusion, with the GO concentration gradient (ΔC) as the driving force for secretion, to describe the transport of GO from the intracellular region to the external environment. As the GO accumulated intracellularly, the concentration gradient between its intracellular and extracellular location increased providing an increased driving force for GO secretion, and hence an increased specific rate of secretion. During the stationary phase, the specific rate of production decreased while the specific rate of secretion remained constant. This translated into the product becoming increasingly extracellular during the stationary phase. Results indicated that as GO was produced in the presence of $Ca(OH)_2$, it was secreted more rapidly into the external medium preventing its intracellular accumulation. On comparison with the NaOH case, in the latter, the secretion in the growth phase was much slower, leading to intracellular accumulation during the phase characterised by a high rate of production. Using ΔC, the transport of GO from the cell associated region to the extracellular region was defined in terms of an overall volumetric GO transport coefficient ($k_s a$) calculated from a generalised transport equation:

$$Rate\ of\ transport = \frac{dC_{GO,E}}{dt} = k_s\, a\left(\Delta C\right)$$

where: k_s = the solid phase mass transfer coefficient representing the inverse of the resistance provided by the solid barrier (i.e. cell wall and slime layer).

a = the hyphal area per unit volume across which the transfer takes place.

where $k_s a$ is the overall resistance of GO transport from the cell associated region through the cell wall and slime layer to the extracellular region and was evaluated graphically as $0.185 \pm 0.020\ h^{-1}$ for NaOH and $0.154 \pm 0.005\ h^{-1}$ for $Ca(OH)_2$. This result may be used on a macro-scale to provide new insight into the secretion of GO into the surroundings in terms of the GO driving force without knowledge of the cell wall characteristics.

The objective of this study was to investigate enzyme location in a fungal system using GO from *A. niger* and *Penicillium* sp. as a model system. The outcomes obtained in this study could then be used for other enzyme and microbial systems. It was found that changing process conditions, such as micro-organism used, growth phase and using different pH control agents has an influence on enzyme location and fungal morphology.

The mixed location of GO in the fungal cultures limits its recovery in that there is a play off between the number of purification steps required and increased theoretical yield. The result will also depend on the step yield employed in the purification process. The results from the study demonstrated the relative benefit of achieving extracellular location in production vs. the downstream process recovery after production.

Since an extracellular location of GO is important for the simplification of the downstream enzyme recovery, purification and enzyme yield of the downstream process, this study illustrated the limiting effect of enzyme transport in attaining maximised extracellular location of GO.

Using GO as a model system it was shown that there were inter-relationships between growth, enzyme production, DSP, enzyme secretion and transport, culture rheology and culture morphology. Further, GO secretion, and its resultant location highlights the limitation of protein transport across the cell envelope, the role of hyphal tips and GO concentration as the driving rate for increased extracellular GO concentration.

Table of Contents

List of Figures

List of Tables

Abbreviations

ABTS	2,2'-azinodi-3-ethylbenzthiazoline-6-sulphonic acid
ATP	Adenosine triphosphate
A. niger	*Aspergillus niger*
ANOVA	Analysis of variance
BCIP	5 – Bromo-4-chloro-3'-Indolylphosphate p Toluidine
BSA	Bovine serum albumin
BQ	Benzoquinone
CBS	Centraalbureau voor Schimmelcultures (Netherlands) (fungal database)
CDW	Cell dry weight
CSIR	Council of Scientific and Industrial Research
CSL	Corn steep liquor
CSTR	Continuous stirred tank reactor
Da	Dalton (equivalent to g mol^{-1})
DMF	Dimethylformamide
DNS	3,5-dinitrosalicylic acid
DSP	Downstream processing
EC	Enzyme Commission number
ELISA	Enzyme-linked immunosorbant assay
ER	Endo Reticulum
FAD	Flavin adenine dinucleotide
GA	Gluconic acid
GO	Glucose oxidase
GO_{gene}	Glucose oxidase gene
GRAS	Generally Recognised as Safe
HPLC	High performance liquid chromatography
HQ	Hydroquinone
IgG	Immunoglobin G
kat	Katal. 1 µmol substrate converted per min ≈ 16.67 nkat
MEA	Malt extract agar
M_w	Molecular weight in g mol^{-1}
NBT	Nitro-Blue Tetrazolium chloride
o.d.	Outer diameter
OTR	Oxygen transfer rate
OUR	Oxygen utilisation rate
PBS	Phosphate buffered saline solution
pCO_2	Partial pressure of CO_2
PEG	Polyethylene glycol

Penicillium sp.	*Penicillium* sp. CBS 120262
pNPP	p-Nitro-phenylphosphate
POD	Peroxidase
RP	Rheological parameter
S	Substrate (i.e. glucose)
SEM	Standard error of the mean
SGS-PAGE	Sodium dodecyl sulphate polyacrylamide gel electrophoresis
TBS	Tris buffered saline solution
TCA	Trichloroacetic acid
TEM	Transmission electron micrograph
TIF	Tagged Image File
U	Enzyme unit. 1 U refers to 1 µmol substrate converted per min
UCT	University of Cape Town
vvm	Volume air per volume medium per minute
YE	Yeast extract

Glossary

Autolysis	The process of self destruction of a cell by the action of enzymes (lysozymes) within it
Bulk flow	The movement of fluid/ molecules driven by pressure
Endoplasmic Reticulum	A system of membranes within the cytoplasm of plant and animal cells. It forms a link between the cell and nuclear membranes and is the site of protein synthesis. It is also concerned with the transport of proteins and lipids within the cell
Eukaryotes	An organism with its genetic material contained within a nucleus
Glycosolytation	The process in which a carbohydrate is joined to another molecule such as a protein to form a glycoprotein. Glycosylation occurs in the Rough Endoplasmic Reticulum (ER) and the Golgi apparatus of cells
Golgi Apparatus	An assembly of vesicles and folded membranes within the cytoplasm of eukaryotic cells that stores and transports secretory products (enzymes) and plays a role in the formation of a cell wall
Homologeous	Native proteins that are derived from the organism
Hetrologeous	Foreign proteins that are expressed from an organism
Iso-electric point	The pH at which a protein carries no net charge. Below the iso-electric point proteins carry a net positive charge, above it a net negative charge. The iso-electric point is of significance in protein purification because it is the pH at which solubility is often minimal
Peroxisomes	Micro bodies which contain H_2O_2 producing oxidase and catalase
Phosphorylation	The introduction of a phosphate group (PO_4^{3-}) to a biomolecule in a reaction that is normally controlled by phosphorylase

Spores	Dormant state in the lifecycle of microbial cells
Turgor pressure	Hydrostatic pressure that is exerted on cell walls to ensure rigidity of a cell
Vesicle	A small, usually fluid-filled, membrane bound sac within the cytoplasm of a cell
Vacuole	Membrane-bound organelle responsible for food digestion, osmotic regulation, and waste product storage

Nomenclature

Latin Symbols

a, b, c, d, e, f and k	constants (depends on the geometry of the system)	
a_{MT}	area across which mass transfer occurs	m^2
A	constant	$cm^2\ s^{-1}\ g^{1/3}\ mol^{-1/3}$
B	constant	$cm^2\ s^{-1}\ mol^{-1/3}$
ΔC	change in concentration	$U\ ml^{-1}$
C_A	concentration of component A	$gmol\ m^{-3}$
C_{AL*}	solubility of component A in the liquid	$mmol\ l^{-1}$
$C_{GO,C}$	cell associated GO concentration	$U\ ml^{-1}$
$C_{GO,E}$	extracellular GO concentration	$U\ ml^{-1}$
C_l	oxygen concentration in the bulk liquid	$mmol\ l^{-1}$
C_m	biomass concentration	$kg\ m^{-3}$
C_{om}	compactness of the mycelial aggregate.	-
C_{sat}	saturated oxygen concentration	$mmol\ l^{-1}$
d	hyphal diameter	µm
d_p	diameter of the mycelial aggregate	m
D	diffusion coefficient of protein at standard conditions, protein at infinite dilution in H_2O at 20 °C	$cm^2\ s^{-1}$
D_A	diffusion coefficient of component A	$m^2\ s^{-1}$
D_p	pellet diameter	mm
F	compactness	-
H	Henry's constant	$atm\ mol\ O_2^{-1}\ mol\ H_2O^{-1}$
k	Boltzman constant of value 1.38066×10^{-23}	$J\ K^{-1}$
k_1, k_2	constants	-
k'	constant	-
k_i	constant	-
k_La	mass transfer coefficient	h^{-1}
k_Sa	overall volumetric GO transport coefficient	h^{-1}
K	consistency index	$Pa\ s^n$
K_c	Casson viscosity constant	$N^{½}\ s^{½}\ m^{-1}$
K_p	plastic consistency index	$Pa\ s^n$

L_b	mean length of hyphal branches	µm
L_d	mean hyphal diameter	µm
L_e	main hyphal length or effective length	µm
L_e^+	effective hyphal length.	-
L_{hgu}	hyphal growth unit length	µm tip^{-1}
L_s	mean length of segments	µm
L_t	total length of hyphae	µm
m	pellet biomass concentration	g l^{-1}
m_{hgu}	hyphal growth mass	g CDW tip^{-1}
M_w	molecular weight	g mol^{-1}
n	flow index	-
n_b	number of branches	-
N	impeller speed	rpm
N_A	rate of mass transfer of component A	gmol s^{-1}
N_A'	Avogadro number of value 6.02 x 10^{23}	mol^{-1}
$N_{A,V}$	volumetric rate of mass transfer of component A	gmol m^{-3} s^{-1}
N_t	number of tips	-
OTR	oxygen transfer rate	mmol l^{-1} h^{-1}
OUR	oxygen utilisation rate	mmol l^{-1} h^{-1}
P	product concentration	g l^{-1}
P_{AG}	partial pressure of component A in the gas phase	atm
P_T	total gas pressure	atm
R^2	regression coefficient	-
R_a	Stokes-Einstein radius = radius of rigid sphere	cm
R_e	radius of equivalent hydrodynamic sphere ($R_e = R_a$)	cm
Re	Reynold's number	-
RF	roughness factor	-
R_g	radius of gyration	cm
R_h	hydrodynamic radius	cm
r_p	product formation rate	g l^{-1} h^{-1}
T	temperature	K
t	time	h
V_{hgu}	hyphal growth volume	m^3 tip^{-1}

w	water content of the mycelium	g g^{-1}CDW
x	amount of GA formed	mole
X	concentration of biomass	g l^{-1}
X_0	concentration of initial biomass	g l^{-1}
X_{max}	maximum biomass concentration	g l^{-1}
y	amount of base consumed	mole
y_{AG}	mole fraction of A in the gas	-
y_d	diffusion distance	m
$Y_{GA/S}$	gluconic acid yield from substrate	g g^{-1}
$Y_{GO/S}$	glucose oxidase yield from substrate	g g^{-1}
$Y_{X/S}$	biomass yield	g g^{-1}

Greek Symbols

α, β	constants	-
α_{GO}	Luedeking-Piret parameter for GO production	U g CDW^{-1}
β_{GO}	Luedeking-Piret parameter for GO production	U g CDW^{-1} h^{-1}
α_r, β_r, γ_r	constants	-
$\dot{\gamma}$	shear rate	s^{-1}
γ_{av}	average shear	s^{-1}
η	dynamic viscosity	Pa s
η_{app}	apparent viscosity	Pa s
$[\eta]$	intrinsic viscosity	Pa s
η_p	plastic viscosity	Pa s
μ	specific growth rate	h^{-1}
μ_{max}	maximum specific growth rate	h^{-1}
ρ	density of fluid	kg m^{-3}
ρ_m	mycelium density	g cells m^{-3}
τ	shear stress	Pa
τ_0	yield stress	Pa
τ_c	Casson yield stress	Pa
ξ	constant	-

Chapter 1 Introduction

A variety of micro-organisms (bacteria, yeast and fungi), both wild type and recombinant such as *Escherichia coli*, *Bacillus subtilis*, *Saccharomyces cerevisiae*, *Aspergillus* sp., *Trichoderma reesei* are used for the production of proteins, enzymes and other bio-products (Middelberg 1995; Gouka *et al*., 1997; Wang *et al*., 2005; Ostergaard and Olsen, 2010). Filamentous fungi are commonly used in the large scale production of industrial enzymes such as glucose oxidase (EC1.1.3.4), laccase (EC 1.10.3.2), catalase (EC 1.11.1.6), lipase (EC 3.1.1.3), α-amylase (EC 3.2.1.1), cellulose (EC 3.2.1.4, EC 3.2.1.9), β-glucanase (EC 3.2.1.6), xylanase (EC 3.2.1.8), lactase (EC 3.2.1.23), pullulanase (EC #.2.1.41) and protease (EC 3.4.2.xx.xx) (Ostergaard and Olsen, 2010). These enzymes are employed in a variety of industries ranging from food, medical, detergent, textiles, tanning, paper and pulp and animal feed. The enzyme glucose oxidase (GO) was studied in this thesis due to its commercial importance in the food and medical industries. In the food industry, it is used to eliminate rancidity and discolouration and to improve food preservation. In the medical field it is used in diagnostic kits (Wong *et al*., 2008). GO is also used for the production of gluconic acid (GA) which is used in the food, beverages, medical and industrial fields (Lockwood, 1975; Ramachandran *et al*., 2006) Other applications of GO (and indirectly H_2O_2) are in biofuel cells, bio-bleaching, mineral leaching and genetic engineering (Wong *et al*., 2008).

Aspergillus spp. and *Penicillium* spp. are used as the main commercial producers of GO (Bucke, 1983; Wong *et al*., 2008). The production and optimisation of GO from fungal cultures have been studied extensively (Nakamatsu *et al*., 1975; Zeletaki and Vas, 1968; Fiedurek *et al*., 1986; Rogalski *et al*., 1988; Traeger *et al*., 1991; Petruccioli *et al*., 1993, 1995, 1997, 1999; Hatzinikoloau and Macris, 1995; Hellmuth *et al*., 1995; Gromada and Fiedurek, 1996; Lu *et al*., 1996; Rando *et al*., 1997; Rothberg *et al*., 1999; Kona *et al*., 2001; Liu *et al*., 2001; Kapat *et al*., 2001; Znad *et al*., 2004). The distribution of GO within fungal cultures is not well defined and there is a controversy in the literature regarding its location in the fungal cell. GO from *A. niger* has been considered to be predominantly an intracellular enzyme (Pazur, 1966; Van Dijken and Veenhuis, 1980; Witteveen *et al*., 1992) although some studies indicate that GO may be located in multiple locations within the *A. niger* culture (Mischak *et al*., 1985; Hatzinikolaou and Macris, 1995). GO from the *Penicillium* sp. has, contrarily, generally been regarded as an extracellular enzyme (Kusai *et al*., 1960; Nakamatsu *et al*., 1975; Petruccioli *et al*., 1993) although intracellular predominance has also been reported (Rando *et al*., 1997).

The location of enzymes in the microbial culture plays an important role in its subsequent downstream recovery and process economics. In any microbial culture, enzymes can be located extracellularly (outside the cell) or intracellularly (inside the cell) or distributed across multiple cell locations. Due to

the multiple locations of GO within the fungal culture, the downstream recovery process of GO for maximum recovery is complicated. A predominantly extracellular or predominantly intracellular location reduces the complexity of enzyme purification and facilitates achievement of a high recovery of the protein. Usually an extracellular location is favoured as this precludes the need for cell disruption and limits the number of proteins and metabolites from which the enzyme must be purified, albeit from a more dilute environment. An intracellular location on the other hand allows concentration of the enzyme by concentration of the cells using a solid-liquid separation step before cell disruption. As an initial step towards optimisation of a GO recovery and purification programme for *Aspergillus* sp. and *Penicillium* sp., it is important to identify and optimise the distribution of enzyme activities in these cultures.

The ability of filamentous fungi to secrete large amounts of homologous (native) enzymes and proteins into the culture medium makes them attractive hosts for heterologous (non-fungal) enzyme and protein production but there are several disadvantages regarding heterologous production with the most important being the lower yields that are obtained compared to that of homologous enzymes (Gouka *et al*., 1997; Torralba *et al*., 1998; Nevalainen *et al*., 2005). Several studies focused on the optimisation of heterologous production using genetic engineering (Archer and Pederby 1997; Conesa *et al*., 2001; Wiebe, 2003; Nevalainen *et al*., 2005; Wang *et al*., 2005; Schroder, 2008) and will not be covered in this thesis. Since enzyme secretion in fungi is postulated to occur at the hyphal tips (Wessels 1990; Worsten *et al*., 1991), the interaction with hyphal morphology and secretion is important to investigate since there is still limited information available on the secretion of enzymes from filamentous fungi compared to that of yeast and higher eukaryotes.

Penicillium spp. is a mycelial culture which possesses viscous non-Newtonian rheological properties. *Aspergillus* spp., on the other hand, grows in a pelleted form resulting in a culture which is usually less viscous and tends to follow Newtonian behaviour for low biomass concentrations changing to non-Newtonian at higher biomass concentrations (Nielsen and Villadsen, 1994). It is known that the rheological properties of the fungal cultivation changes from Newtonian to non-Newtonian with growth (Roels *et al*., 1974). The culture rheology significantly influences the yields and productivities through their influence on physical transport processes, such as mixing, and heat and mass transfer processes (Olsvik and Kristiansen, 1994). This, in turn, influences the operating conditions, and thus affects the growth, morphology and product formation (Olsvik and Kristiansen, 1994). The rheological properties of microbial cultures are influenced by the biomass concentration, the growth rate and morphology (Metz and Kossen, 1977; Charles, 1978; Metz *et al*., 1979; Olsvik and Kristiansen, 1994; Doran, 1999). The morphology is, in turn, affected by factors such as the geometry of the hyphae (length, diameter, and branching frequency), hyphal flexibility and hyphal-hyphal interaction (Olsvik and Kristiansen, 1994).

1.1 Scope of thesis

The production process for product(s) from micro-organisms consists of an upstream and downstream component. The upstream component includes inoculum development of the desired micro-organisms from stock, media preparation and production of product(s) using microbial culture. In this upstream component, factors to be considered include selection of micro-organism, media formulation, inoculum train, sterilisation, reactor type, mode of operation (batch, fed-batch or continuous), process conditions such as growth time, pH, dissolved oxygen (DO) concentration, agitation and temperature. After the production of the desired product(s), such as biomass, proteins, enzymes, organic acids, the product must be recovered to the required purity. In any microbial production system the downstream recovery of the desired product(s) is influenced by its distribution within the micro-organism. In the case of enzyme production the enzyme may either be located intracellularly or extracellurly or distributed across locations. Location will affect the method of enzyme recovery from the culture and the challenges encountered for its purification. This recovery and purification of the product(s) is part of the downstream recovery process (DSP). DSP consists of solid-liquid separations, cell disruption, concentration, separation and formulation. In most instances the upstream and downstream processes or components thereof are optimised separately.

Literature suggests that there are links between location and microbial type, growth and growth conditions. In this study GO produced from *Aspergillus niger* NRRL-3 and *Penicillium* sp. CBS120262 was used as a model system to investigate enzyme location and its impact on DSP. The influence of micro-organism and time of harvest on the location of GO and its subsequent influence on efficiency of the downstream process for recovery of GO activity was studied. The growth rates and productivity of these systems were compared. Through fractionation, GO location was quantified and its impact on DSP analysed. The effect of changing a process condition, in this case the pH control agent, on the location of GO and the fungal morphology was investigated.

The changes in fungal morphology were quantified using image analysis software analySIS®. Simple empirical correlations were developed to provide detailed morphological information while minimising measurement time. Morphological indices such as hyphal length, diameter, total length, effective length, hyphal growth unit and number of hyphal tips were determined for the novel *Penicillium* sp. CBS120262 strain and compared as a function of growth conditions. It is postulated that the morphology of the fungal culture influences the location of GO as well as the suspension viscosity through the influence of growth phase and biomass concentration on morphology.

Morphology is also related to the rheology of the fungal culture. In literature it is shown that pelleted morphology exhibits Newtonian behaviour while mycelial morphology exhibit non-

Newtonian behaviour. With mycelial morphology, as the growth rate of the organism increased, i.e. more hyphae are produced, the culture became more viscous affecting the mass and heat transfer properties of the culture which in turn affect the productivity of the organism. With pelleted morphology the culture suspension does not become as viscous, however mass transfer (oxygen) limitations may occur in the centre of the pellet if the pellet is too large. Also, during the course of a cultivation, the rheological characteristics of the culture become more complex, due to increased biomass concentration or accumulation of complex high molecular weight products or both. Therefore, a reasonable understanding of the rheology of the cultivation is of great importance for the design, scale-up and operation of bioreactors. In this study the characterisation of the culture rheology as a function of biomass concentration, the growth rate and morphology was investigated.

The protein secretion pathway is known for yeast and higher eukaryotes but not for fungi. It has been postulated that protein secretion in filamentous fungi occurs at the hyphal tips. During transit from the intracellular location to the extracellular region, proteins are trapped in the cell wall. In this study the relationship between fungal morphology and enzyme secretion was investigated to increase the understanding of fungal secretion. A new approach was proposed to predict macro scale enzyme secretion where the GO concentration gradient was used as the driving force for secretion. This driving force was used to describe the transport of GO from the intracellular region to the extracellular environment.

Using GO produced from *A. niger* NRRL-3 and *Penicillium* sp. CBS 120262 as a model system to highlight the link between (i) enzyme location, micro-organism used, growth and growth conditions, (ii) enzyme location and DSP to recover and purify the enzyme, (iii) location, growth rate and morphology, (iv) morphology and culture rheology, (v) culture rheology and production, (vi) morphology, secretion and transport of GO

1.2 Stucture of thesis

In Chapter 2 of this thesis, the literature pertaining to GO production and the determination of GO activity is reviewed. The distribution of GO in fungal cultures and its subsequent recovery in the downstream process is considered. Changes in the morphology of the fungal cultures are presented. The relationship between enzyme secretion, transport and diffusion is reviewed. The rheology of fungal cultures in terms biomass concentration, morphology and growth rate is reviewed. At the end of the literature review, key questions (Section 2.11) and hypotheses (Section 2.12) were developed and addressed.

Chapter 3 presents the methodology for the cultivation of *Apergillus niger* NRRL-3 (*A. niger*) and *Penicillium* sp. CBS 120262 (*Penicillium* sp.). Analytical techniques are described with reference to a detailed experimental procedure and validation given as an Appendix for each technique. The methodology of volume corrections to account for base addition and sampling is presented. The quantification of GO activity in the individual fractions for *A. niger* and *Penicillium* sp is described. The qualitative determination of GO in *A. niger* using immunocytochemical labelling is described and the detailed experimental procedure are presented in an Appendix. The sample preparation of the fungal cultures to quantify the changes in fungal morphology using image analysis was described. In Section 3.7 the experimental approach to the study was presented.

In Chapter 4 the production of GO by *A. niger* and *Penicillium* sp. was investigated and its production kinetics described. In this study NaOH was used as the pH control agent since it has been used previously in GO production processes (Blom *et al*., 1952; Li and Chen, 1994; Hellmuth *et al*., 1995). The effect of changing process conditions, such as the pH control agent, on the production of GO from *Penicillium* sp. was investigated. The effect of biomass concentration, growth rate and culture conditions on culture rheology was investigated.

In Chapter 5, the procedure established to determine the distribution of GO activity across the cell components in the fungal culture is described. In this, the culture is separated into the extracellular fraction associated with the supernatant and fractions associated with the mycelia (slime mucilage, cell wall and membrane fragments, and cytoplasm). The fraction of enzyme activity associated with the extracellular fluid and that associated with the mycelial fractions, namely, the cytoplasm, the cell wall and the slime mucilage surrounding the cell, were quantified in Sections 5.1. By using correlations and immunocytochemical studies the diffusion coefficient of GO from *A. niger* through the cell wall was predicted and compared with literature in Section 5.2.

The controvesy in the literature with respect to GO location may, in part, be attributable to the difference in species and in the growth conditions of the fungus, including the growth phase in which the cells were harvested for analysis. To investigate the effect of growth phase on GO location, and its implication with respect to the time of harvest, the *A. niger* and *Penicillium* sp. cultures were harvested in both mid-exponential and stationary phase and GO activity and location were quantified (Section 5.3). In addition, the effect of changing the pH control from NaOH to $Ca(OH)_2$ on the location of GO in *Penicillium* sp. CBS 120262 was studied (Section 5.4).

The recovery of GO in DSP is influenced by both the enzyme location and the relative efficiency, hence number, of separation steps needed. The number of separation steps required is influenced by the complexity of the matrix to be extracted. As a case study, analyses of simulated process yields

were used to demonstrate the consequences of enzyme location on the subsequent protein recovery and purification in Section 5.4.

In Chapter 6 the morphology of the fungal cultures and the secretion of GO are described. The changes in the morphology of an *A. niger* cultivation is presented in Section 6.1. Section 6.2 focuses on *Penicillium* sp. CBS 120262 morphology. Firstly, image analysis routines using analysis® software were developed and validated to analyse *Penicillium* sp. morphology and the number of individual hyphal measurements required for statistically valid results was determined. Secondly, the changes in the morphological indices during cultivation of *Penicillium* sp. CBS120262, quantified through image analysis, were investigated. Thirdly, the effect of using $Ca(OH)_2$ as a different pH control agent on *Penicillium* sp. morphology was investigated. In Section 6.3 the effect of *A. niger* and *Penicillium* sp. morphology on the rheology of the fungal cultures were investigated. The relationship between the changes in the morphological indices of *Penicillium* sp., secretion and transport of GO from the organism is described in Section 6.4 and 6.5. This facilitated the testing of the hypothesis that GO location is largely controlled by mass transport; restrictions on transport from the intracellular region to the external environment under the GO concentration gradient as the driving force for secretion result in the varied location reported.

In Chapter 7, the conclusions drawn from the study are presented and recommendations are made of areas in which future work may yield significant result.

Chapter 2 Literature review

In order to address the scope laid out for this thesis a detailed understanding of the current knowledge is required across the fungal morphology, physiology and the enzyme production process. These topics are considered taking integration of existing microbial and chemical engineering science aspects into consideration. To achieve this, a review of the literature covering the following subsections is conducted: 1) The production of GO (Section 2.1 - 2.5); 2) Its distribution in the fungal culture and its subsequent recovery from the downstream processing (Section 2.6); 3) The morphology of the fungal cultures (Section 2.7); 4) The rheology of fungal culture (Section 2.8); and 5) The relationship between enzyme secretion, transport and diffusion (Section 2.9).

Following these reviews, the key findings for this study are interrelated in Section 2.10 to provide a basis on which to build the key questions and hypotheses addressed in this study, presented in Section 2.11 and 2.12.

2.1 Uses of glucose oxidase (GO)

GO (β-D-glucose:oxygen oxidoreductase, EC 1.1.3.4) is a naturally occurring antioxidant listed under GRAS specifications (Richter, 1983) and is legally accepted in most countries as safe (Schuster *et al*., 2002). Since the 1950's GO has found a wide range of applications, particularly in the food, diagnostic and pharmaceutical fields (Wong *et al*., 2008).

In the food industry GO is used as an additive to remove small quantities of oxygen and glucose from food products to prevent discolouration and rancidity during processing and storage and to improve food preservation. In the diagnostic and pharmaceutical field it is used as a biosensor for the diagnosis of diabetes and various adrenal and pituitary disorders (Richter, 1983). It is also used as an analytical reagent, and as a marker of antigens and antibodies in enzyme immunoassays (Raba and Mottola, 1995). It has been proposed as an anticancer drug, destroying cancerous tissue and cells as a result of hydrogen peroxide (H_2O_2) formation (Raba and Mottola, 1995). GO is also used as a catalyst in the microbial conversion of glucose to gluconic acid. Gluconic acid and its metal salts (gluconates) are excellent sequestering and chelating agents. They are non-toxic, easily bio-degradable and, since these compounds are regarded as "safe", they are used mainly in the food, beverages, pharmaceutical and industrial fields (Lockwood, 1975; Ramachandran *et al*., 2006). Other applications of GO (and indirectly H_2O_2) are in biofuel cells, bio-bleaching, mineral leaching and genetic engineering (Wong *et al*., 2008).

2.2 Properties of GO

GO catalyses the conversion reaction of β-D-glucose to D- gluconic acid and H_2O_2. GO is a glycoprotein with mannose, galactose and glucosamine as integral structural units of the enzyme (Pazur *et al*., 1965). It is also a flavoprotein (Pazur *et al*., 1963; Hendle *et al*., 1992) containing two molecules of flavin adenine dinucleotide (FAD) as a prosthetic group per molecule of enzyme. The flavoprotein removes two hydrogens from β-D glucose on the latter's conversion to Dglucono-δ-lactone. D-glucono-δ-lactone rapidly hydrolyses to D-gluconic acid. The reduced form of enzyme is then re-oxidised by molecular oxygen, producing H_2O_2 as a by-product (Moo-Young, 1985; Wong *et al*., 2008). Figure 2.1 is part of a schematic representation of the kinetic reaction sequence proposed by Atkinson and Lester (1974) and redrawn from Ramachandran *et al*. (2006).

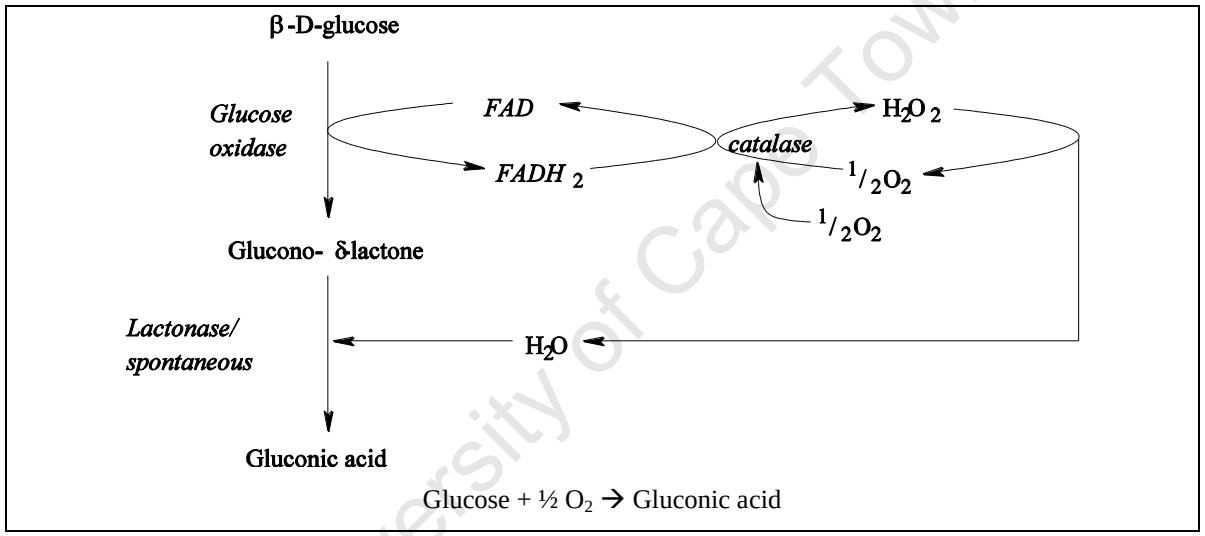

Figure 2.1 Oxidation of glucose by GO (redrawn from Ramachandran *et al*., 2006)

GO from different fungal sources has different properties (Swoboda and Massey, 1965). GO from *A. niger* is a homodimer with an approximate molecular weight between 150,000 and 180,000 Da (Table 2.1) and consists of two identical polypeptide chains covalently linked by disulfide bonds. Each subunit contains one mole of Fe and one mole of FAD. Tsuge *et al*. (1975) reported that the molecule consists of approximately 74% protein, 16% neutral sugar and 2% amino sugars.

GO from *P. amagasakiense* consists of four polypeptide chains with approximate molecular weights of 45,000 Da each and consists of 13% carbohydrate (Hendle *et al*., 1992). Two of these polypeptide chains are held together by a disulphide bond to form a dimer (approximately 81,000 Da) and two dimeric units associate non-covalently to form a tetramer (approximately 160,000 Da) (Rose, 1980). Some of the properties of GO obtained from three different fungal sources is illustrated in Table 2.1 (Swoboda and Massey, 1965).

Table 2.1 Some properties of three GO preparations obtained from fungi (adapted from Swoboda and Massey, 1965)

	Source		
Property	***Aspergillus niger***	***Penicillium amagasakiense***	***Penicillium nonatum***
Average Molecular weight (Da)	186×10^3	154×10^3	152×10^3
Diffusion coefficient ($cm^2\ s^{-1}$)[a]	4.12×10^{-7}	5.02×10^{-7}	5.13×10^{-7}
Sedimentation coefficient (s)[a]	8.00	7.93	8.27
Michaelis-Menten constant (in air, catalase present, pH 5.6)	0.033 M at 25°C	0.015 M at 30°C	0.096 M at 20°C
Standardized activity at 25°C[b]	80	77	64

[a] In aqueous solution and at 20°C.

[b] In units of micromoles per milligram (dry weight), "infinite" glucose concentration, 0.25 mM oxygen, excess catalase, and phosphate or acetate buffer of pH 5.60.

GO activity from *A. niger* has an optimum temperature and pH range of 30 to 50°C and pH 4.5 to 6.5, respectively (Richter, 1983). Rose (1980) reported that GO had its maximum activity at pH 5.6 and temperatures between 35 to 40°C, whereas Nakamatsu *et al*. (1975) reported the maximum activity of GO from *P. pururogenum* to be at pH 5.0 and 35°C. GO from *A. niger* has its isoelectric point at pH 4.2 (Pazur and Kleppe, 1964).

GO is highly selective towards the β-anomer of D-glucose (Keilin and Hartree, 1948; Rohr *et al*., 1983) and any chemical alteration from the basic molecular structure of the substrate results in a considerable reduction in the activity. The β-anomer reacts about 150 times faster than the α-anomer at 20°C (Keilin and Hartree, 1948; Raba and Mottola, 1995). The relative oxidation rates, in the presence of GO as catalyst, for several sugars, given in Table 2.2, illustrate its specificity for β-D-glucose.

Table 2.2 Relative oxidation rates for several sugars (sourced from Raba and Mottola, 1995)

Sugar	**Relative rate of oxidation [a]**
β-D-glucose	100
2-deoxy-D-glucose	25
4,6 Dimethyl-D-glucose	1.22
α-D-glucose	0.64
D-mannose	0.98
D-xylose	0.98
Maltose	0.19
Galactose	0.14
Melobiose	0.11

[a] Rates are normalised to the rate of β-D-glucose oxidation and for the general reaction:
sugar + O_2 → corresponding acid + H_2O_2

2.3 Induction of GO

The synthesis of GO in the micro-organism is induced by glucose and oxygen (Rohr *et al*., 1983; Witteveen *et al*., 1990; Johnson, 1995). The minimum glucose concentration necessary for GO induction is 36 g l^{-1} (Witteveen, 1990) whereas a glucose concentration above 200 g l^{-1} becomes inhibitory (Shuler and Kargi, 1992). On increasing the partial pressure of oxygen from 7.7 ppm to 27.1 ppm, the GO activity can be increased fourfold (Traeger *et al*., 1991). Witteveen *et al*. (1993) indicated that both glucose and molecular oxygen induced the expression of the glucose oxidase gene (GO_{gene}) at the transcription level. Johnson (1995) showed that the effect of glucose and oxygen on GO induction were not independent (Figure 2.3, Section 2.6.4).

$CaCO_3$ can also induce the synthesis of GO (Rohr *et al*., 1983; Petruccioli *et al*., 1995; Hatzinikolaou and Macris, 1995; Liu *et al*., 2001). The optimal suspension concentration is 35 g l^{-1} (Rogalski *et al*., 1988; Petruccioli *et al*., 1995; Liu *et al*., 2001). Hatzinikolaou *et al*. (1996) showed that GO was induced by the addition of $CaCO_3$ at the transcription level. With the addition of $CaCO_3$ to the growth media, the activities of GO and catalase increased while the synthesis of the glycolytic enzyme glucose 6-phosphate isomerase decreased simultaneously (Figure 2.2). They hypothesized that the induction of GO by $CaCO_3$ was accompanied by a metabolic shift from glycolysis in direct oxidation of glucose by GO to the pentose phosphate pathway, shown in Figure 2.2.

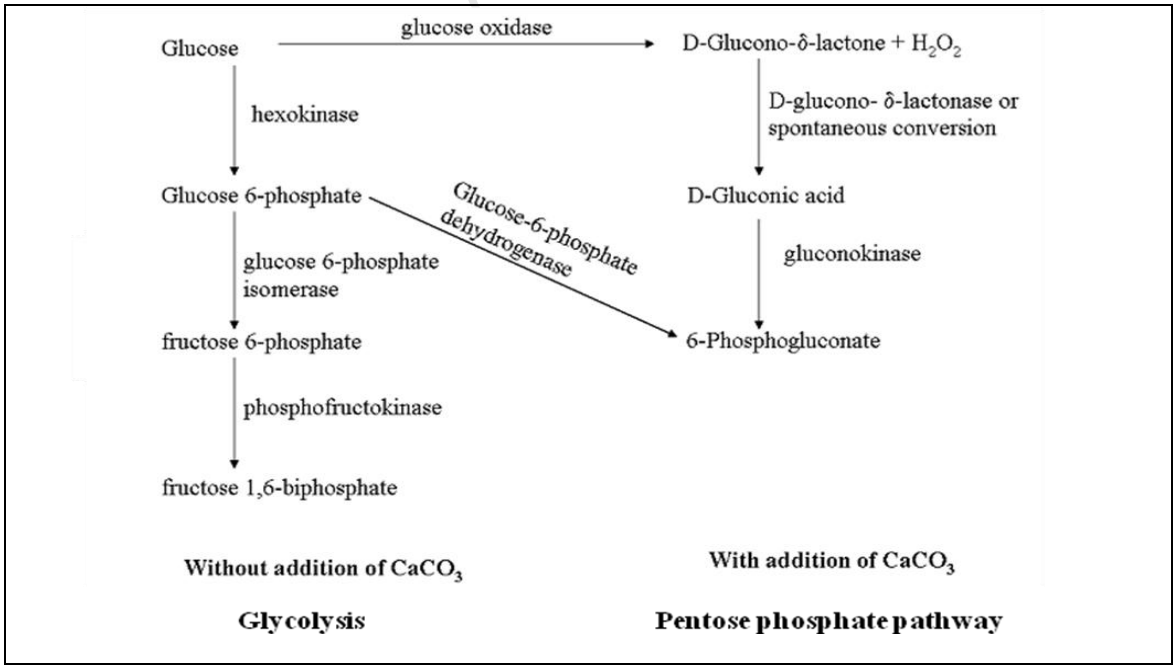

Figure 2.2 The metabolic pathway of glucose with and without the addition of $CaCO_3$ to the growth medium (redrawn from Liu *et al*., 2001)

2.4 Determination of GO activity

The microbial conversion of glucose to gluconic acid is catalysed by GO. The H_2O_2 produced is broken down by co-produced catalase or peroxidase, to oxygen and water. These reactions are described in Eqns 2.1 to 2.3:

$$\text{Glucose} + O_2 + H_2O \xrightarrow{GO} \text{Gluconic acid} + H_2O_2 \quad \textbf{(2.1)}$$

$$H_2O_2 \xrightarrow{catalase\,/\,peroxidase} \tfrac{1}{2}\,O_2 + H_2O \quad \textbf{(2.2)}$$

$$\text{Glucose} + \tfrac{1}{2}\,O_2 \longrightarrow \text{Gluconic acid} \quad \textbf{(2.3)}$$

A standard unit of enzyme activity is defined as the amount which catalyses the conversion of one micromole of the substrate per minute under standard conditions of the assay method.

Various assay methods to determine the activity of GO are described in the literature. The most common assay methods are spectrophotometric. Other methods employed include:

- titration,
- oxygen utilisation rate, and
- electrochemical determination

The spectrophotometric techniques employed either the enzymatic reduction of a coupled chromagen-peroxidase reaction or only the enzymatic reduction of a chromagen. A chromagen substrate, normally colourless, is converted to a coloured complex when added to the reaction mixture and measured at a certain wavelength. Examples of the most common chromagens used in GO assays are benzoquinone, 3,3'-dimethoxybenzidine (o-dianisidine), and 2,2'-azinodi-3-ethylbenzthiazoline-6-sulphonic acid (ABTS).

In the enzymatic reduction of o-dianisidine-peroxidase (Lloyd and Whelan, 1969; Fiedurek *et al*., 1986; Fiedurek and Gromada, 1997, 2000; Fiedurek, 1998; Hatzinikoaou *et al*., 1995; Roche; Seravac; Worthington manual) and ABTS-peroxidase (Hellmuth *et al*., 1995; El-Enshasy, 1998; Kapat *et al*., 1998; Witt *et al*., 1998), the GO is measured by the breakdown of H_2O_2 by peroxidase (POD) and coupled oxidation of the chromagen (dye) to a coloured complex. The rate of increase in absorbance of the coloured complex shows the rate of breakdown of H_2O_2 and hence the activity of GO.

$$\beta\text{-D glucose} + O_2 + H_2O \xrightarrow{GO} \text{Gluconic acid} + H_2O_2 \quad \textbf{(2.4)}$$

$$\text{dye (colourless)} + 2H_2O_2 \xrightarrow{POD} \text{dye (coloured, oxidised)} + 2H_2O + O_2 \quad \textbf{(2.5)}$$

Due to the carcinogenicity of o-dianisdine, the chromagen ABTS which is chemically stable, non-toxic and more sensitive for H_2O_2 detection is preferred (Childs and Bardsley, 1975; Raba and Mottola, 1995). Under the conditions stipulated Kapat *et al*. (1998) expressed their enzyme activity in terms of the Sigma standard activity where 1 U GO (o-dianisidine) = 1.66 U GO (ABTS).

On enzymatic reduction of benzoquinone (BQ) to hydroquinone (HQ) (Ciucu and Patroescu, 1984; Petruccioli *et al*., 1995, 1997, 1999), the rate of increase in absorbance is used to calculate the GO activity. This method does not require any other coupled enzymatic reactions.

$$\beta\text{-D glucose} + O_2 + H_2O + BQ \xrightarrow{GO} \text{Gluconic acid} + HQ \qquad \textbf{(2.6)}$$

In the titration method of Underkofler (1958), used by Zeletaki and Vas (1968), the amount of GO activity is calculated from the amount of HCl added to neutralise the NaOH used to stop the enzymatic reaction. Using a stoichiometric relationship the titration results are converted to manomeric GO units. The manomeric GO unit (Scott, 1953) is defined as that amount of enzyme which will cause the uptake of 10 mm^3 of oxygen per minute under standard conditions (Sarrett unit). Lu *et al*. (1996) and Rothberg (1999) also used a modified version of the titration method of Underkofler (1958).

In the oxygen utilisation method used by Nakamatsu *et al*. (1975), Van Dijken and Veenhuis (1980), Doppner and Hartmeier (1984), Mischak *et al*. (1985), Traeger *et al*. (1991) Li and Chen (1994) and Johnson (1995), the rate of decrease in soluble oxygen after the addition of a sample to an oxygen-saturated buffer containing glucose is measured. The rate of O_2 decrease (in ppm s^{-1}) is converted to GO activity (µmol substrate min^{-1}).

The electrochemical method of Kröger *et al*. (1998) involves the use of screen printed electrodes (containing a rhodinised–carbon working electrode, carbon counter electrode and silver/silver chloride reference electrode) at a working potential of +300 mV. H_2O_2 activity is detected amperometrically by monitoring the current generated by the oxidation of substrate with GO immobilised directly at the working electrode surface.

These different analytical methods have been conducted at different defined conditions and use different definitions for the GO activity unit. A summary of the GO assays, the respective assay conditions (temperature, pH, and substrate concentration) and the definition of the GO unit used in the literature are shown in Table 2.3. It can be seen that comparison of these assays with one another becomes difficult due to the different assay conditions such as: (a) temperature (ranging from 25°C to 37°C), (b) pH (ranging from 5 to 7), (c) different buffers (phosphate, citrate, sodium acetate), and

(d) different substrate (glucose) concentration (ranging from 65 mM to 1 M) and the actual definition of the GO unit.

A common unit or relationship between the different units would facilitate the comparison of two activities. The Commission of Biochemical Nomenclature, Recommendations (1972) recommended that to adhere to SI units, reaction rate should be expressed in moles per second and defined a new unit of enzyme activity to be called katal (symbol, kat). The katal is too large for most purposes and is usually expressed as microkatal, nanokatal or picokatal. The "old" unit (U) may be related to the katal by the following: 1 U catalyses glucose oxidation at a rate of 1 μmol min^{-1} ≈ 16.67 nmol s^{-1}. Therefore 1 U corresponds to 16.67 nkat (NC-IUB, 1979). These conversion factors are included in Table 2.3. Since GO activity is a function of all the operating conditions mentioned above, for direct comparison the effect of the different assay conditions should be taken into account.

2.5 Production of GO by fungal cultures

GO is the essential catalyst for the production of gluconic acid (GA) and both are produced by micro-organisms. The industrial scale production of GA and its metal-salts (gluconates) from glucose has been pioneered by Blom (1952). In this literature review emphasis is placed on the production of GO rather than GA.

Several studies have examined the optimisation of GO production in terms of the selection of the microorganism (Nakamatsu *et al*., 1975; Fiedurek *et al*., 1986; Petruccioli *et al*., 1993), carbon and nitrogen sources (Hatzinikoloau and Macris, 1995, Kona *et al*., 2001; Znad *et al*., 2004; Petruccioli *et al*., 1999), media composition (Rogalski *et al*., 1988; Gromada and Fiedurek, 1996; Hellmuth *et al*., 1995; Hatzinikoloau and Macris, 1995; Petruccioli *et al.*, 1995, 1997; Rando *et al*., 1997; Nakamatsu *et al*., 1975; Liu *et al*., 2001; Lu *et al*., 1996) and the effect of different process conditions, including aeration and agitation (Zeletaki and Vas, 1968; Petruciolli *et al*., 1995; Rothberg *et al*., 1999; Kapat *et al*., 2001, Traeger *et al*., 2001), growth time, (Hatzinikoloau and Macris, 1995), temperature (Hatzinikoloau and Macris, 1995) and pH (Znad *et al*., 2004).

In this literature review the following factors are reviewed pertaining to the production of GO, in accordance with the project scope.

- Organism
- Substrate and media composition
- Oxygen transfer

Table 2.3 Comparison of different GO assays reported in the literature

Principle of assay	Definition of GO unit (U)	Assay conditions	SI GO activity [nkat] Factor*	Comments	Reference
Enzymatic reaction of H_2O_2 coupled with the oxidation of benzoquinone to hydroquinone. Spectrophotometrically @ 290 nm (ε = 2.31 mM^{-1} cm^{-1})	Enzyme activity required to reduce 1 µmol benzoquinone per minute	25°C, pH 5.0, 1 M glucose, sodium citrate buffer	16.67	Method of Ciucu and Patroescu, 1984 as modified by Markwell *et al*., 1989	Petruccioli *et al*. 1995, 1997, 1999
Enzymatic reaction of H_2O_2 coupled with the oxidation of o-dianisidine to coloured complex, quinoneimine dye. Spectrophotometrically @ 525 nm (ε = not specified)	Enzyme activity required to produce 1µmol H_2O_2 per minute	30°C, pH 7.0, 5.6 mM glucose, Tris-phosphate glycerol buffer	16.67	Method of Lloyd and Whelan, 1969 modified by Fiedurek *et al*., 1986	Fiedurek *et al*., 1986 Fiedurek and Gromada, 1997, 2000 Fiedurek, 1998
Enzymatic reaction of H_2O_2 coupled with the oxidation of o-dianisidine to coloured complex, quinoneimine dye. Spectrophotometrically @ 435 nm (ε = not specified)	Enzyme activity required to oxidise 1µmol of glucose per minute.	30°C, pH 5.0, 0.21 M glucose, 0.1 M citrate-phosphate buffer	16.67		Hatzinikoaou *et al*., 1995
Enzymatic reaction of H_2O_2 coupled with the oxidation of o-dianisidine to coloured complex, quinoneimine dye. Spectrophotometrically at 460 nm (ε = not specified)	Enzyme activity required to oxidise 1µmol o-dianisidine per minute	25°C, pH 6.0, 1 M glucose, 0.1 M phosphate buffer	16.67		Worthington manual
Enzymatic reaction of H_2O_2 coupled with the oxidation of o-dianisidine to coloured complex, quinoneimine dye. Spectrophotometrically @ 436nm (ε = 8.3 $mmol^{-1}$ cm^{-1})	Enzyme activity required to convert 1µmol of D-glucose to product in 1 min	25°C, pH 7, Glucose, 100 mM phosphate buffer	16.67		Roche

Principle of assay	Definition of GO unit (U)	Assay conditions	SI GO activity [nkat] Factor*	Comments	Reference
Enzymatic reaction of H_2O_2 coupled with the oxidation of ABTS to a blue-green coloured complex. Spectrophotometrically @ 420 nm (ε =43.2 μmol^{-1} cm^{-1})	Enzyme activity required to oxidise 2 µmol ABTS min^{-1} (this equates to 1 µmol H_2O_2 min^{-1})	30°C, pH 5.0, 100 µM glucose, 100 µM phosphate buffer	16.67	Method of Danneel *et al*., 1993	Rando *et al.*, 1997
Enzymatic reaction of H_2O_2 coupled with the oxidation of ABTS to a blue-green coloured complex. Spectrophotometrically @ 420 nm (ε =43.2 μmol^{-1} cm^{-1})	Enzyme activity required to convert 1 µmol of product in 1 second	25°C, pH 5.8, 315 mM glucose, 0.111 M sodium phosphate buffer, saturated with O_2	1000		Hellmuth *et al.*, 1997 Kapat *et al*., 1998, 2000
Enzymatic reaction of H_2O_2 coupled with the oxidation of ABTS to a blue-green coloured complex. Spectrophotometrically @ 420 nm (ε =43.2 μmol^{-1} cm^{-1})	Enzyme activity required to produce 1 µmol H_2O_2 per minute)	25°C, pH 6, 0.1 M glucose, 0.1 M sodium acetate buffer, saturated with O_2	16.67	Method of Sahm *et al*., 1982	Kalisz *et al*., 1990 Witt *et al*., 1998
Titration method	Sarrett unit which is equivalent to 10 mm^3 oxygen consumption per minute.	30°C, pH 5.9, excess O_2, 1.83 M glucose, phosphate buffer	0.0784	Method of Underkofler, 1958	Zeletaki and Vas, 1968
Titration method	Enzyme activity required to oxidise 1 µmol of β-D-glucose to D-gluconic acid and H_2O_2 per minute	30°C, pH 5.6, 0.11 M glucose, 60 mM sodium acetate buffer	16.67	Modified from method of Underkofler 1958	Lu *et al*., 1996
Titration method	Enzyme activity required for the oxidation of 3 mg glucose to gluconic acid in 15 minutes. This equates to 1.1 µmol glucose per minute	35°C, pH 5.1, 0.17 M glucose, air, acetate buffer	18.34		Rothberg, 1999

Principle of assay	Definition of GO unit (U)	Assay conditions	SI GO activity [nkat] Factor*	Comments	Reference
Oxygen utilisation method. Measuring the rate of decrease in dissolved oxygen concentration	Enzyme activity required to convert 1 µmol O_2 per ml per minute	25°C, pH 5.5, 0.5 M glucose, 0.1 M phosphate buffer, 7 ppm O_2	33.34	Modified from method of Miura *et.al*., 1970	Johnson, 1995
Oxygen utilisation method. Measuring the rate of decrease in dissolved oxygen concentration	Enzyme activity required to oxidise 1 µmol glucose in 1 min	34°C, pH 5.2 65 mM glucose, air, 0.1 M sodium acetate buffer	16.67		Li and Chen, 1994
Oxygen utilisation method. Measuring the rate of decrease in dissolved oxygen concentration with a polarographic needle electrode	Enzyme activity required to oxidise 1 µmol glucose in 1 min	35°C, pH 5.1, 65 mM glucose, 0.1 M acetate buffer	16.67		Traeger *et al*., 1991
Manometrically with a Warburg apparatus	Enzyme activity required for O_2 uptake of 10 mm^3 per minute	30 °C, pH 5.9, 0.1 M phosphate buffer containing 0.4% sodium salt of dehydroacetic acid and 3.3% glucose	0.0784		Scott, 1953
Manometrically with a Warburg apparatus	Enzyme activity required for 1 µl oxygen uptake per hour	37°C, pH 5.6, 0.5 M glucose, air, 0.25 M phosphate buffer	0.119		Nakamatsu *et al*., 1975
Electrochemically at + 300mV By determining hydrogen peroxide activity.				Using a rhodinised-carbon working electrode, carbon counter electrode and silver/silver chloride reference electrode at a potential of + 300 mV.	Kroger *et al*., 1998

* Use this factor to convert the non-GO activity unit (U) to the SI GO activity unit (nkat) with glucose as the substrate
1 mol glucose → 1 mol H_2O_2 which reacts with 1 mol o-dianisidine or 1 mol benzoquinone
1 mol O_2 → 2 mol glucose (from Reaction 2.3)
µmol H_2O_2 min^{-1} or µmol glucose min^{-1} is converted to nkat by multiplying by a factor of 16.67
µmol O_2 min^{-1} is converted to nkat by multiplying by a factor of 33.34
10 mm^3 O_2 min^{-1} is converted to nkat by multiplying by a factor of 0.0784 (Using the solubility of O_2 in water at 30°C to be 7.53 mg l^{-1})
µl O_2 h^{-1} is converted to nkat by multiplying by a factor of 0.119 (Using the solubility of O_2 in water at 37°C to be 6.86 mg l^{-1})

2.5.1 Microorganisms and the production of GO

The most common fungal sources of GO are *Aspergillus niger*, *Penicillium notatum*, *Penicillium glaucum*, *Penicillium amagasakiense*, and *Penicillium purpurogenum* (Lockwood, 1975). Commercial preparations are obtained from *A. niger* and *P. amagasakiense* (Nakamatsu *et al*., 1975; Atkinson and Muvituna, 1991; Bucke, 1983). GO can also be produced using a recombinant *Saccharomyces cerevisiae* containing gene sequences from *A. niger* (Kapat *et al*., 2001). Interest in the wild-type fungal system remains due to the patent position of the recombinant system. GO is produced by the micro-organism as a defensive agent and subsequently has anti-microbial properties due to the formation of H_2O_2 (Petrucuccioli *et al*., 1999). H_2O_2 is broken down by catalase, which is produced concurrently with GO, to oxygen and water.

The difference in GO activity produced by wild type, mutant and recombinant organisms are illustrated in Table 2.4. The commercial production of GO depends on the organism used. Nakamatsu *et al*. (1975) reported significant variations across species of the same genus, e.g. *P. purpurogenum* produces up to ten times more GO than *P. amagasakiense*. Mutagenesis has been used to select mutants of *A. niger* and *P. variabile* with increased GO production rates (Petruciolli *et al*., 1997). Mutants of the same microbial species can have different GO production rates due to metabolic differences (Witteveen *et al*., 1990). The use of recombinant organisms, such as *S. cerevisiae* can also improve GO production but use is subject to patent issues. Generally, the mutant and recombinant organisms produce higher GO activities than wild type organisms, while *Penicillium sp*. are a better producers of GO than *A. niger sp*.

Table 2.4 GO produced from wild type, mutant and recombinant organisms

Organism used	GO produced[a]	Reference
Wild type or Parent organism		
A. niger NRRL-3	22.2 nkat ml^{-1}	Hellmuth *et al*., 1995
A. niger G-IV-10	4.82 U ml^{-1} (80.3 nkat ml^{-1})	Fiedurek and Gromada, 1997
P. variabile P16	18.6 U ml^{-1} (310.0 nkat ml^{-1})	Petruccioli *et al*., 1997
Mutant organism		
A. niger G-IV-10 Mutant M-6	8.57 U ml^{-1} (142.9 nkat ml^{-1})	Fiedurek and Gromada, 1997
P. variabile P16 Mutant M-80.10	25.6 U ml^{-1} (426.8 nkat ml^{-1})	Petruccioli *et al*., 1997
Recombinant organism		
A. niger NRRL-3 (GOD 3-18)	76.7 nkat ml^{-1}	Hellmuth *et al*., 1995
S. cerevisiae	10.3 U ml^{-1} (171.7 nkat ml^{-1})	Hong *et al*., 1998

[a] Multiply GO activity (U) by a factor specified in Table 2.3 to convert GO activity to nkat.

2.5.2 Substrate and media composition

A representative selection of media compositions reported in literature for the production of GO from *A. niger* (Table 2.5a) and *Penicillium spp*. (Table 2.5b) are given. The main carbon sources used to produce GO are glucose (Rogalski *et al*., 1988; Traeger *et al*., 1991; Hellmuth *et al*., 1995; Hatzinikolaou and Macris, 1995; Li and Chen, 1994; Johnson, 1995; El-Enshasy, 1998; Petruccioli et al., 1995, 1997; Nakamatsu *et al*., 1975; Petruccioli *et al*., 1993), sucrose (Hatzinikolaou and Macris, 1995; Zeletaki and Vas, 1968; Rando *et al*., 1997) and molasses (Hatzinikolaou and Macris, 1995) while other carbon sources such as fructose, galactose, lactose and starch can also be used. Glucose is the best carbon source for the production of GO. This is in line with the specificity of GO for β-D-glucose (Table 2.2) and the induction of GO reported by Witteveen (1990) and Johnson (1995). Molasses consists mainly of sucrose. If invertase is present it will convert sucrose to glucose and fructose.

Organic nitrogen sources such as peptone, corn steep liquor, urea, yeast extract and inorganic sources such as nitrates and ammonium salts are used for the production of GO. The salts and trace elements in the media are required for the regulation of cell metabolism and as co-factors for enzymes. These are supplied in varying concentrations to the various media.

To neutralise the organic acid formed and to maintain a constant pH, a source of alkalinity is required: NaOH, $Ca(OH)_2$ and $CaCO_3$ have been reported. Across the above mentioned studies, the various pH control agents were used without noting its effect on GO production. However, Petruccioli *et al*. (1995) studied the effect of $CaCO_3$, NaOH and NaOH plus $CaCl_2$ on the production of GO and catalase from *Penicillium variable* P16. They found more GO was produced (± 19.3 U ml^{-1}) when 35 g l^{-1} $CaCO_3$ was added initially to the bioreactor with no further pH control compared to when 8M NaOH was used (< 2 U ml^{-1}) to maintain the pH at 6.0. $CaCO_3$ has been reported to induce the synthesis of GO (Petrucciolli *et al*., 1995; Hatzinikolaou and Macris, 1995; Liu *et al*., 2001). Hatzinikolaou *et al*. (1996) showed that GO was induced by the addition of $CaCO_3$ and that the induction occurred at the transcription level. It was also shown that with the addition of $CaCO_3$, the production of the glycolytic enzyme, glucose-6-phosphate isomerase decreased. Hatzinikolaou *et al*. (1996) proposed that the addition of $CaCO_3$ to the growth medium caused a metabolic shift from glycolysis to a different pathway, such as the pentose phosphate pathway. The optimum concentration of $CaCO_3$ was found to be 40 and 50 g l^{-1} for the sucrose and molasses experiments. Other authors found the optimal $CaCO_3$ concentration to be 35 g l^{-1} (Rogalski *et al.*, 1988; Petruccioli *et al.*, 1995; Liu *et al.*, 1999).

Table 2.5a Media composition for GO production using *A.niger spp*.

	Rogalski *et al*., 1988	**Traeger *et al*., 1991**	**Hellmuth *et al*., 1995**	**Hatzinikolaou and Macris, 1995**	**Zeletaki and Vas, 1968**	**Li and Chen, 1994**	**Johnson, 1995**	**El-Enshasy 1998**
Organism	*A.niger* G-13 mutant	*A. niger* (RLL 126/1-2)	*A.niger* NRRL-3 (GOD 3-18)	*Aniger* ATCC strains and wild type *A.niger* BTL	*A. niger* strain 1026/5	A. niger ATCC 9029	A. niger NRRL-3	*A.niger* NRRL-3 (GOD 3-18)
Carbon source (in g per liter):								
Glucose	80	100	80	80 or		60	100	80
Sucrose				80 or	50 or 70			
Beet Molasses				80				
Other					7.5 citric acid			
Nitrogen source (in g per liter):								
Inorganic:								
$(NH_4)_2NO_3$						0.3		
$(NH_4)_2HPO_4$	0.388			0.4				
$NaNO_3$			3				1.20	3
Organic:								
Peptone*	30			10				
Cornsteep liquor (CSL)*		20			20	8 ml		
Yeast Exract (YE)*							0.50	2
Urea						2.0		
$Ca(NO_3)_2.4H_2O$					2			
Phosphate (in g per liter):								
KH_2PO_4	0.188	1	1	0.2	0.25	0.25	0.50	1
Other salts (in g per liter):								
$MgSO_4.7H_2O$	0.156	0.25		0.2	0.25	0.25	0.20	0.5
KCl			0.5		0.25			0.5
$FeSO_4.7H_2O$								0.01
$FeCl_3.6H_2O$					0.01			
$MgSO_4$			0.5					
FeSO4			0.01					
Trace elements							0.04 ml **	
pH control:								
NaOH			2.5 M			5 M	5 M	2.5 M
$CaCO_3$				40 g l^{-1} 50 g l^{-1} when used with molasses				
$Ca(OH)_2$	25 %(w/w)							
Antifoam	0.25 ml/l Durapol		SP1 reagent			20% KM-70 agent	0.25 ml/L Sigma Antifoam 289	Reagent SP1

* The approximate nitrogen content is 13% for peptone, 11% for yeast extract and 8% for corn steep liquor

** From Witteveen (1990). Trace metal solution of Vishniac and Santer (1957)

Table 2.5b Cultivation media for GO production using *Penicillium spp*.

	Petruccioli *et al*., 1997, 1995	**Rando *et al*., 1997**	**Nakamatsu *et al*., 1975**	**Nakamatsu *et al*., 1975**	**Nakamatsu *et al*., 1975**	**Petruccioli *et al*., 1993**
Organism	**Wild type *P.variable* P16 and mutant strain M-80-10**	***P. pinophilum***	***Penicillium* species (Media A)**	***Penicillium* species (Media B)**	***Penicillium* species (Media C)**	***P. variable* P16**
Glucose	80		40	60	40	80
Sucrose		40				
Galactose						
Beet Molasses						
$(NH_4)_2SO_4$						
$(NH_4)_2HPO_4$						
$NaNO_3$	5	1.9	2	7	2	5
Peptone	3		3[#]	3[#]		3
CSL						
YE						
Soybean meal extract					5	
Hycase[##]						
KH_2PO_4	1	1.5	1.0	1.0	1.0	1
$Na_2PO_4.2H_2O$		4.45				
$MgSO_4.7H_2O$		0.20	0.50	0.5	0.5	0.5
KCl	0.5		0.5	0.5	0.5	
$FeSO_4.7H_2O$	0.01		0.01		0.01	0.5
$CaCl_2.2H_2O$		0.02				
Trace elements		10 ml				
Vitamins		10 ml				
pH control:						
NaOH						
$CaCO_3$	35 g l^{-1}					35 g l^{-1}
Antifoam	2ml/l Silicon antifoam					

2.5.3 Oxygen transfer

Molecular oxygen induces the expression of the GO_{gene} at the transcription level (Johnson, 1995; Witteveen *et al.*, 1993; Mischak *et al.*, 1985).

Fungal GO production is a highly aerobic process and due to oxygen's low solubility in aqueous solutions (7.53 mg l^{-1} at 30°C in water), it is the first substrate to become limiting. The dissolved oxygen concentration in the culture depends on temperature, media composition, biomass concentration, agitation and aeration rate, impeller and reactor geometry and cell growth (Kapat *et al.*, 2001).

To ensure the culture does not become oxygen limited, the oxygen transfer rate (OTR, [mmol l^{-1} h^{-1}]), and its utilisation rate (OUR, [mmol l^{-1} h^{-1}]), need to be matched, according to Eqn 2.7. This relationship controls the resultant dissolved oxygen concentration.

$$OTR = k_l a\left(C_{sat} - C_l\right) = OUR \qquad \textbf{(2.7)}$$

where $k_l a$ is the mass transfer coefficient [h^{-1}], C_{sat} is the saturated oxygen concentration [mmol l^{-1}] and C_l is the oxygen concentration in the bulk liquid [mmol l^{-1}].

The agitation speed and air flow rate are typically used to influence the $k_l a$ or OTR in the bulk medium through (Clarke *et al.*, 2006b). Excessive increasing of the agitation speed can lead to injury of the mycelial filaments due to shear. With *A. niger*, efficient bulk oxygen transfer may not suffice as mass diffusion limitations arise within the pellet due to an increase in the pellet diameter.

Previous studies by Zeletaki and Vas (1968) indicated that the GO activity increased two fold for an oxygenated culture compared to an aerated culture owing to the influence of oxygen partial pressure on the dissolved saturation concentration via Henry's law (Equation 2.8).

$$P_{AG} = P_T\, y_{AG} = H C^*_{AL} \qquad \textbf{(2.8)}$$

where P_{AG} is the partial pressure of component A in the gas phase [atm], P_T the total gas pressure [atm], y_{AG} the mole fraction of A in the gas phase, H is Henry's constant [atm mole O_2^{-1} mole H_2O^{-1}], and C^*_{AL} is the solubility of component A in the liquid phase [mmol l^{-1}].

Johnson (1995) found that by increasing the oxygen partial pressure for an *A. niger* cultivation in a 7 litre Chemap bioreactor from 0.21 to 0.75 atm, at an optimal glucose concentration of 100 g l^{-1}, an aeration rate of 1.5 vvm (volume air per volume bioreactor per minute) and agitation speed of 600 rpm, the final GO activity in this low biomass system increased from 2.1 U ml^{-1} to 4.5 U ml^{-1}. Increasing the oxygen concentration from 0.75 atm to 1.0 atm did not further increase the final level of GO produced (Figure 2.3).

Since GO production is a highly aerobic process and oxygen has a low solubility in aqueous solutions, oxygen vectors such as the hydrocarbons, n-dodecane, n-hexadecane and soybean oil have been added to the culture medium to increase the oxygen transfer rate (Li and Chen, 1994; Clarke *et al.*, 2006b). Hydrocarbons are largely immiscible in the culture medium; however, Li and Chen (1994) proposed that they act as an active intermediate in the oxygen transport from the gas bubbles to the aqueous phase. They showed that, with the addition of 5% n-dodecane at various times (0, 8, 16 h) to the *A. niger* culture, an increase in GO production of 67%, 125% and 15% was achieved compared to the control.

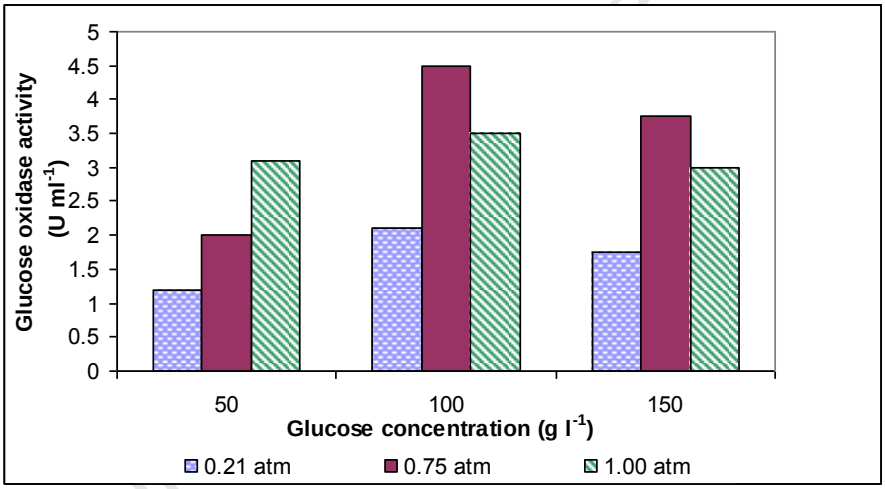

Figure 2.3 Effect of glucose and oxygen on maximum GO levels (redrawn from Johnson, 1995)

Increasing the rate of agitation increases the $k_l a$ and hence OTR. This ensures that the cultivation productivity does not decrease due to oxygen limitation. If the agitation is too high, it leads to hyphal damage due to shear which impacts negatively on the productivity. Petruccioli *et al.* (1995), using *P. variabile* P16, showed that by increasing the agitation rate from 300 rpm to 400 rpm an increase in GO activity from 6.3 U ml^{-1} (105.0 nkat ml^{-1}) to 19.3 U ml^{-1} (321.7 nkat ml^{-1}) results after 90 h. However, a further increase in agitation to 500 rpm, 700 rpm and 900 rpm resulted in a dramatic decrease in GO to 12.7 U ml^{-1} (211.7 nkat ml^{-1}), 3.21 U ml^{-1} (53.5 nkat ml^{-1}) and 2 U ml^{-1} (33.3 nkat ml^{-1}), respectively. Observations under a light microscope did not show mycelial differences when varying the agitation.

2.6 Location of GO in *Aspergillus spp*. and *Penicillium spp*.

2.6.1 Downstream processing of microbial enzymes

The location of the enzyme refers to its distribution in the microbial culture and plays an important role in the subsequent downstream recovery process of the enzyme. In microbial cultures, enzymes may be found in the extracellular and/or intracellular location. In the extracellular location it can be found either excreted into the bulk culture fluid or supernatant or associated with the cell in the capsular material or slime mucilage. In the intracellular location it is found either associated or bound to cell structures such as organelles, cell wall and membranes or soluble in the cytoplasm.

Figure 2.4 illustrates a typical downstream process (DSP) for the recovery of intracellular and extracellular enzymes. Enzyme recovery is typically initiated with the separation of the solids (biomass) and liquids (supernatant) after which the enzyme is recovered from either the solid or liquid streams. The extracellular location of an enzyme facilitates its recovery because it precludes the need for a cell disruption step and limits the number of other proteins and metabolites from which the enzyme must be purified. Although recovery of an intracellular enzyme realises the disadvantages mentioned above, the enzyme is readily concentrated by concentration of the cells before cell disruption and separation from the solids. It is desirable that the enzyme product is located exclusively in one or other of these locations as processing of both the cell lysate and supernatant together requires enzyme purification from a dilute and complex solution and is not typically practical.

Solid-liquid separation can be achieved by centrifugation or filtration. Mechanical cell disruption using high pressure homogenisers, bead mills or ultrasonic disintegrators are usually preferred (Harrison, 1991; Balasundaram *et al*., 2009). Lysing of the cells can also be induced by chemically killing the cells or by radically altering the pH, temperature or osmotic properties of the growth medium (Harrison, 1991; Fiedurek, 1998; Balasundaram *et al*., 2009), but is inefficient, particularly for fungi, and introduces further contaminating solutes. After cell disruption the cell debris is removed typically by centrifugation prior to protein recovery. In some instances the protein can be extracted from the whole cell lysate using, for example, expanded bed adsorption.

Ultrafiltration, which removes most of the water and other residual small molecules such as amino acids and sugars, is sufficient to provide a crude extract from the supernatant. From the cell lysate an additional selective protein separation step, such as precipitation, size separation or chromatography, is required (Harrison, 2011). If the enzyme is required in a liquid form as a crude extract, stabilizers such as potassium sorbate or glycerine are added. However, if the enzyme is to be sold as a powder,

the ultrafiltered liquid is spray-dried and blended with carriers to the correct activity. Speciality enzymes, or those requiring greater purity, are subjected to multiple purification stages including large-scale chromatography such as ion-exchange, gel filtration or affinity chromatography (Gray and Tribe, 1979).

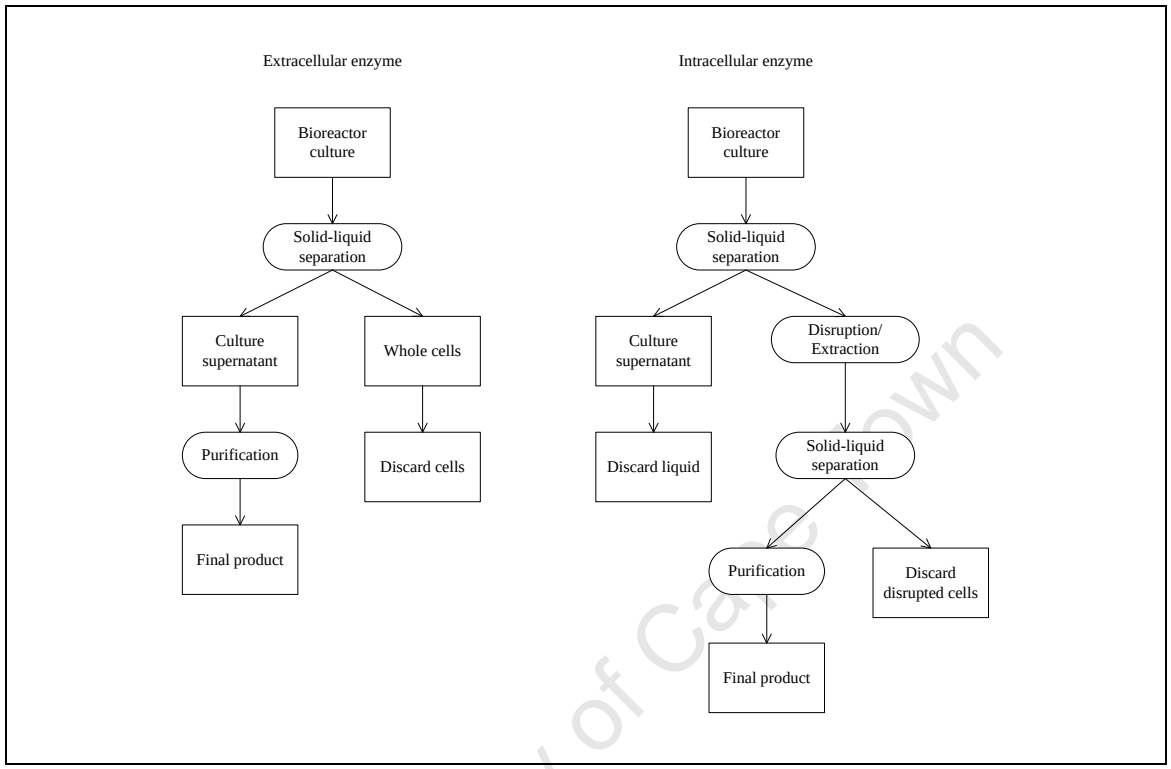

Figure 2.4 Downstream recovery procedures for extracellular and intracellular enzymes (modified from Gray and Tribe, 1979)

Some of the analytical techniques used in literature to fractionate *A. niger* and *Penicillium* spp. cultures to recover the intracellular GO are summarised in Table 2.6. The fungal cells were recovered by means of filtration or centrifugation and washed to remove residual media. The cells were resuspended in either buffer or distilled water (pre-treatment). The buffers used for resuspending the cells included sodium acetate, citrate phosphate, McIlvaine and phosphate (with and without EDTA) and ranged in concentration from 50 mM to 100 mM and pH 4 to 7. The cell suspension was then disrupted by means of sonication, homogeniser, French press or a commercial blender (cell disruption). The disrupted cell suspension was further pre-treated to "leach" GO from the fragments (treatment) and the cell debris was removed by means of centrifugation (solid separation). Any additional treatment of the cell debris such as washing and resuspension are shown in the "final treatment steps" column of Table 2.6. The cell extract was recovered from the cell debris and used in the GO assay (Section 2.6) to quantify the GO associated with the cell debris. This intracellular location includes GO associated or bound to cell structures such as organelles, cell wall and membranes and soluble in the cytoplasm.

Table 2.6 Comparison of the different separation processes used in literature to measure the intracellular GO activity

Solid separation, washing and pre-treatment steps	Cell disruption step	Treatment, solid separation and final treatment steps	Organism	References
Filter, wash several times with water, add 60 mM sodium acetate buffer pH 5.6; 0.2 g mycelium ml^{-1} acetate buffer	Disrupt for 10 min at 0-10°C using Sonic Dismembrator	Maintain broken mixture at 4°C for over 24 h, centrifuge at 15000 rpm for 30 min at 2°C	*A. niger* ZBY-7	Lu *et al*., 1996
Filter, wash several times with distilled water, add mycelium to double distilled water (0.2 g mycelium ml^{-1})	Glass cell homogeniser	Centrifuge at 2000 g for 10 min	*A. niger* ZBY-7	Liu *et al.*, 1999
Filter, wash on sieve with 160 µm pore size, resuspend in 0.1 M citrate-phosphate buffer, pH 4	Disrupt in commercial blender at maximum speed for 3 min. Resulting suspension subjected to sonication (8 x 1 min periods)	Not mentioned	*A. niger* BTL	Hatzinikolaou and Macris, 1995
Centrifuge 20 ml at 6000 rpm for 15min, wash twice with deionised water, resuspend in 0.1 M phosphate buffer pH 6.0 to initial volume of 20 ml	Cool in ice water, homogenise (3 times for 30 s each) with Cell Homogeniser	Centrifuge at 6000 rpm for 10 min, harvest cell debris and wash twice with cold deionised water. Resuspend in 0.1 M phosphate buffer pH 6.0 to final volume of 5 ml	*P. variabile* P16	Petruccioli *et al.*, 1997
Centrifuge at 6000g for 10 min, add 3 ml 0.1 M McIlvaine buffer, pH 5.5 to 2.0 g wet weight	Homogeniser with glass pestle at 7000 rpm with 20 passes of the pestle	Add 97 ml of 0.1 M McIlvaine buffer to homogenised mycelium	*A. niger* G-IV-10	Gromada and Fiedurek, 1996
Filter with 45 µm Millipore membrane, volume of sample used is increased from 1 ml to 20 ml	French press	Not mentioned	*A. niger* NRLL3	Johnson, 1995
Filter, wash several times with water, resuspend filter cake in 5 cm^3 double distilled water. Mycelium suspension cooled in ice water	Ultrasonic Homogeniser (5 x for 3 min) at 20.5 kHz, 100 W cm^{-2}	Centrifuge at 8000 g	*A. niger* RRL 12-6/1-2	Traeger *et al.*, 1991
Filter, wash until pH of washings is 6.5 - 7.0 (Citric acid cultivation), press between filter paper to remove excess water. Use ratio of 10 ml extraction medium to 1 g wet weight	Homogeniser	For extraction of intra- cellular GO 0.1M phosphate buffer + 1mM EDTA, pH 6.0 was used. All operations carried out in the cold, centrifuge at 6000 g for 20 min	*A. niger* B60	Mischak *et al.*, 1985
Filter, wash extensively with demineralized water, suspend mycelium in 50 mM potassium phosphate buffer, pH 7.0	Disrupt for 5 min at 0 - 4°C with ultrasonic disintegrator (20 kHz)	Centrifuge at 20000 g for 20 min	*A. niger*	Van Dijken and Veenhuis, 1980

2.6.2 Controversy regarding GO location in fungal cultures

Literature findings relating to the location of GO in *A. niger* are contradictory, both with regard to the distribution between extra- and intracellular locations and, in the case of an intracellular location, with regard to the identification of the exact intracellular site (cytoplasm or cell wall and membrane associated). GO from *A. niger* has been considered to be predominantly an intracellular enzyme (Pazur, 1966; Van Dijken and Veenhuis, 1980; Witteveen *et al.*, 1992), although it has been recognised that multiple GO locations may exist within the *Aspergillus* culture (Mischak *et al.*, 1985; Hatzinikolaou and Macris, 1995).

Van Dijken and Veenhuis (1980) performed cytochemical labelling of GO in *A. niger* and showed it was located intracellularly in cytoplasmic microbodies, identified as peroxisomes. They suggested that any extracellular GO resulted from autolysis. Subsequently, Witteveen *et al*. (1992), using immunocytochemical labelling, showed that the bulk of GO was localised in the cell wall and attributed the peroxisome location to be an artefact of the analytical method used. A cell wall location was further supported by the observation that while GO was present in the lysate of intact mycelia, it was absent in the lysate of protoplasts (Witteveen *et al*., 1992).

Mischak *et al.* (1985) examined the distribution of GO between intra- and extracellular locations in *A. niger*, and reported a predominantly extracellular location. These authors observed that 75% of the total GO was present in the culture fluid, only 17% of which could be accounted for by autolysis. Since the extracellular location was observed in a Mn^{2+} deficient medium only, Witteveen *et al*. (1992) suggested that the extracellular location might be a consequence of an altered cell wall composition resulting from Mn^{2+} deficiency, thus allowing a cell-wall localised GO to enter the culture fluid and, therefore, making this result compatible with their result of a cell wall locality. The alteration of cell wall composition had previously been associated with Mn^{2+} deficiency during production of citric acid by *A. niger* (Kisser *et al*., 1980). However, Mn^{2+} has also been observed to induce slime mucilage around the cell (Kisser *et al*., 1980; Mischak *et a*l., 1985) which traps GO, making it appear intracellular through diffusional limitations (Mischak *et al*., 1985). Hence it can be proposed that the extracellular location in a Mn^{2+} deficient medium is due to the absence of enzyme entrapment and not a result of a cell wall locality. An extracellular location of GO is also suggested by the glycoprotein structure of the enzyme (Pazur *et al*., 1965).

The location of GO in *Penicillium spp*. has generally been regarded as extracellular (Kusai *et al*., 1960; Nakamatsu *et al.*, 1975; Petruccioli *et al*., 1993) although intracellular predominance has also been reported (Rando *et al*., 1997). The multiple locations reported for GO in *Aspergillus* sp. and *Penicillium spp*. are shown in Table 2.7.

The discrepancies in the literature may, in part, be attributable to the difference in the growth phase in which the cells were harvested for analysis. Hatzinikolaou and Macris (1995) observed the ratio of extracellular to total GO activity in an *A. niger* culture varied from about 0.1 at the initial stages of growth to about 0.25 after 96 hours. Pluschkell *et al*. (1996) reported the increase in ratio of extracellular GO activity from recombinant *A. niger* from between 0.35 and 0.40 during early growth (20 h) to 0.9 at the end of growth (200 h). Interestingly, reports by Johnson (1995) suggest that GO from wild-type *A. niger* NRRL-3 is associated with both the culture fluid (extracellular) and the mycelial pellets (intracellular). The extracellular GO accounted for approximately 30% of the total enzyme produced after a 30 h growth period. During the rapid growth phase (6-19 h) the enzyme was predominantly intracellular. GO trapped in the mucilage layer is another possible location (Mischak *et al.*, 1985; Johnson, 1995). They postulate that this mucilage entraps GO on its excretion from the cell, thereby causing it to remain associated with the mycelium, thus appearing intracellular.

To date no attempt has been reported in the literature to resolve the differences in GO location in fungal cultures.

Table 2.7 Review of reported locations of GO in *Aspergillus spp*. and *Penicillium spp*. at the outset of this study

Organism	Extracellular	Intracellular (includes cell wall and membrane fragments)	Reference
A. niger		Predominant	Pazur, 1966
A. niger		Predominant	Van Dijken & Veenhuis, 1980
A. niger N400 (CBS 120.49)		Predominant	Witteveen *et al.*, 1992
A. niger B60	74%	26%	Mischak *et al.*, 1985
A. niger BTL	25% (96 h culture) 10% (early exponential)	75%	Hatzinilolaou and Macris, 1995
Recombinant *A. niger* NRRL-3 (GOD3-18)	90% (stationary) 40% (exponential)		Pluschkell et al., 1996
A. niger NRRL3	30% (stationary)		Johnson, 1995
P. amagasakiense	Predominant		Kusai *et al.*, 1960
Penicillium sp.	Predominant		Nakamatsu *et al.*, 1975
P. variabile P16	Predominant		Petruccioli *et al.*, 1993
P. pinophilum DSM 11428	20 – 40% (due to lysis)	60 – 80%	Rando *et al.*, 1997

2.7 Morphology of fungal cultures

In submerged fungal cultures the filamentous morphology of the microorganism can vary between "mycelial" and "pellet" forms (Metz and Kossen, 1977). The complex morphology of the microorganism is of importance because it can influence the productivity, rheology, mass and heat transfer (Metz and Kossen, 1977; Whitaker and Long, 1973; Braun and Vecht-Lifshitz, 1991). Variation in the location of GO may be linked to culture morphology and cell wall structure. *A. niger* provides a model for pelleted morphology while *Penicillium* sp. displays mycelial morphology.

2.7.1 Physiology of fungi

Fungi can be classified (Atkinson and Mavituna, 1991) as lower fungi and higher fungi. The lower fungi (Myxomycotina) consist of the subdivisions Mastigomycotina and Zygomycotina and slime molds. The higher fungi comprise yeast (Ascomycotina), Basidiomycotina and Fungi Imperfecti (Deuteromycotina). *Aspergillus* and *Penicillium* are Imperfect Fungi (Deuteromycota)

The higher fungi are essentially aerobic. They form long branched filamentous hyphae which can be 4 to 20 μm wide, and may or may not have cross walls or septa (Aiba, 1965). A section of a hypha (Aiba, 1965) is illustrated in Figure 2.5 and the size and properties of parts of a fungal hypha are summarized in Table 2.8.

Figure 2.6 illustrates a range of morphological forms of filamentous fungi in submerged cultures ranging between the two extremes of freely dispersed mycelia and pellets with clumps as the intermediate form (Amanullah *et al*., 2000).

C.W.	Cell wall
F	Fibrous layer
M	Mitochondria
N	Nucleus
S.P.	Pore in the septum
S	Septum
R	Endoplasmic reticulum
N.M.	Nuclear membrane
N.P.	Pore in the nuclear membrane
C.M.	Cell membrane

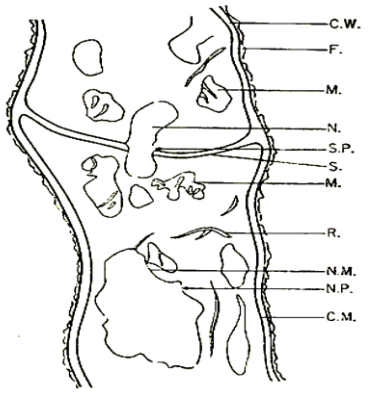

Figure 2.5 Diagram of a fungal hypha (sourced from Aiba, 1965)

Table 2.8 Size and properties of fungal components (sourced from Atkinson and Mavituna, 1991; Aiba, 1965)

Component	Size (µm)	Comments
Outer fibrous layer	0.1 – 0.5	Very electron-dense material
Cell Wall	0.1 – 0.25	*Zygomycetes*, *Ascomycetes* and *Basidiomycetes* contain chitin (2-26% dry weight); *Oomycetes* contain cellulose, not chitin, while yeast cells contain glucan (29%), mannan (31%), protein (13%) and lipid (8.5%)
Cell membrane	0.007 - 0.01	Much folded, double-layered membrane; semi-permeable to nutrients
Endoplasmic reticulum	0.007 - 0.01	Highly invaginated membrane or set of tubules, probably connected with both the cell membrane and the nuclear membrane and concerned in protein synthesis and probably other metabolic functions
Nucleus	0.7 - 3	Surrounded by a double membrane (10 nm), containing pores (40 - 70 nm wide); flexible and contains cytologically distinguishable chromosome. Nucleolus about 3 nm. In *Actinomycetes* there is no nuclear membrane. The nucleus is capable of migration.
Mitochondria	0.5 - 1.2 by 0.7 - 2	Analogous to those in animal and plant cells, containing electron transport enzymes and bounded by an outer membrane and an inner membrane forming cristae; probably develop by division of pre-existing mitochondria
Inclusions		Lipid and glycogen-like granules are found in some fungi. Ribosomes in all fungi.

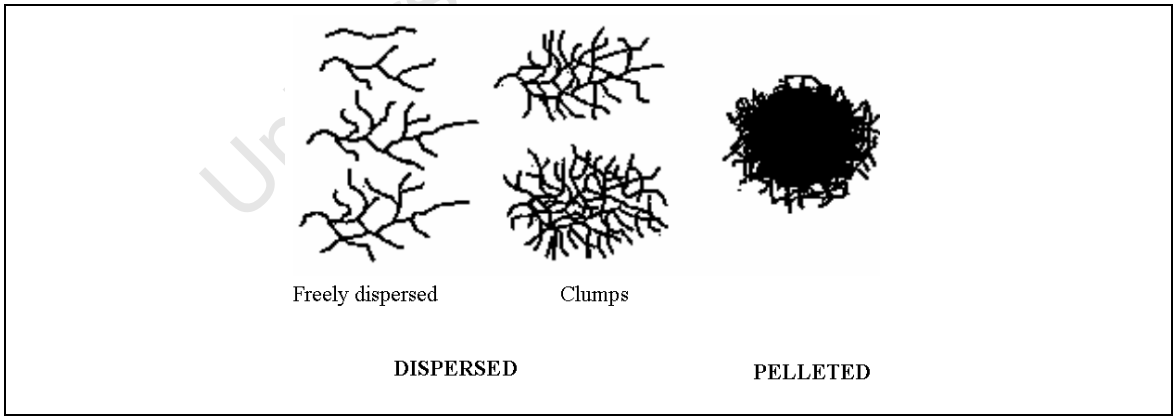

Figure 2.6 Range of morphological forms in submerged cultures of filamentous fungi (sourced from Amanullah *et al*., 2000)

2.7.2 Growth of filamentous fungi

Under favourable conditions, spores of fungi such as *Aspergillus* spp. and *Penicillium* spp. germinate into active growing hyphae as shown in Figure 2.7a (Nielsen, 1996).

The single germ tube emerging from the germinated spore and the hyphal length extends at an exponential rate (Equation 2.9) until it reaches a maximum hyphal extension rate at which point linear growth (Equation 2.10) is achieved (Prosser, 1995). During growth, the extension of the hyphae occurs only at the apical tips as shown in Figure 2.7b. These extend linearly at rates depending on the hyphal composition and environmental conditions (Pazouki and Panda, 2000, Prosser, 1995). Although the hyphae grow only at the tips, the total length of the mycelium increases exponentially with the increasing number of tips due to branching (Yang *et al*., 1992). Together with tip extension this formation of branches enables the fungi to "spread out". In terms of growth kinetics, branch formation may be considered equivalent to cell division in unicellular microorganisms (Prosser, 1995). Branching frequency is an indication of the rate of formation of new tips within a hyphal element (Nielsen, 1996). The mycelium grows rapidly in favourable conditions and is densely branched with large hyphal diameters but in poor growth conditions it has fewer branches with small hyphal diameters i.e. long threads with very few branch points enabling it to seek a better growth environment (Nielsen, 1993).

$$L = L_0 e^{k_1 t} \qquad \textbf{(2.9)}$$

$$L = L_0 + k_2 t \qquad \textbf{(2.10)}$$

where L and L_0 represent hyphal length at time t and at the beginning of the appropriate growth phase and k_1 and k_2 are constants.

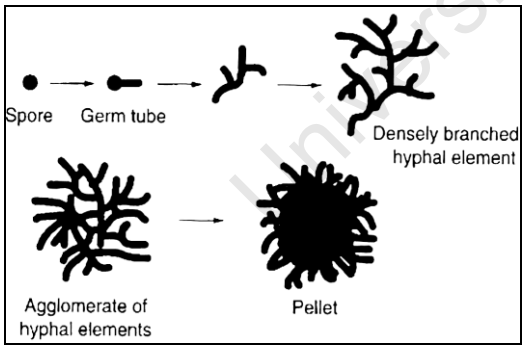

Figure 2.7a Development of a hyphal element from a spore (sourced from Nielsen, 1996)

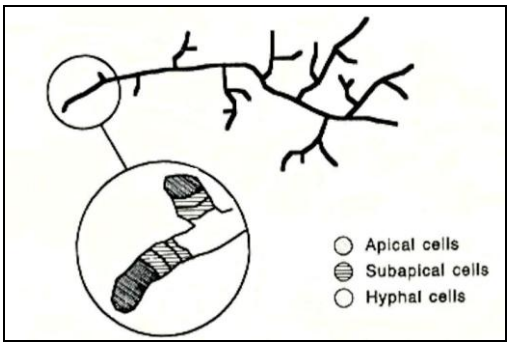

Figure 2.7b Apical tip of hyphal element (sourced from Nielsen, 1994)

Therefore for filamentous fungi, growth only occurs at the hyphal tips and where new tips are created by branching and fragmentation of the hyphae due to shear stress (Znidarsic and Pavko, 2001; Lejeune and Baron, 1998). Mycelial fragmentation is common in fungal cultures. It has been associated with high agitation and increased levels of vacuolisation (Papagianni and Moo-Young, 2002; Paul *et. al*., 1994; Papagiani *et. al*., 1999; Belmar-Beiny and Thomas, 1991).

Vacuolisation is normally found in older hyphae. This is a natural ageing process in fungi which tends to weaken the hyphae. When shear is applied, it accelerates their fragmentation. Certain conditions, such as oxygen limitation or supplying glucose at the maintenance rate, contribute to vacuolisation of hyphae and subsequent fragmentation (Righelato *et.al*., 1968; Paul *et al*., 1994). Vacuolisation was shown to be more pronounced in the mycelial growth form (Papagianni and Moo-Young, 2002).

2.7.3 Quantitative representation of hyphal morphology

Until the 1970's little quantitative work was reported on the morphology of fungi. Fungal morphology was referred to qualitatively as "long filamentous mycelium", "short fragmented mycelium", "highly branched mycelium", etc. Early investigations were based on time-consuming manual measurements from an electronic digitiser (Metz *et al*., 1981). This method was slow, labour-intensive and not particularly accurate or precise. An alternative method was developed by Adams and Thomas (1988) to represent the morphology of fungal organisms quantitatively using image analysis which is faster, more accurate and reproducible. Algorithms to quantify the morphology of dispersed mycelia using semi-automatic and automatic methods were developed by Packer and Thomas (1990), and Tucker *et al*. (1992) and for pellet morphology by Cox and Thomas (1992) and Reichl *et al*. (1992).

To characterize the hyphal morphology of fungi, a number of morphological indices can be used (Metz *et al*., 1981; Grimm *et al*., 2005). These have been described by Metz *et al*. (1981) and are detailed in Figure 2.8:

Morphological indices		
L_t	Total length of hyphae (sum of all hyphal lengths)	
L_e	Main hyphal length or effective length	
L_d	Mean hyphal diameter	
n_b	Number of branches	
L_b	Mean length of branches	
L_s	Mean length of segments (length from tip to 1st branch point)	
N_t	Number of tips	
L_{hgu}	Hyphal growth unit (also known as branching frequency)	$L_{hgu} = L_t/N$
L_{e+}	Dimensionless effective length	$L_{e+} = L_e/L_d$

Figure 2.8 Morphological indices used to describe mycelium (adapted from Metz *et al*., 1981, Grimm *et al*., 2005)

The dimensions of hyphae are used to calculate the following morphological indices:

- hyphal growth unit: the average total length of hyphae associated with a growing tip, L_{hgu} ($L_{hgu} = L_t/N_t$). It is often referred to as the branching frequency, where $L_{hgu} = L_t/n_b$ (Caldwell and Trinci, 1973)
- dimensionless effective length: L_e^+ ($L_e^+ = L_e/L_d$)
- hyphal growth unit volume V_{hgu} or hyphal growth unit mass m_{hgu}: Conversion between the different hyphal growth unit definitions can be made using Equation 2.11, where d is the hyphal diameter, ρ_m is the mycelium density and *w* is the water content of the mycelium (Nielsen, 1992).

$$m_{hgu} = \rho_m (1-w) V_{hgu} = \rho_m (1-w) \frac{\pi}{4} d^2 L_{hgu} \qquad \textbf{(2.11)}$$

The quantification of the morphology of pellets is more complex as individual hyphae cannot be distinguished. Therefore, different morphological indices are used (Cox and Thomas, 1992), namely

- perimeter
- area of pellet
- compactness, F': the ratio of the projected area of the hyphae in a clump to the projected area of the clump after filling in any voids
- circularity ratio: the relationship between pellet perimeter and the dense core area of the pellet. This is 1 for circular objects and greater than 1 for others. The circularity ratio is an estimate of clump roughness or hairiness and is given by:

$$Circularity = \frac{perimeter^2}{4\pi\, area} \qquad \textbf{(2.12)}$$

Fluoresence techniques can be used to determine active growing tips. A stain such as Chalcofluor White is added to a hyphal sample and viewed under UV excitation. The stain binds selectively to cellulose and chitin, and since the cell wall of fungi consists of varying amounts of cellulose and chitin, it fluoresces in accordance with this variation. Actively growing tips appear intensely bright while non-active or broken tips do not fluoresce (Amanullah, 2002). Semi-automatic image analysis is then used to determine quantitatively the fraction of actively growing mycelial tips.

2.7.4 Pellet morphology and formation

Pellets can be classified into three groups: 1) fluffy loose pellets which have a compact centre and a much looser outer zone; b) compact smooth pellets, where the whole pellet is compact and the outside of the pellet is smooth; c) hollow smooth pellets, where the centre is hollow owing to autolysis and the outside is smooth (Clark, 1962; Steel *et al*., 1954).

A typical pellet consists of three regions: the growing region at the outer shell, the non-growing region of mycelial biomass and the hollow centre (Wittler *et al*., 1986). The growth of pellets is restricted to the surface of the pellet while cell lysis occurs at the centre of the pellet due to nutrient limitation, in most cases oxygen.

Pellet formation can also be classified into two types, namely coagulating and non-coagulating (Pazouki and Panda, 2000). In the coagulating type, the spores conglomerate at an early stage of development to form pellets while in the non-coagulating type one spore grows out to form one pellet. Pellets of *A. niger* are of the coagulating type (Galbraith and Smith, 1969).

Many factors influence pellet formation (Braun and Vecht-Lifshitz, 1991; Papagianni, 2004). These factors can be divided into microbiological (inoculum type and level, growth rate), chemical (type and ratio of carbon and nitrogen sources, media composition, surface active agents, dissolved oxygen, carbon dioxide) and physical (pH, temperature and shear forces). However, it is difficult to assign a specific factor that is responsible for a change in morphology since varying one factor may change more than one parameter (Braun and Vecht-Lifshitz, 1991; Papagianni, 2004).

The inoculum amount, type (spore or vegetative) and age are important factors in fungal cultures (Tucker *et al*., 1992; Papagianni and Moo-Young, 2002). High spore inoculum concentrations favour mycelial growth, while a low spore inoculum concentration (below 10^8 spores ml^{-1}) favours pellet formation (Van Suijdam *et al*., 1980). However, spore agglomeration can occur in high spore inoculums resulting in pellet formation (Galbraith and Smith, 1969). The size of pellets is also influenced by the size of the inoculum. A large inoculum (10^8 spores ml^{-1}) of *A. niger* resulted in a large number of fine pellets, while much larger pellets were formed at inoculum levels of 10^5 spores ml^{-1} (Johnson, 1995, Papagianni and Moo-Young, 2002). For a *P. chrysogenum* culture with an inoculum of 10^4 spores ml^{-1}, the pellets remained small but became more numerous in comparison to an inoculum concentration of 10^3 spores ml^{-1} (Papagianni, 2004).

During growth the morphology of the organism changes. This, in turn, affects the nutrient consumption and the oxygen uptake rate in submerged cultures. Several authors studied the effect

of dissolved oxygen on the morphology of fungal cultures (Kobayashi *et al*., 1973; Van Suijdam and Metz 1981a; Zeletaki and Vas, 1968) and reported changes from thicker shorter and more highly branched mycelia to more flexible and thinner hyphae. Due to oxygen's low solubility in water (7.53 mg l^{-1} at 30°C), and thereby limited driving force, as the pellet size increases, autolysis of the core occurs because less oxygen is able to diffuse to the centre of the pellet. Li and Chen (1994) used hydrocarbons to act as an oxygen transfer enhancer in *A. niger* cultures and observed no morphological changes. As a consequence of microbial respiration during growth CO_2 is produced which influences the morphology of several filamentous microorganisms (McIntyre and McNeil, 1997). For *P. chrysogenum*, CO_2 stimulated chitin synthesis at the hyphal tip and subapical cell wall. Chitin is a compound of cell wall which increases its plasticity and has been linked to increased branching (Edwards and Ho, 1988).

Agitation causes the dispersion of spore agglomerates (Metz and Kossen, 1977). Increased agitation gives rise to smaller and more compact pellets (Metz and Kossen, 1977), since the hyphae becomes shorter, thicker and more branched (Van Suijdam and Metz, 1981a), while lower agitation favours the development of fluffy looser pellets (Metz and Kossen, 1977; Berovic *et al*., 1993). Pellets of approximately 1200 μm initial diameter were reduced to a final stable size of approximately 900 μm when agitation was greater or equal to 600 rpm ($u_t \geq 2.03$ m s^{-1}) (Casas-Lopez *et al*., 2005). Strong agitation can also cause the break-up of pellets (Metz and Kossen, 1977) since high agitation rates leads to high energy dissipation rates which is related to high shear stresses. Increased agitation leads to a decrease in the mean effective hyphal length (Van Suijdam and Metz, 1981a). Morrison and Righelato (1974) and Miles and Trinci (1983) showed that at a stirrer speed of 1000 rpm the length of the hyphal growth unit of *P. chrysogenum* decreases with an increase in the dilution rate. In contrast, when *P. chrysogenum* was grown in glucose-limited continuous culture, at a stirrer speed of 500 rpm, the hyphal growth unit length increased with an increase in dilution rate (Miles and Trinci, 1983), but at 1000 rpm it did not vary with dilution rate (van Suijdam and Metz, 1981a). Observations made by Petruccioli *et al*. (1995) under a light microscope did not show any mycelial difference with varying speed rates from 300 to 900 rpm. Agitation also influences the structure and survival of pellets once they have been formed since during mixing the mycelia in the dispersion zone around the impeller gets damaged more easily and the greater the movement of mycelia through this zone the greater the damage and the lower the productivity.

2.8 Rheology of fungal cultures

The performance of a bioreactor is influenced by the rheological properties of the microbial cultivation. These rheological properties greatly affect the fluid mixing, mass- and heat transport (Charles, 1978; Metz *et al*., 1979). This in turn influences the operating conditions, and thus growth, morphology and product formation (Olsvik and Kristiansen, 1994). It therefore has an important influence on product yields. During the course of a cultivation, the rheological characteristics of the culture often become more complex, due to the increased biomass, accumulation of high-molecular-weight products or both (Manchanda *et al*., 1982). A reasonable understanding of the rheology of the cultivation is therefore of great importance for the design, scale-up and operation of bioreactors.

The rheological properties of microbial cultures are determined by the biomass concentration, the growth rate and morphology (Metz and Kossen, 1977; Charles, 1978; Metz *et al*., 1979; Olsvik and Kristiansen, 1994; Doran, 1999). The morphology is in turn affected by factors such as the geometry of the hyphae (length, diameter, and branching frequency), hyphal flexibility and hyphal-hyphal interaction (Olsvik and Kristiansen, 1994).

2.8.1 Definitions and rheogram

Rheology is the science of deformation and flow of fluids. A fluid is a substance which undergoes continuous deformation when subjected to a shearing force. When a force is applied to a fluid, it normally flows; the viscosity of the fluid is its resistance to motion and can be represented as

$$\tau = -\eta \frac{dv}{dy} \qquad \textbf{(2.13)}$$

where τ is the force per unit area, known as shear stress [Pa], η is the viscosity [Pa s], dv/dy is the velocity gradient, known as shear rate [s^{-1}] and is denoted by the symbol $\dot{\gamma}$. Equation 2.13 is known as Newton's law of viscosity.

The generalised relationship between shear stress and shear rate for a fluid is given by Equation 2.14.

$$\tau = \tau_0 + K\left(\dot{\gamma}\right)^n \qquad \textbf{(2.14)}$$

where τ is the shear stress applied on the fluid [Pa]; τ_0 is the yield stress [Pa]; $\dot{\gamma}$ is the shear rate [s^{-1}]; K is the consistency index [Pa s^n] and n is the dimensionless flow index.

Fluids can be classified as Newtonian or non-Newtonian. Equation 2.14 can be reduced to several forms depending on the values of τ_0 and n. In Table 2.9 the fluids are classified according to their rheological behaviour and Figure 2.9 depicts the flow curves (rheogram) of these fluids. The viscosity of Newtonian fluids is independent of the shear rate and is sometimes called the dynamic viscosity (η). This is not the case for non-Newtonian fluids, as the viscosity is dependent on the shear rate applied to the fluid and is defined as apparent viscosity (η_{app}). It is therefore meaningless to specify the apparent viscosity of a non-Newtonian fluid without noting the shear stress or shear rate at which it was measured (Doran, 1999). Common types of non-Newtonian fluids include pseudoplastic, dilatant, Bingham plastic and Casson plastic. Bingham and Casson plastics fluids do not produce motion until a yield stress has been applied (τ_0). For a Bingham plastic fluid when the yield stress is exceeded and flow is initiated, the Bingham fluid behaves like a Newtonian fluid. For Casson fluids, as soon as the yield stress has been exceeded the fluid shows pseudoplastic behaviour (Doran, 1999). In this literature review time-dependent and visco-elastic fluids are not covered.

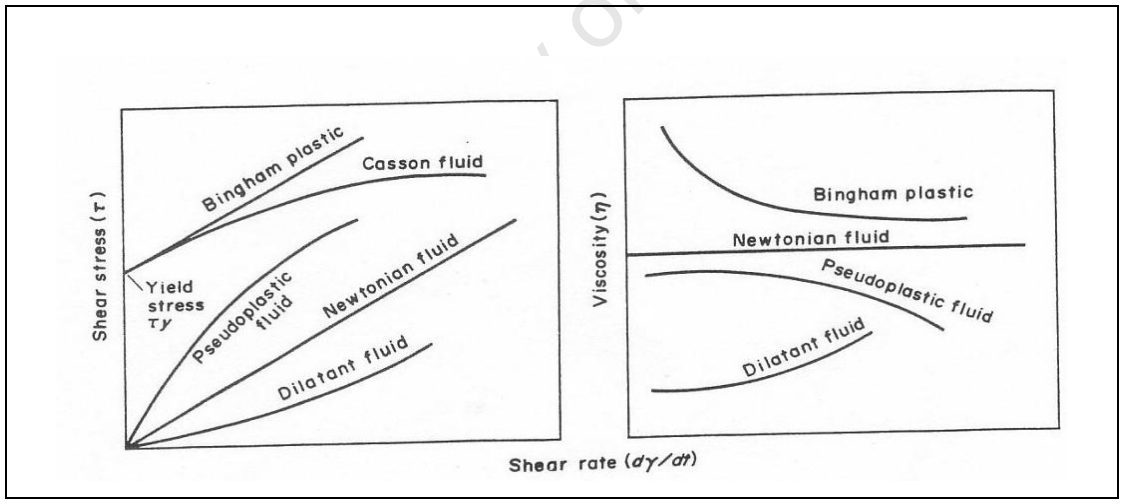

Figure 2.9 Rheogram of typical Newtonian and non-Newtonian fluids (Moo-Young, 1985)

In a bioreactor both agitation and aeration influence the mixing of the culture. Adequate mixing ensures that all the cells are in contact with oxygen and nutrients in the liquid phase and that there are no stagnant regions in the bioreactor. Increasing agitation enhances mixing and mass transfer, but may have a detrimental effect on the cells which lead to cell damage and cell death. The shear rate in a stirred tank reactor varies from very high values close to the impeller to low values near the wall of the reactor (Van Suijdam and Metz, 1981b; Atkinson and Mavituna, 1991).

Table 2.9 Classification of fluids according to their rheological behaviour. (Atkinson B. and Mavituna F., 1991; Doran, 1999)

Fluid	Equation	Apparent viscosity, ($\eta_{app} = \tau\,\gamma^{-1}$)	Examples
Newtonian	$\tau = \eta\gamma$ n= 1 $\tau_0 = 0$	Constant $\eta_{app} = \eta$	All gases, water, dispersions of gases in water, low molecular weight liquids, aqueous solutions of low molecular weight components
Non-Newtonian Pseudoplastic (power law) shear thinning	$\tau = K\gamma^n$ n < 1 $\tau_0 = 0$	Decreases with increasing shear rate $\eta_{app} = K\gamma^{n-1}$	Rubber solutions, adhesives, polymer solutions, some melts, some greases, starch suspensions, cellulose acetate, mayonnaise, some soap and detergent slurries, some paper pulps, paints, biological fluids
Dilatant (power law) shear thickening	$\tau = K\gamma^n$ n > 1 $\tau_0 = 0$	Increases with increasing shear rate $\eta_{app} = K\gamma^{n-1}$	Some cornflour and sugar solutions, starch, quicksand, wet beach sand, iron powder dispersed in low viscosity liquids
Bingham plastic	$\tau = \tau_0 + K_p\gamma$ n = 1 $\tau_0 > 0$	Decreases with increasing shear rate when yield stress τ_0 is exceeded $\eta_{app} = \frac{\tau_0}{\gamma} + K_p$	Some plastic melts, margarine, cooking fats, some greases, chocolate mixtures, toothpaste, some soap and detergent slurries, some paper pulps
Casson plastic (Combination of Bingham plastic and Pseudoplastic)	$\tau^{\frac{1}{2}} = \tau_0^{\frac{1}{2}} + K_p\gamma^{\frac{1}{2}}$	Decreases with increasing shear rate when yield stress τ_0 is exceeded $\eta_{app} = \left[\left(\frac{\tau_0}{\gamma}\right)^{\frac{1}{2}} + K_p\right]^2$	Blood, tomato ketchup, orange juice, melted chocolate, printing ink

It is therefore difficult to define an average shear rate in the culture and the subsequent viscosity, especially for non-Newtonian fluids. The relationship developed by Metzer and Otto (1957) between the impeller speed and the average shear in a stirred tank for Newtonian fluids is given in Equation 2.15

$$\gamma_{av} = k'N \quad \textbf{(2.15)}$$

where k' is a constant independent of the rheological characteristics of the fluid, but dependent on the impeller geometry (Table 2.10); N is the impeller speed [rev min^{-1}].

Table 2.10 Experimental values of K for pseudoplastic fluids (Margaritis and Zajic, 1978)

Impeller system	k'
Curved-blade paddle	7
Paddle	10 – 13
Six-blade turbine	10 – 13
Propeller	10
Anchor	20 - 25
Helical ribbon	30

The power law model is commonly used to describe the rheological behaviour of filamentous cultures (Metz *et al*., 1979; Charles, 1978; Allen and Robinson, 1990; Olsvik and Kristiansen 1994; Goudar *et al*., 1999; Pedersen *et al*., 1993). Others authors have described the rheological properties of filamentous cultures as Bingham (Allen and Robinson, 1990; Metz *et al*., 1979) or Casson (Allen and Robinson, 1990; Metz *et al*., 1979; Roels *et al*., 1974). Both the Bingham and Casson models include yield stress but the Casson model is a better fit at low shear rates than the Bingham model (Metz *et al*., 1979; Roels *et al*., 1974). The Herschel-Bulkley model, which combines the power law with a yield stress ($\tau = \tau_0 + K_p \gamma$), is sometimes used.

The rheological correlations for *A. niger* and *P. chrysogenum* cultures are given in Table 2.11. The parameters used in these rheological characterisation are defined as follows: K is the consistency index [N s^n m^{-1}], K_c is the Casson viscosity [N s $m^{-2}]^{1/2}$, X is the biomass concentration [g l^{-1}], d_p is the diameter of the mycelial aggregate [m], n is the flow behaviour index [-], L_{hgu} is the hyphal growth unit length [m tip^{-1}], RF is the roughness of mycelial aggregates [-], C_{om} is the compactness of the mycelial aggregate [-], τ_0 yield stress [N m^{-2}], and η_p is the plastic viscosity [Pa s^{-1}]. The rheological parameters (RP) (Metz *et al*., 1973) used in Table 2.11 to correlate the rheological properties with the suspension properties typically include the various consistency indices (K, K_p, K_c), or yield stress (τ_0) in the form of:

$$RP = constant\,(X)^{\alpha}\left(L_{e+}\right)^{\beta}\left(L_{hgu}\right)^{\gamma} \quad \textbf{(2.16)}$$

$$RP = constant\,(X)^{\alpha}\left(RF\right)^{\beta}\left(compactness\right)^{\gamma} \quad \textbf{(2.17)}$$

Table 2.11 Rheological correlations for *A. niger* and *P. chrysogenum* cultures (Heydarian *et al*., 1999)

Microorganism	Rheological model	Variation of theological parameters [a]	Shear range (s^{-1})	Viscometer	Comments	References
A. niger (dispersed mycelia)	Power law	$K = 0.308\ X^{3.15}\ d_p^{0.229}$ $n = 0.559\ X^{-0.058} d_p^{-0.082}$	30 – 200	Pipe flow	$2.3 < X < 11.2$	Fatile, 1985
A. niger (dispersed mycelia)	Power law Bingham Casson	$K = 4.3 \times 10^{-4} X^{3.3}$ $\tau_0 = 0.02X^{2.3}$ $K_c = 0.048X^{0.26}$ $\tau_0 = 2.5\times 10^{-3} X^3$	50 – 650 for all three models	Coaxial cylinder	Power law was preferred; morphology changes were not considered	Allen and Robinson, 1990
P. chrysogenum (dispersed mycelia)	Casson	$\tau_0\ \alpha\ X^{2.5}$ $K_c = 1.4 \times 10^{-3}\ XL_{hgu}^{0.6}$	-	Turbine impeller	Flexibility can affect rheology	Metz *et al*., 1979
P. chrysogenum (dispersed mycelia)	Power law Bingham Casson	$K = 3.6 \times 10^{-3} X^{2.5}$ $\tau_0 = 0.043X^{2.1}$ $\eta_p = 2.2 \times 10^{-3} X^{0.78}$ $\tau_0 = 8.3 \times 10^{-3} X^{2.5}$ $K_c = 0.047X^{0.19}$	50 – 650 for all three models	Coaxial cylinder	Morphology changes not considered; power law was preferred	Allen and Robinson, 1990
P. chrysogenum (dispersed mycelia)	Herschel-Bulkley Casson	$K = aX^{2.8}RF^{0.7}C_{om}^{1.2}$ $1\text{-}n = bX^{0.7}RF^{0.6}C_{om}^{0.9}$ $\tau_0 = cX^{3.2}RF^{0.6}C_{om}^{1.5}$ $\tau_0 = eX^{2.9}RF^{0.6}C_{om}^{1.0}$ $Kc = fX^{1.2}RF^{0.1}C_{om}^{1.0}$	3.5 - 75.8 for both models	Turbine impeller	Morphological measurement was for clump, which is more than 90% of total	Olsvik *et al*., 1993
P. chrysogenum (dispersed mycelia)	Casson	$\tau_0 = aX^2$	-	Turbine impeller	-	Roels *et al*., 1974

[a] a, b, c, d, e and f are constant parameters

The rheological properties of filamentous cultures change from Newtonian to non-Newtonian as the growth rate increases and products are formed (Roels *et al*., 1974). The rheology of yeast cultures below 10% solids and dilute filamentous cultures is usually Newtonian (Doran, 1999). As mentioned in Section 2.7 the filamentous growth forms of fungal suspensions can be divided into the mycelial and the pellet form. *Penicillium* is a mycelial culture which possesses viscous non-Newtonian rheological properties. *Aspergillus*, however, grows in a pelleted form resulting in a culture which is usually less, viscous and tends to follow Newtonian behaviour. However, limitations in mass transfer of medium components into (and out of) the pellet as well as intraparticle transport are typical (Nielsen and Villadsen, 1994; Olsvik and Kristiansen, 1994). Figure 2.10 illustrates the effect of the different morphological forms on the rheological properties of filamentous fungi (Kim *et al*., 1983). The pelleted form is more closely Newtonian in behaviour than the filamentous form, with the consistency index, n, for pellets closer to unity. The consistency index, and therefore the apparent viscosity, can differ by several orders of magnitude depending on cell morphology (Moo-Young, 1985).

Figure 2.10 The effect of different morphological forms on the rheological properties of filamentous fungi (Kim *et al*., 1983)

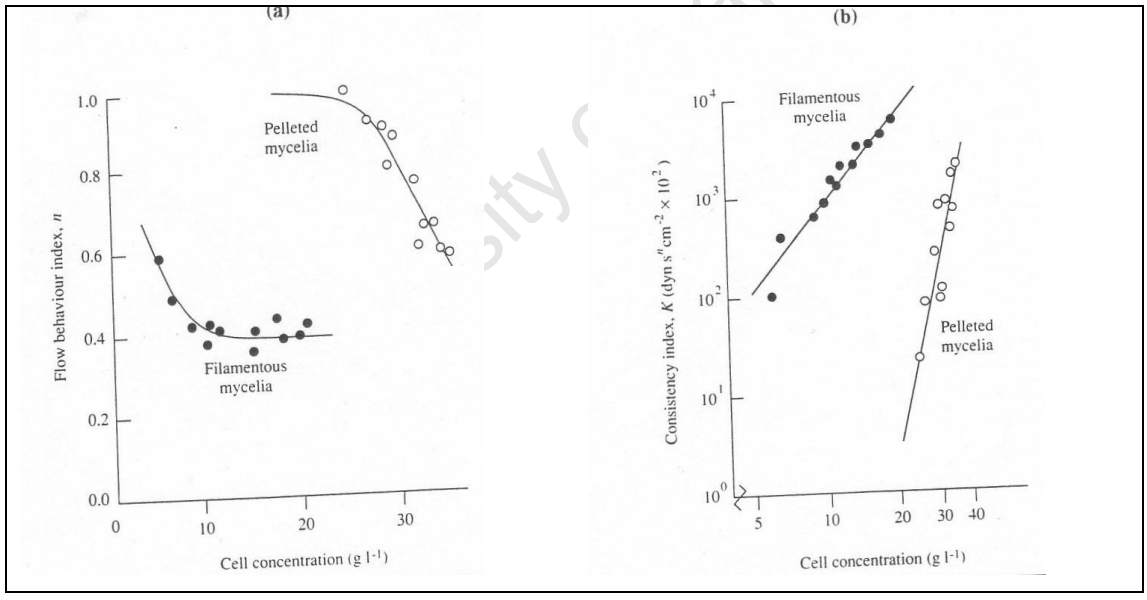

The rheological properties of a fungal culture affect the turbulence characteristics of the fluid such as mixing, heat and mass transfer processes (Metz *et al*., 1979). This in turn influences the operating conditions and thus affect growth, morphology and product formation (Olsvik and Kristiansen, 1994). For shear thinning systems (n<1), low viscosities results in regions of high shear rate (near the impeller) and very high viscosities in region with low shear rate (near the wall) in the reactor. Only a small part of the bioreactor, around the impeller, is maintained at the optimal condition. Increasing the agitation rate improves the overall homogeneity, but raises the

power consumption and may damages the cells due to the high shearing (Van Suijdam and Metz, 1981a). On the other hand, in the pellt form, the viscosity of the cultivation is typically lower and the rheological properties Newtonian. The Newtonian fluid is characterised by good bulk phase mass and heat transfer properties. Moreover, the pellet formation facilitates the separation of fluid in downstream processes (Van Suijdam *et al.* 1981a) and is an attractive growth form for cultivation of fungi.

The rheological properties of microbial cultures are determined by the biomass concentration, the growth rate and morphology (Metz and Kossen, 1977; Charles, 1978; Metz *et al*., 1979; Olsvik and Kristiansen, 1994; Doran, 1999). The morphology is in turn affected by factors such as the geometry of the hyphae (length, diameter, and branching frequency), hyphal flexibility and hyphal-hyphal interaction (Olsvik and Kristiansen, 1994).

2.8.2 Effect of biomass concentration on fungal rheology

Generally, an increase in biomass concentration leads to high viscosity. Typical correlations between biomass concentration and viscosity (or shear stress) has been proposed by several authors (Table 2.11). Allen and Robinson (1990) showed that the correlation of the consistency index, K with biomass concentration, X to be dependent on the type of strain used, and thus on mycelial morphology.

The flow behaviour index, n and flow consistency index K of a *P. chrysogenum* suspension are given in Table 2.12. Pedersen *et al*. (1993) also found n to decrease with increasing biomass concentration and reached a final level between 0.4 and 0.5 for biomass concentrations higher than between 10 and 15 g kg^{-1}. Literature data on filamentous fungi illustrates that the consistency index, K vary with biomass concentration to the power of 2 to 4 and that the flow behaviour index, n decrease from 1 to a value between 0.2 and 0.4 with an increase in biomass concentration (Allen and Robinson, 1990)

Table 2.12 Biomass concentration, flow behaviour index and consistency index for a *P. chrysogenum* suspension (Mukataka, *et al*., 1980)

X (g l^{-1})	n (-)	K (g cm sec^{n-2})
9.1	0.37	30.2
8.0	0.37	21.7
7.1	0.40	16.1
6.1	0.43	10.4
4.5	0.50	6.7

2.8.3 Effect of fungal morphology on fungal rheology

The rheological properties of the cultivation medium are closely related to the various changes in the morphology of the micro-organism (Charles 1978; Packer and Thomas, 1990; Riley et al., 2000). Morphology is also influenced by a number of process variables which can be controlled to a certain extent in most microbial cultivation processes, such as growth rate, medium composition, oxygen tension, and shear stress (Van Suijdam and Metz, 1981a).

Roels *et al* (1974) have found that the Casson equation was superior to the power law and Bingham plastic equation for two different strains of *P. chrysogenum*. They also found that its viscosity was higher when the cells were growing as filaments instead of as pellets.

Metz *et al*. (1979) found quantitative relationships between the size and shape of filamentous suspensions of two strains of *P. chrysogenum* grown in batch culture, and steady shear viscosity measurements of these suspensions:

$$\tau_c = 1.67 \times 10^{-4} C_m^{2.5} (L_e^+)^{0.8} \quad \textbf{(2.18)}$$

$$K_c = 5.454 \times 10^{-3} C_m^{1.0} (L_{hgu})^{0.6} \quad \textbf{(2.19)}$$

where τ_c is the Casson yield stress [N m^{-2}], K_c is the Casson constant [$N^{1/2}$ $s^{1/2}$ m^{-1}] C_m is the biomass concentration [kg m^{-3}], L_e^+ is the effective hyphal length [-], and L_{hgu} is the hyphal growth unit [m tip^{-1}].

The extend of branching of hyphal cells can also affect rheology. Cultures of sparsely branched mycelia (mycelial morphology) are more viscous than cultures of highly branched mycelia (pelleted morphology). Metz *et al*. (1979) hypothesised that branching frequency affected hyphal flexibility. The changes in the flexibility of the hyphae may be due to changes in cell wall composition, changes in branching pattern or diameter of the hyphae, or variations in osmotic pressure (Metz *et al*., 1979). Pace (1980) found that suspensions containing short mycelia, compared with those containing long mycelia, typically show lower apparent viscosities. Olsvik and Kristiansen (1992) found that the effects of the growth rate on the rheological properties of the culture depend on the dissolved oxygen concentration.

2.8.4 Effect of growth rate on fungal rheology

Van Suijdam *et al*. (1981a) showed that, for a *P. chrysogenum* culture, the hyphal length increased with increased growth rate, an increase in hyphal length typically lead to increased viscosity. It was also shown that the higher the n index, the shorter the mean hyphal length (Olsvik and Kristiansen, 1992). It was shown that the "morphology-index", K/x increased with the biomass, which implied that the influence of the biomass concentration on broth viscosity increased as the biomass concentration increased. It should be mentioned that for these relationships 90% of the hyphae existed in small clumps and any relationships between hyphal geometry of freely dispersed hyphae and rheological parameters may thus not be reliable (Olsvik and Kristiansen, 1994). Morphological studies by Pace (1980) showed that the mean hyphal length increased with the biomass concentration, although n was constant, thus indicating no relationship between n and hyphal length. Johansen *et al.* (1998) found that a threefold increase in hyphal length increased the apparent viscosity of the broth by a factor of seven.

Further literature suggests that the growth phase of the micro-organism may influence both the rheology and enzyme location (Olsvik and Kristiansen, 1992; Zeletaki and Vas 1968). An increase in growth rate also leads to an increase in apical tips (Chang and Trevithick, 1974) which has been associated with an increased extracellular enzyme location. Both the rheology and location have been associated with specific morphological characteristics namely; an increase in hyphal length has been corresponded to an increase in viscosity (van Suijdam and Metz, 1981a) and an increase in apical tips with an increase in extracellular enzyme location (Chang and Trevithick, 1974).

2.9 Protein secretion, transport and diffusion

2.9.1 Protein secretion

Protein secretion in filamentous fungi is postulated to occur at the hyphal tip (Wessels 1990; Wösten *et al*., 1991). Chang and Trevich (1974) hypothesised that enzymes are excreted by the apical tips of the organism and, during transit from the intracellular location to the extracellular region, are trapped in the cell wall (Figure 2.11). The accumulation of secreted proteins at the hyphal tips supports this hypothesis (Chang and Trevithick, 1970; Wösten *et al*., 1991; Gordon *et al*., 2000; Amunallah *et al*., 2002) and that secretion is dependent on the number of actively growing hyphal tips (Amunallah *et al*., 2002). Wösten *et al*. (1991) used immunochemical techniques to demonstrate that glucoamylase secretion in *A. niger* occurred predominantly at the

tips of the growing hyphae. Fluorescence experiments conducted by Gordon *et al*. (2000) revealed that the expression of GLA::sGFP (glucoamylase::green fluorescent protein fusion) resulted in fluorescence that was localised in the hyphal cell walls and septa, and that it was the most intense at the hyphal apices.

The relationship between fungal morphology and protein secretion is illustrated in Figure 2.12 for an extracellular protease and shows that the pelleted form of growth is associated with significantly lower protease secretion levels into the bulk medium than that of the filamentous growth form (Papagianni and Moo-Young, 2002).

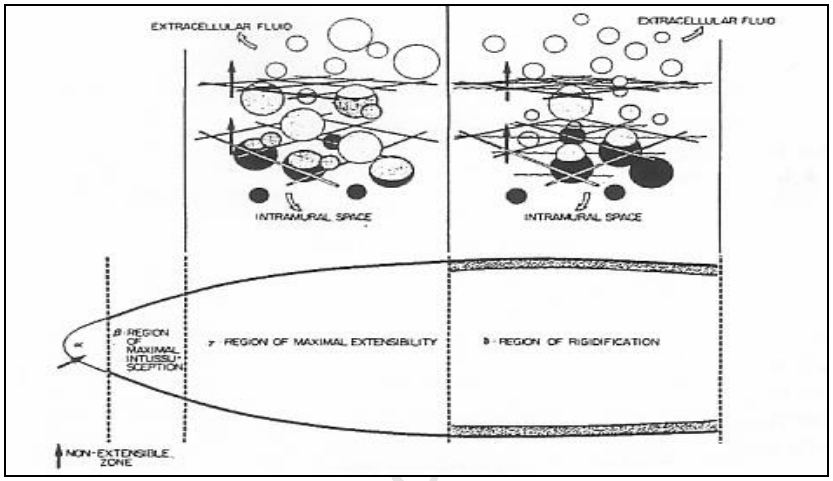

Figure 2.11 Excretion of proteins through a fungal cell wall (sourced from Chang and Trevich, 1974)

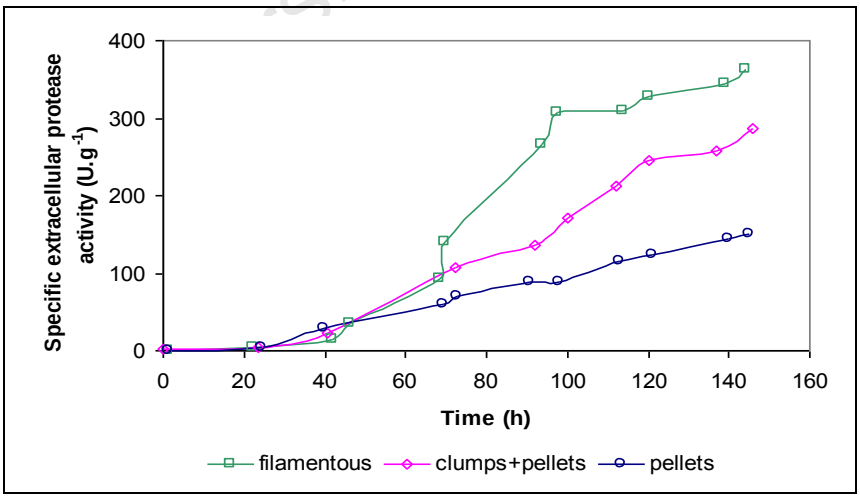

Figure 2.12 The effect of *A. niger* growth form on specific extracellular protease activities in bioreactor cultures (adapted from Papagianni and Moo-Young, 2002)

Since the knowledge of fungal secretion pathways is still limited, the better known secretion pathways in yeast and higher eukaryotes are used to explain a fungal secretion pathway (Conesa *et*

al., 2001; Pederby, 1994). In this hypothetical protein secretory pathway in filamentous fungi (Figure 2.13), proteins are produced and then transferred to the lumen of the endoplastic reticulum (ER) where the post-translational processes such as protein folding, glycosylation, disulfide bridge formation, and phosphorylation begin (Pederby, 1994). With the exception of membrane proteins, the majority of proteins secreted by filamentous fungi are glycosylated. It is proposed that the proteins are secreted as fast as they are synthesized i.e. equivalent to constitutive secretion in mammalian cells. This early step in the secretory pathway can be a bottleneck in the secretion process, because partially folded structures (such as unglycosylated proteins) may remain in the ER for an extended time (Pluschkell *et al*., 1996). Vesicles on the ER lumen carry the protein molecules to a Golgi-like system. Finally, these vesicles transfer the proteins to the tip of the growing hyphae where they fuse with the plasma membrane and release their contents into the periplasmic space. There is also speculation concerning the possible involvement of vacuoles in the secretory pathway. Fungi appear to differ with respect to the location of enzymes after they are released at the surface of the plasma membrane. Casadevall *et al*. (2009) suggested that fungi use vesicular transport to deliver these enzymes from the periplasmic space across the cell wall into the external environment.

Since the fungal cell wall is the most important barrier encountered by these secreted proteins (Chang and Trevich, 1974; Pederby, 1994). Vainstein and Pederby (1991) studied the secretion of invertase by *A. niger* and *A. nidulans*. In *A. niger*, the distribution of the enzyme is 70% cell bound and 30% secreted, but in *A. nidulans*, the enzyme is distributed more equally. When the cell-wall of *A. nidulans* is removed, the level of secretion of invertase increased to approximately 90%.

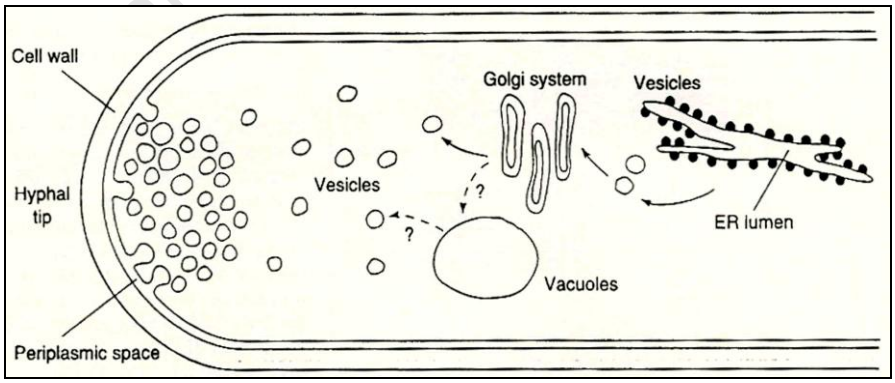

Figure 2.13 A secretory pathway in filamentous fungi (sourced from Pederby, 1994)

The cell wall is a structure that provides osmotic and physical protection to the cell from the environment and determines the shape of the cell (Klis *et al*., 2002). Cell walls that are newly synthesised have plastic or viscoelastic properties and respond to the internal turgor pressure

within the hyphae (Chang and Trevich, 1974). With time the cell walls become more rigid as a result of cross-linking of chitin microfibrils to a glucan matrix in the wall (Wessels, 1990) and become more resistant to the turgor forces. The turgor pressure which is generated within the hyphae acts as the driving force for hyphal extension (Robson, 1999). The growth of the hyphal cell wall involves the apposition of wall material (mainly polysaccharide polymers) from the inside to the outside of the wall (Wessels, 1993). At the apical tip, the wall polymers are plastic while from the subapical region to the extension zone (Figure 2.8) the wall polymers become more cross-linked which results in a very rigid structure that is assumed to be non-porous to large molecules. These observations led Wessels (1993) to propose a "bulk-flow" hypothesis to explain the passage of proteins through the cell wall.

The extensive studies of de Nobel *et al*. (1989, 1990a, b, 1991) and Klis *et al*. (1994, 2002, and 2006) on the yeast cell wall are used to explain the fungal cell wall. The composition and structure of the cell wall of *S. cerevisiae* (Klis, 1994) is illustrated in Figure 2.14. Typically the cell wall consists of two layers, the inner polysaccharide layer which provides mechanical strength, shape and elasticity to the wall and an outer protein layer which determines most of the surface properties of the cell and protects the inner layer from foreign molecules. The inner layer consists mainly of β1,3-glucan and β1,6-glucan which is complexed with chitin while the outer layer consists of glycosylated mannoproteins (Klis, 2002). The majority of the mannoproteins are covalently linked to the inner glucan layer (Klis, 1994). Fungal cell walls contain α-glucan and high levels of chitin whereas yeast cells have no α-glucan and lower levels of chitin (Klis, 2006). Analyses of cell wall components of *Aspergillus* have shown that the fungal cell walls are composed of β-1,3-glucan, β-1,6-glucan, linear β-1,3/1,4-glucan, chitin and mannoproteins (Fontaine *et al*., 2000).

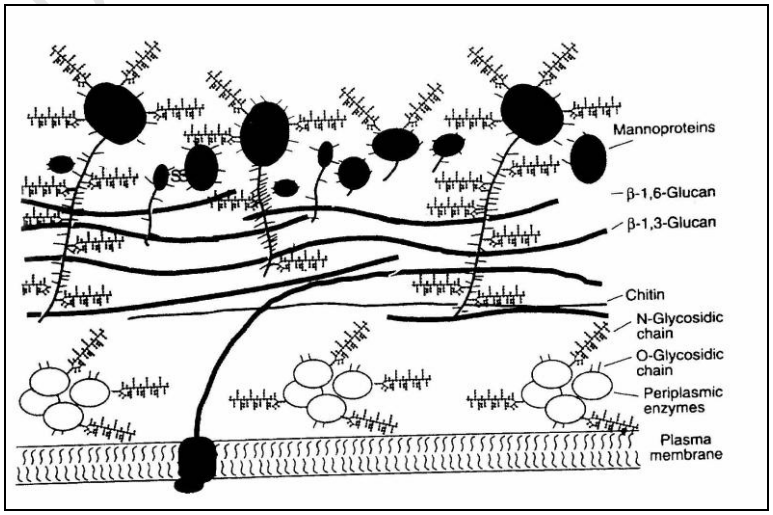

Figure 2.14 Composition and structure of the cell wall of *S. cerevisiae* (sourced from Klis, 1994)

It is now recognised that the mannoproteins play an important role in the permeability of the cell wall (Zlotnik *et al*. 1984; De Nobel *et al*. 1990b). The external mannoprotein layer determines the cell wall porosity (Zlotnik *et al*. 1984; De Nobel *et al*. 1989, 1990b, 1991) and the disulfide bridges between the mannoproteins affect the cell wall porosity (De Nobel *et al*. 1990b). The extent to which a protein is passed through the cell wall depends on the pore size of the cell wall, the characteristics of the secreted protein including the molecular weight, the amount of glycolsylation and the charge (De Nobel *et al*., 1989). Stationary phase yeast cells have a considerably higher turgor pressure compared to exponential phase cells. Due to increased levels of trehalose, the cell wall becomes thicker. The stationary phase cell walls are more resistant to β1,3-glucanase digestion and showed a considerable reduction in cell wall porosity compared with exponentially growing cells (De Nobel *et al*., 1990b). The number of disulfide bridges in the wall increases 6 to 7 fold in the stationary phase (De Nobel *et al*., 1990b). De Nobel *et al*., (1991) further showed cyclic variation in the permeability of the cell wall Cell wall porosity also depends on a number of factors that can be manipulated externally. These include growth medium composition, local oxygen concentration, cell turgor, growth phase (De Nobel and Barnett, 1991), temperature variation kinetics, osmotic pressure variation kinetics (Gervais and Martinez de Maranon, 1995), pH of the suspending medium (Shaeiwitz *et al*., 1989), among others. Also, the treatment of yeast cells with chemicals such as dithiothreitol has been shown to increase cell wall porosity (De Nobel *et al*., 1989). Cell wall degrading β-1,3-glucanase has been used successfully to manipulate the porosity of the yeast cell wall thereby improving the selective release and recovery of homologous proteins in yeast (Asenjo *et al*., 1993; Shen *et al*., 1989).

The ability of filamentous fungi to secrete large amounts of homologous (native) enzymes and proteins into the culture medium makes them attractive hosts for heterologous (non-fungal) enzyme and protein production (Torralba *et al*., 1998, Gouka *et al*., 1997). Concentrations of secreted homologous proteins are usually large e.g. 30 g l^{-1} cellulase from *Trichoderma reesei* and 20 g l^{-1} glucoamylase from *Aspergillus nige*r (Pederby, 1994), compared to heterologous proteins which have improved from the mg l^{-1} range (Gouka *et al*., 1997) to the g l^{-1} range (Nevalainen *et al*., 2005). Due to the lower production levels encountered in heterologous protein production, research started to focus on the genetics and molecular biology of protein secretion in filamentous fungi with focus on genetic modification of the secretion pathway such as signal sequence, translational fusions, transcriptional regulations, translational fusions, glycosylation and modifying the levels of chaperones to improve heterologous protein production. Recent research also focussed on metabolic engineering of the glycosylation pathway in fungi due to the interdependencies between glycosylation, protein production, secretion and activity (Deshpande et al., 2008; Shoji et al., 2008; Nevalainen K.M.H et al., 2005; Punt et al., 2002; Conesa et al., 2001; Archer 2000; Gordon et al., 2000; Archer and Pederby, 1997; MacKenzie et al., 1993).

2.9.2 Protein transport and diffusion

The transport of molecules through membranes can be against the concentration gradient, i.e. moving from a lower to higher concentration, where active transport occurs, which requires the expenditure of energy as ATP.

Diffusion, on the other hand, is the transport of molecules through the membranes from a high to a lower concentration and is controlled according to Fick's Law of diffusion (Equation 2.20). In Equation 2.20 the mass flux of species A (J_A, gmol s^{-1} m^{-2}) is for unidirectional steady-state diffusion in a stagnant medium where the mass flux is proportional to the concentration gradient:

$$J_A = -\mathrm{D_A}\frac{dC_A}{dy_d} = \frac{N_A}{a_{MT}} \qquad \textbf{(2.20)}$$

where N_A is the rate of mass transfer of component A [gmol s^{-1}], a_{MT} is the area across which mass transfer occurs [m^2], D_A is the diffusion coefficient of component A [m^2 s^{-1}], C_A is the concentration of component A [gmol m^{-3}] and y_d is the distance [m].

Tyn and Gusek (1990) carried out a study whereby the diffusion coefficients of proteins (at infinite dilution in water) were predicted using several correlations (Table 2.13). The hydrodynamic radius in the Einstein-Stokes equation is that of a hydrated molecule since enzymes can not be classified as hard spheres because they are non-spherical, dynamic, and solvated in solution. The hard sphere radius is therefore changed to the hydrodynamic radius or the radius of gyration to account for the size and the shape of the protein. The radius of gyration is related to the hydrodynamic radius by the expression $R_g = 1/\xi\ R_h$ where ξ is a constant which presumably depends on the configuration of the protein molecule (Tyn and Gusek., 1990). The hydrodynamic radius R_h (cm) can be calculated using Equation 2.21 (Armstrong *et al*., 2004):

$$R_h = \left(\frac{3[\eta]M_w}{10\pi N_A}\right)^{1/3} \qquad \textbf{(2.21)}$$

where [η] is the intrinsic viscosity [ml g^{-1}], M_w is the molecular weight [g mol^{-1}], N_A' is the Avogadro's number which is 6.02 x 10^{23} mol^{-1}.

Table 2.13 Proposed correlations to estimate protein diffusion coefficients D (adapted from Tyn and Gusek., 1990)

Correlation	Principle	Equation
Stokes-Einstein Equation	Relates the diffusivity (D) of a rigid spherical protein in dilute aqueous solvent where k is the Boltzman constant and has a value of 1.38066 x 10^{-23} J K^{-1}, R_a Stokes-Einstein radius of the protein and η is the solvent viscosity.	$D = \frac{kT}{6\pi\eta R_a}$ **(2.22)**
Polson Method (1)	Use the molecular weight of protein to determine the diffusivity. A' is a constant and has a value of 2.85 x 10^{-5} cm^2 s^{-1} $g^{1/3}$ $mol^{-1/3}$.	$D = \frac{A'}{\sqrt[3]{M_w}}$ **(2.23)**
Polson Method (2)	Use the molecular weight of protein as well as the intrinsic viscosity to determine the diffusivity. B' is a constant and has a value of 4.185 x 10^{-5} cm^3 s^{-1} $mol^{1/3}$.	$D = \frac{B'}{\sqrt[3]{M_w[\eta]}}$ **(2.24)**
Modified Stokes-Einstein Equation	Use an equivalent hydrodynamic radius (R_e) or radius of gyration (R_g) instead of a rigid sphere. where $R_e = \xi R_g$	$D = \frac{kT}{6\pi\eta\xi R_g}$ **(2.25)**
Correlation of Tyn and Gusek (1990)	Inverse correlation between diffusivity and the radius of gyration. The constant has the dimensions: cm^2 s^{-1} Å.	$D = \frac{1.69x10^{-5}}{R_g}$ **(2.26)**

2.10 Summary of literature findings

The production of GO by fungi has been investigated by various authors. Studies by these authors emphasise the different types of organisms (wild-type, mutant or recombinant), various carbon and nutrient sources as well as the influence of process conditions such as pH, aeration and agitation on the production of GO and its productivity.

GO is distributed in several locations throughout the fungal culture, namely extracellular, intrapellet (external to the cell but associated with the mucilage layer surrounding the hyphae) or, intracellular (either bound to the cell wall and membrane or in the cytoplasm of the fungal cell). Controversy exists in the literature over the location of GO in both *A.niger* and *Penicillium* sp.

The morphology of *A. niger* is pelleted and that of *Penicillium* sp. is mycelial. The morphology of the organism is important because it can influence the productivity, rheology, mass and heat transfer of a culture. Factors that can influence the morphology of the micro-organism are:

inoculum type and level, growth rate of the organism, media composition, dissolved oxygen and carbon dioxide, pH of the culture, temperature and agitation as well as the effect of shear stress.

Fungal rheology is affected by the biomass concentration, growth phase and fungal morphology which in turns affect the productivity of the cultivation. *A. niger*'s pelleted morphology exhibits non-viscous Newtonian behaviour while *Penicillium* sp. viscous non-Newtonian behaviour.

Protein secretion is hypothesed to occur at the hyphal tips. During growth the apical tips are postulated to become less porous which leads to its entrapment within the hyphal cell. From the information given in this literature study, the relationships between protein production, location, fungal morphology, protein secretion, transport and diffusion to the external environment remain incompletely described.

2.11 The focus of the current study

The present study aims to study the GO systems from *Aspergillus niger* NRRL-3 and *Penicillium* sp. CBS 120262 in terms of production of GO as well as the location of GO within these organisms. The location of GO is investigated under changing process conditions such as time of harvest and pH control agents on GO location in order to resolve the controversy in the literature on dominant location within the different fungal cell types. Characterisation of the distributed location within the cell will inform integration between the production phase and DSP. These multiple locations have an influence on the recovery of GO through its downstream recovery process, subsequent to its production. In turn, they are influenced by the production environment. An important factor to take into account with respect to the location of the enzyme is the fungal cell wall and its relation to protein secretion.

A novel technique was developed using image analysis software to study hyphal morphology and to relate it to GO secretion and transport. The rheology of *A. niger* and *Penicillium* sp. was investigated in terms of the biomass concentration, growth rate and morphology and compared with literature. The diffusion coefficient of GO was quantified using electron micrographs of *Aspergillus niger*. This study aims to identify factors influencing protein secretion in fungi using GO as a case study, in order to enhance enzyme recovery in the DSP.

2.11.1 Research hypotheses

In this thesis, the following three hypotheses are tested:

1. GO is found in several locations in fungi, namely in the envelope, supernatant, cytoplasm and gel layer surrounding cells. These locations and the quantitative split of GO across them is a function of micro-organism type, growth phase and growth conditions.

2. The location of GO plays a key role in its recovery in the downstream process; hence a structured approach to both the selection of the production system and the design of the downstream enzyme recovery process needs to take cognizance of the location in order to maximize yield.

3. The growth phase of the fungus influences both cell morphology and the location of GO. The growth phase and morphology plays a role in secretion of GO. The GO concentration gradient between the intracellular and the extracellular regions can be described as the driving force for secretion and the transport of GO out of the cell.

2.11.2 Key questions

In light of the current literature, the following key questions were developed and are addressed in the thesis:

1. Where is GO located in each organism nominated for GO production and what quantity of GO is in each fraction?
2. How does location of GO change with changing process conditions such as micro-organism used, growth rate and pH control agent?
3. How does the location of GO influence the downstream process used to recover and purify the enzyme?
4. How do the growth rate, GO location and morphology relate to one another?
5. What effect does the morphology have on the rheology of the fungal culture and consequently the attainable optimum process conditions?
6. How does the rheology influence the production of GO?
7. What is the relationship between morphology, secretion and transport of GO?

Chapter 3 Materials and methods

In this chapter the methodology for the cultivation of *A. niger* NRRL-3 and *Penicillium* sp. CBS 120262 are described in Section 3.1 and 3.2; and the subsequent analyses for cell dry weight (CDW), glucose concentration, gluconic acid (GA), glucose oxidase (GO) activity, morphology and viscosity are described in Section 3.3 and Appendix A. In Section 3.4 the methodology of volume corrections are described to account for base addition and sampling. The quantification of GO activity in the individual fractions are described in Section 3.5 and the qualitative determination of GO in *A. nige*r using immunocytochemical labelling in Section 3.6.

3.1 Culture conditions for *Aspergillus niger* NRRL-3 and *Penicillium* sp. CBS 120262

3.1.1 Microorganisms and culture maintenance

A. niger NRRL-3 and *Penicillium* sp. CBS 120262, the latter kindly supplied by the Council for Scientific and Industrial Research (CSIR, South Africa), were used throughout this study. *Penicillium* sp. CBS 120262 was isolated from a soil sample taken from the Northern Province of South Africa by the CSIR (Simpson *et al*., 2007). Cultures were maintained on Malt Extract Agar (MEA) for Yeast and Molds (MEAYM; Bacteriological Analytical Manual Online) between 4 and 6°C and sub-cultured every month. MEA contained the following per litre: malt extract (bacteriological) 20 g; glucose 20 g; peptone (bacteriological) 1 g; agar 20 g.

3.1.2 Inoculum and bioreactor medium

The media composition of Hellmuth *et al.* (1995) was used for the inoculum and bioreactor cultivations of *A. niger* (Table 3.1):

Table 3.1 Composition of *Aspergillus niger* inoculum and bioreactor medium (Hellmuth *et al*., 1995)

Chemical	Concentration ($g\ l^{-1}$)
Glucose	100
$NaNO_3$	3
Yeast Extract	2
KH_2PO_4	1
$MgSO_4.7H_2O$	0.5
KCl	0.5
$FeSO_4.7H_2O$	0.01
Sigma Antifoam 209	0.25 ml l^{-1}

For *Penicillium* sp., the inoculum medium (from CSIR) and bioreactor medium (Rogalski *et al*., 1988) are tabulated in Table 3.2 and Table 3.3 respectively.

Table 3.2 Inoculum medium for *Penicillium* sp. CBS 120262 (from CSIR)

Chemical	Concentration ($g\ l^{-1}$)
Glucose	10
Peptone	5
KH_2PO_4	1
$MgSO_4.7H_2O$	0.5
Agar	15

Figure 3.3 Bioreactor medium for *Penicillium* sp. CBS 120262 (Rogalski *et al*., 1988)

Chemical	Concentration ($g\ l^{-1}$)
Glucose	80
Peptone	30
$(NH_4)_2HPO_4$	0.388
KH_2PO_4	0.188
$MgSO_4.7H_2O$	0.156
Sigma Antifoam 209	0.25 ml l^{-1}

3.1.3 Inoculum development

3.1.3.1. *Aspergillus niger*

Spores from the MEA plate were suspended in a 1% peptone solution to a concentration of 5 x 10^7 spores ml^{-1} and 30 ml of the spore suspension was added to 600 ml of the inoculum medium (final spore concentration of 2.5 x 10^6 spores ml^{-1}). The 600 ml inoculum medium was prepared as follows: Glucose and $MgSO_4.7H_2O$ were autoclaved together while the other salts were autoclaved separately. Carbon (glucose) and nitrogen ($NaNO_3$ and yeast extract) sources were separated to prevent loss due to the Maillard reaction. The magnesium and phosphate sources were separated to minimise loss by reaction and precipitation (Pirt, 1975). The pH of the salts solution was adjusted to pH 6.2 with 0.2 ml 5M NaOH. After sterilisation, the contents of the two separate flasks were added together in a sterile 3-l Buchner conical flask. The flask inoculated with spore suspension was incubated at 30°C and 120 rpm until a pH of 5 had been reached (about 17 to 19 h) when it was used as the inoculum for the bioreactor at 10% (v/v).

3.1.3.2. *Penicillium* sp. CBS 120262

A 1000 ml inoculum medium (Table 3.2), excluding the agar, was prepared. A 250 ml aliquot of the inoculum medium (Table 3.2) was transferred to a wide bottom Erlenmeyer flask (capacity 2000 ml, height 155 mm, bottom diameter 195 mm, neck diameter 40 mm). Four flasks were used in total. Agar was added separately (3.75 g each) to the four flasks. The flasks were sterilised at 121°C for 20 min. Spores from the MEA plate were transferred to each of the wide bottom

Erlenmeyer flasks (with the solidified media) using a Nichrome wire (Three to five loops). The spores were harvested after seven days into 0.1% (v/v) sterile Tween-80 solution and collected into a 100 ml sterile Schott bottle. A 100 ml spore suspension containing 4 x 10^8 spores ml^{-1} was used as the inoculum for the bioreactor (1.7% (v/v)).

3.2 Experimental setup and reactor conditions

A 7.0-l Chemap laboratory bioreactor (supplied by Chemapec) with a 6-l working volume was used. The equipment layout for the batch experiments is shown in Figure 3.1. Agitation was achieved by 90 mm o.d., 20 x 20 mm 4 bladed Rushton turbines driven by a central base shaft. The temperature was controlled by appropriate cooling and heating of a 0.7 l min^{-1} water stream passing through two stainless steel heat transfer coils. The pH of the cultivation was monitored by a Mettler Toledo (Type 465-50-57) pH electrode which was connected to a UCT pH controller driving a UCT peristaltic dosing pump which controlled the pH. The base was drawn from a reservoir which was placed on a scale pan. Dissolved oxygen was monitored using a Mettler Toledo 4100 meter connected to a sterilisable Mettler Toledo InPro 6000 oxygen electrode. The air supply was passed through a rotameter and carbon filter before entering the reactor. The exhaust gases left the top of the bioreactor via a condenser cooled with tap water and through a carbon filter to avoid contaminating the laboratory with *A. niger* and *Penicillium* sp. spores and to provide a sterile barrier for the bioreactor. A steam-sterilised sample port at the base of the vessel enabled samples to be removed aseptically.

The base case conditions for *A. niger* and *Penicillium* sp. cultivations are provided in Table 3.4. During the cultivation the amount of base added to maintain a constant pH was noted. Samples were taken aseptically at discrete intervals and the sample volume was noted. The samples were analysed for CDW; reducing sugar; GA concentration and GO activity. GO activity was measured as extracellular (supernatant) activity and total (cell lysate) activity. A portion of the sample was used for morphology measurements. At the end of the cultivation the culture was harvested to determine the location of GO through fractionation experiments.

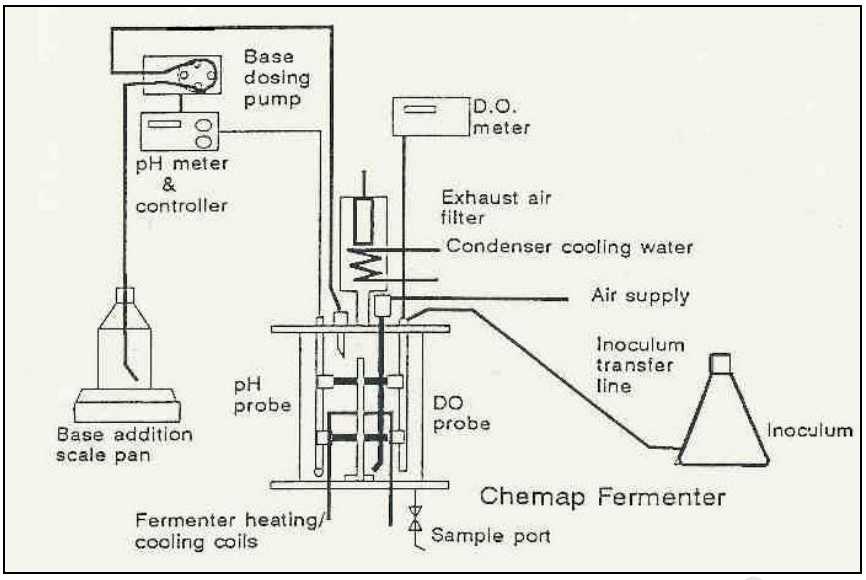

Figure 3.1 Equipment setup of laboratory bioreactor (sourced from Johnson, 1995)

Table 3.4 Base case condition for *A. niger* and *Penicillium* sp. cultivations

Organism	***Aspergillus niger* NRRL-3**	***Penicillium* sp. CBS 120262**
Temperature	30°C	28°C
pH	5.5	6.5
Aeration (0.21 atm O_2)	0.8 vvm	1.0 vvm
Agitation	500 rpm	300 – 600 rpm
pH control agent	5 M NaOH	5 M NaOH

3.3 Analytical techniques

The principles of the techniques, their detection limits and reproducibility are described in this section. The detailed methodology is presented in Appendix A.

3.3.1 Cell dry weight (CDW)

Centrifugation was found unable to separate the biomass from the suspension owing to small density difference and complex morphology. Filtration was therefore used as the preferred method of solid-liquid separation. CDW was determined gravimetrically by filtering a 20 ml sample through a pre-dried 0.45 µm Millipore filter and drying the sample to constant mass at 80°C in duplicate (Appendix A.1). The subsequent supernatant was used in various assays.

3.3.2 Reducing sugar

The glucose concentration was determined as reducing sugar in the supernatant using a modification of the standard dinitrosalicylic acid colorimetric method (Miller, 1959) according to the procedure set out in Appendix A.2. The method measures the presence of free carbonyl group (C=O) (which is also known as reducing sugars) and is based on the oxidation of the aldehyde functional group with simultaneous reduction of 3,5-dinitrosalicylic acid (DNS) to 3-amino,5-nitrosalicyclic acid under alkaline conditions. These reactions are presented below:

$$\text{aldehyde group} \xrightarrow{oxidation} \text{carboxyl group}$$

$$\text{3,5-dinitrosalicyclic acid} \xrightarrow{reduction} \text{3-amino, 5-nitrosalicyclic acid}$$

The assay was calibrated using a dilution series from 0.1 to 1.0 g l^{-1} glucose (standard curve). The absorbance of the solution was measured at 510 nm with a spectrophotometer. The glucose concentration was determined relative to the predetermined standard curve. The maximum coefficient of variance of the assay was less than 6%.

3.3.3 Gluconic acid (GA)

The GA concentration in the supernatant was measured by HPLC. A Waters Fast Fruit Juice Column (50 Å, 7µm, 7.8 x 150mm) was used with 0.01 M H_2SO_4 as the mobile phase at a flow rate of 1ml min^{-1} and a temperature of 50°C in conjunction with the UV detector at 210 nm. The assay was calibrated using a dilution series from 0.1 to 10 g l^{-1} D-Gluconic acid lactone solution (Appendix A.3). Gluconic acid had an average residence time of 5.20 ± 0.14 minutes. The GA concentration was determined relative to the predetermined standard curve. Maximum errors of 6.7% and 19% were determined with 25 and 10 µl injection volumes respectively.

3.3.4 Base addition

A 5 M NaOH and 3.4 M $Ca(OH)_2$ solution was used during batch cultivations to neutralise the GA produced during the conversion of glucose to GA. The base addition was monitored gravimetrically. Direct correlation was found between the base added and the amount of GA (measured by HPLC) produced (Figure 4.4 and Johnson, 1995). The conversion to GA ranged between 85 and 100% (Johnson, 1995).

3.3.5 Glucose oxidase (GO) activity

GO activity was measured by the oxygen utilisation method of Miura (1970) as modified by Johnson (1995) (Table 2.3 and Appendix A.4). The reaction mixture consisted of a 0.1 M phosphate, 0.5 M glucose buffer at pH 5.5. A YSI 5739 field dissolved oxygen electrode was used to measure the decrease in dissolved oxygen over 250 seconds and the activity related to the oxygen consumption rate in the presence of excess glucose. The oxygen consumption rate in the overall reaction under the controlled conditions refers to the equivalent glucose consumption rate and GA production rate. One unit (U) of GO activity was defined as the amount of enzyme that catalysed the oxidation of 1 µmol glucose in 1 min at pH 5.5 and 25°C. Following comparison with the different assay methods reported, this method was selected over the spectrophotometric ones (o-dianisdine and ABTS) because it could be used to measure the activity of GO both in solution (supernatant and cytoplasm) and in cell lysate suspensions, was inexpensive, and not subject to interferences under conditions used.

3.3.6 Morphology

3.3.6.1 Sample preparation

Samples from *A. niger* and *Penicillium* sp. cultures were mixed with an equal volume of a fixative immediately on sampling (Packer and Thomas, 1990) and stored at 4°C for later analysis. The fixative consisted of 13 ml 40% formaldehyde and 5 ml glacial acetic acid added to 200 ml 50% (w/v) ethanol. On analysis, samples were diluted with fixative to ensure that no overlapping of the hyphal elements occurred. A 0.8 ml aliquot of Lactophenol Tryphan Blue stain was added to 9.2 ml of the fixed and diluted sample to enhance visualisation (Packer and Thomas, 1990). A 20 µl drop of the diluted suspension was mounted on a microscope slide as a wet preparation. For *A. niger* samples, instead of a wet preparation, the slide was allowed to air dry and the excess dry fixative-stain solution was washed away with 70% ethanol to give a clear glass slide with stained pellets.

3.3.6.2 Image analysis

An Olympus BX 40 microscope was used to view the glass slides under bright field at various magnifications (100 to 400 times). Images of individual freely dispersed mycelia were captured using an Olympus U-TOV-5XC digital camera and saved as TIF files. Using image analysis software analySIS® (www. soft-imaging.net) the micrographs were converted from colour to an 8-bit grey scale image. Using automatic thresholding at a pre-set value (67 and 194 for *Penicillium* sp. and between 5 and 185 for *A. niger*), the image was converted into a binary image with the white hyphal strands being of interest. The threshold range represented the upper and lower limits

of the grey phase. Using the detect function, the white image was temporarily changed to a red image and the resulting image analysed, using the image analysis software analysis®, to determine the automatic values of 'minimum and maximum feret diameters', 'minimum diameter', 'shape factor', 'area' 'convex area', 'perimeter', 'max X' and 'max Y' as defined in Table 3.5.

Table 3.5 Definitions of morphological indices (as defined by analySIS® software) used in this study

Index	Diagram	Definition
Feret $_{min}$	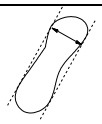	The minimum distance between parallel tangents at opposite particle borders
Feret $_{max}$	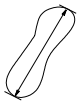	The maximum distance between parallel tangents at opposite particle borders
Diameter $_{min}$		The minimum diameter of a particle (for angles in the range 0° through 179° with step width 1°)
Shape factor	 0.5 0.8 1	Describes the "roundness" of a particle. A spherical particle has a shape factor of 1 and for other particles it is smaller than 1.
Area		The area of a particle is the product of the number of pixels of the particle and the calibration factor in X and Y direction
Convex area		The area of the convex cover of the particle
Perimeter		The sum of the pixel distances along the closed boundary
Max X	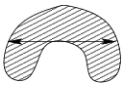	The maximum length of all horizontal distances contained within the particle
Max Y		The maximum length of all vertical distances contained within the particle

Towards the end of growth the older hyphae became vacuolated. To eliminate interference from vacuolation, the image processing routine was modified to reduce the "holes" representing vacuoles by using various filters. A sharpen filter was used to enhance the edges of the hyphae. After the binarising step various morphological filters, such as dilation and erosion, were used. The dilation filter was used to fill the holes by enlarging the white objects to make the hyphal

edges appear continuous. The erosion filter was used thereafter to subtract the extra thickness of the hyphae while still keeping the hyphae intact by reducing the white objects.

3.3.7 Viscosity measurements

Viscosity measurements were made off-line at room temperature using a Paar Physica MC1 rotational viscometer and the data was logged using US200 software (Paar Physica, Germany). Two measuring devices were used to determine the media, supernatant and culture viscosities. The concentric cylinder spindles Z1-DIN (DIN # 53453), also known as the double gap (gap width of 0.5 mm, sample volume of 17 ml, viscosity range between 0.001 Pa s to 1.30 Pa s) was used. The Z1-DIN is ideal for measuring the viscosity of media, supernatant and culture samples with low biomass concentration except when the mycelial size was greater than the 0.5 mm gap width. For samples where the large mycelia size (> 0.5 mm) caused error with the Z1-DIN spindle, the Z2-DIN spindle was preferred. This was also found for high biomass concentrations. The cup and bob, Z2-DIN (DIN # 53019) had a gap width of 1.9 mm, sample volume of 100 ml and a viscosity range of 0.02 Pa s to 15 Pa s.

3.4 Volume corrections

During the course of fungal growth, large samples (± 100 to 200 ml) were removed to measure the concentrations of reducing sugars, CDW, GA, total GO and extracellular GO as well as for morphology and viscosity analyses. By taking large samples, unconverted glucose was removed from the bioreactor preventing its subsequent conversion to CDW, GA and GO. This affected the apparent yield if not accounted for. As glucose was converted to GA, the pH decreased. Base was added automatically to maintain the pH at a constant value i.e. pH 5.5 and 6.5 for *A. niger* and *Penicillium* sp., respectively. This base addition diluted the culture. At a molarity of 5M NaOH, approximately 600 ml of base was added to maintain a constant pH through the batch cultivation due to the formation of GA. To account for the removal of glucose on sampling prior to conversion, removal of the biomass catalyst and dilution through pH control, volume corrections were made to the measured concentrations of glucose, CDW, GA and GO to enable an accurate determination of kinetics and yield data by including the effect of sample volume, sample frequency and base addition.

The volume correction system developed to account for the base addition and sampling is shown in Table 3.6. A spreadsheet example is given in Appendix D.1 and the statistics used to analyse the data in Appendix D.2. At each time interval when a sample was taken, the weight of the base

added and the sample volume taken was noted. The weight of the base was converted to volume added during the sampling interval using the specific gravity of a 5M NaOH solution as 1.2. The specific gravity of 3.4 M $Ca(OH)_2$ (25% $Ca(OH)_2$ was 1.164. Samples were taken directly after the addition of the basic solution. The measured data of batch cultures is shown in Appendix C.

Time has been uncoupled as after base addition (t_b) and after sampling (t_s). The initial volume ($V_{reactor,t0}$) of the batch cultivation was 6000 ml. The resultant reactor volume ($V_{reactor}$) was calculated by the addition of base (V_{NaOH}) (Eqn 3.1) and the subtraction of sample (V_{sample}) (Eqn 3.2). The measured glucose concentration (C_s) was modified to the corrected glucose concentration ($C_{s,actual}$) by taking into account the change in reactor volume, the amount of glucose removed from the reactor ($m_{s,out}$) on sampling, the amount of glucose remaining ($m_{s,remaining}$) in the reactor and the amount of glucose used ($m_{s,used}$) by the microorganism for the production of biomass, GA and GO (Eqns. 3.3 to 3.7).

$$V_{t_{1(i)}}^{reactor} = V_{t_0}^{reactor} + V_{t_{1(i)}}^{NaOH} - V_{t_0}^{sample} \quad \textbf{(3.1)}$$

$$V_{t_{1(i+1)}}^{reactor} = V_{t_{1(i)}}^{reactor} - V_{t_{1(i+1)}}^{sample} \quad \textbf{(3.2)}$$

$$m_{t_{1(i+1)}}^{s,out} = V_{t_{1(i+1)}}^{sample} \text{ x } C_{t_{1(i+1)}}^{s} \quad \textbf{(3.3)}$$

$$m_{t_{1(i)}}^{s,remaining} = V_{t_{1(i)}}^{reactor} \text{ x } C_{t_{1(i)}}^{s} \quad \textbf{(3.4)}$$

$$m_{t_{1(i+1)}}^{s,remaining} = m_{t_{1(i)}}^{s,remaining} - m_{t_{1(i+1)}}^{s,out} \quad \textbf{(3.5)}$$

$$m_{t_{1(i)}}^{s,used} = m_{t_0}^{s,remaining} - m_{t_{1(i)}}^{s,remaining} \quad \textbf{(3.6)}$$

$$C_{t1(i+1)}^{s,actual} = m_{t_{1(i+1)}}^{s,remaining} / V_{t_0}^{reactor} \quad \textbf{(3.7)}$$

To verify that the procedure was correct a mass balance was performed on glucose so that, glucose IN = glucose OUT + glucose USED + glucose REMAINING in reactor.

The same procedure was followed to calculate the corrected concentrations of the products CDW, GA and GO activities (total and extracellular).

Table 3.6 Procedure for calculating the corrected glucose concentrations using volume corrections

	Time (h)	Measured glucose ($g\ l^{-1}$)	Base added (ml)	Sample Volume (ml)	Reactor Volume (ml)	Glucose taken out of reactor (g)	Glucose remaining in reactor (g)	Glucose used (g)	Corrected glucose ($g\ l^{-1}$)
Initial	t_0	$C^s_{t_0}$	0	$V^{sample}_{t_0}$	$V^{reactor}_{t_0}$	$m^{s,out}_{t_0}$	$m^{s,remaining}_{t_0}$	$m^{s,used}_{t_0}$	$C^{s,actual}_{t_0}$
After base addition	$t_{1(i)}$	$C^s_{t_{1(i)}}$	$V^{NaOH}_{t_{1(i)}}$		$V^{reactor}_{t_{1(i)}}$		$m^{s,remaining}_{t_{1(i)}}$	$m^{s,used}_{t_{1(i)}}$	
After sampling	$t_{1(i+1)}$	$C^s_{t_{1(i+1)}}$		$V^{sample}_{t_{1(i+1)}}$	$V^{reactor}_{t_{1(i+1)}}$	$m^{s,out}_{t_{1(i+1)}}$	$m^{s,remaining}_{t_{1(i+1)}}$		$C^{s,actual}_{t_{1(i+1)}}$

The difference between the measured concentration (unmodified values) and corrected concentrations (modified values) for glucose, CDW, GA and GO was analysed using a one-tailed t-test at 95% confidence interval (null hypothesis that there is no difference). In a number of the runs the sample concentrations did not satisfy the null hypothesis and therefore it was decided to use the volume corrected values throughout to ensure uniformity in the subsequent calculations. The actual data used for subsequent calculations is shown in Appendix E.

3.5 Quantification of GO activity in the individual culture fractions

The distribution of GO activity through the fungal culture was determined by separation of the culture into the extracellular fraction and the fractions associated with the mycelia (slime mucilage, cell wall and cytoplasm), according to the procedure outlined below and shown in Figure 3.2, followed by an analysis of the activity (Section 3.3.5) in each of the fractions. The calculations used are detailed in Appendix B.

The total GO activity was determined from an analysis of the activity in the entire culture suspension following disruption of the mycelia with a French Press (2 passes at 20 MPa). Studies by Johnson, 1995 showed that 2 passes at 20 MPa was sufficient for complete disruption of the filaments.

The supernatant from another culture sample was separated by vacuum filtration through a 0.45 µm Millipore filter followed by washing of the mycelia with distilled water on the filter. The supernatant and wash water were combined for the analysis of the activity in the extracellular fluid. This provided quantification of the extracellular GO.

The washed mycelia were suspended in phosphate buffer at pH 5.5 and disrupted with a French Press as before. The disrupted suspension was filtered through a 0.45 µm Millipore filter to separate the cell wall and membrane fragments, from the liquid containing the cytoplasm and slime mucilage. The cell wall and membrane fragments were resuspended in phosphate buffer at pH 5.5 for the analysis of the activity in the cell debris fraction.

The slime mucilage was separated from the cytoplasm via ethanol precipitation, followed by recovery of the precipitate after centrifugation (12000g, 10 min, 4°C). The activity of the cytoplasm was determined from the liquid and the precipitate was dissolved in 0.1 M NaOH to obtain the activity in the slime mucilage.

The activity lost due to separation was calculated using a mass balance and the data were corrected to that which would be attained assuming complete recovery in each of the separation steps. The corrected data were used in the calculation of the percentage activity in each fraction (Appendix B.2).

3.6 Immunocytochemical labelling

Immunocytochemical labelling was performed on an *A. niger* stationary phase sample (25 h) to provide a qualitative indications of the location of GO in the fungus. The procedures and reagents used for labelling are detailed in Appendix A.5.

Firstly, the purity of the commercial GO from Seravac Pty Ltd (Epping, Cape Town) was determined by SDS-PAGE, running a 12% separating gel and 6.5% stacking gel to ensure that GO does not require further purification. Electrophoresis was carried out at a constant voltage of 200 V for approximately 90 min. After electrophoresis, the gel was stained in a Coomassie Brilliant Blue R-250 solution for 30 min. Thereafter, the gel was destained in a 7% acetic acid solution overnight.

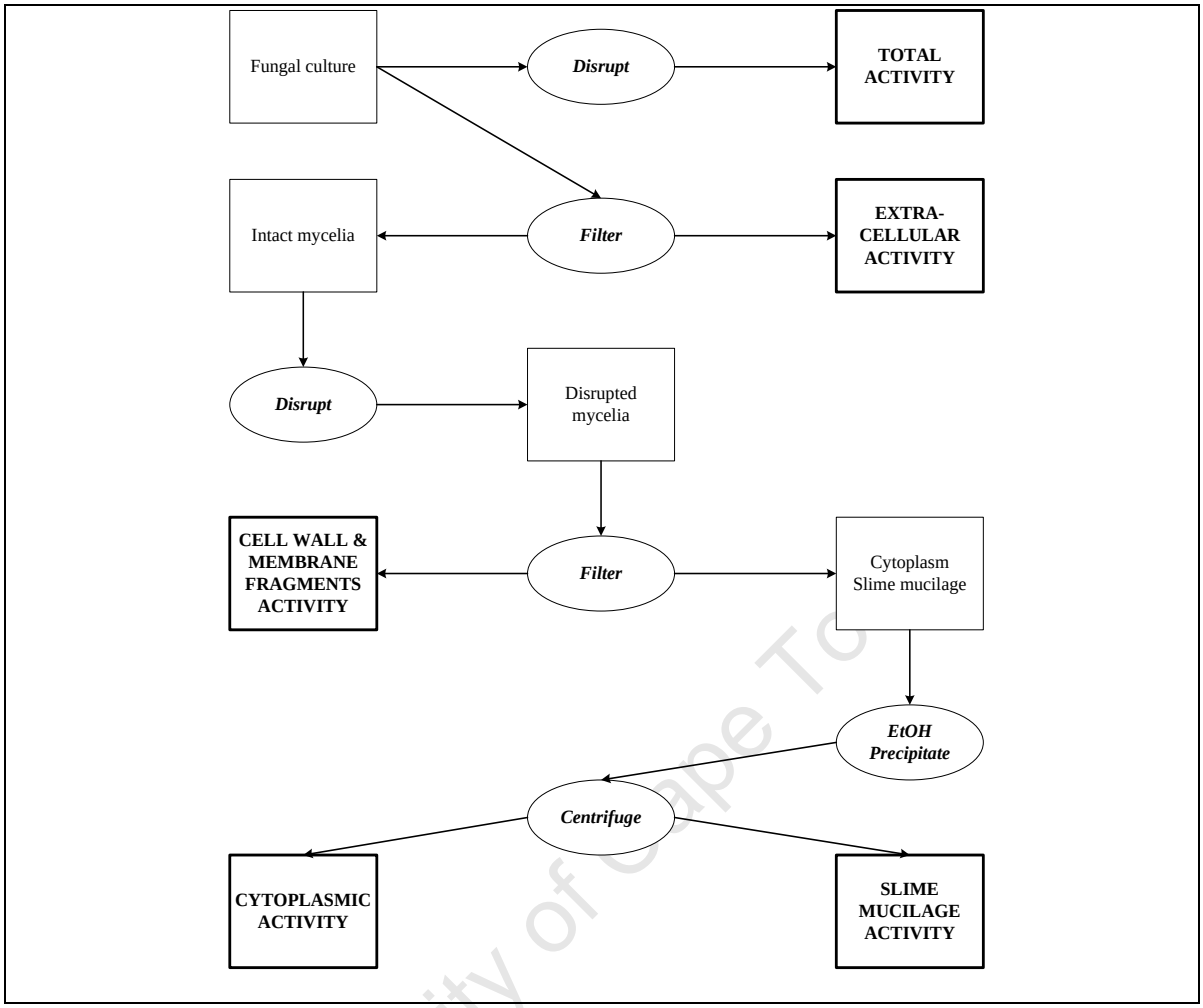

Figure 3.2 Procedure for the separation of GO into the individual fractions

Primary rabbit polyclonal antibodies, immunoglobin G (IgG), were raised against a commercial GO obtained from Seravac Pty Ltd (Epping, Cape Town, South Africa). Pre-immune serum was collected prior to immunization with GO to check if the animals expressed pre-existing anti-fungal antibodies. An enzyme-linked immunosorbent assay (ELISA) was performed (Harlow and Lane 1988) on the rabbit serum to identify the fractions with the highest titre. IgG was purified from the serum by fractional precipitation with PEG 6,000 and the concentration was determined by the absorbance at 280 nm ($\varepsilon_{280\,nm}^{1mg/ml}$ = 1.64).

To prepare cell extracts, fungal cells were ruptured by a French Press, followed by incubation with 1% Triton X100. The extract was clarified by centrifugation (15000g, 15 min, 4°C), and the supernatant was transferred to a clean container. Proteins were precipitated by the addition of trichloroacetic acid (TCA) to a final concentration of 5%. The suspension was centrifuged and the supernatant was removed. The pellet was washed with acetone to remove residual TCA and redissolved in a minimal volume of phosphate-buffered saline (PBS). Pure, commercial GO and

cell extracts were separated by reducing 12% sodium dodecyl sulphate–polyacrylamide gel electrophoresis (SDS-PAGE) (20 V, 90 min, 4°C), transferred onto nitrocellulose (20 V, overnight) and stained with Ponceau S. The membrane was probed with purified IgG to determine specificity and to identify any cross-reactivity with other *A. niger* proteins. For immunogold transmission electron microscopy, mycelial pellets were fixed with 2% paraformaldehyde and 2% glutaraldehyde in PBS (pH 7.4), dehydrated in a graded ethanol series and embedded in LR White resin.

Ultra-thin sections were collected onto nickel grids and blocked with tris-buffered saline containing 1% fish skin gelatin, 0.8% bovine serum albumin (BSA) and 20 mM glycine for an hour. The sections were washed, probed with IgG (ranging from 2.5 to 10 μg/ml at a final volume of 5 ml, 2 h) and detected with 10 nm gold-conjugated goat anti-rabbit IgG (1/200 dilution, 5 μl, 1 h). The sections were contrasted with uranyl acetate/lead citrate and examined on a transmission electron microscope at 80 kV.

3.7 Experimental approach

The aim of this thesis was to investigate the production and location of GO in *A. niger* NRRL-3 and *Penicillium* sp. CBS120262, and the impact of location on product recovery. The growth, substrate utilisation and product formation (CDW, GA, total and extracellular GO) were quantified. In literature GO has been associated with different locations in the fungal culture. In this thesis, the location of this enzyme and the amounts associated with each fraction (cell wall and membrane fragments, supernatant, cytoplasm and gel) were determined. Quantitatively, this was done by separation of the culture into the different fractions and determination of the activity of GO in each fraction by measuring the rate of consumption of dissolved oxygen in the GO-catalysed conversion of glucose to GA. These results were supported by labelling of the GO produced from *A. niger* NRRL-3 with a gold-labelled antibody generated in response to GO and its observation by transmission electron microscopy. The latter gave a qualitative measure of the location of GO in *A. niger* NRRL-3 with specific reference to that fraction associated with the cell envelope.

Analysis of the inconsistency of the literature with respect to GO location in filamentous fungi suggests that the micro-organism used and the growth phase of the micro-organism may influence both the morphology and the GO location. This hypothesis was test experimentally. The correlation between morphology and GO location was reviewed in the literature and, where

necessary, verified or determined experimentally. Image analysis of micrographs was undertaken to view the changes of the hyphae during growth and thereby provide indices to describe the morphology. The morphology, growth rate and location of GO were correlated. The influence of changing process conditions, such as changing the pH control agent, on the production and location of GO as well as the morphology of *Penicillium* sp. CBS 120262 was investigated.

It is known that the rheological properties of a microbial culture changed from Newtonian to non-Newtonian with growth. Therefore, the characterisation of the culture rheology of the microbial suspension as a function of growth phase as well as biomass concentration, culture conditions and morphology was undertaken.

The relative rates of GO production and secretion were quantified using the GO activity as a function of growth phase and location the cause of the location profile. A generalised mass transfer approach was investigated to predict the secretion profiles obtained. The results from the immunocytochemical labelling and literature correlations were used to predict the diffusion coefficient of GO required for the mass transfer analysis. The influence of GO location on its subsequent recovery through downstream processing (DSP) was discussed as was the potential to influence this.

Chapter 4 Production of GO from *A. niger* NRRL-3 and *Penicillium* sp. CBS 120262

In this chapter the production of GO from batch *A. niger* NRRL-3 and *Penicillium* CBS 120262 cultivations was investigated and their time-based growth profiles with respect to substrate utilisation and product formation (CDW, GA, total and extracellular GO) are described in Section 4.1. Kinetics parameters are also compared. In Section 4.2 the effect of using $Ca(OH)_2$ instead of NaOH as pH control agent for the production of GO from *Penicillium* sp. CBS 120262 was investigated and compared. The rheology of *A. niger* and *Penicillium* sp. was discussed in Section 4.3.

4.1 Batch cultivation of *A. niger* and *Penicillium* sp.

4.1.1 Time profiles

The growth parameters of replicate *A. niger* and *Penicillium* sp. batch cultivations are shown in Figures 4.1 and 4.2 respectively. The procedure for volume corrections, set out in Section 3.4 and Appendix D, was used to correct concentrations of glucose, CDW, GA, total and extracellular GO for sampling and dilution. The specific gravity for a 5 M NaOH solution is 1.2. The measured batch cultivation data are set out in Appendix C and the volume corrected data are set out in Appendix E.

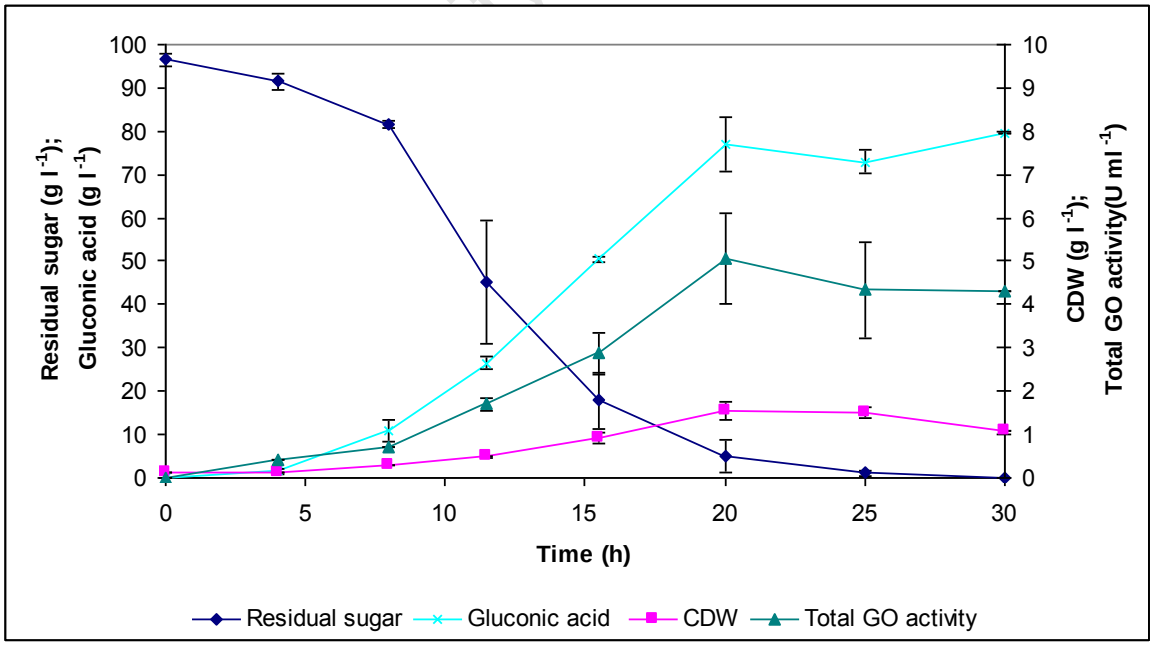

Figure 4.1 Batch culture of *A. niger* (◆) Residual sugar; (✳) Gluconic acid; (■) CDW; (▲) Total GO activity (mean of two values)

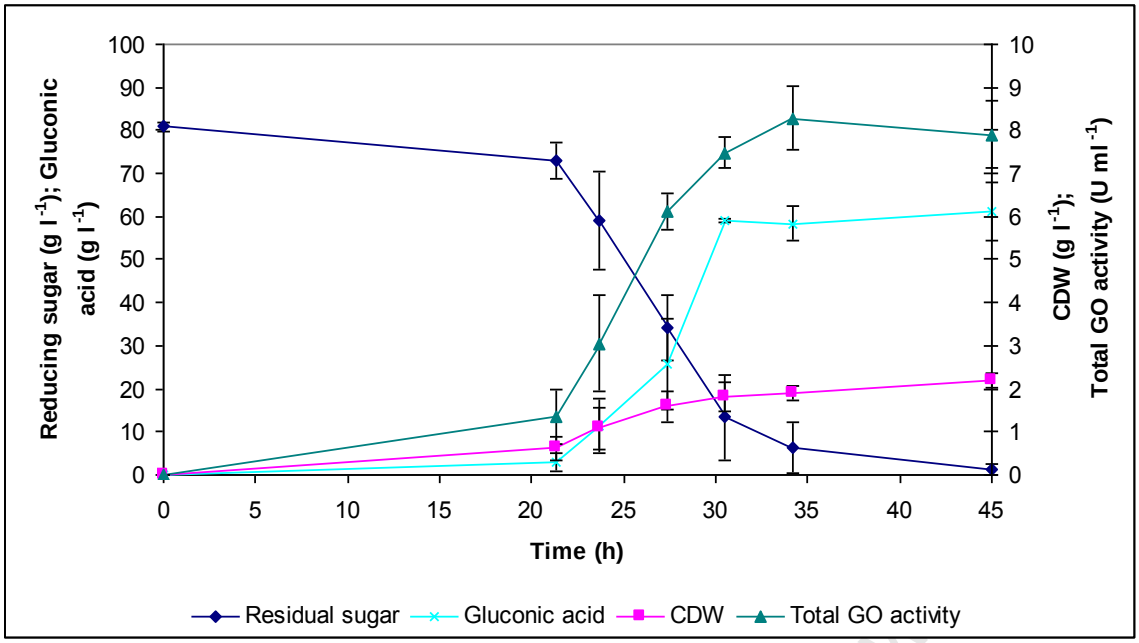

Figure 4.2 Batch culture of *Pencillium* sp. (◆) Residual sugar; (✳) Gluconic acid; (■) CDW; (▲) Total GO activity (mean of three values)

The batch cultures of *A. niger* (Figure 4.1) and *Penicillium* sp. (Figure 4.2) were in stationary phase respectively by 25 h and 45 h as indicated by the negligible residual reducing sugar concentration and no further increase in biomass concentration. *A. niger* had a lag phase of less than 4 h compared to a lag phase for *Penicillium* sp approaching 20 h. The longer lag phase was attributed to different inoculum development procedures for the two organisms. *Penicillium* sp. was developed from a spore inoculum and *A. niger* from a mycelial inoculum (Section 3.1.3).

The amount of base added during growth to the cultures to maintain a constant pH of 5.5 for *A. niger* and 6.5 for *Penicillium* sp. and to neutralise the GA formed is shown in Figure 4.3. The concentration of GA formed was measured directly by HPLC or indirectly by the addition of base to maintain a constant pH since there was a direct correlation between moles base added and moles GA produced (Figure 4.4). The direct relationship between OH^- ions consumed and GA produced is given as:

$$y = 1.1593\ x + 0.0471 \qquad \textbf{(4.1)}$$

where x moles of GA produced and y moles OH^- ions consumed with a regression coefficient of 0.9973. This relationship was valid for both the *A. niger* and *Penicillium sp.* systems illustrating the dominance of GA in acidification of the medium. The moles of OH^- ions used and GA formed were calculated as follows:

$$moles\ OH^{-} = \frac{mass\ NaOH\ solution\ added\ *\ Molarity\ of\ NaOH\ solution}{density\ of\ NaOH\ solution} \quad \textbf{(4.2)}$$

$$moles\ GA = \frac{GA\ concentration\ *V_{reactor}}{M_w\ GA} \quad \textbf{(4.3)}$$

where the mass of the NaOH solution added was the cumulative amount in grams, the molarity of the NaOH solution was 5M, the density of the 5M NaOH solution was 1.2 g ml^{-1}, the GA concentration in g l^{-1} was obtained from HPLC analysis, $V_{reactor}$ was 6 litres and the molecular weight (M_w) of GA was 196 g mol^{-1}.

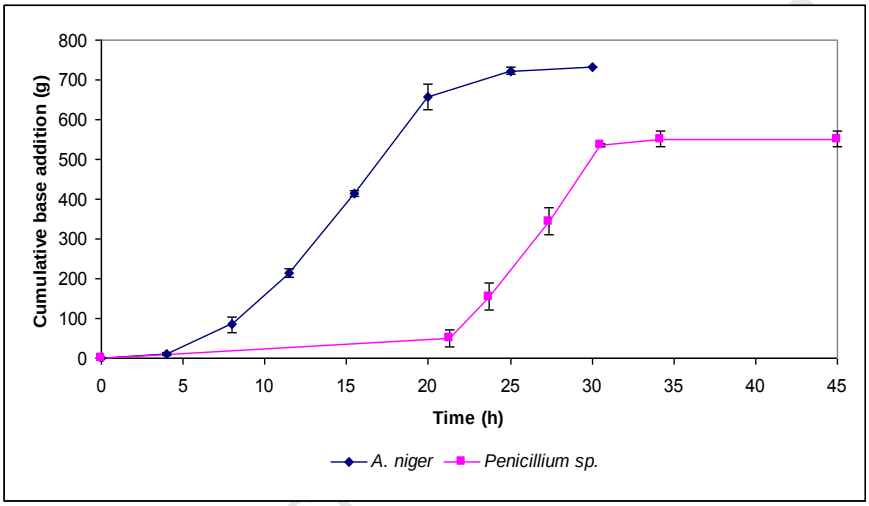

Figure 4.3 Addition of 5 M NaOH to *A. niger* (◆) and *Penicillium* sp. (■) cultures

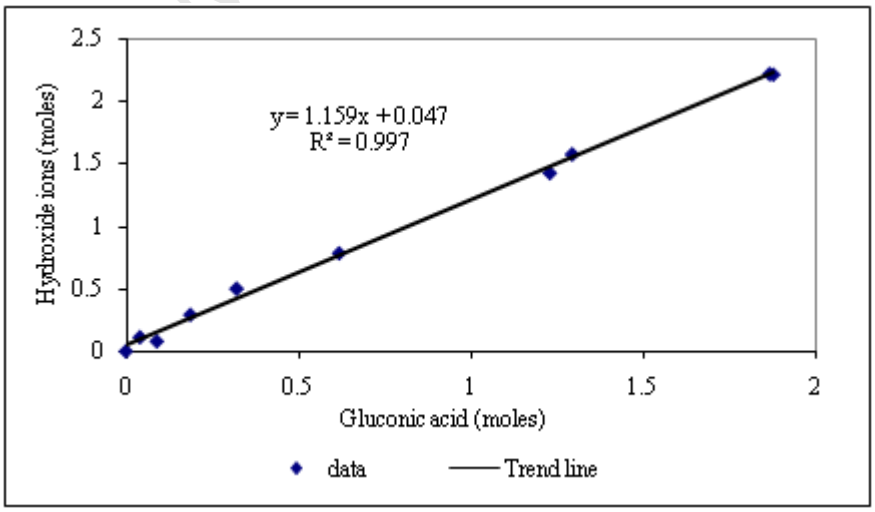

Figure 4.4 Correlation between moles NaOH added and moles GA produced for *A. niger* and *Penicillium* sp.

4.1.2 Reproducibility

The reproducibility of the two batch cultures of *A. niger* and three *Penicillium* sp. cultures for reducing sugar, CDW, GA, total and extracellular GO concentrations were assessed using a single factor ANOVA analysis. It was shown that the respective concentrations at each point in the time profile did not differ significantly at a 95% confidence interval.

4.1.3 Kinetic parameters of batch *A. niger* and *Penicillium* sp. cultures

The kinetic parameters, maximum yield coefficients ($Y_{X/S}^{max}$, $Y_{GA/S}^{max}$, $Y_{GO/S}^{max}$), maximum specific GO activity, maximum specific GA produced, specific growth rate and overall productivities were determined for batch cultures of *A. niger* and *Penicillium* sp. (Table 4.1).

Table 4.1 Kinetic parameters of *A. niger* NRRL-3 and *Penicillium* sp. CBS 120262 batch cultures

	A. niger	***Penicillium* sp.**
$Y_{X/S}^{max}$ [g CDW (g glucose)$^{-1}$]	0.015 ± 0.004	0.028 ± 0.0002
$Y_{GA/S}^{max}$ [g GA (g glucose)$^{-1}$]	0.85 ± 0.04	0.76 ± 0.08
$Y_{TotalGO/S}^{max}$ [U GO (g glucose^{-1}]	53.55 ± 5.08	101.06 ± 10.95
[µkat GO (g glucose)$^{-1}$]*	(1.786 ± 0.1695)	(3.370 ± 0.365)
Maximum Specific Total GO activity [U GO (g CDW)$^{-1}$]	2838 ± 76	3598 ± 423
[µkat GO (g CDW)$^{-1}$]*	(114.43 ± 17.26)	(119.94 ± 14.11)
Maximum Specific GA produced [g GA (g CDW)$^{-1}$]	56.47 ± 16.04	27.26 ± 4.88
μ_{max} [h^{-1}]	0.15 ± 0.02	0.16 ± 0.001
Overall biomass productivity [g l^{-1} h^{-1}]	0.04 ± 0.02	0.04 ± 0.01
Overall GA productivity [g GA l^{-1} h^{-1}]	2.8 ± 0.2	1.46 ± 0.04
Overall Total GO productivity [U l^{-1} h^{-1}]	0.19 ± 0.03	0.19 ± 0.01
([nkat l^{-1}h^{-1}]) *	(6.79 ± 0.47)	(6.17 ± 0.44)
Overall Extracellular GO productivity [U l^{-1} h^{-1}]	0.04 ± 0.004	0.08 ± 0.01
([nkat l^{-1}h^{-1}]) *	(1.49 ± 0.01)	(2.54 ± 0.24)

* Conversion of this data from U to nkat has used a conversion factor of 33.34 as described in Section 2.5, Table 2.3

Fungal cells do not grow by fission (bacteria) or by budding (yeast) but increase by polar growth in which the hyphae elongate and branches are formed to "spread out" to seek nutrients. The maximum amount of biomass that was produced for *A. niger* and *Penicillium* sp. was 1.56 and 2.20 g l^{-1} from 100 g l^{-1} and 80 g l^{-1} glucose respectively. This translates to a yield coefficient of 0.015 ± 0.004 g CDW (g glucose)$^{-1}$ for *A. niger* and 0.028 ± 0.0002 g CDW (g glucose)$^{-1}$ for *Penicillium* sp. These low yields where the result of nitrogen limitation. The N-limited media was selected to limit the biomass

concentration, to avoid mass transfer limitations through viscosity. Most of the glucose was converted to GA. Although the morphologies were different for *A. niger* (pellet) and *Penicillium* sp. (mycelial), the growth of the organisms was similar and was well represented by the exponent growth rate constant μ, with μ_{max} of 0.15 ± 0.02 h^{-1} and 0.16 ± 0.001 h^{-1} for *A. niger* and *Penicillium* sp. respectively.

Both fungi were excellent GA producers with yield coefficients (mass/mass) of 0.85 ± 0.04 g GA g^{-1} glucose for *A. niger* after 25 h and 0.76 ± 0.08 g GA g^{-1} glucose for *Penicillium* sp. after 45 h, compared to a theoretical yield coefficient of 0.98 g g^{-1} (0.9 mol mol^{-1}) (Ramachandran *et al*., 2006). The maximum specific GA produced is 56.47 ± 16.04 g GA g^{-1} CDW for *A. niger* and 27.26 ± 4.88 g GA g^{-1} CDW for *Penicillium* sp.

Although the overall biomass and total GO productivity are the same for both *A. niger* and *Penicillium* sp. after 25 h and 45 h at 0.04 g l^{-1} h^{-1} and 0.19 U l^{-1} h^{-1} respectively, the overall extracellular GO productivity of *Penicillium* sp. is double than that of *A. niger*. If the 20 h lag phase was removed by manipulation of the inoculum (as required to maximise the economics and minimise the environmental burden of the bioprocess), the productivity of *Penicillium* would be up to 1.8 fold greater than that of *A.niger*.

The maximum GO activity was 4.7 U ml^{-1} (156.7 nkat ml^{-1}) at 25 h for *A. niger* and 8.1 U ml^{-1} (270.0 nkat ml^{-1}) for *Penicillium* sp. at 45h. Simpson (2005) reported the total activity of GO produced from *Penicillium* sp. at 45 h as 10.1 U ml^{-1} (168.4 nkat ml^{-1}). The overall GO yield from glucose $Y_{GO/S}$ was 53.55 ± 5.08 (U g^{-1} glucose) (1.786 ± 0.1695 μkat g^{-1}) for *A. niger* and 101.06 ± 10.95 (U g^{-1} glucose) (3.370 ± 0.365 μkat g^{-1}) for *Penicillium* sp. The overall specific GO activity was 2838 ± 76 U g^{-1} biomass (114.43 ± 17.26 μkat g^{-1}) for *A. niger* and 3598 ± 423 U g^{-1} (119.94 ± 14.11 μkat g^{-1}) for *Penicillium* sp.

GO is a primary metabolite (Miron *et al*., 2004) and can be represented by the Luedeking-Piret product model, given in Equation 4.4. This unstructured model combines growth and non-growth-associated contributions towards product formation. The product formation rate (r_p) depends upon both the growth rate $\frac{dX}{dt}$ term and the instantaneous biomass concentration X.

$$\frac{dP}{dt} = r_p = \alpha \frac{dX}{dt} + \beta X \qquad \textbf{(4.4)}$$

where α and β are the Luedeking-Piret equation parameters respectively for growth (α ≠ 0, β = 0) and non-growth (α = 0, β ≠ 0) associated product formation. Integration of Equation 4.4 (where P = P_0 at t = 0) with the integrated logistic equation (Equation 4.5b) yields Equation 4.6 (Wang *et al*., 2006):

The logistic equation is of the form:

$$\frac{dX}{dt} = \mu_{max} X \left(1 - \frac{X}{X_{max}}\right) \quad \textbf{(4.5a)}$$

and its integrated form

$$X = \frac{X_0 \exp^{\mu_{max} t}}{1 - \frac{X_0}{X_{max}}(1 - \exp^{\mu_{max} t})} \quad \textbf{(4.5b)}$$

where X and X_0 are the cell mass and the initial cell mass [g l^{-1}]; X_{max} is the asymptotic maximum cell mass [g l^{-1}] and μ_{max} is the maximum specific growth rate [h^{-1}].

$$P(t) = P_0 + \alpha X_0 \left\{ \frac{e^{\mu_{max} t}}{\left[1 - \left(\frac{X_0}{X_{max}}\right)\left(1 - e^{\mu_{max} t}\right)\right]} - 1 \right\} + \beta \frac{X_{max}}{\mu_{max}} \ln\left[1 - \frac{X_0}{X_{max}}\left(1 - e^{\mu_{max} t}\right)\right] \quad \textbf{(4.6)}$$

The Excel function Solver was used to determine the parameters X_o, X_{max}, α and β in Equation 4.6 by keeping the value of μ_{max} constant at 0.15 h^{-1} for *A. niger* and 0.16 h^{-1} for *Penicillium* sp. for the first data set (Run 1). The μ_{max} values (Table 4.1) were obtained from experimental data that was fitted to the Monod equation in Section 4.1.3. These constants for *A. niger* and *Peniciilium* sp., are summarized in Table 4.2. The prediction from Equation 4.6 is compared with the second data set (Run 2) in Fig. 4.5. The Luedeking-Piret model fit to the two data sets shows the characteristic S-shaped curve and shows good agreement between the model and data. In Figure 4.6 the regression coefficient (R^2) for the parity of the measured data and the Luedeking-Piret data for both runs indicate R^2 values of 0.94 and 0.98 for *A. niger* and 0.90 and 0.95 for *Penicillium* sp. respectively. These R^2 values indicate that the Luedeking-Piret model is an appropriate model to represent the GO activity data.

The parameters μ_{max}, X_0, X_{max} α_{GO} and β_{GO} *A. niger* and *Penicillium* sp. are summarised in Table 4.2. The maximum biomass concentration that was obtained from the model was 1.8 g l^{-1} and 2.5 g l^{-1} for *A. niger* and *Penicillium* sp. respectively. The results obtained for α_{GO} and β_{GO} confirmed that the

product GO (Equation 4.1) was growth-associated with an α_{GO} value of 2.6 x 10^3 U g CDW^{-1} for *A. niger* and 3.3 x 10^3 U g CDW^{-1} for *Penicillium* sp. and β_{GO} value of 0 U g CDW^{-1} h^{-1}.

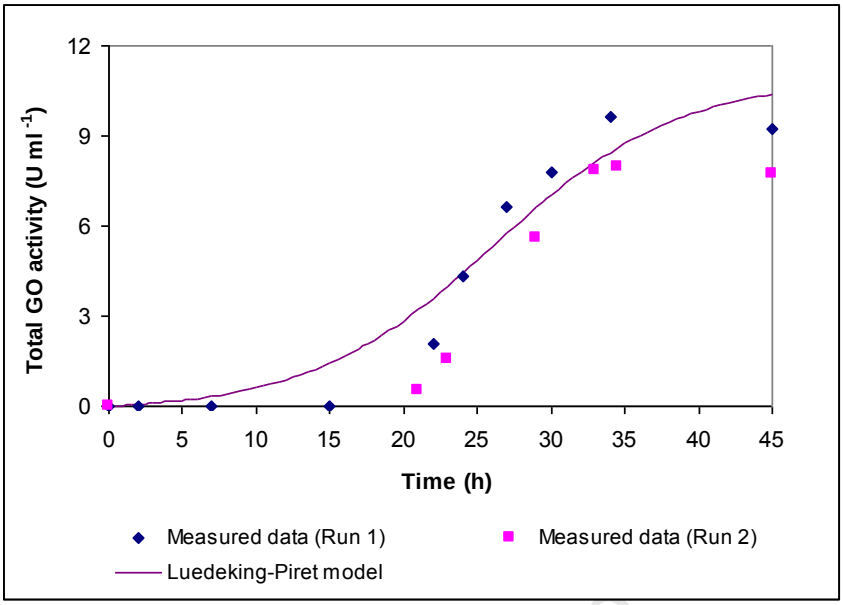

Figure 4.5 The production of GO during a batch *Penicillium* sp. culture (◆) and Luedeking–Piret model (—)

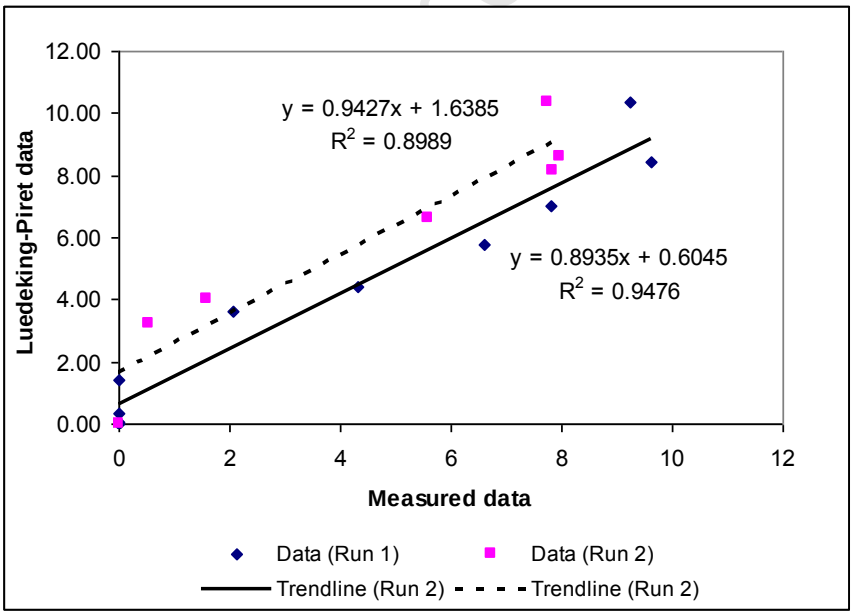

Figure 4.6 Comparison of GO production using the corrected data and the Luedeking-Piret model data for GO production

Table 4.2 The parameters μ_{max}, X_0, X_{max}, α_{GO} and β_{GO} for GO production by *A. niger* and P*enicillium* sp.

Parameters	*A. niger*	*Penicillium* sp.
μ_{max}	0.15 h^{-1}	0.16 h^{-1}
X_0	0.32 g l^{-1}	0.05 g l^{-1}
X_{max}	1.8 g l^{-1}	2.5 g l^{-1}
α_{GO}	2.6 x 10^3 U g^{-1}	3.3 x 10^3 U g^{-1}
β_{GO}	0 U g^{-1} h^{-1}	0 U g^{-1} h^{-1}
R^2	0.94 and 0.98	0.90 and 0.95

Since *Penicillium* sp. produced more biomass and GO from glucose than *A. niger* (Table 4.1) it was used to study the effect of changing process conditions, such as the pH control agent used, on the production of GO.

4.2 The effect of using $Ca(OH)_2$ as pH control agent on the production of GO by *Penicillium* sp. CBS 120262

NaOH was used as the pH control agent for batch cultures of *A. niger* and *Penicillium* sp. since it has previously been used in GO production processes (Blom *et al*., 1952; Li and Chen, 1994; Hellmuth *et al*., 1995). Several authors used $CaCO_3$ or $Ca(OH)_2$ for pH control of *Aspergillus* (Rogalski *et al*., 1988; Hatzinikolaou and Macris, 1995; Liu *et al*., 1999, 2001) and *Penicillium* (Petruccioli *et al*., 1995, 1997) as discussed in Section 2.5.2. These authors hypothesized that the addition of calcium induces the production of GO at the transcription level as discussed in Section 2.4 and 2.6. In this study $Ca(OH)_2$ was chosen since the solubility of $Ca(OH)_2$ in water at 20°C is higher (1.17 g l^{-1}) than that of $CaCO_3$ (0.013 g l^{-1}); hence did not interfere with the gravimetric measurement of biomass.

The procedure for volume corrections, set out in Section 3.4 and Appendix D, was used to calculate the corrected concentrations of glucose, CDW, GA, total and extracellular GO. The specific gravity for a 25% (w/v) $Ca(OH)_2$ (3.4 M) solution was 1.164. The measured batch cultivation data are set out in Appendix C and the volume corrected data are set out in Appendix E.

As described in Section 4.1, a similar correlation between GA and $Ca(OH)_2$ was found for *Penicillium* sp. when the pH was maintained at a value of 6.5. The relationship between the moles of hydroxide ions (OH^-) used to neutralise the GA formed during growth for $Ca(OH)_2$ is

$$y = 1.1684\ x - 0.2776 \qquad \textbf{(4.7)}$$

where x moles of GA produced and y moles OH^- ions consumed with a regression coefficient of 0.9877. These ratios (Equation 4.1 and 4.7) can be used to determine GA concentration indirectly.

The cultivations using the respective pH control agents NaOH and $Ca(OH)_2$ were performed in duplicate. One data set for each pH control agent was used to generate Figure 4.7. The reproducibility of the two batch cultures of *Penicillium* sp. (for each pH control agent) regarding the corrected glucose, CDW, GA and GO concentrations was assessed using a single factor ANOVA analysis. For each pH control agent, the respective concentrations at each time point in the profile did not vary significantly at a 95% confidence interval. Figure 4.7 (a) to (f) illustrates typical batch profiles for glucose utilisation measured as reducing sugar and product formation (CDW, GA, total GO and extracellular GO) for the NaOH and $Ca(OH)_2$ systems as well as the cumulative amount of base added to maintain pH.

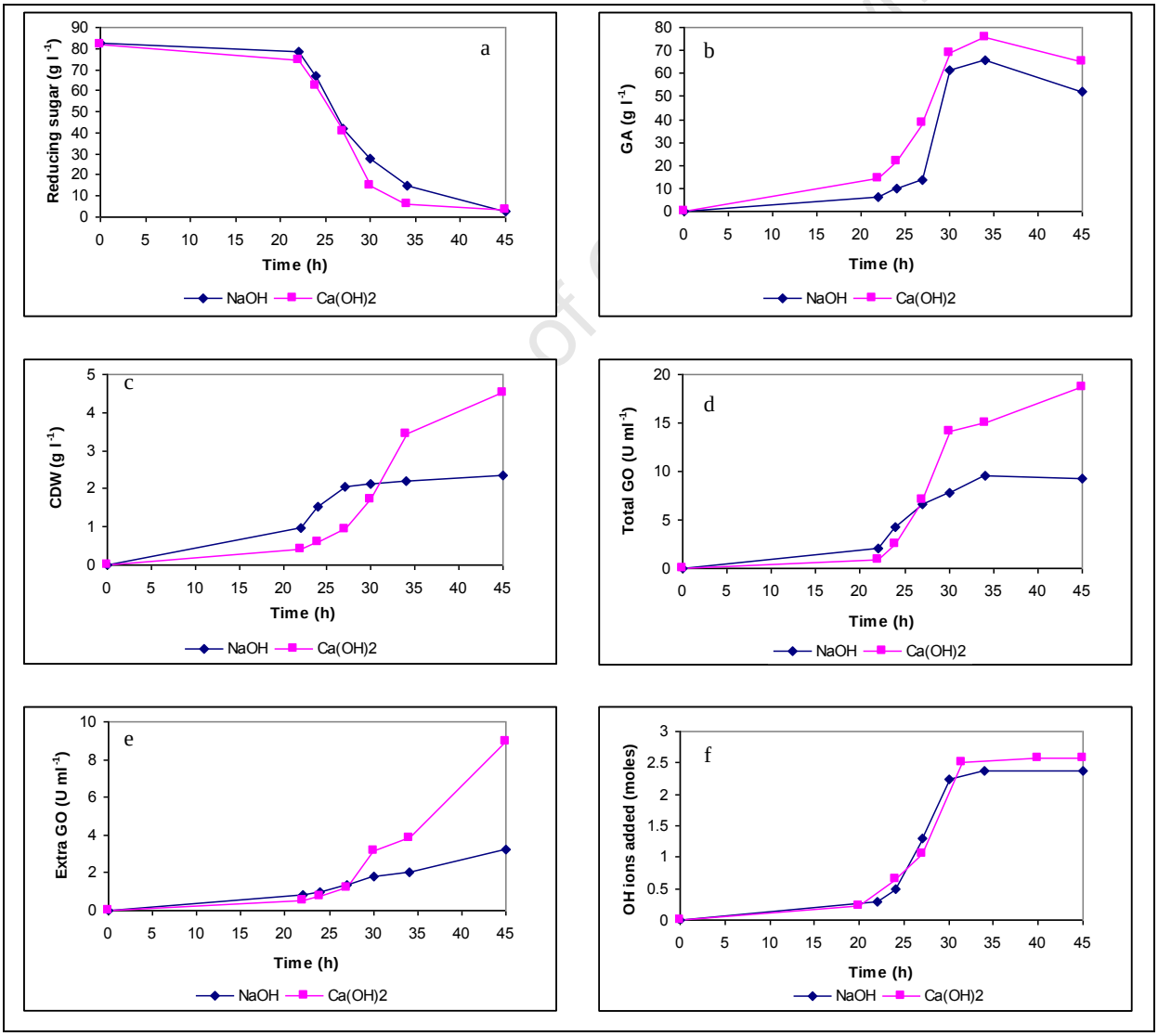

Figure 4.7 *Penicillium* sp. CBS 120262 batch profiles using NaOH (◆) and $Ca(OH)_2$ (■) as pH control agents: a) sugar consumption, b) GA production, c) biomass formed as CDW, d) total GO activity, e) extracellular GO activity and f) moles OH^- ions added.

Using $Ca(OH)_2$ for pH control, more biomass (4.5 g l^{-1} CDW), total GO (18.8 U ml^{-1} (626.8 nkat ml^{-1})) and GA (65 g l^{-1}) were produced than with NaOH (CDW, 2.4 g l^{-1}; GO, 9.2 U ml^{-1} (306.7 nkat ml^{-1}); GA, 52 g l^{-1}). The cumulative amount of OH^- ions added to the cultivation to maintain the pH at 6.5 and to neutralise the organic acid produced was 2.57 and 2.38 moles for $Ca(OH)_2$ and NaOH respectively. The volumetric activity of GO in the supernatant and culture lysate, was higher for $Ca(OH)_2$ at 8.9 U ml^{-1} (296.7 nkat ml^{-1}) and 47.6% of the total activity than for NaOH at 3.2 U ml^{-1} (106.7 nkat ml^{-1}) and 34.8% of total activity, indicating that GO production was enhanced by using $Ca(OH)_2$ for pH control. Studies by Petrucciolli *et al*. (1995) using *Penicillium variabile* P16 showed that on addition of 35 g l^{-1} $CaCO_3$, GO production increased to approximately 15 U ml^{-1} at 45 h, compared to 2 U ml^{-1} when NaOH was used. Various authors reported that $CaCO_3$ had a strong inducing effect on GO synthesis (Petrucciolli *et al*., 1995; Hatzinikolaou and Macris, 1995; *Liu et al*., 2001). This might be due to GO induction that was accompanied by a metabolic shift from glycolysis to the pentose phosphate pathway (Section 2.6).

The kinetic parameters maximum yield, maximum specific GO activity, maximum specific GA concentration, specific growth rate and overall productivities on use of NaOH and $Ca(OH)_2$ (in duplicate) are summarised in Table 4.3.

Table 4.3 Kinetic parameters of *Penicillium* sp. CBS 120262 batch cultivation using NaOH or $Ca(OH)_2$ as pH control agent

	***Penicillium* sp. CBS 120262 cultivation using:**	
	NaOH	**$Ca(OH)_2$**
$Y_{X/S}^{max}$ [g CDW (g glucose)$^{-1}$]	0.028 ± 0.0002	0.07 ± 0.01
$Y_{GA/S}^{max}$ [g GA (g glucose)$^{-1}$]	0.76 ± 0.08	0.80 ± 0.04
$Y_{TotalGO/S}^{max}$ [U GO (g glucose)$^{-1}$]	101.1 ± 11	248 ± 21
[µkat GO (g glucose)$^{-1}$]*	(3.37 ± 0.365)	(8.3 ± 0.7)
Maximum Specific Total GO activity [U GO (g CDW)$^{-1}$]	3598 ± 423	4556 ± 549
[µkat GO (g CDW)$^{-1}$]*	(119.9 ± 14.11)	(152 ± 18)
Maximum Specific GA produced [g GA (g CDW)$^{-1}$]	27.26 ± 4.88	14.00 ± 0.42
μ_{max} [h^{-1}]	0.16 ± 0.01	0.19 ± 0.01
Overall biomass productivity [g l^{-1} h^{-1}]	0.04 ± 0.01	0.10 ± 0.00
Overall GA productivity [g GA l^{-1} h^{-1}]	1.46 ± 0.04	1.42 ± 0.05
Overall Total GO productivity [U l^{-1} h^{-1}]	0.19 ± 0.01	0.46 ± 0.05
(nkat l^{-1} h^{-1})*	(6.17 ± 0.44)	(15.3 ± 1.7)
Overall Extracellular GO productivity [U l^{-1} h^{-1}]	0.08 ± 0.01	0.17 ± 0.04
(nkat l^{-1} h^{-1})*	(2.54 ± 0.24)	(5.8 ± 1.4)

* Conversion of this data from U to nkat has used a conversion factor of 33.34 as described in Section 2.5, Table 2.3

The maximum yield of biomass, and total GO yield from glucose was highest in the $Ca(OH)_2$ cultivation (0.07 g CDW g^{-1} glucose; 248 U GO g^{-1} glucose (8.3 μkat GO g^{-1} glucose)) than in NaOH (0.028 g CDW g^{-1} glucose; 101 U GO g^{-1} glucose (3.37 μkat GO g^{-1} glucose)). The yield of GA from glucose for NaOH and $Ca(OH)_2$ were 0.76 g GA g^{-1} glucose and 0.8 g GA g^{-1} glucose respectively. The specific growth rates were similar (0.19 h^{-1} for $Ca(OH)_2$ and 0.16 h^{-1} for NaOH). The specific GO activity also varied marginally between 3598 U GO g^{-1} CDW (119.9 μkat GO g^{-1} CDW) for NaOH to 4556 U GO g^{-1} CDW (152 μkat g^{-1}) for $Ca(OH)_2$. The productivity of total GO production was higher for $Ca(OH)_2$ than for NaOH by a factor of 2.4. The kinetic parameters especially the overall productivity in Table 4.3 clearly illustrates that *Penicillium* sp. was a dominant GA producer compared to the amount of biomass and GO produced.

The Luedeking-Piret parameters X_o, X_{max}, α_{GO} and β_{GO} were determined by keeping the value of μ_{max} constant at 0.19 h^{-1} for *Penicillium* sp. when $Ca(OH)_2$ was used as the pH control agent for the first data set (Run 1). The μ_{max} value (Table 4.3) was obtained from experimental data that was fitted to the Monod equation in Section 4.2. These constants were fitted to Equation 4.6 and compared with the second data set (Run 2) and the results with the R^2 values summarised in Table 4.4 with those constants obtained for the NaOH cultivation. For the $Ca(OH)_2$ cultivations the R^2 values of 0.90 and 0.92 for parity between the measured data and the Luedeking-Piret data indicate that the Luedeking-Piret model illustrated an appropriate fit to the GO activity data.

The maximum biomass concentrations obtained from the model were 2.5 g l^{-1} and 4.7 g l^{-1} for the NaOH and $Ca(OH)_2$-controlled *Penicillium* sp. cultivations respectively. The results obtained for α_{GO} and β_{GO} confirmed that the product GO (Equation 4.1) was growth-associated with an α_{GO} value of 3.3 x 10^3 U g CDW^{-1} for NaOH- and 4.7 x 10^3 U g CDW^{-1} for $Ca(OH)_2$-controlled cultivations and β_{GO} value of 0 U g CDW^{-1} h^{-1}. The rate of GO production can be written as: $r_{p,GO} = 3.3 \times 10^3 \mu X$ for NaOH and $r_{p,GO} = 4.5 \times 10^3 \mu X$ for $Ca(OH)_2$ cultivations.

Table 4.4 The parameters μ_{max}, X_0, X_{max}, α_{GO} and β_{GO} for GO production of *Penicillium* sp. batch cultivations using NaOH or $Ca(OH)_2$ as pH control agent

	NaOH	$Ca(OH)_2$
μ_{max}	0.16 h^{-1}	0.19 h^{-1}
X_0	0.05 g l^{-1}	0.02 g l^{-1}
X_{max}	2.5 g l^{-1}	4.7 g l^{-1}
α_{GO}	3.3 x 10^3 U g^{-1}	4.5 x 10^3 U g^{-1}
β_{GO}	0 U g^{-1} h^{-1}	0 U g^{-1} h^{-1}
R^2	0.90 and 0.95	0.90 and 0.92

4.3 Rheology of *A. niger* and *Penicillium* sp. cultures

During the course of a cultivation, the rheological characteristics of the culture often becomes more complex, due to the increased biomass and accumulation of high-molecular-weight products (Manchanda *et al*., 1982). In literature pelleted morphology exhibits Newtonian behaviour at low to medium biomass concentrations while mycelial morphology exhibits non-Newtonian behaviour. With mycelial morphology, as the growth rate of the organism increases (i.e. more hyphae are produced), the culture broth becomes more viscous which, in turn, affects the mass and heat transfer properties of the culture as well as the productivity of the organism. With pelleted morphology, the culture broth does not demonstrate these limitations in bulk mass transfer; however, intra-pellet mass transfer limitations may result in oxygen limitation occurring in the centre of the pellet if the pellet is too large. Therefore, a reasonable understanding of the rheology of the cultivation is of great importance for the design, scale-up and operation of bioreactors since the performance of a bioreactor is influenced by the rheological properties of the microbial cultivation. These rheological properties greatly affect the fluid mixing, mass and heat transfer (Charles, 1978; Metz *et al*., 1979) which in turn influences the operating conditions, and thus affect the growth, morphology and product formation (Olsvik and Kristiansen, 1994).

4.3.1 Validation of viscosity measurements

The range of impeller speeds used for *Penicillium* sp. cultivation were between 300 and 600 rpm while a constant impeller speed of 500 rpm for *A. niger* cultivations was maintained. These speeds can be expressed as impeller tip speed [m s^{-1}] using Equation 4.8:

$$\text{Impeller tip speed} = \pi N D \qquad \textbf{(4.8)}$$

where N is impeller speed (rpm) and D is impeller diameter (D = 0.08 m). The impeller tip speed at the various agitation speeds are given in Table 4.5 and the average shear rate was calculated using Equation. 2.15 with a k' value of 10 (Metzer and Otto, 1957; Margaritis and Zajic, 1978).

A Paar Physica Rheolab MC1 rheometer was used to measure the shear rate, shear stress and viscosity of samples. The double gap (dgap) spindle Z1 was used for low viscosity liquids (η < 200 mPa s) and suspensions with particle size < 500 μm since the internal and external gap width was 0.5 mm. The Z2 spindle was used for medium to high viscosity liquids (20 to 15 000 mPa s) and suspensions with particle size < 1900 μm since the gap width was 1.90 mm. A shear rate of 100 s^{-1} was used in calculations of the apparent viscosities and compared with literature data.

Table 4.5 Impeller tip speed and average shear rate for different impeller speeds

Speed [rpm]	Impeller tip speed [$m.s^{-1}$]	$\gamma_{av} = k'N$ [s^{-1}] where k' = 10
300	1.26	50.0
350	1.47	58.3
400	1.68	66.7
450	1.88	75.0
500	2.09	83.3
550	2.30	91.7
600	2.51	100.0

Calibrations at 25°C with Newtonian fluids such as water, sucrose solutions and a Brookfields 50.4 mPa.s calibration fluid were performed. The power law was used to calculate the rheological indices n and K. The viscosity was calculated at a shear rate of 100 s^{-1} and compared with the theoretical values in Table 4.6. The results in Table 4.6 showed that the viscosity obtained with the double gap spindle, Z1, was close to the theoretical values whereas the viscosities obtained from the Z2 spindle were much higher than that of the theoretical values. The geometric details of these systems are specified in Section 3.3.7. The ratio of the viscosity values from the Z2 to the Z1 spindles varies from a factor of 4.4 for water to a factor of 3.6 for 20% sucrose to 1.6 for 40% sucrose to 1.3 for 60% sucrose and to a factor of 1.1 for a Brooksfields calibration oil. This indicated that as the viscosity of the liquid increased the difference between the viscosity values for Z2 and Z1 became less. Since rheological properties are intrinsic properties of the fluid, these should not be influenced by the measuring technique or instrument (Olsvik and Kristiansen, 1994). The results in Table 4.6 indicate that it is not the case in this study.

Table 4.6 Viscosity values and power law indices (K and n) at 25°C for water, sucrose solutions and a 50.4 mPa s Brookfields calibration fluid using Z1 and Z2 spindles

	Water	20 % sucrose	40 % sucrose	60 % sucrose	Brookflieds calibration fluid
Theoretical value* (mPa)	0.89	1.71	5.21	44.0	50.4
			dgap or Z1 spindle		
Viscosity (mPa.s)	0.89	1.70	4.91	44.4	46.7
Power law indices	K = 7.21 x 10^{-4} $Pa.s^n$ n = 1.03	K = 1.45 x 10^{-3} $Pa.s^n$ n = 1.03	K = 4.26 x 10^{-3} $Pa.s^n$ n = 1.02	K = 4.72 x 10^{-2} $Pa.s^n$ n = 0.99	K = 4.64 x 10^{-2} $Pa.s^n$ n = 1.00
			Z2 spindle		
Viscosity (mPa.s)	3.89	6.07	7.98	55.48	50.7
Power law indices	K = 9.91 x 10^{-5} $Pa.s^n$ n = 1.60	K = 4.37 x 10^{-4} $Pa.s^n$ n = 1.44	K = 4.38 x 10^{-4} $Pa.s^n$ n = 1.54	K = 4.56 x 10^{-2} $Pa.s^n$ n = 1.03	K = 3.98 x 10^{-2} $Pa.s^n$ n = 1.05
			Ratio of viscosity from Z2 to viscosity from Z1		
	4.37	3.57	1.63	1.25	1.08

* Theoretical value from CRC Handbook, 58th edition

Limitations using the rheometer to measure viscosity was that the rheometer have a ball-bearing drive and cannot measure as accurately as an air-bearing drive at low shear rates $\gamma < 1\ s^{-1}$, there was also a lot of scatter in the data at shear rates lower than 100 s^{-1}. The Z2 spindle gave higher than 1 value for the power law index n when it was used for suspensions with low biomass concentration. The Z2 spindle should be used for liquids with viscosities > 10 mPas, with the transition viscosity region of between 44 and 50 mPas.

Since the rheological properties of filamentous cultivations are normally considered to be a function of the biomass concentration and the morphology of the micro-organism (Charles, 1978; Metz et al., 1979) the rheology of *A. niger* and *Penicillium* sp. CBS 120262 was investigated in terms of the biomass concentration and the fungal morphology.

The shear stress and shear rate rheograms for supernatant and culture samples were obtained during the cultivations using a double gap (dgap) spindle Z1 or Z2 spindle. The shear rate range between 100 and 1000 s^{-1} was used to obtain the raw data. The US200 software package was used to calculate the rheology parameters of the Ostwald or Power law (K and n), Bingham (τ_0 and K_p), Herschel-Bulkley (τ_0 and K_p and n) and Casson (τ_0 and K_p) models in the shear rate range of 150 – 500 s^{-1}. These results as well as the shear rate range that was used and the shear stress range obtained are summarised in Appendix G.

4.3.2 The effect of biomass concentration on *A. niger* and *Penicillium* sp. cultures

In order to study the effect of biomass concentration on the culture rheology biomass was harvested at the end of the cultivation and filtered using Whatman filter paper. Biomass suspensions were prepared using this supernatant with a range of different biomass concentrations. The biomass concentrations were plotted against the respective consistency indexes and yield stresses were obtained from the rheology models (Ostwald or power law, Bingham, Herschel-Bulkley and Casson) presented in Table 4.7. For *A. niger* the values of the constant varies, even by an order of magnitude while the changes in the exponent is similar and in the same order of magnitude. The correlation of K and X (Table 4.7) varied according to the type of strain used, and thus on the fungal morphology as shown below for the Ostwald model:

A. niger (pellets) (present study)	$K = 4.0 \times 10^{-5} X^{4.1}$
A. niger (dispersed mycelia) (literature)	$K = 4.3 \times 10^{-4} X^{3.3}$
P. chrysogenum (literature)	$K = 3.6 \times 10^{-3} X^{2.5}$
Penicillium sp. (present study)	$K = 1.3 \times 10^{-3} X^{2.3}$

Table 4.7 Rheological correlations for *A. niger* and *Penicillium* spp. cultures

Microorganism	Rheological model	Variation of rheological parameters [a]	Shear range (s^{-1})	Viscometer	Comments	References
A . niger (clumps/pellets)	Power law Bingham Casson	$K = 4.0 \times 10^{-5}X^{4.1}$ $\tau_0 = 6.0 \times 10^{-3}X^{2.8}$ $K_c = 0.025\ X^{0.48}$ $\tau_0 = 1.8\times 10^{-3}\ X^{3.0}$	150 – 500 for all three models	Coaxial cylinder	Morphology changes were not considered; 1<X<14 g l^{-1} Power law was preferred	Present study
A. niger (dispersed mycelia)	Power law Bingham Casson	$K = 4.3 \times 10^{-4}X^{3.3}$ $\tau_0 = 0.02\ X^{2.3}$ $K_c = 0.048\ X^{0.26}$ $\tau_0 = 2.5\times 10^{-3}\ X^{3}$	50 – 650 for all three models	Coaxial cylinder	Morphology changes were not considered; 2<X<15 gl^{-1} Power law was preferred;	Allen and Robinson, 1990
P. chrysogenum (dispersed mycelia)	Power law Bingham Casson	$K = 3.6 \times 10^{-3}X^{2.5}$ $\tau_0 = 0.043\ X^{2.1}$ $\eta_p = 2.2 \times 10^{-3}X^{0.78}$ $\tau_0 = 8.3 \times 10^{-3}X^{2.5}$ $K_c = 0.047\ X^{0.19}$	50 – 650 for all three models	Coaxial cylinder	Morphology changes not considered; 2<X<15 gl^{-1} Power law was preferred	Allen and Robinson, 1990
Penicillium sp. CBS120262 (dispersed mycelia)	Power law Bingham Herschel-Bulkley Casson	$K = 1.3 \times 10^{-3}X^{2.3}$ $\tau_0 = 0.02\ X^{2.0}$ $K_p = 2.7 \times 10^{-3}\ X^{2.0}$ $\tau_0 = 4.9 \times 10^{-2}X^{1.4}$ $K_c = 0.040\ X^{0.16}$ $\tau_0 = 0.022\ X^{1.6}$	150 – 500 for all 4 models	Coaxial cylinder	Morphology changes not considered; 1<X<14 g l^{-1}	Present study

These indices for the respective rheology models of *A. niger* pellets were used to calculate the apparent viscosity at a shear rate of 100 s^{-1} and presented in Figure 4.8. The apparent viscosity at 100 s^{-1} for the three models (Ostwald, Bingham and Herschel-Bulkley) is similar while that of the Casson model is lower. The apparent viscosity of the four models are linear (Newtonian) at biomass concentrations lower than 4 g l^{-1} and at biomass concentrations higher than 4 g l^{-1} it increased exponentially (non-Newtonian) (Figure 4.8).

Figure 4.9 illustrated the change in the power law index (n), consistency index (K) and the apparent viscosity at 100 s^{-1} for *A. niger* using the Ostwald model. The high value for n (n >1) at the beginning was due to the Z2 spindle that had been used to measure the viscosity of pellets and gave erroneous readings at very low CDW concentrations (Section 4.3.1) but it does follow the trend of decreasing

with increasing CDW concentration. The decrease in n is slight (1.4 to 1.3) up to a biomass concentration of 4 gl^{-1} then it decreased from 1.3 to 0.4. The viscosity of the suspension culture changed linearly from 2.8 to 4.5 mPa s for biomass concentrations ranging from 0 to 4 g l^{-1} and increased exponentially from 4.5 to 86 mPa s for biomass concentrations from 4 to 14 g l^{-1}. For *A. niger* cultures the viscosity remains Newtonian up to 4 g l^{-1} and became non-Newtonian for biomass concentrations greater than 4 g l^{-1}. This result is in accordance with Warren *et al*. (1995). According to Charles (1978), the consistency index K, which is a direct measure of viscosity at a given shear rate is shown in Figure 4.9.

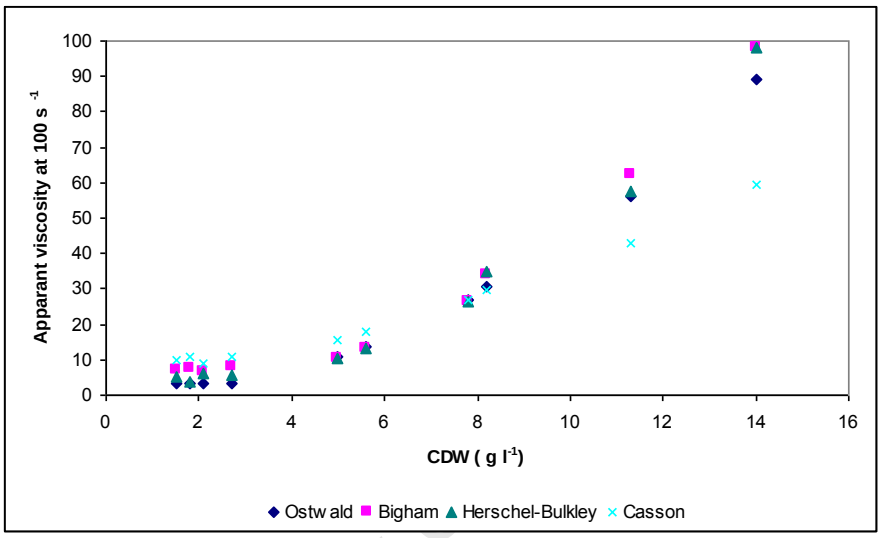

Figure 4.8 Apparent viscosity of *A. niger* vs. biomass concentration at 100 s^{-1} for different rheology models

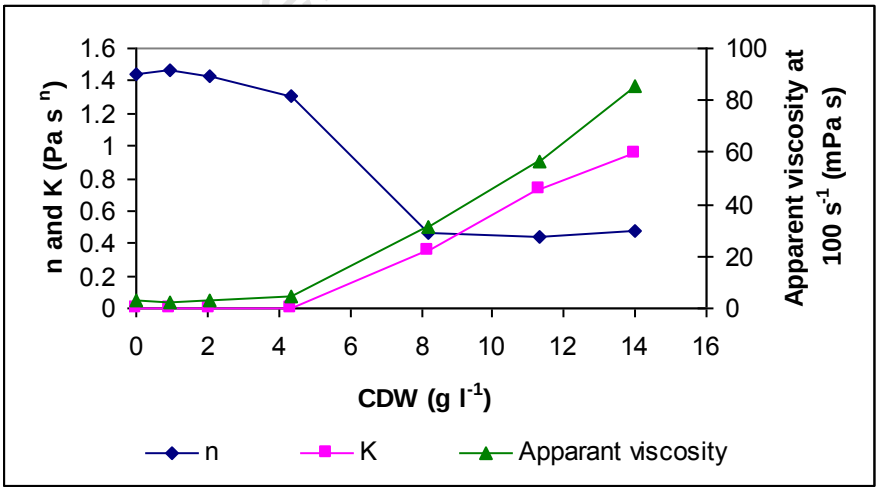

Figure 4. 9 The power law index, consistency index and apparent viscosity at 100 s^{-1} for different *A. niger* biomass concentrations

The apparent viscosity of the *A. niger* supernatant and the suspension during the 25 h duration of the cultivation changed minimally from 1.1 mPa s to 1.3 mPa s and 2.3 to 2.8 mPa s respectively. These results indicate the Newtonian behaviour of the supernatant and suspension as well as the negligible influence of biomass in the range of 0 to 1.8 g l^{-1}.

For *Penicillium* sp. the effect of biomass concentration on its apparent viscosity gave similar profiles as *A. niger* except that the Newtonian portion is up to ± 2 g l^{-1} instead of 4 g l^{-1} (Figure 4.10). Thereafter it increased exponentially to an apparent viscosity of 50 mPas which is approximately 50% lower than the apparent viscosity of *A. niger* at 14 g l^{-1} CDW. The Casson model is still lower than the other models for both *A. niger* and *Penicillium* sp.

In Figure 4.11 the n index followed the pseudo-plastic trend in that it decreased as the apparent viscosity increased while the K index followed the apparent viscosity profile. The n index decreased slightly from 1.5 to 1.4 to a biomass concentration of 2.5 g l^{-1}, then decreased from 1.4 to 0.4 to a biomass concentration of 10 g l^{-1}, thereafter a small further decrease from 0.4 to 0.2 occurred on increase of biomass concentration to 25 g l^{-1}. The non-Newtonian behaviour of the *Penicillium* culture was reached at a lower biomass concentration than for *A. niger*. The apparent viscosity increased linearly from 2.5 to 4.6 mPa s for biomass concentrations ranging from 0 to 3.2 g l^{-1} and increased exponentially to 196 mPa s at a biomass concentration of 25 g l^{-1}.

The supernatant viscosity of the *Penicillium* sp. cultivations remained constant at approximately 1.2 mPa s. The culture viscosity changed during the 45 h cultivation from 1.2 to 4.3 mPa s^{-1}.

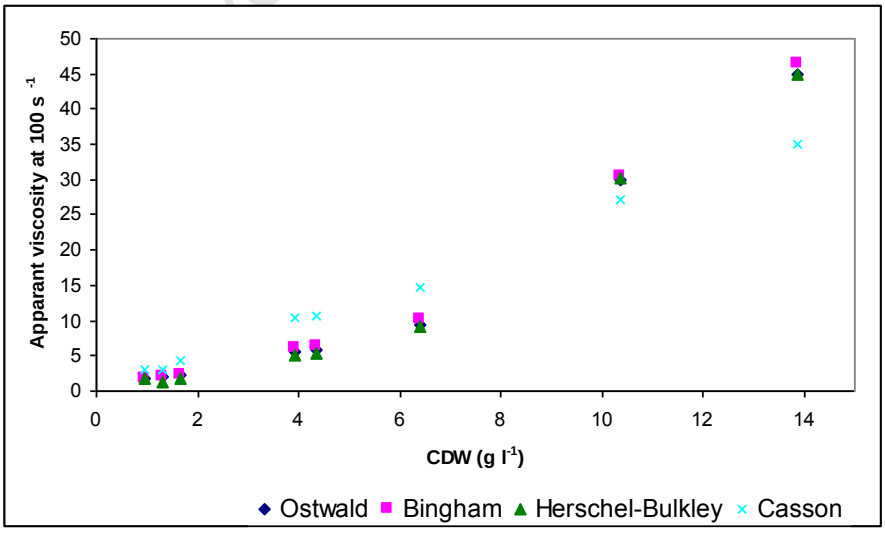

Figure 4.10 Apparent viscosity of *Penicillium* sp. vs. biomass concentration at 100 s^{-1} for different rheology models

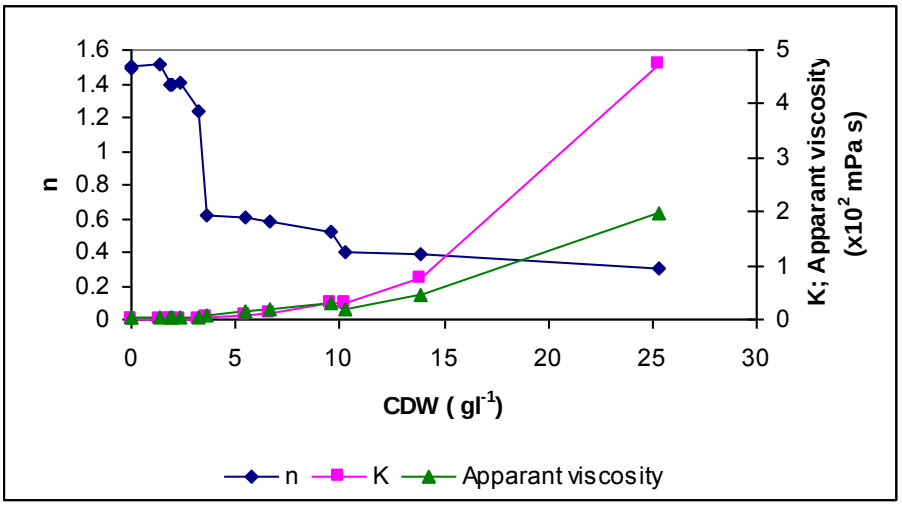

Figure 4.11 The power law index, consistency index and apparent viscosity at 100 s^{-1} for different *Penicillium* sp. biomass concentrations

The effect of using $Ca(OH)_2$ as pH control agents instead of NaOH on the biomass concentration and culture rheology was investigated and the results of the different rheology models are summarised in Table 4.8. From Table 4.8 it was shown that the values of the constant varies, even an order of magnitude while the changes in the exponent was small.

The change in the apparent viscosity during the cultivations using NaOH and $Ca(OH)_2$ as pH control agents are shown in Figure 4.12. The Ostwald rheology model was used to calculate the apparent viscosity. The apparent viscosity at the beginning of the cultivation was 1 mPa s and during the cultivation the apparent viscosity increased to 4.3 mPa s and 3.3 mPa s using NaOH and $Ca(OH)_2$ as pH control agent. This result indicates that the apparent viscosity of the *Penicillium* sp. culture is influenced by the pH control agent, albeit a small influence. It can be expected that culture morphology would influence viscosity. Culture morphology is presented later in Section 6.2.3.

The effect of biomass concentration on the apparent viscosity of *A. niger* and *Penicillium* sp. showed similar trends to that of literature but was less pronounced because the biomass concentrations were low during the cultivations (1.56 g l^{-1} for *A. niger* and 2.20 g l^{-1} for *Penicillium* sp.). The effect of using different pH control agents on the apparent viscosity of *Penicillium* sp. delivered a similar outcome.

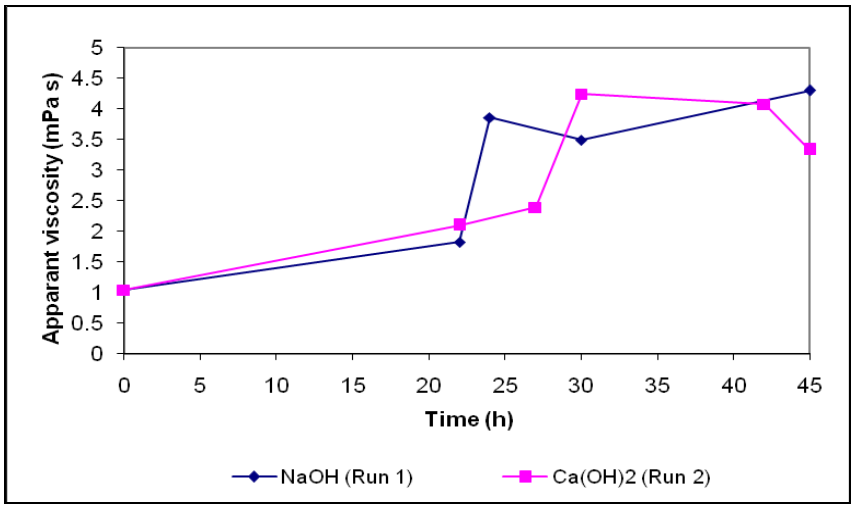

Figure 4.12 Apparent viscosity at 100 s^{-1} for NaOH- and $Ca(OH)_2$-controlled cultivations

Table 4.8 Rheological correlations for *Penicillium* sp. cultures using NaOH and $Ca(OH)_2$ as pH control agents

Microorganism	Rheological model	Variation of rheological parameters	Shear range (s^{-1})	Viscometer	Comments	References
Penicillium sp. CBS120262 Using NaOH as pH control agent	Power law Bingham Herschel-Bulkley Casson	$K = 1.3 \times 10^{-3} X^{2.3}$ $\tau_0 = 0.02\ X^{2.0}$ $K_p = 2.7 \times 10^{-3}\ X^{2.0}$ $\tau_0 = 4.9 \times 10^{-2} X^{1.4}$ $K_c = 0.040\ X^{0.16}$ $\tau_0 = 0.022\ X^{1.6}$	150 – 500 for all 4 models	Coaxial cylinder	Morphology changes not considered; $1<X<14$ g l^{-1}	Present study (From Table 4.7)
Penicillium sp. CBS120262 using $Ca(OH)_2$ as pH control agent[1]	Power law Bingham Herschel-Bulkley Casson	$K = 3.0 \times 10^{-4} X^{3.5}$ $\tau_0 = 0.01\ X^{2.5}$ $K_p = 7.0 \times 10^{-4}\ X^{2.3}$ $\tau_0 = 7.8 \times 10^{-3} X^{2.6}$ $K_c = 0.042\ X^{0.27}$ $\tau_0 = 2.4 \times 10^{-3} X^{3.0}$	150 – 500 for all 4 models	Coaxial cylinder	Morphology changes not considered; $1<X<21$ g l^{-1}	Present study
Penicillium sp. CBS120262 using $Ca(OH)_2$ as pH control agent[2]	Power law Bingham Herschel-Bulkley Casson	$K = 4.5 \times 10^{-4} X^{3.4}$ $\tau_0 = 0.08\ X^{2.5}$ $K_p = 4.0 \times 10^{-4}\ X^{2.2}$ $\tau_0 = 4.9 \times 10^{-2} X^{2.5}$ $K_c = 0.05\ X^{0.28}$ $\tau_0 = 0.022\ X^{2.9}$	150 – 500 for all 4 models	Coaxial cylinder	Morphology changes not considered; $0.5<X<11$g l^{-1}	Present study

[1] The CDW included the $Ca(OH)_2$ that was present when the sample was taken.

[2] The CDW was washed with 4N HCl to dissolve the $Ca(OH)_2$.

4.4 Conclusions

The growth of *A. niger* NRRL-3 and *Penicillium* sp. CBS120262 and associated production of GO was quantified, compared and the appropriate reproducibility was established. In both cultures GO was associated with growth. While glucose induces GO production, it was efficiently metabolised to GA. There was a direct relationship between the amount of GA produced and the amount of base needed to neutralise GA providing an indirect measure of GA produced. *Penicillium* sp. supported a higher biomass concentration, higher volumetric GO concentration and higher specific GO activity on reaching stationary phase than *A. niger*. A larger fraction of the GO produced from *Penicillium* was extracellular compared to *A. niger*.

Since *Penicillium* sp. was shown to produce more biomass and GO than *A. niger* it was used to study the effect of changing the pH control from NaOH to $Ca(OH)_2$ on the production of GO. Using $Ca(OH)_2$ as pH control agent influenced the production of GO favourably with an increase in the GO and biomass productivity. Specifically the extracellular GO activity increased 2.8 fold while the overall GO activity increased 2 fold.

Results indicated that with an increase in biomass concentration the culture apparent viscosity of *A. niger* and *Penicillium* sp. increased and that the rheological correlations obtained compared favourably with that of literature.

Chapter 5 Location of GO in *A. niger* NRRL-3 and *Penicillium* sp. CBS 120262

This chapter focused on four primary aspects. Firstly, the distribution of GO in *A. niger* was quantified in an attempt to explain the controversy in the literature regarding its location. Secondly, the influence of micro-organism used and its growth phase on enzyme location was examined. Thirdly, the effect of growth conditions, such as increasing the Ca^{2+} concentration, on the location of GO in *Pencillium* sp. cultures was investigated. Lastly, the effect of enzyme location on the subsequent protein recovery and purification processes was demonstrated through the analysis of the process yields through a series of simulated process trains. The calculations used in the procedure to determine the distribution of GO activity in the multiple sites are described in Appendix B.

5.1 Enzyme distribution in *A. niger* NRRL-3 cultures

Since enzyme location impacts enzyme recovery significantly, this study quantified the enzyme distribution between the extracellular fluid, cell wall and membrane fragments, cytoplasm and slime mucilage fractions in *A. niger*. The culture was separated into the individual fractions and the GO activity in each determined. The enzyme location across the mycelial fractions was further assessed through immunocytochemical labelling of GO.

The distribution of GO activity in the cell suspension was determined at the end of duplicate A. *niger* batch cultures when the total enzyme activity was highest (Figure 4.1). The extracellular fluid and the mycelia were separated and the mycelia were further divided into discrete fractions of slime mucilage, cytoplasm and cell wall and membrane fragments (Section 3.5). The fractional enzyme activities in each of the extracellular fluid, slime mucilage, cytoplasm and cell wall were determined and are presented in Table 5.1.

In early stationary phase, the enzyme activity was found to be predominantly associated with the mycelial fraction, with only 38% present in the extracellular fluid. This is contrary to the results of Mischak *et al*. (1985), who reported a predominantly extracellular location (75%). These authors conducted their studies in a Mn^{2+} deficient medium in which slime production was negligible suggesting that under conditions where slime production was significant, the finding of an intracellular location might be erroneously attributed to enzyme entrapment in the slime. In this study, however, only 16% of the total activity, in the mycelial associated fraction was due to entrapment in the slime

mucilage while approximately half of the total activity could be attributed to a truly intracellular location, namely the cytoplasm plus the cell wall and membrane fragments.

Table 5.1 The percentage of GO activity in the individual fractions of the *A. niger* culture harvested at early stationary phase

Location	Percentage GO activity		
	Batch 1	Batch 2	Average ± stdev
Extracellular fluid	42	33	38 ± 5
Slime mucilage	10	21	16 ± 6
Cell wall and membrane fragments	32	37	34 ± 2
Cytoplasm	16	9	12 ± 3
Extracellular liquid phase[1]	68	63	66 ± 3
Intracellular[2]	48	46	47 ± 1

[1] Extracellular liquid phase = extracellular fluid + slime mucilage + cytoplasm

[2] Intracellular = cell wall and membrane fragments + cytoplasm

Both cell wall and membrane fragments, and cytoplasm fractions contained appreciable GO activity, estimated as 34% and 12% of total GO respectively. A predominantly cell wall location was reported by Witteveen *et al*. (1992) and a predominantly cytoplasmic location by Van Dijken and Veenhuis (1980) (Table 2.7). The analyses of the activities in the mycelial fractions presented here suggest that, contrary to a dominant location, the enzyme is located in multiple sites.

To examine this contradiction in GO location, the intracellular presence of GO was further investigated using immunocytochemical labelling of the GO in the mycelia. Antibodies to the purified GO protein for *A. niger* were generated in rabbits (Technical assistance of the Animal Research Unit at the Faculty of Health Sciences acknowledged). SDS-PAGE and a Western Blot were used to confirm that the antibodies were specific for GO from *A. niger* and did not cross react with other *A. niger* proteins (Figure 5.1).

Transmission electron micrographs (TEM) of sections of *A. niger* mycelia at the end of duplicate batch cultures were examined. These micrographs showed GO in the cell wall and cytoplasm in viable (Figure 5.2a) and non-viable cells (Figure 5.2b). The labelling in these micrographs was confirmed to be specific for GO since the labelling using the pre-immune serum was statistically insignificant (95% confidence interval). In addition, the electron micrographs, showed a dependence of the location of enzyme on the cell viability. Although the enzyme was present in both the viable and non-viable cells, significant cytoplasmic enzyme was only observed in the non-viable cells. In the viable cells, the enzyme was predominantly associated with the cell wall with negligible amounts observed in the cytoplasm. These results indicate a statistical variation in the cell population, with respect to the cell

viability of the individual cells, with a corresponding variation in the intracellular site of the enzyme. This suggests that the conflicting intracellular sites reported in the literature may, at least in part, be a consequence of cells of different viability in the various studies exhibiting correspondingly different enzyme sites. When considering the viable cells alone, the results presented here support a significant fraction of GO associated with the cell wall location in agreement with the findings of Witteveen *et al.* (1992).

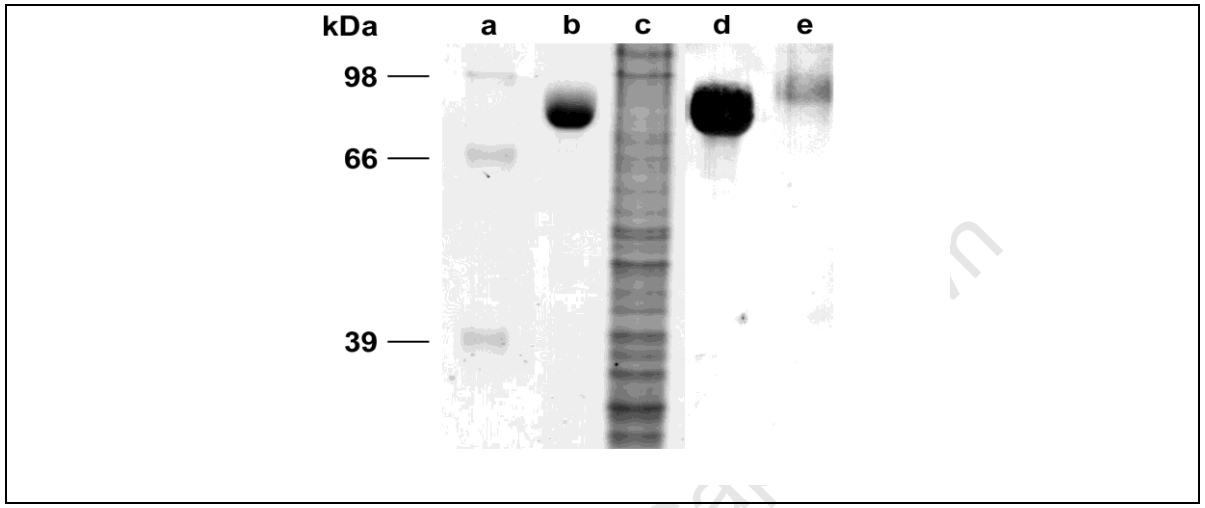

Figure 5.1 Combined SDS-PAGE (a –c) and Western blot (d and e). Lane a) Molecular marker (98, 66, 39, 21 6/4 Da), b) 5 µg commercial GO, c) 20 µl TCA homogenate, d) 5 µg commercial GO, e) 20 µl TCA homogenate

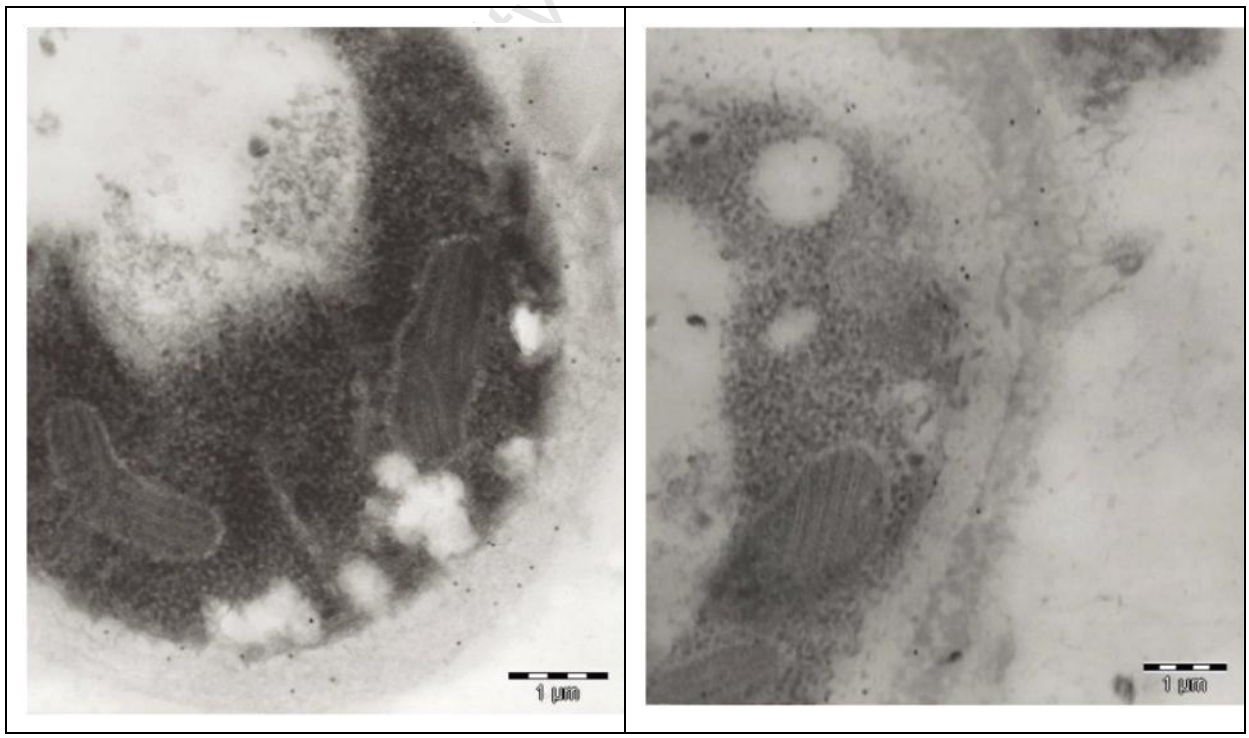

Figure 5.2(a) Transmission electron micrographs showing immunocytochemical labelling of GO in *A. niger* NRRL-3 depicting a viable cell after 25 hrs: 5 µg/ml of IgG (x 50,000)

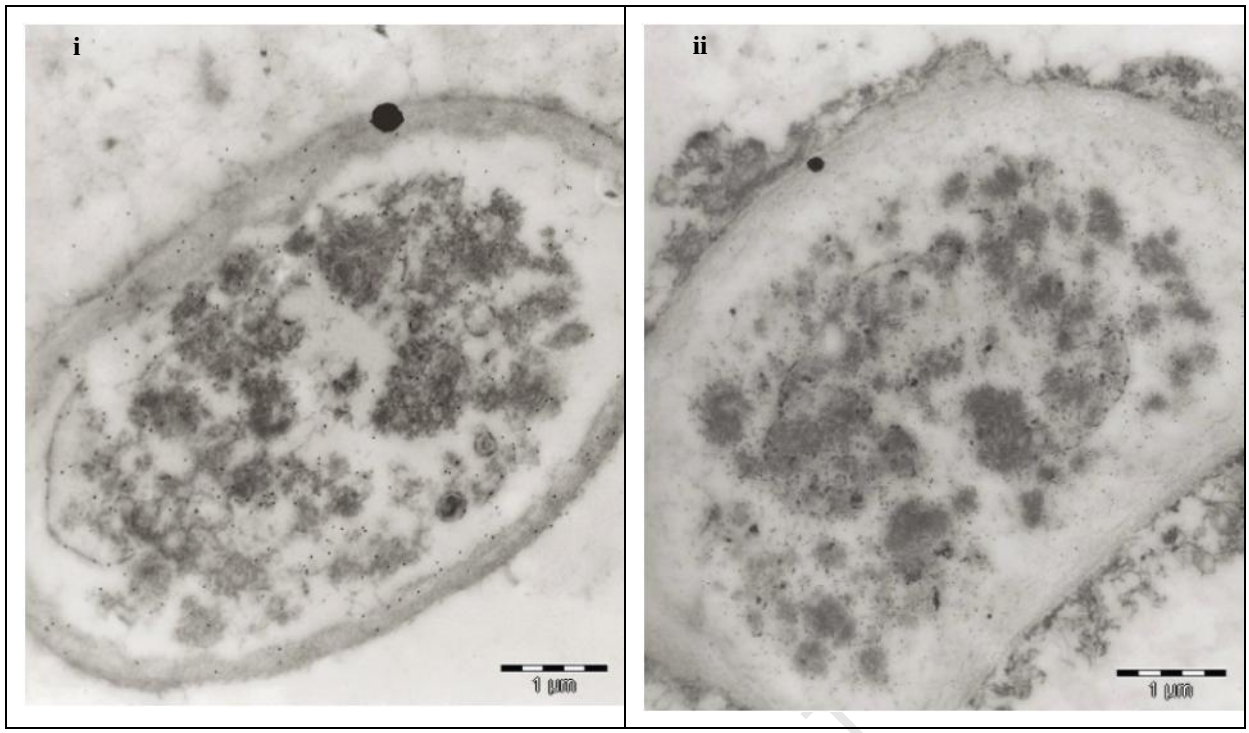

Figure 5.2(b) Transmission electron micrographs showing immunocytochemical labelling of GO in *A. niger* NRRL-3 depicting a non-viable cell after 25 hrs: 5 µg/ml of IgG ((i) magnification of 20,000 and (ii) magnification of 12,000)

An association of the enzyme with the cell wall was supported by the model of Chang and Trevithick (1974), based on the relative sizes of the enzyme and the pores in the cell wall. Measurements of the average pore size of the cell wall indicated that they were too small to allow passage of the enzyme. However, this average value was largely dependent on the pore size of the lateral walls in the hyphae. Further, it is reported that the apical tips are more porous than the lateral walls (Chang and Trevithick, 1974). Consequently, it may be postulated that enzyme secretion occurs dominantly through the apical tips and the enzyme becomes trapped in the cell wall as the porous apical wall is transformed into the non-porous lateral wall. Their model was based on the relative size of the enzyme, hence the diffusion of GO from *A. niger* is explored in the Section 5.1.1.

5.2 Diffusion coefficient of GO from *A. niger*

Diffusion is the transport of molecules from a high to a lower concentration and is represented by Fick's Law of diffusion (Equation 2.18) where the mass flux is proportional to the concentration gradient. The proportionality factor is the diffusion coefficient. The diffusion coefficient of GO across the cell envelope of *A.niger* was determined using an electron micrograph and correlations that was used to predict protein diffusion coefficients.

In Figure 5.2a an electron micrograph of an *A. niger* pellet at 25 h prepared according to the methodology presented in Section 3.6 is shown. The gold particles, labelling the GO antibody developed (Section 3.6), indicated the location of GO in the fungus which was mainly bound to the cell wall as discussed in Section 5.1. At 25 h the percentage GO associated with the cell wall was 34 ± 2%. The cell wall thickness measured from Figure 5.2a using analySIS® software was approximately 128.6± 8.3 nm, which is in agreement with the size range of the cell wall of fungi of between 100 and 250 nm (Atkinson and Mavituna, 1991 and Aiba, 1965). Therefore, the distance through which the GO molecule must diffuse to get to the external medium is approximately 130 nm. Messing *et al*. (1974) indicated that the size of a GO unit is 0.0084 µm and that the GO molecule can not enter a pore size less than 0.0168 µm (0.0084 x 2 = 0.0168). The diffusion coefficient of GO from *A. niger* was reported to be 4.12 x 10^{-7} cm^2 s^{-1} (Swoboda and Massey, 1965).

An initial estimate of the diffusivity of GO from *A. niger*, correlations from a study by Tyn and Gusek (1990) to predict the diffusion coefficients of proteins (Table 2.13) was used. The enzyme GO is made up of two identical subunits of M_w of approximately 80 kDa. The manomeric molecule is a compact spheroid with approximate dimensions of 60 Å x 52 Å x 37 Å. The corresponding dimensions of the dimer are 70 Å x 55 Å x 80 Å (http://chem.ch.huji.ac.il). Estimating the average molecular weight of the GO dimer as 180 kDa and the hydrodynamic radius as the largest of the three dimensions (80 Å), the diffusion coefficient can be calculated as 5.1 x 10^{-7} cm^2 s^{-1} and 2.1 x 10^{-7} cm^2 s^{-1} according to Eqn. 2.19 and Eqn 2.22 respectively. This is in agreement with the diffusion coefficient of 4.1 x 10^{-7} cm^2 s^{-1} obtained by Swoboda and Massey (1965) for GO from *A. niger* as well as a calculated and experimental diffusion coefficient value of 5.45 x 10^{-7} cm^2 s^{-1} and 5.13 x 10^{-7} $cm^2 s^{-1}$ for GO (Aragon and Hahn, 2006). Rinas *et al*. (2005) on the other hand reported a value of 5.6 x 10^{-6} cm^2 s^{-1} through regression.

5.3 The influence of micro-organism and growth phase on the distribution of GO in *Penicillium* sp. CBS 120262 and *A. niger* NRRL-3 cultures

5.3.1 Micro-organism

Using biomass fractionation as described in Section 3.5, the distribution of GO activity in the stationary phase cultures of *Penicillium* sp., and *A. niger* were compared (Table 5.2). In both *Penicillium* sp. and *A. niger* cultures, the GO activity was located in multiple sites, distributed between the extracellular fluid, slime mucilage, cell wall and membrane fragments and cytoplasm, although in different proportions. In *Penicillium* sp. cultures, the GO activity was located predominantly in the extracellular fluid (59%) while in *A. niger* cultures, only 38% of the GO activity was found in this

location, the majority being associated with the cell, intracellularly (46%) or trapped in the slime mucilage (16%). Notably, the cell envelope associated fraction was greatly reduced in *Penicillium* sp. (10%) compared with *A. niger* (34%). The extracellular predominance of GO in *Penicillium* sp. CBS 120262 cultures (59%) was in agreement with that reported for the *Penicillium* spp. used (Table 2.7) by Kusai *et al.* (1960), Nakamatsu *et al.* (1975) and Petruccioli *et al.* (1993), although Rando *et al.* (1997) reported an 80% intracellular activity in *P. pinophilum*. The predominance of cell associated GO in *A. niger* cultures (46%) is in agreement with Pazur (1966), van Dijken and Veenhuis (1990), Witteveen *et al.* (1992) and Hatzinilolaou and Macris (1995). Mischak *et al.* (1985), however, reported a predominance of GO (74%) in the extracellular fluid of *A. niger* (Table 2.7).

Table 5.2 GO location in duplicate stationary phase cultures of *Penicillium* sp. CBS 120262 and *A.niger* NRRL-3 (reported as % of total)

	Extracellular Fluid	Slime mucilage	Cell wall and membrane fragments	Cytoplasm	Intra-cellular*
Penicillium sp	59 ± 9	9 ± 2	10 ± 2	22 ± 6	32 ± 3
A. niger	38 ± 5	16 ± 6	34 ± 2	12 ± 3	46 ± 2

* Intracellular = cytoplasm plus cell wall and membrane fragments

Multiple sites for the location of enzymes in fungi could be explained by the intracellular synthesis of proteins during microbial growth and their subsequent secretion into the extracellular fluid (Peberdy 1994). The diffusion of a protein through the cell wall depends on its size relative to the porosity of the wall (Peberdy 1994) and it was postulated to more likely occur through the porous apical hyphal tips, rather than through the less porous lateral walls (Chang and Trevithick 1974; Wörsten et al.1991). As the hyphae lengthen, the porous apical walls are converted to the less porous lateral walls, and during transit, the proteins may become trapped in the wall (Chang and Trevithick 1974). This hypothesis pertaining to the secretion of fungal proteins may account for a proportion of the GO activity remaining in the cytoplasm, while the rest is either in the extracellular fluid or associated with the cell wall, and membrane. Under conditions where slime is produced, some of the GO may also be trapped in the slime mucilage (Mischak *et al.*, 1985).

The larger portion of GO activity in the extracellular fluid in the *Penicillium* sp. as opposed to that in the *A. niger* cultures was largely attributable to lower amounts being trapped in the cell wall, membrane and slime mucilage during transit from the cytoplasm to the extracellular fluid. In *Penicillium* sp., the GO activity in the cell wall and membrane (10%) was considerably lower than that in *A. niger* (34%). Similarly, in *Penicillium* sp., the GO activity in the slime mucilage (9%) was lower

than that in *A. niger* (16%). The greater entrapment of *A. niger* GO in the cell wall and membrane might be explained by the larger size of *Aspergillis* GO (186 kDa) (Swoboda and Massey, 1965)) relative to *Penicillium* GO (*P. amagasakiense* 154 kDa; *P. notatum* 152 kDa) (Swoboda and Massey, 1965). The greater entrapment of *A. niger* GO in the slime mucilage might be a consequence of the larger *A. niger* GO, but might also be due to the relatively lower diffusivity of this protein. The diffusion coefficients of GO from *A. niger* and *P. amagasakiense* are reported as 4.12×10^{-7} and 5.02×10^{-7} $cm^2.s^{-1}$, respectively (Swoboda and Massey, 1965). Differences in the cell wall structures of these organisms have not been studied. The GO entrapment in the cell wall and slime mucilage had a significant influence on the GO activity in the extracellular fluid. Despite the greater amount of GO activity in the *Penicillium* sp. cytoplasm (22%) than in the *A. niger* cytoplasm (12%), the fraction of GO in the extracellular fluid in the *Penicillium* sp. cultures (59%) was 1.6-fold higher than that in the *A. niger* cultures (38%), due to reduced entrapment in the cell envelope.

5.2.2 Growth phase

To investigate the effect of the growth phase on GO location and its implication with respect to time of harvest, the GO distribution during the mid-exponential phase in the *Penicillium* sp. and *A. niger* cultures was quantified and compared with that found in the stationary phase cultures. The distribution of GO in mid-exponential phase was determined in the 27 h *Penicillium* sp. culture (Figure 4.2) and in the 15.5 h *A. niger* culture (Figure 4.1). The distribution of the GO activity in the mid-exponential phase cultures, provided in Table 5.3, differed widely from that in the stationary phase cultures (Table 5.2). In particular, the mid-exponential phase GO activity in *Penicillium* sp. and *A. niger* cultures resided predominantly in the intracellular (53%) and extracellular (46%) fractions respectively, opposite to that found in the stationary phase cultures.

The degree of entrapment in the cell wall and slime mucilage played a dominant role in the variation in GO location with growth phase. As *Penicillium* sp. progressed from exponential growth to the stationary phase, a decrease in GO in both the cytoplasm (35% to 22%) and in the cell wall (18% to 10%) was observed. A decrease in the GO trapped in the slime mucilage (17% to 9%) was also observed. In *A. niger* cultures, the GO in the cytoplasm decreased from 16% to 12% but entrapment in the cell wall increased from 26% to 34% as did the entrapment in the slime mucilage (12% to 16%). In both *Penicillium* sp. and *A. niger* cultures, the fraction of GO in the cytoplasm decreased with the progression from the active growth phase to the stationary phase (1.6-fold and 1.3-fold respectively). In *Penicillium* sp. cultures this translated to a decreased intracellular GO (2.4-fold). The extracellular GO fraction was further enhanced by a decrease in the GO trapped in the slime mucilage (1.9-fold). In *A. niger* cultures, in contrast, an increased entrapment in the cell wall (1.3-fold) eclipsed the decrease in the cytoplasm and a marginal increase in the intracellular GO fraction (1.1-fold) resulted. The

increased entrapment in the slime mucilage (1.3-fold) further decreased the fraction of GO found extracellularly.

Table 5.3 GO location in mid-exponential phase cultures of *Penicillium* sp. CBS 120262 and *A. niger* NRRL-3 (reported as % of total)

	Extracellular fluid	Slime mucilage	Cell wall and membrane fragments	Cytoplasm	Intra-cellular*
Penicillium sp	30 ± 1	17 ± 2	18 ± 2	35 ± 2	53 ± 1
A. niger	46 ± 2	12 ± 2	26 ± 4	16 ± 1	42 ± 3

*Intracellular = cytoplasm plus cell wall and membrane fragments

The variation in the distribution of GO on progression from the active growth phase to the stationary phase between the two organisms suggests differing limiting stages in the secretion and entrapment of the enzyme in these organisms. In order to compare the differences in the enzyme secretion and entrapment, the specific GO in each location was calculated by multiplying the total specific GO activity by the fraction of GO in each of the locations and is compared in Table 5.4. The specific GO activity, rather than their volumetric equivalents, was examined so as to negate the influence of cell concentration on GO activity, since cellular growth had not yet been optimised.

The stationary phase total specific GO activity for *Penicillium* sp. was 3591 U g^{-1} (120 µkat g^{-1}), 25% higher than for *A. niger* at 2867 U g^{-1} (96 µkat g^{-1}). Similarly, in the mid-exponential phase the total specific GO activity for *Penicillium* sp. of 3813 U g^{-1} (127 µkat g^{-1}) was higher than for *A. niger* at 3152 U g^{-1} (105 µkat g^{-1}). This indicates that while *Penicillium* sp. and *A. niger* had similar growth rates (0.15 h^{-1} and 0.16 h^{-1} respectively), the amount of GO produced per cell was 1.2-fold higher for *Penicillium* sp. than that produced by *A. niger*. Further, for both species the total specific GO activity was higher in the exponential growth phase than in the stationary phase, whereas the volumetric GO activity was maximum in the stationary phase where the cell concentration was highest.

During the progression from the mid-exponential to stationary phase in *Penicillium* sp. cultures, the specific GO activity decreased from 1335 U g^{-1} (44 µkat g^{-1}) to 790 U g^{-1}(26 µkat g^{-1}) (1.7-fold) in the cytoplasm and from 686 U g^{-1} (23 µkat g^{-1}) to 359 U g^{-1} (12 µkat g^{-1}) (1.9-fold) in the cell wall and membrane fragments. Conversely the specific GO activity in the extracellular fluid increased from 1144 U g^{-1} (38 µkat g^{-1}) to 2119U g^{-1} (71 µkat g^{-1}) (1.9-fold).

Table 5.4 Specific GO activity in stationary and mid-exponential phases in *Penicillium* CBS 120262 and *A. niger* NRRL-3

	Total	Extra-Cellular fluid	Slime mucilage	Cell wall and membrane fragments	Cytoplasm
Penicillium sp **- Mid-exponential phase (27 h)**					
% GO		30	17	18	35
Specific GO activity (U g^{-1})	3813	1144	648	686	1335
(µkat g^{-1})	(127)	(38)	(22)	(23)	(44)
Penicillium sp – **Stationary phase (45 h)**					
% GO		59	9	10	22
Specific GO activity (U g^{-1})	3591	2119	323	359	790
(µkat g^{-1})	(120)	(71)	(11)	(12)	(26)
***A. niger* - Mid-exponential phase (15.5 h)**					
% GO		46	12	26	16
Specific GO activity (U g^{-1})	3152	1450	378	820	504
(µkat g^{-1})	(105)	(48)	(13)	(27)	(17)
***A. niger* - Stationary phase (25 h)**					
% GO		38	16	34	12
Specific GO activity (U g^{-1})	2867	1089	459	975	344
(µkat g^{-1})	(96)	(36)	(15)	(33)	(12)

Similarly, during the progression from mid-exponential to stationary phase in *A. niger* cultures the specific GO activity in the cytoplasm decreased from 504 U g^{-1} (17 µkat g^{-1}) to 344 U g^{-1}(12 µkat g^{-1}) (1.5 fold). In contrast to *Penicillium* sp., however, the specific GO activity in the cell wall and membrane fragments increased from 820 U g^{-1} (27 µkat g^{-1}) to 975 U g^{-1} (33 µkat g^{-1}) (1.2-fold) and the specific GO activity in the extracellular fluid decreased from 1450 U g^{-1} (48 µkat g^{-1}) to 1089 U g^{-1} (36 µkat g^{-1}) (1.3-fold). Further, the specific GO activity in the slime mucilage decreased in *Penicillium* sp. from 648 U g^{-1} (22 µkat g^{-1}) to 323 U g^{-1} (11 µkat g^{-1}) (2.0-fold) and increased in *A. niger* from 378 U g^{-1} (13 µkat g^{-1}) to 459 U g^{-1} (15 µkat g^{-1}) (1.2-fold).

These trends mirror those observed in the percentage GO activity in the locations (Table 5.3) and suggest that transport of the GO from the cell may be the rate limiting step and is only partially achieved during the rapid enzyme production associated with the growth phase. The decrease of specific GO in the extracellular fluid of *A. niger* as the culture progresses from exponential growth phase to stationary phase raises the question as to whether it would be better to harvest this organism during the exponential phase instead of the stationary phase. In the exponential phase, maximal CDW has not yet been reached (Figures 4.1 and 4.2), and so a compromise is required between the specific

GO activity produced, the CDW attained and the extracellular GO fraction. For the *Penicillium* sp. cultures, where the specific GO activity increased as the culture progressed from exponential to stationary phase with increasing CDW, the volumetric GO activity and extracellular fraction of GO reached a maximum in the stationary phase, where it is clearly preferable to harvest the culture.

5.4 The effect of increasing Ca^{2+} availability by using $Ca(OH)_2$ as pH control agent, on the location and recovery of GO in *Penicillium* sp. CBS 120262

The distribution of GO activity in the cell suspension was determined at the end of *Penicillium* sp. batch cultures using $Ca(OH)_2$ as pH control agent. The GO activity found in each of the fractions: extracellular fluid, slime mucilage, cytoplasm and combined cell wall and membrane fragments were quantified and are compared with those of NaOH in Table 5.5. In $Ca(OH)_2$ cultures, the GO was located predominantly in the extracellular fluid (93%) while in the NaOH cultures only 59% of the GO activity was found in this location which translates to a 1.6 fold increase.

Table 5.5 Fractionation of GO across the cell location for stationary phase *Penicillium* sp. CBS 120262 cultures using NaOH or $Ca(OH)_2$ as pH control agents

	Average % GO activity and standard deviation of *Penicillium* sp.	
	NaOH*[1]	**$Ca(OH)_2$**
Extracellular fluid	59 ± 9	93 ± 0.1
Slime mucilage	9 ± 2	1 ± 0.5
Cell wall and membrane fragments	10 ± 2	3 ± 1
Cytoplasm	22 ± 6	3 ± 0.4
Intracellular*[2]	32 ± 3	6 ± 0.3

*[1] Values from Table 5.2

*[2] Intracellular = cytoplasm plus cell wall and membrane fragments

The $Ca(OH)_2$ results indicate that the progression of GO from the cytoplasm through the cell wall and slime mucilage to the extracellular medium was fast compared to that of NaOH for the same duration (45 h). This is demonstrated by the specific productivity of the extracellular GO which increased by a factor of approximately two. For example, the fraction of GO in the cytoplasm was 7.3-fold lower than that of NaOH. The fraction of GO trapped in the cell wall and membrane fragments was 3.3-fold lower than NaOH, indicating that $Ca(OH)_2$ might assist in increasing the permeability of the cell wall.

Similarly, the GO trapped in the slime mucilage after progression from the cell wall was 9-fold lower than for NaOH.

5.5 Impact of enzyme location on downstream recovery

The results of enzyme location reported above has significant consequences for the efficacy of downstream enzyme recovery (Section 2.8.1). Typically downstream unit operations either recover and purify the enzyme from the extracellular culture supernatant phase (Fig. 5.3 A) or from the biomass phase, the latter after disruption to release intracellular content. The advantage of having the majority of enzyme in the extracellular liquid is the simplified purification process, owing to fewer contaminating proteins in the extracellular fluid than in the cell extract. Processing of an intracellular enzyme necessitates cell disruption followed by the fractionation of the enzyme from a more complex mix of metabolites typically requiring more process steps. Since it is generally only economically viable to purify the enzyme from either the liquid or the solid, a choice has to be made as to whether the liquid stream or the solids portion are to be processed after solids separation with the enzyme located in the other fractions being lost. This loss is likely to be even greater since the maximum enzyme recovery is reduced due to losses during purification, the latter being affected by number of process steps. Therefore, under conditions where the enzyme is partitioned equally between the extracellular fluid and mycelia, processing of either of the liquid or solid streams alone is unsuitable.

An alternative downstream processing option is investigated for this mixed location product, involving disruption of the mycelia before separation, followed by processing of the liquid stream (Figure 5.3B). Part of the enzyme associated with the mycelia would be released into the liquid stream, thereby increasing the activity in this stream. Under these conditions, the activity in the liquid stream includes the activity in the cytoplasm, the slime mucilage and extracellular fluid, with the remaining activity being discarded with the cell wall fragments.

In the case of the GO activity in the stationary phase cultures, processing the liquid after solids separation would lead to a maximum possible recovery of 59% and 38%, in *Penicillium* sp. and *A. niger* respectively, with the rest being lost through discarding the solids (Table 5.6).

Purifiying GO following cell disruption of the stationary phase cultures would result in a maximum possible enzyme recovery of 90 and 66% for *Penicillium* sp. and *A. niger* respectively (Table 5.6). Similar trends were evident when examining the recovery of activity from the liquid from cultures harvested in mid-exponential phase. Inclusion of a disruption stage prior to solids separation

increased the possible recovery from 30% to 82% for *Penicillium* sp. and from 46% to 74% for *A. niger* (Table 5.6).

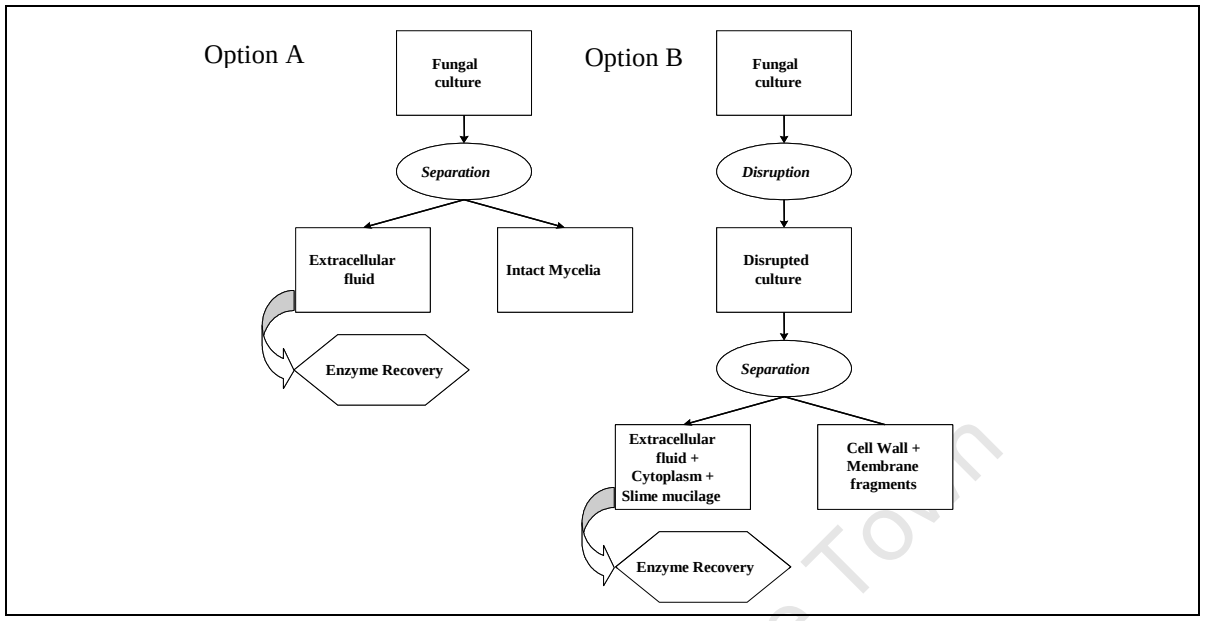

Figure 5.3 Recovery of GO activity from a liquid stream with (B) and without (A) disruption of the mycelia

Table 5.6 Comparison of the maximum possible recovery of GO activity in *Penicillium* CBS 120262 and *A. niger* NRRL-3 cultures in stationary and mid-exponential phases (reported as % of total)

	Max. recovery from liquid (no disruption stage) [*1]	Max. recovery from liquid (disruption stage included) [*2]
Stationary phase		
Penicillium sp	59 ± 9	90 ± 2
A. niger	38 ± 5	66 ± 3
Mid-exponential phase		
Penicillium sp	30 ± 1	82 ± 3
A. niger	46 ± 2	74 ± 4

[*1] Liquid refers to contribution from extracellular fluid

[*2] Liquid refers to contribution from extracellular fluid + cytoplasm + slime mucilage

Investigating the effect of $Ca(OH)_2$ on the recovery of GO from the liquid phase after disruption of the culture and recovery of the liquid phase without disruption was compared with the NaOH cultivation in Table 5.7. For $Ca(OH)_2$ there was a marginal increase in maximum theoretical recovery from 93% without disruption to 97% with disruption, while there was an increase in the maximum theoretical recovery of GO from the NaOH cultivation from 59% to 90% by disrupting the culture first.

Table 5.7 Comparison of the maximum possible recovery of GO activity in *Penicillium* sp. CBS 120262 using NaOH or $Ca(OH)_2$ as pH control agents (reported as % of total)

	Recovery from liquid (no disruption)	Recovery from liquid (disruption)
NaOH*	59 ± 9*	90 ± 2*
$Ca(OH)_2$	93 ± 0.1	97 ± 0.8

* Values from Table 5.5

The results were further analysed to consider the impact of mixed location on downstream processing (DSP) using cultures of *A. niger* and *Penicillium* sp. grown using NaOH for pH control to evaluate the potential value of purifying GO from the liquid after solids separation in comparison to purifying the GO from the liquid after disruption and solids separation (extracellular, cytoplasmic and mucilage associated product). The impact of the number of purification stages in these two alternatives needs was also assessed. As a case study it was assumed that three purification stages (e.g. ultra-filtration, selective precipitation and crystallisation) suffice to purify GO from the extracellular fluid (Route 1), whereas disruption and five purification stages (e.g. ultra-filtration, selective precipitation (x2), affinity chromatography and crystallization) were required to obtain the same purity of GO from the combined cell extract including extra- and intra-cellular proteins (Route 2). It was assumed that the yield of each recovery stage was 97%. By combining these yields with the specific GO activity at the time of harvest (stationary phase or exponential phase), the specific GO activity after recovery was calculated and is presented in Table 5.8. By normalising the activity recovered with respect to recovery of GO from the extracellular fluid from stationary phase *A. niger* cultures, comparison is easily made across micro-organism used, harvest time and process route.

The normalised values increased significantly if the disruption stage was included, despite the need for extra processing stages. In stationary phase cells, this value increased from 1 to 1.59 and 1.94 to 2.71 for *A. niger* and *Penicillium* sp. respectively. Similarly, in mid-exponential phase cells, this value increased from 1.33 to 1.95 and 1.05 to 2.62 for *A. niger* and *Penicillium* sp. respectively. For the recovery of GO from the mixed location environment achieved in the presence of NaOH, there is a definite benefit potential in recovering GO from the combination of the extracellular fluid and cell extract. Economic analysis remains to be considered.

When comparing the specific GO recovered for each organism in the two different growth phases, it is evident that the greatest capacity of *A. niger* cells to produce GO activity was in the growth phase, a capacity which decreased during the transition to stationary phases, when the cell concentration was substantially increased. This clearly demonstrates a need for a compromise between the high GO production per cell and low cell concentration on the one hand, and lower GO production per cell and high cell concentration on the other.

Table 5.8 Comparison of predicted GO recovery from *A. niger* NRRL-3 and *Penicillium* CBS 120262 cultures across two process routes, relative to GO recovery from extracellular fluid of *A. niger*. Route 1 considers recovery of the extracellular GO using three disruption and purification steps. Route 2 considers recovery from the liquid phase resulting after cell disruption using a subsequent five step process train. (a) Stationary phase cultures (b) Mid-exponential cultures

Portion to be processed	Microorganism	Number of recovery stages at 97% yield	Maximum theoretical recovery (%)	Overall GO activity recovered*	GO in extract/ GO in extracellular fluid of *A. niger*
(a)					
Extracellular fluid	*A. niger*	3 stages	38	0.35 of 2867 U g^{-1} = 994 U g^{-1}	1.00
Extract from extracellular fluid plus cell lysate	*A. niger*	Disruption and 5 stages	66	0.55 of 2867 U g^{-1} = 1576 U g^{-1}	1.59
Extracellular fluid	*Penicillium* sp	3 stages	59	0.54 of 3591 U g^{-1} = 1934 U g^{-1}	1.94
Extract from extracellular fluid plus cell lysate	*Penicillium* sp	Disruption and 5 stages	90	0.75 of 3591 U g^{-1} = 2692 U g^{-1}	2.71
(b)					
Extracellular fluid	*A. niger*	3 stages	46	0.42 of 3152 U g^{-1} = 1323 U g^{-1}	1.33
Extract from extracellular fluid plus cell lysate	*A. niger*	Disruption and 5 stages	74	0.62 of 3152 U g^{-1} = 1943 U g^{-1}	1.95
Extracellular fluid	*Penicillium* sp	3 stages	30	0.27 of 3813 U g^{-1} = 1044 U g^{-1}	1.05
Extract from extracellular fluid plus cell lysate	*Penicillium* sp.	Disruption and 5 stages	82	0.68 of 3813 U g^{-1} = 2604 U g^{-1}	2.62

* Calculated as the product of the combined stage yields, the maximum recovery and the specific GO activity. As an example: For the recovery of extract from the extracellular fluid for stationary phase *A. niger*, where three purification stages are required, GO recovered = 0.97^3*0.38*2867 U g^{-1}= 0.35*2867 U g^{-1}. Similarly, for the recovery from the extracellular fluid cell lysate, where six purification stages are required GO recovered = 0.97^6*0.66*2867 U g^{-1}= 0.55*2867 U g^{-1}.

Since the specific GO recovered was based on an assumed 97% yield in each purification stage (Table 5.8), the sensitivity of the data to different yields was assessed by comparing the normalised values at 98%, 97%, 95%, 85% and 80% step yields (Table 5.9). In Table 5.9 the relative yields are considered in each case as a fraction of that obtained on recovery of extracellular GO using a three-step process at the defined yield. The overall yield of GO recovery from the extracellular fluid of *A. niger* where only three purification stages were involved decreased with a decreasing unit operation yield from 1.00 at

97% step yield to 0.80 at 90% step yield, 0.67 at 85% step yield and 0.56 at 80% step yield. This decrease is accentuated with increased number of downstream unit operations. Using disruption and five purification stages, recovery of GO decreased from a normalised 1.00 at a 97% step yield in the absence of disruption to 0.64 at 90% step yield, 0.45 at 85% step yield and 0.31 at 80% step yield.

The recovery from the liquid after disruption, where 5 purification stages were required, decreased significantly as the yield decreased, such that at 85% yield, little or no difference was obtained in the recovery of GO, irrespective of the purification programme. Hence the benefit of disruption before solids separation and purification of the combined cell extract and extracellular fluid resulting in a greater recovery of GO activity holds only at high recovery yields on individual unit operations. At low yields, this route is doubly unfavourable, leading to both a reduced GO recovery and at a higher recovery cost.

Expanding the case study for $Ca(OH)_2$, it was assumed that three purification stages (e.g. ultra-filtration, selective precipitation and crystalisation) would suffice to purify the GO from the extracellular fluid, whereas five purification stages (e.g. ultra-filtration, selective precipitation (x2), affinity chromatography and crystallization) are required to obtain the same purity of GO from the extracellular fluid plus the cell extract. In the case of $Ca(OH)_2$ two extra steps were included to remove the insoluble Ca^{2+} (dissolving Ca^{2+} with 4N HCl and then water washing) before the biomass was disrupted to release the intracellular content. It was further assumed that the yield of each recovery stage was 97%. By combining these yields with the specific GO activity at the time of harvest (stationary phase), the specific GO activity after recovery was calculated (Table 5.10). These were normalised with respect to recovery of GO from the extracellular fluid from the NaOH cultivation.

The normalised values (Table 5.10) increased significantly if the disruption stage was included, despite the need for extra processing stages. For the 97% yield per stage case study in stationary phase, this value increased from 1 to 1.39 for NaOH whereas for the $Ca(OH)_2$ case the value decreased from 1.66 to 1.49. Therefore in GO recovery, there was a definite benefit in recovering GO from the combination of the extracellular fluid and cell extract in the NaOH case but not in the $Ca(OH)_2$ case for which greater than 90% extracellular location was shown.

Table 5.9: Sensitivity analysis of the predicted recovery of GO from stationary and mid-exponential phase *A. niger* NRRL-3 and *Penicillium* sp. CBS120262 cultures

Approach	**Microorganism**	**Number of recovery stages**	**GO in extract/ GO in extracellular fluid of *A. niger***					
			98% yield per stage	**97% yield per stage**	**95% yield per stage**	**90% yield per stage**	**85% yield per stage**	**80% yield per stage**
Extracellular fluid	*A. niger* in stationary phase	3 stages	1.00	1.00	1.00	1.00	1.00	1.00
Extract from fluid and cell lysate	*A. niger* in stationary phase	Disruption and 5 stages	1.63	1.59	1.49	1.27	1.07	0.89
Extracellular fluid	*Penicillium* sp. in stationary phase	3 stages	1.94	1.94	1.94	1.94	1.94	1.94
Extract from fluid and cell lysate	*Penicillium* sp. in stationary phase	Disruption and 5 stages	2.79	2.71	2.54	2.16	1.82	1.52
Extracellular fluid	*A. niger* in growth phase	3 stages	1.33	1.33	1.33	1.33	1.33	1.33
Extract from fluid and cell lysate	*A. niger* in growth phase	Disruption and 5 stages	2.02	1.95	1.84	1.56	1.31	1.10
Extracellular fluid	*Penicillium* sp. in growth phase	3 stages	1.05	1.05	1.05	1.05	1.05	1.05
Extract from fluid and cell lysate	*Penicillium* sp. in growth phase	Disruption and 5 stages	2.70	2.62	2.46	2.09	1.76	1.47

Table 5.10: Sensitivity analysis of the predicted recovery of GO from stationary phase *Penicillium* sp. CBS 120262 cultures using NaOH or $Ca(OH)_2$ as pH control agents

Approach	**Microorganism**	**Number of recovery stages**	**GO in extract/ GO in extracellular fluid of *Penicillium* sp. (NaOH)**					
			98% yield per stage	**97% yield per stage**	**95% yield per stage**	**90% yield per stage**	**85% yield per stage**	**80% yield per stage**
Extracellular fluid	*Penicillium* sp. NaOH	3 stages	1.00	1.00	1.00	1.00	1.00	1.00
Extract from fluid and cell lysate	*Penicillium* sp. NaOH	Disruption and 5 stages	1.43	1.39	1.31	1.11	0.94	0.78
Extracellular fluid	*Penicillium* sp. $Ca(OH)_2$	3 stages	1.66	1.66	1.66	1.66	1.66	1.66
Extract from fluid and cell lysate	*Penicillium* sp. $Ca(OH)_2$	Disruption and 7 stages	1.57	1.49	1.34	1.03	0.77	0.57

5.6 Conclusions

GO activity was shown to be located in multiple sites in both *Penicillium* sp. and *A. niger* cultures carried out under standard conditions *viz.* in the extracellular fluid, slime mucilage surrounding the cell, cytoplasm and cell wall and membrane fraction. The distribution between these sites depended on the micro-organism used and on the growth stage in which it was harvested. The results showed that as the cultures moved from active growth to the stationary phase, more enzyme was secreted from the cytoplasm. In *Penicillium* sp. this resulted in an increase in GO activity in the extracellular fluid. In *A. niger* cultures, however, the concurrent increased GO entrapment in the cell envelope reduced the fraction of GO activity in the extracellular fluid. Since the distribution of activity varied with growth phase, the GO recovered depended on the time at which the culture was harvested.

The specific GO activity in *A. niger* decreased on progression from growth to stationary phase. Further, increased entrapment of GO in the cell envelope of stationary phase *A. niger* was observed. This illustrates the need for an optimisation approach to select preferred harvest time which gives integrated consideration of enzyme location, specific activity and biomass concentration.

The overall specific GO activity in *Penicillium* sp. was 1.2-fold greater than that in *A. niger*. This indicated that *Penicillium* sp. showed a better productivity of GO activity than *A. niger*, since the specific growth rates of the two organisms were the same. Further, the maximum cell concentration was enhanced in the *Penicillium* culture, resulting in a greater volumetric GO activity. These observations, and the coincident occurrence of the maximal specific GO activity, maximal cell concentration and maximal extracellular location, makes *Penicillium* sp. CBS 120262 a preferred choice over *A. niger* NRRL-3 for GO production.

The GO activity recovered at the end of the process depends not only on the organism, growth phase and time of harvest, but also on the purification programme used. When comparing recovery directly from the extracellular fluid (after solids separation) with recovery from the combination of the extracellular fluid and cell extract (after disruption and solids separation), it was clear that the relative merits of these two routes, in either organism, depended strongly on the recovery yield attainable in each step. Where a 97% yield for each step is achieved, and recovery and purification is achieved by a three step process in the absence of cell disruption or a five step process following cell disruption, the inclusion of cell disruption is shown to increase enzyme recovery from cultures demonstrating multiple sites of enzyme location, significantly.

The use of $Ca(OH)_2$ as pH control agent affected the location of GO in the stationary phase culture of *Penicillium* sp. The fraction of GO in the extracellular medium in the presence of $Ca(OH)_2$ compared to that of NaOH at the same time point (45 h) increased by 1.6-fold. The fraction of GO trapped in the cell wall and membrane fragments was 3.3-fold lower than NaOH, indicating that $Ca(OH)_2$ might assist in increasing the permeability of the cell wall. Similarly, the GO trapped in the slime mucilage after progression from the cell wall was 9-fold lower than for NaOH.

In all cultures, a proportion of the GO was associated with the cell envelope. This was accentuated in the presence of NaOH and particularly with *A. niger*. It has been postulated previously that enzyme secretion occurs dominantly through the apical tips and that the enzyme becomes trapped in the cell wall as the porous apical wall is transformed into the non-porous lateral wall. To further investigate this, the secretion of GO and its subsequent location in the fungi was further expanded by investigating the morphology of the micro-organism and the relative rates of enzyme formation and secretion in the next chapter.

Chapter 6 Fungal Morphology and GO transport

The morphology of the fungal cultures changes during growth and influences the productivity and viscosity of the culture. To date, investigation of the relationship between morphology and GO secretion presented in the literature has been limited to macro-morphology using systems of *Aspergillus* characterised by a pelleted growth, unlike the mycelial growth characteristic of *Penicillium*. These relationships are further investigated in this chapter with the emphasis on mycelial *Penicillium* cultures. Since the production of GO was higher in *Penicillium* sp cultures (Section 4.1.3) and its shift to a predominant extracellular location of more marked (Section 5.3), the study was focussed on the changes in *Penicillium* sp. morphology and associated GO location, with limited study of *A. niger* cultures. The changes in the morphology of an *A. niger* cultivation is presented in Section 6.1.

Section 6.2 focuses firstly on *Penicillium* sp. CBS 120262 morphology. The work of Metz *et al*. (1981), Adams and Thomas (1988), Packer and Thomas (1990), Tucker *et al*. (1992), Cox and Thomas (1992), and Reichl *et al*. (1992) was used as a starting point for use of image analysis to quantify the morphological changes during cultivation. A set of semi-automated image analysis routines was developed using the image analysis software analySIS®. These routines yielded morphological indices through empirical correlations with the outputs of the analySIS® software. The semi-automatic image processing steps were validated by comparison with the manual measurements and the number of individual hyphal measurements required for statistically valid results was determined. Secondly, the changes in the morphological indices during cultivation of *Penicillium* sp. CBS 120262, quantified through image analysis, were investigated. Thirdly, the effect of using $Ca(OH)_2$ as a different pH control agent on *Penicillium* sp. morphology was investigated.

In Section 6.3 the effect of *A. niger* and *Penicillium* sp. morphology on the rheology of the fungal cultures was investigated. The relationship between the changes in the morphological indices of *Penicillium* sp., secretion and transport of GO from the organism is described in Sections 6.4 and 6.5

6.1 *Aspergillus niger* NRRL-3 morphology

The coagulating nature of *A. niger* spores, following inoculation of a shake flask using a spore suspension washed off an agar plate is illustrated in Figure 6.1. From these coagulating spores, clumps (Fig. 6.2a) formed which developed into pellets. These pellets changed in shape and size from fluffy pellets during the growth phase (Fig 6.2b) into pellets with a looser outer zone (Fig.6.2c) to more compact pellets with a hairy perimeter in the stationary phase (Fig. 6.2d).

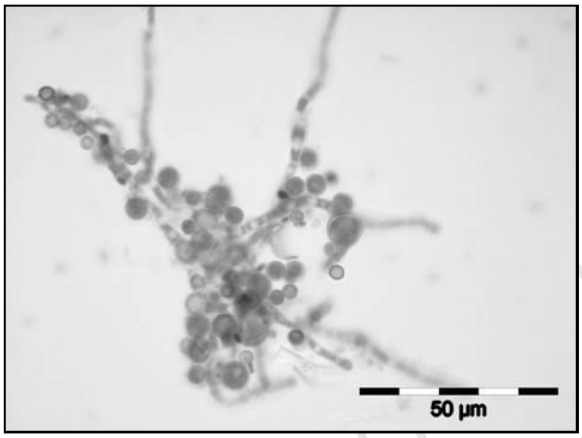

Figure 6.1 *A. niger* spore coagulation to form pellets at 9 h after inoculating a shake flask

In order to quantify the changes in morphology, image analysis was used for a 48 h bioreactor study on *A. niger*. Discrete morphological samples were taken at 0, 15.5, 25 and 48 h. Sample preparation and image analysis, described in Sections 3.3.6 were used to quantify the changes in morphology from "loose" clumps to compact pellets with a hairy perimeter (Figure 6.2). The morphological indices, pellet diameter, area, compactness factor F and circularity factor (also known as the roughness factor RF) were determined for 50 pellets. The F factor is the ratio of the projected area of the pellet to the projected area of the pellet after filling in any voids observed by image analysis and is estimated by Equation 6.1. The RF factor relates the pellet perimeter to the dense core area of the pellet and provides an estimate of the clump roughness or 'hairiness' (Tucker *et al*., 1992) as estimated by Equation 6.2.

$$F = \frac{projected\ \ area\ of\ \ pellet}{projected\ \ area\ of\ \ pellet\ \ after\ \ filling\ \ in\ voids} = \frac{area}{convex\ area} \qquad \textbf{(6.1)}$$

$$R = \frac{perimeter^2}{4\pi\, x\, area} \qquad \textbf{(6.2)}$$

The automatic values of 'area', 'convex area', 'perimeter', as defined in Table 3.5, were used to estimate the F and R indices. The average pellet diameter was measured manually using the 'line' command from the analySIS® software. The average and standard deviation of these indices for 50 pellets are summarised in Table 6.1.

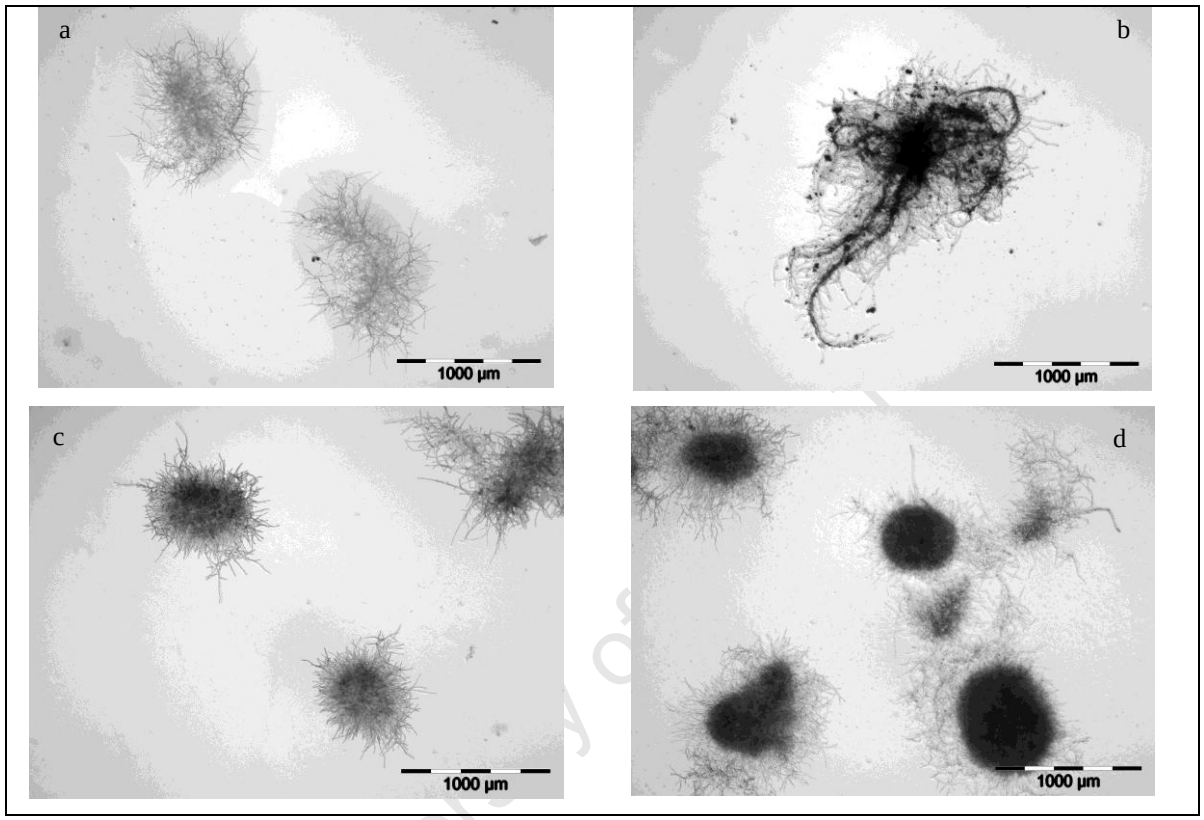

Figure 6.2 Morphological changes of *A. niger* NRRL-3 pellets at (a) 0 h, (b) 15.5 h, (c) 25h and (d) 48 h in a Chemap bioreactor

Table 6.1 Changes in the morphological indices area, convex area, perimeter, pellet diameter, roughness and compactness during growth for 50 *A. niger* pellets

	Time (h)			
Indices (avg ± stdev)	**0**	**15.5**	**25**	**48**
Area (mm^2)	1.102 ± 0.663	0.422 ± 0.284	0.397 ± 0.191	0.375 ± 0.182
Convex area (mm^2)	1.946 ± 1.172	0.827 ± 0.355	0.784 ± 0.368	0.585 ± 0.237
Perimeter (mm)	45.59 ± 24.86	36.24 ± 12.82	35.11 ± 15.20	21.92 ± 11.36
Pellet diameter (mm)	1.22 ± 0.07	0.72 ± 0.037	0.69 ± 0.010	0.72 ± 0.005
Roughness(-)	164 ± 91.7	328 ± 193.5	261 ± 122.4	138 ± 118.7
Compactness (-)	0.55 ± 0.11	0.48 ± 0.12	0.51 ± 0.07	0.64 ± 0.15

The changes in the average area and diameter of the *A. niger* pellets are illustrated in Figure 6.3. The pellets have an approximate area and diameter of 1.10 mm^2 and 1.22 mm on inoculation of the bioreactor with a shake flask culture grown for 18 hours. At mid-exponential phase (15.5 h) in the stirred tank bioreactor, the average area and diameter decreased to approximately 0.422 mm^2 and 0.72 mm. In early stationary phase at 25 h the average area and diameter decreased to 0.397 mm^2 and 0.69 mm. In late stationary phase at 48 h the area and diameter were little changed at 0.375 mm^2 and 0.72 mm respectively. Figure 6.2 and 6.3 clearly indicate how the pellets changed from a large, hairy open pellet with a large area and diameter at the beginning of the cultivation to smaller, more compact pellets with a rim of loose hyphae at the end of the cultivation. With growth the hairiness of the pellet, shown by RF, decreased from a maximum value of 328 at 15.5 h to 138 at 48 h while the compactness of the pellet, shown by F, increased with time from 0.48 to 0.64 for the same period, as clearly illustrated in Figures 6.2 and 6.4.

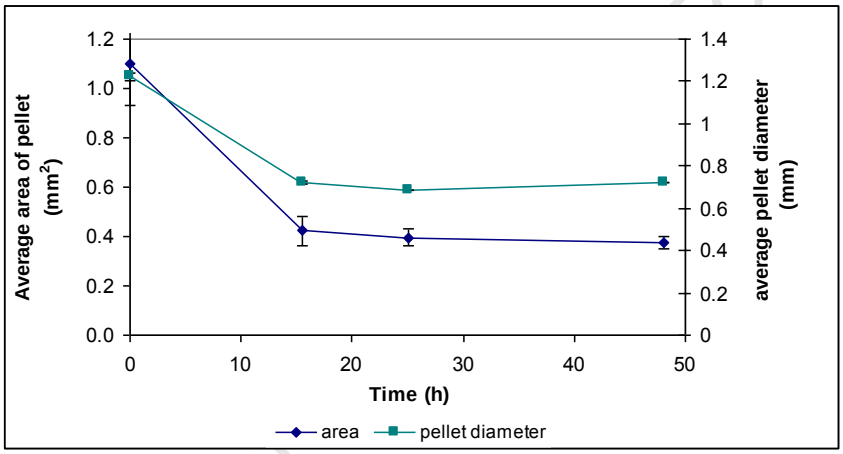

Figure 6.3 Change in the average area and pellet diameter of *A. niger* pellets during growth (n = 50)

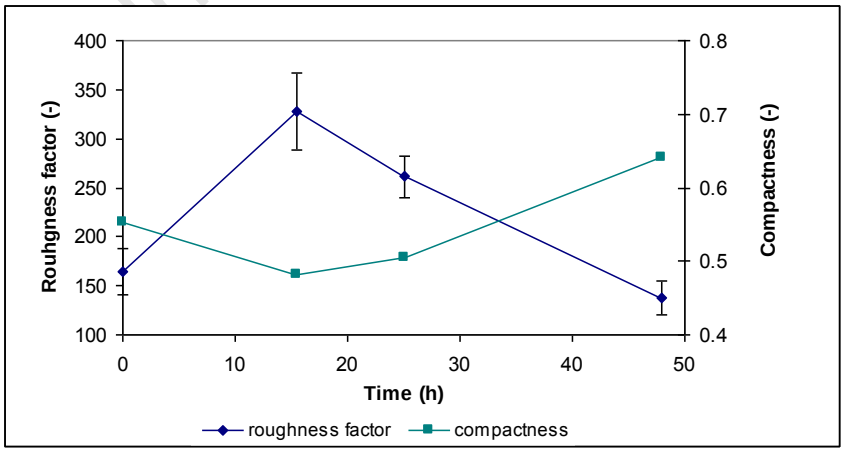

Figure 6.4 The change in the roughness and compactness of *A. niger* pellets during growth (n = 50)

6.2 *Penicillium* sp. CBS 120262 morphology

Investigating the morphology of samples of a *Penicillium* sp. prepared from batch cultivation according to Section 3.3.6, it was noticed that the hyphae remained freely dispersed and no clumps or pellet morphology was observed such as seen with *A. niger*. It was noted that clumping or overlapping of hyphal elements was present when the samples were not sufficiently diluted. Emphasis was placed on correlations between morphology and enzyme secretion for *Penicillium* sp. as this was selected as the preferred organism for GO production.

6.2.1 Image analysis method validation

Images of micro-organisms give a qualitative understanding of morphological change during growth. During growth, the hyphae consist of a population of different cells ranging from growing, productive cells to inactive, vacuolated, non-productive cells (Müller *et al*., 2002). Quantifying these different cell types as well as the relative distribution of hyphal tips and lateral walls gives a better understanding of the system and makes comparisons with other systems more reliable. A culture of *Penicillium* sp. CBS120262 in early exponential growth (22 h) was used for the validation of the image analysis method. Sample preparation is described in Section 3.3.6.1.

The work of Metz *et al*. (1981), Adams and Thomas (1988), Packer and Thomas (1990), Tucker *et al*. (1992), Cox and Thomas (1992), and Reichl *et al*. (1992) was used as the basis to investigate image analysis as a means to quantify changes in morphology. The image analysis software analySIS® was used to develop image analysis routines to analyse *Penicillium* sp. morphology, whereafter these were validated.

As mentioned in Section 2.7.3, early investigations by Metz *et al*., (1981) were based on manual measurements from photographs using an electronic digitiser. Since this method was time-consuming, labour intensive and imprecise, image analysis routines were developed by Adams and Thomas (1988) and refined by Packer and Thomas (1990), Tucker *et al*. (1992), Cox and Thomas (1992), to yield faster, more accurate and reproducible quantitative image analysis. Algorithms to quantify the morphology of dispersed mycelia, clumps and pellet morphologies using *Penicillium chrysogenum, Streptomyces clavuligerus, Streptomyces tendae and Aspergillus niger* using semi-automatic and automatic methods were developed (Packer and Thomas, 1990; Tucker *et al*., 1992; Cox and Thomas, 1992; Reichl *et al*., 1992). The principle stages in image analysis are 1) image capture and enhancement, 2) segmentation, 3)

object detection, and 4) measuring and analysis (Adams and Thomas, 1988; Packer and Thomas, 1990; Tucker *et al*., 1992; Cox and Thomas, 1992). In image capture, micrographs are obtained from a camera mounted on the microscope. The quality of the pictures is enhanced by improving the edges of hyphal features. The image is "segmented", i.e., all greyness levels above a preset level are treated as being of interest and the image is binarised (black and white image). The binary image is then reduced by "skeletonization" i.e, the mean pixels between the edges of the objects are found. Skeletons are then analysed for length and any branches of lengths greater than a preset number of pixels are removed by the skeletons. The processed binary image is then passed to the measurement and analysis phase of the program

6.2.1.1 Image processing routine

Using the image analysis software analySIS®, the light micrographs generated at 100 fold magnification were converted from colour (Figure 6.5a) to an 8-bit grey scale image (Figure 6.5b). Using automatic thresholding at a pre-set range between 67 and 194, the image was converted into a binary image with the white hyphal strands being of interest (Figure 6.5c). Using the detect function, the white image was temporarily changed to a red image and the resulting image was analysed using the image analysis software analySIS® (Figure 6.5d) to determine the automatic values of 'minimum diameter', 'minimum and maximum feret diameters' and 'shape factor' as defined in Table 3.5.

In stationary phase cultures, the older hyphae became vacuolated (Figure 6.6a). To eliminate interference from vacuolation, the image processing routine was modified to reduce the "holes" representing vacuoles by using various filters. A 'sharpen' filter was used to enhance the edges of the hyphae before applying the threshold. After the binarising step (Figure 6.6b), the morphological filters 'dilation' and 'erosion' were used to remove discontinuities (Figures 6.6c and d). The dilation filter was used to fill the holes by enlarging the white objects to make the hyphal edge appear continuous. The erosion filter was used thereafter to subtract the extra thickness of the hyphae while still keeping the hyphae intact by reducing the size of the white hyphal strands.

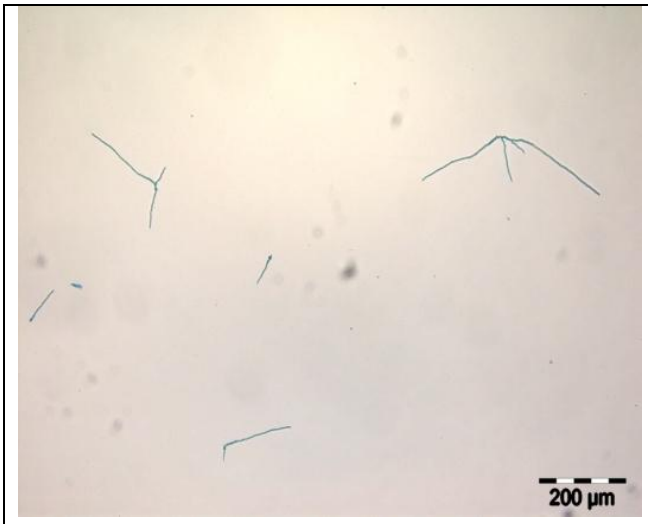

(a) Initial colour image of individual hyphae

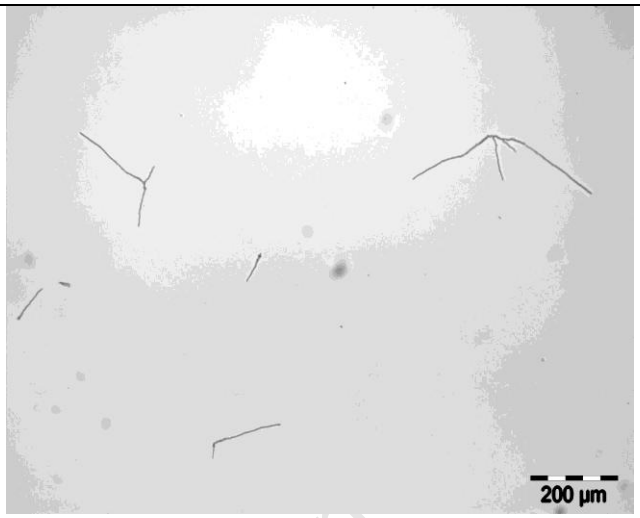

(b) 8-bit grey scale image

(c) Binarised image after being thresholded between the range 67 and 194

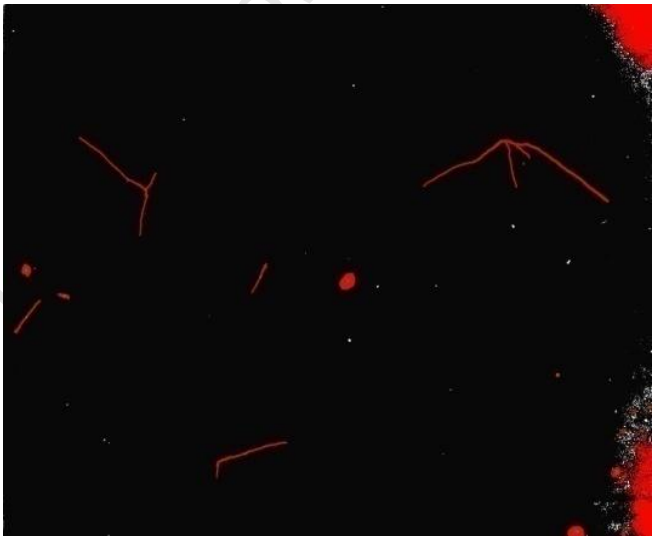

(d) The temporary red images are detected for feret min', 'feret max', 'diameter min' and 'shape factor'

Figure 6.5 Image processing routines for individual *Penicillium* sp. CBS 120262 hyphae, illustrated in early exponential phase of batch cultures

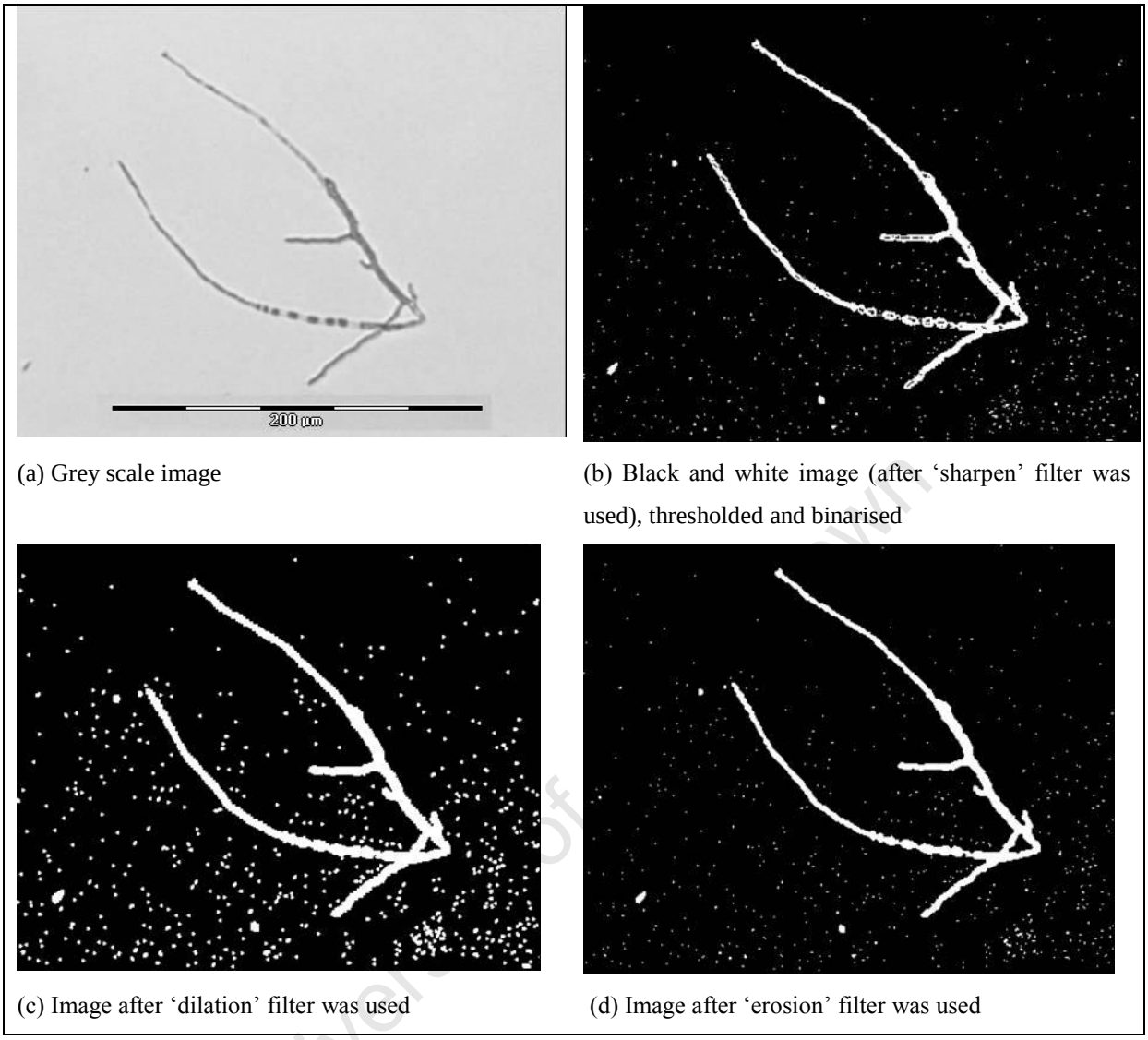

(a) Grey scale image

(b) Black and white image (after 'sharpen' filter was used), thresholded and binarised

(c) Image after 'dilation' filter was used

(d) Image after 'erosion' filter was used

Figure 6.6 Image processing routines which include the 'sharpen', 'dilation' and 'erosion' filters to eliminate interference from vacuolation in individual *Penicillium* sp. CBS 120262 hyphae during stationary phase of batch cultures

6.2.1.2 Validation of manual and semi-automatic image analysis procedures

The following morphological indexes, as described by Metz *et al*. (1981) (Figure 2.8), were obtained for this study: the main hyphal length (L_e), total hyphal length (L_t), hyphal diameter (L_d) and number of tips (N_t) of the individual filaments. For the L_e, L_t and L_d indices, three different sets of forty measurements of individual hyphae from *Penicillium* sp. CBS 120262 cultures at early exponential phase (22 h) were analysed both manually and semi-automatically. For the manual measurements, the L_e, L_t and L_d indices were determined using the manual line command from the analySIS® software. This command was used to manually measure the distance between two points and was denoted by a straight line. The number of

tips was counted manually using the 'touch count' command of the analysis® image analysis software. In the semi-automatic procedure L_e, L_t and L_d were determined from empirical correlations using the '$feret_{min}$', '$feret_{max}$', '$diameter_{min}$' and 'shape factor' values obtained from the analysis® software. The correlations developed between L_e, L_t, L_d and '$feret_{min}$', '$feret_{max}$', '$diameter_{min}$' and 'shape factor' are shown in Equations 6.3 to 6.5.

$$\textit{Main Length, } L_e = feret_{max} \quad \textbf{(6.3)}$$

$$\textit{Total Length, } L_t = (feret_{max} + feret_{min}) \quad \textbf{(6.4)}$$

$$\textit{Hyphal diameter, } L_d = average\ (diameter_{min} \times shape\ factor;\ feret_{min} \times shape\ factor) \quad \textbf{(6.5)}$$

A comparison between the manual and semi-automatic procedure to determine the L_e, L_t and L_d indices showed that the ratio of the manual measurements to semi-automatic measurements varied from 0.98 to 1.0 for L_e, 1.01 to 1.07 for L_t and between 1.03 and 1.05 for L_d for triplicate samples (Table 6.2). The semi-automatic techniques provided a reliable representation of the manual measurements. Statistical analysis (t-test at 95% confidence) confirmed that there was no difference between the manual and semi-automatic values for determining L_e, L_t and L_d (data not shown).

Table 6.2 Comparison between the manual and semi-automatic procedures for determining L_e, L_t and L_d for forty individual *Penicillium* sp. CBS 120262 hyphae in triplicate samples

		Manual	Semi-Automatically	Ratio of manual to semi-automatically
Main hyphal length L_e, µm	(#1)	157	161	0.98
	(#2)	146	149	0.98
	(#3)	169	169	1.00
Total hyphal length L_t, µm	(#1)	232	216	1.07
	(#2)	204	196	1.04
	(#3)	275	277	1.01
Hyphal diameter L_d, µm	(#1)	3.9	3.7	1.05
	(#2)	3.8	3.7	1.03
	(#3)	3.8	3.7	1.03

The parameters L_e, L_t and L_d were used to calculate the indices for the hyphal growth unit or branching frequency, L_{hgu}, and the dimensionless effective length, L_{e+}, defined in Section 2.7.3 using both the manual and semi-automatic procedures. The ratios of the manual to semi-automatic measurements for L_{hgu} varied from 0.98 to 1.05 while the ratios for L_{e+} varied from 0.91 to 0.96 respectively (Table 6.3). The semi-automatic values for L_e, L_t and L_d (calculated from Equations 6.1 to 6.3) could be used in the determination of L_{hgu} and L_{e+}.

Table 6.3 Comparison between the manual and semi-automatic procedure for determining L_{hgu} and L_{e+} for forty individual *Penicillium* sp. CBS 120262 hyphae in triplicate samples

		Manual	Semi-Automatically	Ratio of manual to semi-automatically
Hyphal growth unit L_{hgu} µm tip^{-1}, $L_{hgu} = L_t/N$	(#1)	59	56	1.05
	(#2)	54	55	0.98
	(#3)	60	54	1.03
Dimensionless effective length L_{e+}, $L_{e+} = L_e/L_d$	(#1)	40	44	0.91
	(#2)	38	40	0.95
	(#3)	44	46	0.96

6.2.1.3 Number of measurements acquired

The number of hyphal measurements is important to ensure the statistical significance of the data. The comparison of the L_e, L_t, N_t, L_d, L_{hgu} and L_{e+} for triplicate measurements of 20, 40, 60 and 100 individual hyphae are presented in Table 6.4. To evaluate the required number of individual hyphae for the statistical significance of data, the average values, standard deviation, standard error of the mean (SEM) and values at ± 95% confidence interval were compared for each sample and are summarised in Table 6.4 and Figure 6.7. The SEM was calculated as the quotient of the standard deviation of the population and the number of samples processed n. The SEM values decreased as the number of individual hyphae processed increased. Based on the diminishing returns with respect to decreased error with increasing sample number, the evaluation of fifty individual micro-organisms was selected for subsequent studies.

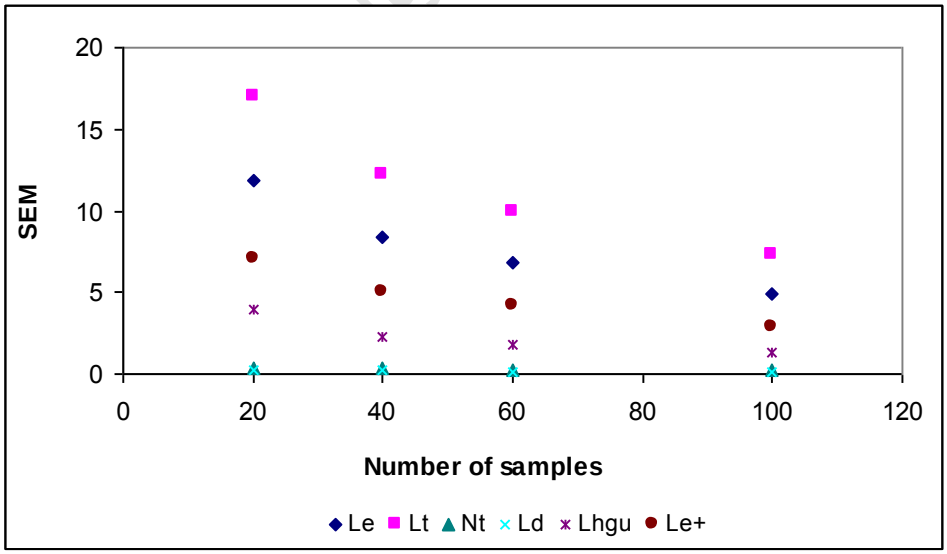

Figure 6.7 SEM values for longest hyphal length L_e, total hyphal length L_t, number of hyphal tips N_t, hyphal diameter L_d, hyphal growth unit L_{hgu} and dimensionless effective length L_{e+} and the number of hyphae analysed

Table 6.4 Comparison of L_e, L_t, N_t, L_d of individual hyphae for a range of 20 to 100 samples

	L_e (µm)	L_t (µm)	N (-)	L_d (µm)	L_{hgu} (-)	L_{e+} (-)
N = 20 (#1)						
Average ± stdev	160.4 ± 56.9	212.7 ± 82.2	3.67 ± 1.24	3.34 ± 1.15	54.70 ± 12.33	56.50 ± 34.02
Standard Error	12.7	18.4	0.292	0.257	2.91	7.61
Confidence - 95%	133.8	174.2	3.05	2.81	48.6	40.6
Confidence + 95%	187.1	251.1	4.28	3.88	60.8	72.4
N = 20 (#2)						
Average ± stdev	147.8 ± 53.4	194.7 ± 76.2	3.60 ± 1.57	3.39 ± 1.08	56.57 ± 17.90	50.09 ± 31.45
Standard Error	11.9	17.0	0.35	0.24	4.00	7.03
Confidence - 95%	122.8	159.0	2.87	2.89	48.2	35.37
Confidence + 95%	172.8	230.4	4.34	3.90	65.0	64.80
N = 20 (#3)						
Average ± stdev	172.5 ± 57.0	235.1 ± 85.8	4.55 ± 2.28	4.09 ± 1.19	55.93 ± 13.47	48.97 ± 29.09
Standard Error	12.7	19.2	0.51	0.27	3.01	6.51
Confidence - 95%	145.8	195.0	3.48	3.54	49.6	35.36
Confidence + 95%	199.2	275.3	5.62	4.65	62.23	62.59
N = 40 (#1)						
Average ± stdev	160.7 ± 52.8	216.5 ± 77	3.97 ± 1.82	3.71 ± 1.38	56.09 ± 13.88	51.67 ± 31.69
Standard Error	8.34	12.2	0.30	0.22	2.25	5.01
Confidence - 95%	143.8	191.8	3.37	3.27	51.53	41.54
Confidence + 95%	177.6	241.1	4.57	4.15	60.65	61.81
N = 40 (#2)						
Average ± stdev	149.0 ± 48.7	196.1 ± 75.1	3.70 ± 1.59	3.67 ± 1.20	55.03 ± 14.30	45.72 ± 25.39
Standard Error	7.71	11.9	0.25	0.19	2.26	4.01
Confidence - 95%	133.4	172.1	3.19	3.28	50.45	37.60
Confidence + 95%	164.6	220.1	4.21	4.05	59.61	53.84
N = 40 (#3)						
Average ± stdev	169.5 ± 50.8	226.6 ± 72.6	4.48 ± 1.99	3.68 ± 1.18	54.15 ± 13.38	53.18 ± 29.00
Standard Error	8.0	11.6	0.32	0.19	2.12	4.59
Confidence - 95%	153.2	203.0	3.83	3.30	49.87	43.91
Confidence + 95%	185.7	250.1	5.11	4.06	58.43	62.46
N = 60 (#1)						
Average ± stdev	156.6 ± 53.0	208.4 ± 77.5	3.93 ± 1.73	3.54 ± 1.34	54.32 ± 13.30	52.98 ± 32.19
Standard Error	6.8	10.0	0.23	0.17	1.75	4.16
Confidence - 95%	142.9	188.4	3.48	3.19	50.82	44.66
Confidence + 95%	170.2	228.5	4.39	3.88	57.82	61.29
N = 60 (#2)						
Average ± stdev	142.2 ± 45.0	186.8 ± 69.0	3.53 ± 1.58	3.76 ± 1.11	55.37 ± 14.13	42.17 ± 23.06
Standard Error	5.8	8.9	0.20	0.14	1.82	2.98
Confidence - 95%	130.5	168.9	3.13	3.47	51.72	36.22
Confidence + 95%	153.8	204.6	3.94	4.05	59.02	48.13
N = 60 (#3)						
Average ± stdev	163.8 ± 50.7	219.6 ± 74.7	4.28 ± 1.98	3.76 ± 1.19	54.90± 13.43	50.31 ± 27.75
Standard Error	6.5	9.6	0.26	0.15	1.73	3.58
Confidence - 95%	150.8	200.3	3.77	3.45	51.45	43.14
Confidence + 95%	176.9	238.9	4.79	4.07	58.39	57.48
N = 100 (#1)						
Average ± stdev	152.6 ± 49.2	206.4 ± 74.0	3.95 ± 1.76	3.58 ± 1.21	54.09 ± 12.94	49.89 ± 29.64
Standard Error	4.9	7.3	0.18	0.12	1.29	2.93
Confidence - 95%	142.9	191.8	3.60	3.35	51.52	44.07
Confidence + 95%	162.2	220.9	4.3	3.82	56.66	55.71
N = 100 (#2)						
Average ± stdev	149.4 ± 51.7	198.8 ± 78.1	3.84 ± 1.89	3.84 ± 1.14	55.00 ± 15.50	44.39 ± 27.69
Standard Error	5.2	7.8	0.19	0.11	1.55	2.78
Confidence - 95%	139.2	183.3	3.46	3.61	51.93	38.87
Confidence + 95%	159.7	214.3	4.22	4.07	58.08	49.91
N = 100 (#3)						
Average ± stdev	160.6 ± 51.9	215.4 ± 76.2	4.34 ± 1.90	3.58 ± 1.09	52.49 ± 13.52	50.44 ± 26.31
Standard Error	5.2	7.6	0.19	0.11	1.35	2.63
Confidence - 95%	150.3	200.2	3.96	3.36	49.81	45.22
Confidence + 95%	170.9	230.5	4.72	3.80	55.17	55.66

6.2.2 Morphology as a function of growth phase

To illustrate the impact of growth phase on hyphal morphology, micrographs at 24 h (early growth phase) and at 45 h (late stationary phase) are shown in Figure 6.8. At 24 h the hyphae appeared freely dispersed with a few branches (± 4 branches), while increased branching (± 7 branches) was observed at 45 h. Throughout the cultivation, the hyphae remained freely dispersed and no pellet formation was observed. The hyphal morphologies associated with different phases of growth during batch culture were quantified by the measurement of morphological indices as a function of batch culture time and are presented in Figure 6.9 with data tabulated in Appendix F.

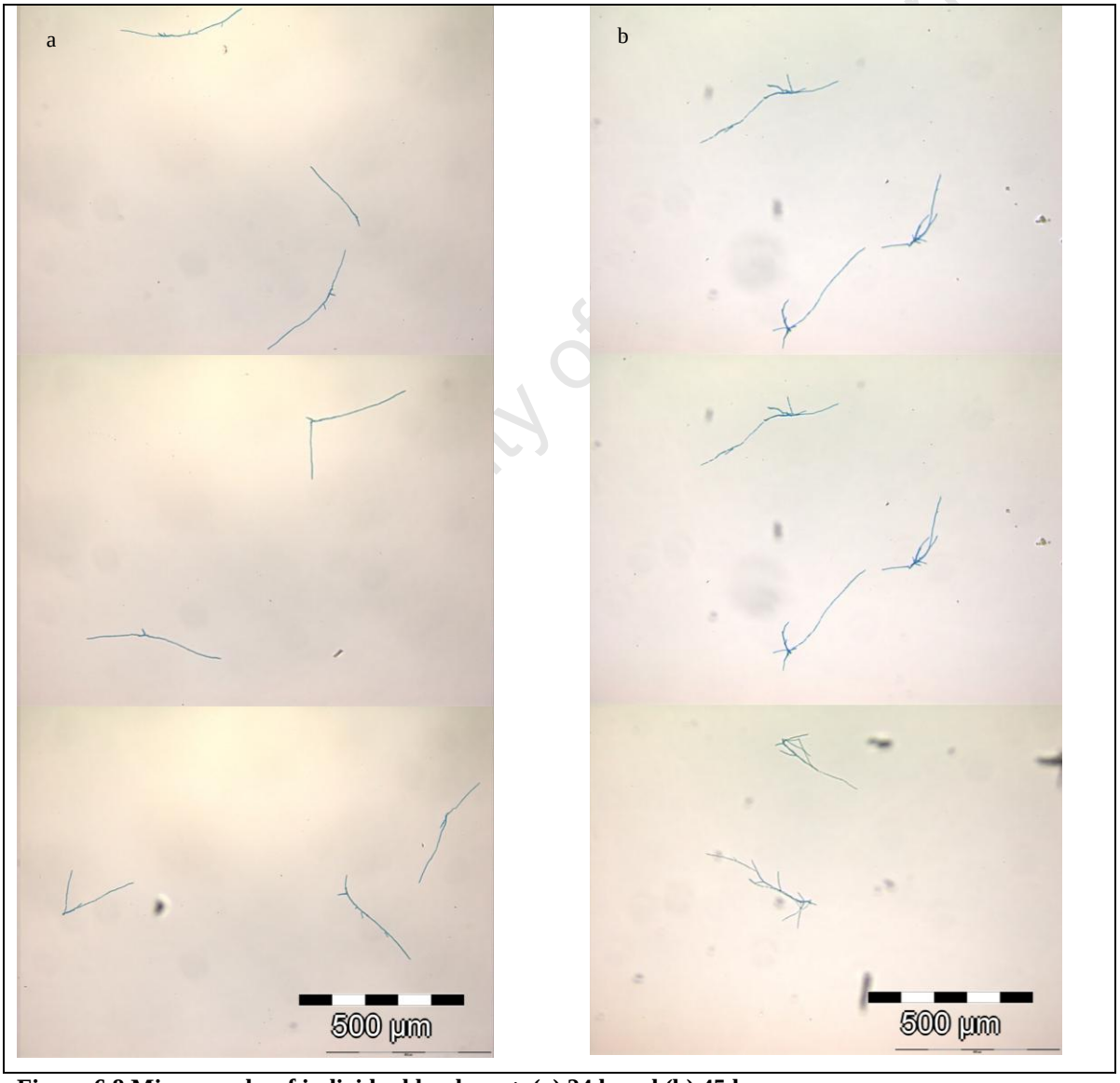

Figure 6.8 Micrographs of individual hyphae at (a) 24 h and (b) 45 h

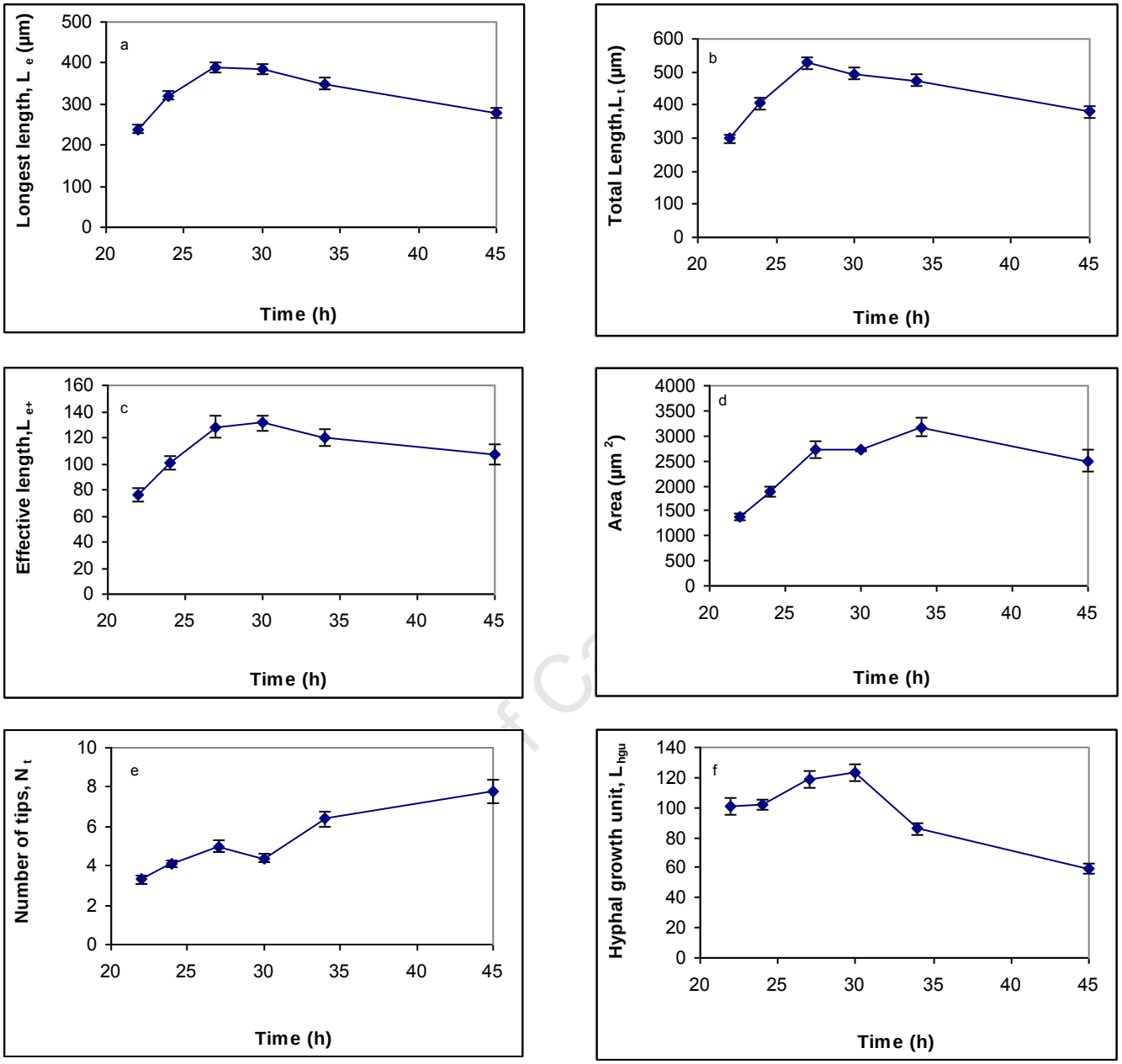

Figure 6.9 Changes in morphological parameters (a) longest hyphal length, L_e, (b) total hyphal length, L_t, (c) effective dimensionless length, L_{e+}, (d) hyphal area A, (e) number of hyphal tips, N_t (f) hyphal growth unit, L_{hgu} during the growth of *Penicillium* sp. CBS120262. The error bars represent the standard error of the mean (SEM) (n = 50)

During active growth (22 - 27 h), the L_e index (Figure 6.10a), L_t index (Figure 6.10b) and L_{e+} index (Figure 6.10c) increased from 240, 300 and 76 µm at 22 h to a maximum of 390, 527 and 128 µm at 27 h respectively, indicating that the hyphae became longer during this period. The corresponding L_d index remained constant at 3.5 ± 1.0 µm, indicating no change in fungal diameter (figure not shown). The area

of the individual hyphae increased from approximately 1380 μm^2 to 2500 μm^2 during active growth and reached a maximum of 3200 um^2 at 34 h, thereafter it decreased to 2500 μm^2 at 45h (Figure 6.10d). Additionally, the average number of hyphal tips per hyphal body increased from three to five during the active growth period from 22 h to 27 h (Figure 6.10e) while the L_{hgu} index increased from 100 μm tip^{-1} at 22 h to 119 μm tip^{-1} at 27 h (Figure 6.6f). During the transition from the active growth to the stationary phase (27 to 45 h), the $L_{e,}$ L_t and L_{e+} indices decreased to 280, 380 and 110 μm respectively indicating a shortening of the hyphae as well as becoming thinner (L_d index of 3.0 ± 0.9 μm). The number of tips increased to eight tips per hyphal body, indicating that the hyphae became more branched as shown by the decrease in the L_{hgu} index to 60 μm tip^{-1}.

6.2.3 Effect of using $Ca(OH)_2$ as a pH control agent on the morphology of *Penicillium* sp. CBS 120262

To illustrate the change of hyphal morphology during growth in the presence of an increased calcium concentration, owing to the use of $Ca(OH)_2$ as pH control agent, micrographs of cultures were taken at 24 h (mid-exponential phase) and at 45 h (late stationary phase) as shown in Figure 6.10. In general, hyphae were freely dispersed at 24 h with a few branches, while greater branching was evident at 45 h. At 45h, vacuolisation could be seen in some of the hyphae. Vacuolisation was normally observed in older hyphae (Figure 6.6) and is a natural ageing process in fungi.

To investigate the effect of $Ca(OH)_2$ on hyphal morphology, the progression of a number of morphological indices was traced during growth as described in Section 6.2.2 and illustrated in Figure 6.11. The morphological indices used were: hyphal area (A), number of tips (N_t), main hyphal length (L_e),total hyphal length (L_t), dimensionless effective length (L_{e+}) and hyphal growth unit (L_{hgu}). These were compared with those from growth using NaOH as pH control agent.

During growth, the morphological indices for $Ca(OH)_2$ showed marked differences from those obtained for NaOH. At the end of growth, the area (Fig. 6.11a) of the hyphae was larger by a factor of 1.9 (4722 μm^2). There were 19 tips per hyphal body (Fig. 6.11b) compared to the 8 tips per hyphal body for NaOH. The hyphae became longer with the L_e index (Fig. 6.11c), L_t index (Fig 6.11d) and the L_{e+} index (Fig. 6.11e) increasing to 359, 549 and 266 μm at the end of the cultivation. Interestingly, the L_e and L_t indices of NaOH with maximum values of 390 and 527 μm at 27 h are similar to $Ca(OH)_2$ at the end of the

cultivation. At 45 h the hyphae were more branched, as indicated by a lower L_{hgu} (33 µm tip^{-1} for $Ca(OH)_2$ vs. 59 µm tip^{-1} for NaOH (Fig. 6.11f)) and higher tip number.

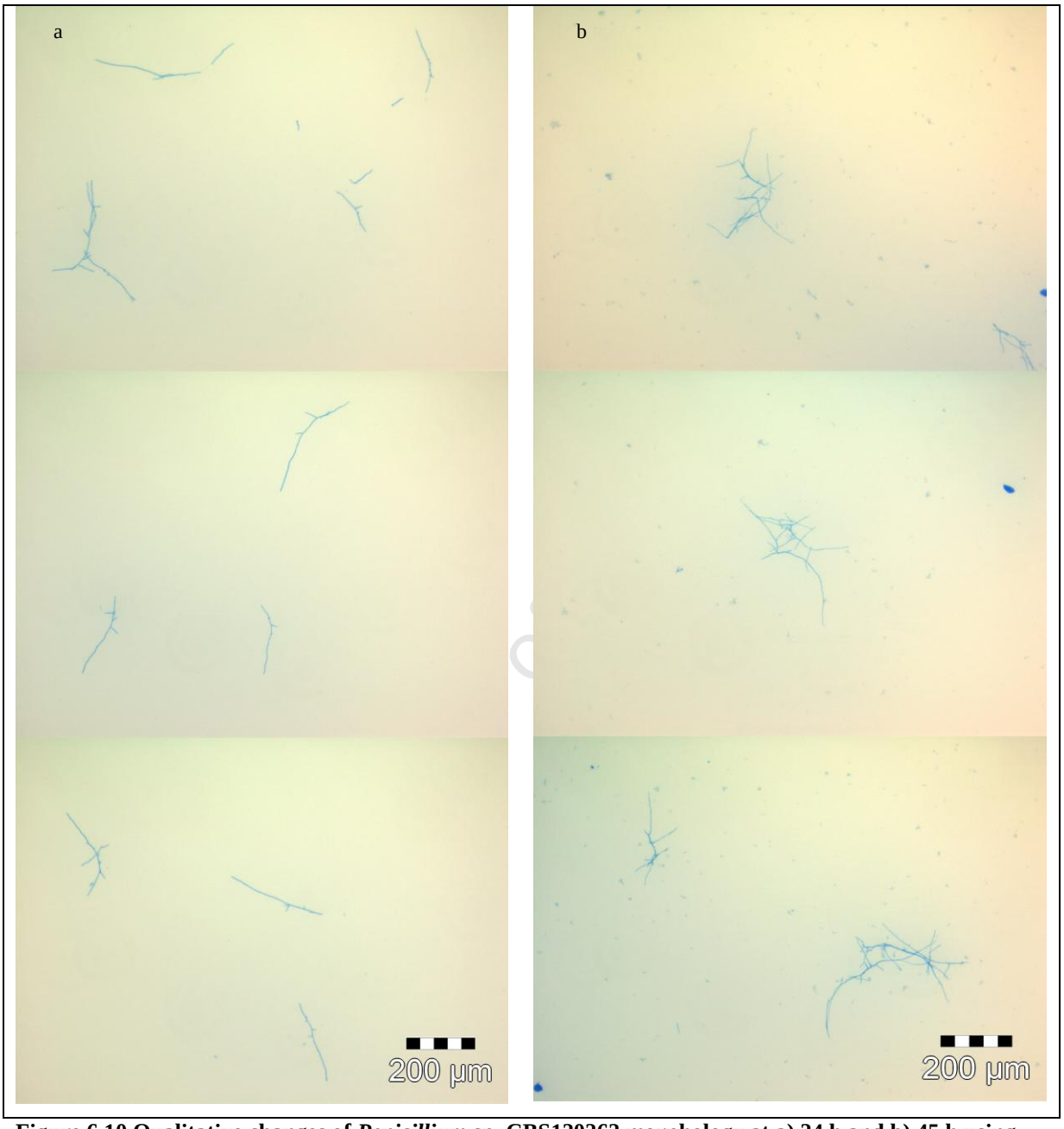

Figure 6.10 Qualitative changes of *Penicillium* sp. CBS120262 morphology at a) 24 h and b) 45 h using $Ca(OH)_2$ as pH control agent

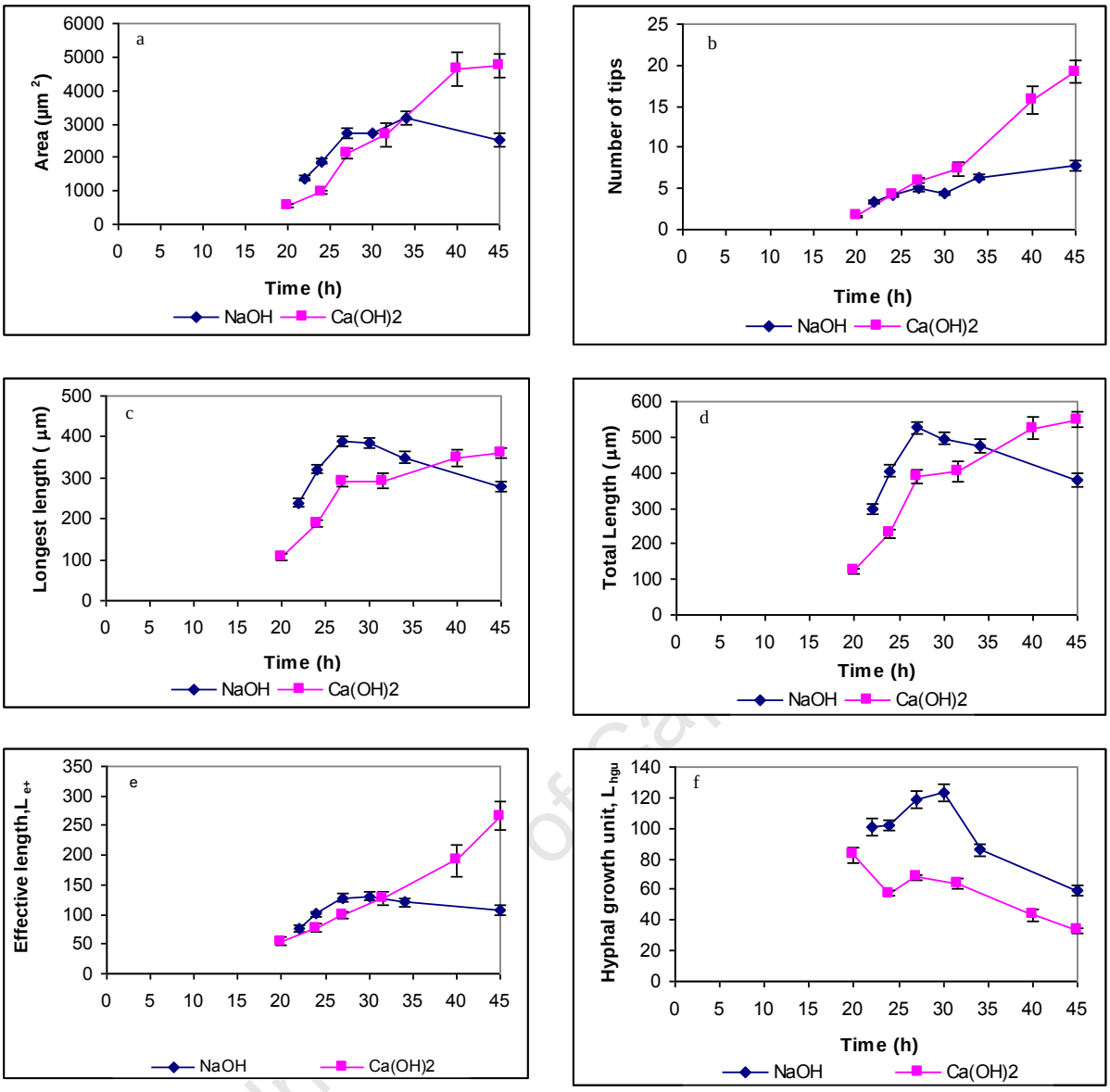

Figure 6.11 Comparison of the change in morphological parameters (a) hyphal area A, (b) number of hyphal tips N_t, (c) longest hyphal length L_e, (d) total hyphal length L_t, (e) effective dimensionless length L_{e+}, (f) hyphal growth unit L_{hgu} during growth for *Penicillium* sp. CBS 12026 using NaOH (◆) and $Ca(OH)_2$ (■). The error bars represent the standard error of the means (SEM) (n = 50)

The Ca^{2+} gradient has been postulated to play an important role in the regulation of hyphal apices and the formation of branches (Jackson and Heath, 1993; Gow, 1995; Trinci, 1990). The internal [Ca^{2+}] may affect the transport of cell wall vesicles and the fusion of vesicles to the protoplasmic membrane (Gow, 1995; Trinci, 1990). This study suggests that if Ca^{2+} influences the formation of branches, i.e. more apical tips (i.e lower L_{ghu}) and vesicle transport, i.e. more GO can be released from the larger number of tips to

the extracellular medium and therefore increases the extracellular GO. This suggests that the higher the number of tips, the higher the amount of extracellular GO secreted into the culture media.

6.3 The effect of *A. niger* NRRL-3 and *Penicillium* sp. CBS 120262 morphology on the rheology of the fungal culture

Since the rheological properties of the cultivation medium are closely related to the various changes in the morphology of the organism (Charles 1978; Packer and Thomas, 1990; Riley *et al*., 2000), the rheology of *A. niger* and *Penicillium* sp. cultures in terms of their morphology was investigated. The morphological indices as determined in Section 6.1 and Section 6.2 were related to rheological parameters (RP) and compared to literature.

Metz *et al*. (1979) found quantitative relationships between the size and shape of filamentous suspensions of two strains of *P. chrysogenum* grown in batch culture, and steady shear viscosity measurements of these suspensions according to Equations 2.18 and 2.19.

$$\tau_c = 1.67 \times 10^{-4} C_m^{2.5} (L_e^+)^{0.8} \quad \textbf{(2.18)}$$

$$K_c = 5.454 \times 10^{-3} C_m^{1.0} (L_{hgu})^{0.6} \quad \textbf{(2.19)}$$

Since *A. niger* cultivation is a mixture of pellets and clumps the roughness factor RF and the compactness factor together with the diameter of the pellet or clump were related to the rheology of the cultivation (Olsvik *et al*., 1993). A modification of the relationship of Metz *et al*. (1979) (Equation 2.16) by Riley *et al*. (2000) was used to describe the influence of cell dry weight (X) and the morphology indices (roughness factor RF and compactness factor C) upon the viscosity of the *A. niger* cultivation (Equation. 2.17):

$$RP = \text{constant } (X)^{\alpha}. (L_{e+})^{\beta}. (L_{hgu})^{\gamma} \quad \textbf{(2.16)}$$

$$RP = \text{constant } (X)^{\alpha}. (RF)^{\beta}. (C)^{\gamma} \quad \textbf{(2.17)}$$

Equations 2.16 and 2.17 were used respectively to describe the influence of cell dry weight and the morphology indices upon the viscosity of the *Penicillium* sp. CBS 120262 and *A. niger* cultivations. The values of the constant, α, β and γ were obtained using multiple regression (Solver function in Excel) of the data presented in Appendix G and are compared to the results of various authors in Table 6.5

Table 6.5 Comparison of rheological correlations for *Penicillium* sp. and *A. niger* cultures

Reference	Relationship	Organism
Metz *et al*. 1979	$K_c = 5.454 \times 10^{-3} X^{1.0} (L_{hgu})^{0.6}$	*P. chrysogenum* (freely
	$\tau_0 = 1.67 \times 10^{-4} X^{2.5} (L_{e+})^{0.8}$	dispersed)
Tucker and Thomas, 1993	$K = \text{constant } X^{2.8} RF^{0.7} C^{1.2}$	*P. chrysogenum* (clumps)
Tucker 1994	$K = 6.6 \times 10^{-5} X^{2.3} RF^{-0.96} C^{0.79}$	*P. chrysogenum* (clumps)
Riley *et al*. 2000	$K = X^2 \times (5 \times 10^{-5} \times L - 10^{-3})$	*P. chrysogenum* (clumps)
Present study	$K_c = 4.3 \times 10^{-4} X^{0.9} L_{hgu}^{1.0}$	*Penicillium* sp CBS
	$\tau_0 = 5.3 \times 10^{-4} X^{1.6} L_{e+}^{0.80}$	120262 (freely dispersed)
Olsvik *et al*. 1993	$K = -0.56 + 0.0018 X^{1.7} RF$	*A. niger* continuous
		(pellets)
Olsvik & Kristiansen, 1994	$K = 0.38 + 4.8 \times 10^{-5} X^{2.9} RF$	*A. niger* fed batch
		(pellets)
Present study	$K = 3.2 \times 10^{-6} X^{1.4} RF^{1.7} C^{1.1}$	*A. niger* batch (pellets)
Present study	$K = 2 \times 10^{-4} RF + 0.0746$	*A. niger* batch (pellets)

In all the correlations in Table 6.5, the impact of the biomass concentration varied with the exponent value from 1.0 to 2.9. There is an approximate direct correlation with biomass concentration for freely dispersed mycelial, and an exponent approaching two for the biomass concentration for both clumps and pellets, which is consistent with the viscosity of particle suspensions. The exponent values for the morphological indices for freely dispersed mycelia varied between 0.6 and 1.0 for L_{hgu} and remained constant at 0.8 for L_{e+}, while for the clump/pellet parameters RF and C the exponent value varied from -0.96 to 1.7 and 0.79 to 1.2 respectively.

Paul *et al*. (1994) and Packer and Thomas (1990) reported that 80% to 90% of a *P. chrysogenum* culture to be in the clump form. Under these conditions, relating the culture rheological properties to the morphology of only freely dispersed hyphae are not reliable (Tucker *et al*. 1992; Tucker and Thomas, 1993). During the cultivation of *Penicillium* sp. CBS 120262 in this study, the majority of the hyphae was present in the freely dispersed form. This may be attributed to the lower cell dry weight of 2.2 g l^{-1} during *Penicillium* sp. CBS 120262 cultivation compared to the 12 g l^{-1} obtained during the cultivation of *P.*

chrysogenum in the previous studies. This is supported by McIntyre et al. (1998) who found that the majority of the hyphae presented in the freely dispersed form during cultivation *P. chrysogenum* at a biomass concentration of between 4 and 5 g l^{-1} CDW.

Petersen *et al*., 2008 used particle size distribution data with multivariate models for the prediction of rheological properties of *Aspergillus oryzae* fed-batch fermentations conducted in 550 L pilot scale tanks. In this approach the particles were not classified into freely dispersed, clumps or pelleted forms and therefore did not report on the morphological indices such as roughness, compactness or maximum hyphal dimensions. This technique used all the particles in the suspension and not only a diluted sample to eliminate hyphal overlapping for microscopic observation and provides a link between operating conditions, micro-organism and rheology.

6. 4 Relationship between morphology and GO secretion

During the active growth phase from 22 to 27 h for the NaOH cultivation, the volumetric rate of GO secretion increased from 0.04 U ml^{-1} h^{-1} to a maximum at 0.13 U ml^{-1} h^{-1}, as the number of hyphal tips increased from 3 to 5 per hyphal body (Fig. 6.12). Thereafter the rate of GO secretion decreased from 0.13 U $ml^{-1}h^{-1}$ at the end of the active growth phase (27 - 34 h) to a constant 0.11 U ml^{-1} h^{-1} during the late stationary phase (34 – 45 h) as the number of hyphal tips increased further from 5 to 8 per hyphal body. Previously it was suggested by Chang and Trevitick (1974), Wessels (1990) and Worsten *et al*. (1991) that secretion occurred at the hyphal tips. In accordance with this, it was shown that during the active growth phase (22 – 27 h) of *Penicillium* sp., GO secretion increased over 3-fold as the number of tips increased. Further, an attenuation in the increase in the number of tips corresponded to a marginal decrease in GO secretion during the stationary phase (27 – 45 h). The relationship between GO secretion and N_t supports the postulation of decreased enzyme secretion through hyphal tips in the stationary phase owing to decreasing porosity of the cell wall. Conversely, the GO secreted from the hyphal tips with the pH control agent $Ca(OH)_2$ increased throughout the culture time of 45 h (Fig. 6.12). The growth moved from exponential to stationary phase between 35 and 45 h. In late exponential phase, the GO secretion rate was 0.4 U ml^{-1} h^{-1} at 16 hyphal tips per hyphal body. The maximum GO secretion rate from 19 hyphal tips per hyphal body in early stationary phase of the $Ca(OH)_2$ cultivation was 0.70 U ml^{-1} h^{-1}.

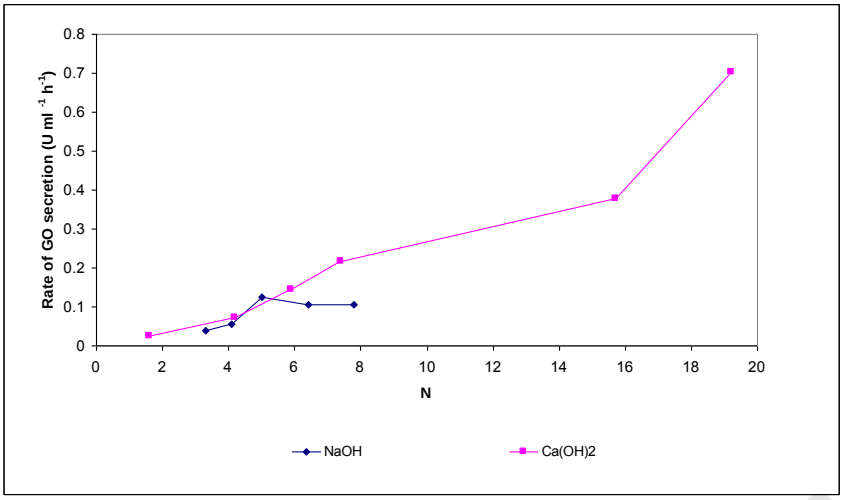

Figure 6.12 Relationship between the volumetric rate of GO secretion and number of tips (N) during the growth of *Penicillium* sp. CBS 120262 cultivations using NaOH (◆) and Ca(OH)$_2$ (■)

The relationships between the specific rate of GO production and secretion as well as N_t and L_{hgu} indices during the batch culture using NaOH and Ca(OH)$_2$ are shown in Fig. 6.13a and Fig. 6.13b respectively. For the NaOH-controlled culture the late growth phase, early stationary phase and the stationary phase can be divided as 22 – 27 h, 27 – 34 h and 34 – 45 h respectively (Fig. 4.2). When Figures 4.7 (c and d) and Fig. 6.14b are studied together it appeared that for the Ca(OH)$_2$-controlled culture the exponential growth phase extended beyond 35 hours. The maximum specific GO production rate of 327.8 U $g^{-1}h^{-1}$ was observed early in the active phase (24 h) for NaOH-controlled culture whereas for the Ca(OH)$_2$-controlled culture it was 1119.3 U $g^{-1}h^{-1}$ (27 h) which was 3.4 fold higher than for the NaOH-controlled culture. Thereafter for the NaOH-controlled culture, the specific GO production rate decreased to 169.8 U g^{-1} h^{-1} at 34 h with no net production observed towards the end of the stationary phase, while with Ca(OH)$_2$ addition, a sudden decrease in production after 27 h was observed. Conversely, the specific secretion rate, the specific secretion rate/ tip and specific secretion rate/ L_{hgu} increased to a maximum of 42.8 U $g^{-1}h^{-1}$, 6.9 U $g^{-1}h^{-1}$ tip^{-1} and 4.1 x 10^5 U tip g^{-1} h^{-1} m^{-1} respectively at 34 h for the NaOH-controlled culture and showed little change towards the end of the cultivation. For the Ca(OH)$_2$--controlled culture, the maxima were found at 81.6 U $g^{-1}h^{-1}$, 4.3 U $g^{-1}h^{-1}$ tip^{-1} and 24.6 x 10^5 U tip g^{-1} h^{-1} m^{-1} at 45 h, which is consistent with the continued growth of the Ca(OH)$_2$-controlled culture. During active growth the specific secretion rate was consistently lower than the production rate, indicating an accumulation of intracellular GO. The secretion rate remained fairly constant during the stationary phase despite the decrease in the production rate, corresponding to a shift towards extracellular location of GO. This could imply that the GO accumulated in the hyphal cell during cultivation may be in response to the transport of GO across the cell envelope being the limiting factor to its extracellular accumulation.

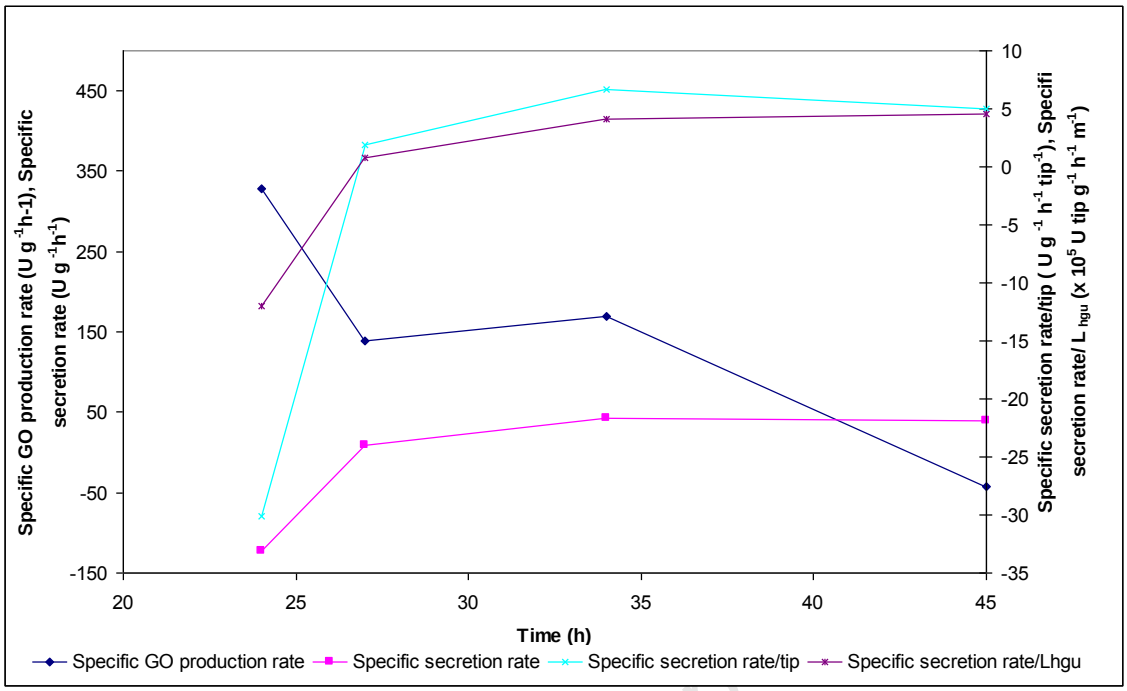

Figure. 6.13a Relationship between specific GO production rate, specific GO secretion rate, specific secretion rate/ tip, specific secretion rate/ L_{hgu} with time using NaOH as pH control agent

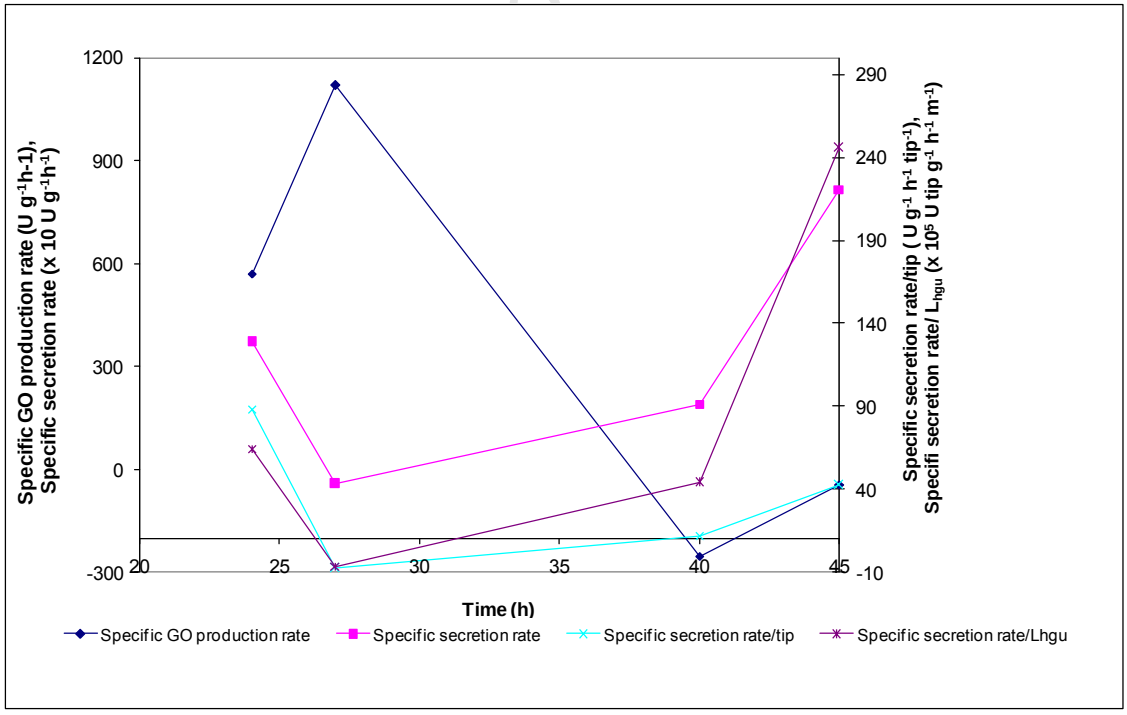

Figure. 6.13b Relationship between specific GO production rate, specific GO secretion rate, specific secretion rate/ tip, specific secretion rate/ L_{hgu} with time using $Ca(OH)_2$ as pH control agent

6.5 GO transport from the intracellular region to the extracellular surroundings

The rates of change in the total, cell associated and extracellular GO activity illustrated the change in location of GO during growth using NaOH (Fig. 6.14a) and $Ca(OH)_2$ (Fig. 6.14b) as pH control agents. The cell associated GO was determined as the difference between the total GO produced and the extracellular GO secreted. There were three distinct regions during the batch bioprocess: Region A corresponding to the active growth phase, Region B the late growth phase and Region C the early stationary phase. For NaOH and $Ca(OH)_2$ the active growth phase (Region A) was from 22 to 27 h and 20 to 27 h respectively, late growth phase (Region B) from 27 to 34 h and 27 to 45 h and early stationary phase (Region C) from 34 to 45 h for the NaOH- controlled culture.

For the NaOH cultivation, in Region A there was a rapid increase in the rates of production of total and cell associated GO activity with a more gradual increase in extracellular GO activity. The maximum total GO production and cell associated GO accumulation rates at 27 h were 1.43 U $ml^{-1}h^{-1}$ and 1.11 U $ml^{-1}h^{-1}$ respectively, while the maximum rate of secretion to extracellular GO was 0.31 U ml^{-1} h^{-1}. These rates suggest that the intracellular accumulation of GO was partially the result of limitation in the secretion rate. While for growth in the presence of $Ca(OH)_2$, the maximum total GO production rate and accumulation of cell associated GO rate at 27 h were 1.50 U $ml^{-1}h^{-1}$ and 1.36 U ml^{-1} h^{-1} respectively, the rate of secretion to extracellular GO only increased to 0.14 U $ml^{-1}h^{-1}$. Since the rates of secretion of GO in this region were 4.6 and 10.7 fold slower respectively than the rate of production, the rapid GO production rate translates primarily into a cell associated GO accumulation rate.

During the early stationary phase (Region B) there was a reduction in the rates of increase in total, cell associated and extracellular GO activity under standard conditions. The rate of cell associated GO accumulation at 34 h was negligible while the total GO activity increased at 0.2 U ml^{-1} h^{-1}, suggesting that the export of GO was no longer rate limiting. The rate of extracellular GO activity remained in the range 0.2 to 0.25 U ml^{-1} h^{-1} between 28 and 32 hours. With elevated Ca^{2+} concentrations on using $Ca(OH)_2$ as pH control agent, the rates of increase of total and cell-associated GO decreased to 0.58 U $ml^{-1}h^{-1}$ and 0.2 U ml^{-1} h^{-1} while the extracellular GO rate increased to 0.38 U $ml^{-1}h^{-1}$. At the end of the fermentation (45 h) for the $Ca(OH)_2$-controlled culture, the total, cell associated and extracellular GO activity rates increased to 1 U ml^{-1} h^{-1}, 0.3 U ml^{-1} h^{-1} and 0.7 U ml^{-1} h^{-1}, respectively. This finding is supported with an increase in the longest hyphal length (Fig.6.11 c), number of tips (Fig. 6.11b), CDW (Fig. 4.7c), volumetric total (Fig. 4.7d) and extracellular GO (Fig. 4.7 e) activity

The production and secretion rates of GO in Region C decreased to zero between 34 and 45 h for the culture controlled with NaOH.

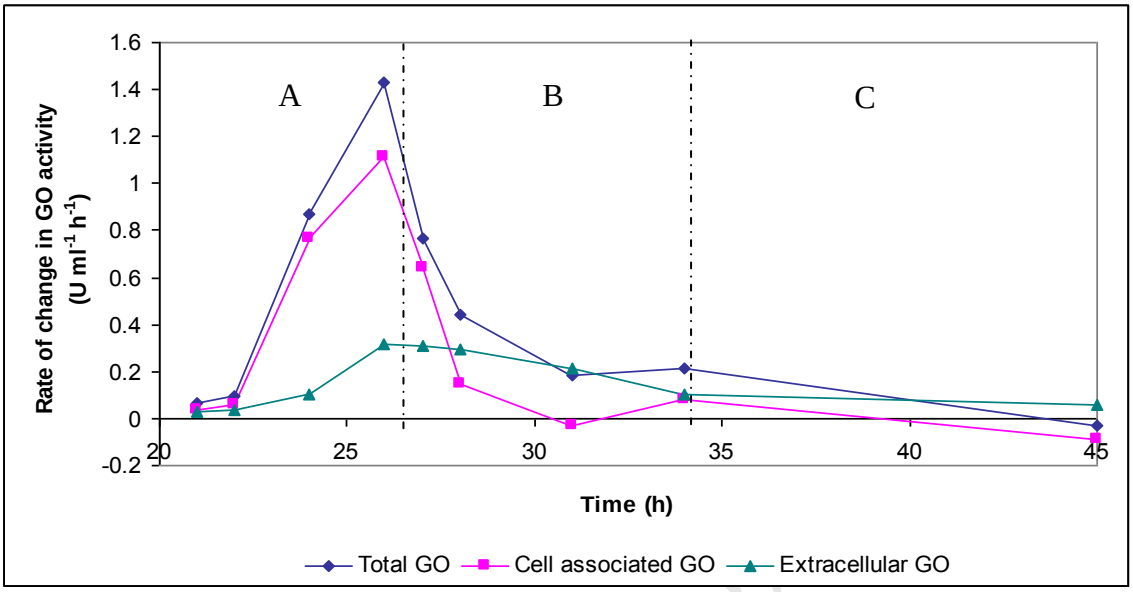

Figure. 6.14a Rate of change in total, cell associated and extracellular GO with time when NaOH was used as pH control agent

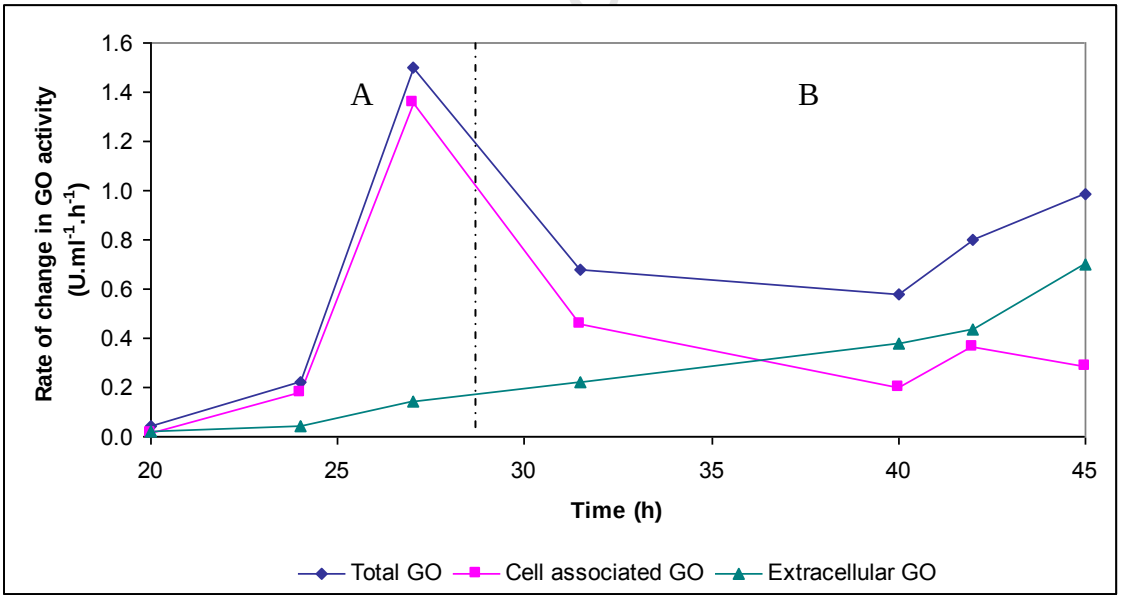

Figure. 6.14b Rate of change in total, cell associated and extracellular GO with time when $Ca(OH)_2$ was used as pH control agent

As GO was produced, it was transported from the cell associated location into the extracellular region. Using a mass transfer approach across a boundary based on Fick's law of diffusion (Doran, 1999), it is proposed that the transport of GO from the cell associated region to the extracellular region can be represented in Fig. 6.15. It was assumed that the cell envelope, which comprised the cell wall and membrane fragments and slime layer, represented the major resistance to mass transfer from the cell-associated region to the extracellular region. Under these conditions, there would be negligible internal resistance to mass transfer with the cell associated GO concentration ($C_{GO,C}$) equal to the GO concentration at the internal cell wall interface ($C_{GO,CWi}$). Further, the concentration of GO at the cell wall-extracellular region interface ($C_{GO,CWj}$) would equal the GO concentration in the extracellular fluid as external agitation dominated external mass transfer resistance. The concentration gradient (ΔC), the driving force for GO transfer, can then be defined as the difference between the cell associated ($C_{GO,C}$) and extracellular GO ($C_{GO,E}$) concentrations.

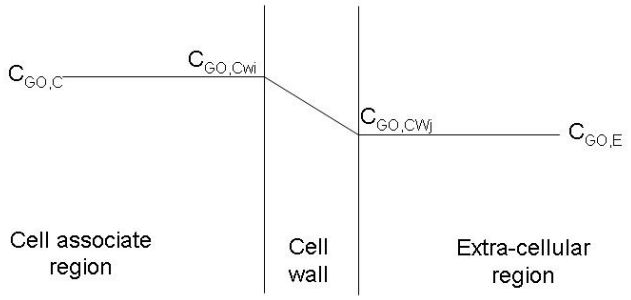

Figure. 6.15 Proposed transport of GO from the cell associate region to the extracellular region

The change in ΔC during the growth phase is shown in Fig. 6.16. During the active growth phase for NaOH-controlled growth (22 – 27 h), ΔC increased 2-fold to 2.69 x 10^3 U ml^{-1} while for $Ca(OH)_2$ – controlled growth (20 - 27 h), ΔC increased 2.3-fold to 3.17 x 10^3 U ml^{-1} . During early stationary phase (27 – 34 h) for the NaOH-controlled culture, ΔC increased further to 3.63 x 10^3 U ml^{-1} but at a slower rate than during active growth. ΔC then decreased during the late stationary phase (34 - 45 h) to 2.69 x 10^3 U ml^{-1}. Whereas for the $Ca(OH)_2$–controlled culture, ΔC decreased during the stationary phase from 3.17 x 10^3 U ml^{-1} to 1.62 x 10^3 U ml^{-1} which translated to a reduction in the concentration driving force compared to the NaOH culture. The total GO activity curve for the NaOH-controlled culture showed a similar profile to that for ΔC (NaOH) and reached a maximum of 55.4 x 10^3 U at 34 h, thereafter it decreased to 51.5 x 10^3 U at 45 h. The total GO activity curve for the $Ca(OH)_2$ -controlled culture on the other hand increased from active growth (41.6 U ml^{-1}) phase to the end of the stationary phase (109.9 U ml^{-1}) resulting in a 2.6 fold increase. Although the total GO activity for the $Ca(OH)_2$ culture increased

during growth, the concentration driving force between the intracellular region and the external environment decreased indicating that as GO was produced it gets secreted into the external medium compared to the delay in GO secretion for the NaOH culture.

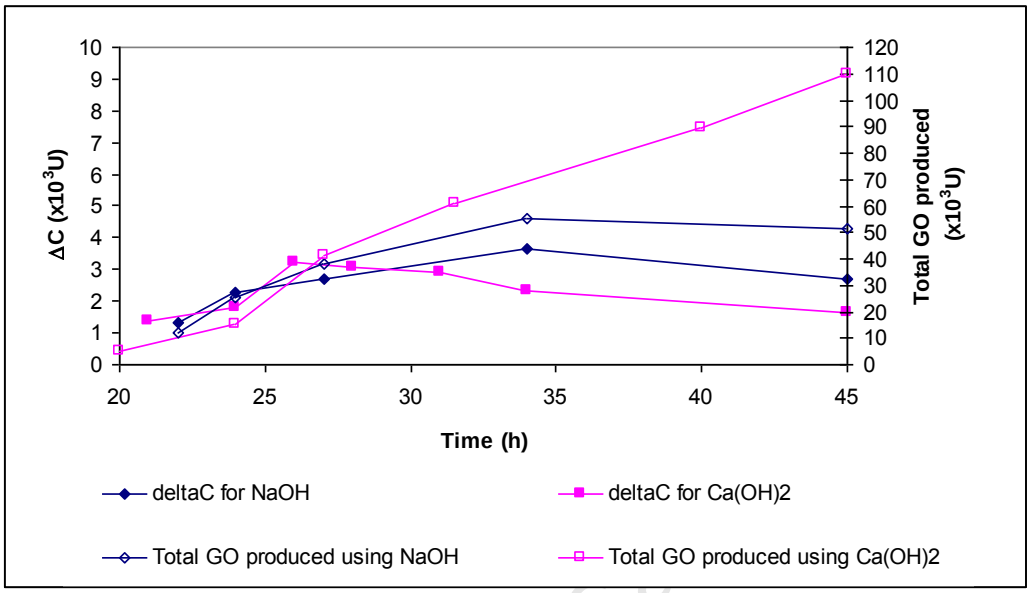

Figure. 6.16 Change in the concentration gradient (delta C) between the cell associated and extracellular GO and total GO activity of *Penicillium* sp. CBS 120262 in a batch culture, grown using NaOH or Ca(OH)$_2$ as the pH control agent

Using ΔC, the transport of GO from the cell associated region to the extracellular region was defined in terms of an overall volumetric GO transport coefficient ($k_s a$) calculated from re-arranging Equation 2.20 (Fick's law of diffusion)

$$J_A = -\mathrm{D_A}\frac{dC_A}{dy_d} = \frac{N_A}{a_{MT}} \qquad \textbf{(2.20)}$$

to

$$N_A = \left(\frac{-D_A\, a_{MT}}{\Delta y}\right)\Delta C$$

and the rate of transport can be written as:

$$Rate\ of\ transport = \frac{dC_{GO,E}}{dt} = k_s\, a\left(\Delta C\right) \qquad \textbf{(6.6)}$$

where: k_s = the solid phase mass transfer coefficient representing the inverse of the resistance provided by the solid barrier (i.e. cell wall and slime layer).

a = the hyphal area per unit volume across which the transfer takes place.

Integration of Equation 6.6 yields:

$$\ln\left(1-\frac{C_{GO,E}}{C_{GO,C}}\right)=(k_s a)t \qquad \textbf{(6.7)}$$

By plotting $\ln\left(1-\frac{C_{GO,E}}{C_{GO,C}}\right)$ vs. t the slope, k_sa, which is the overall resistance of GO transport from the cell associated region through the cell wall and slime layer to the extracellular region was evaluated graphically as 0.185 ± 0.020 h^{-1} for the NaOH-controlled culture and 0.154 ± 0.005 h^{-1} for the $Ca(OH)_2$-controlled culture. Equation 6.8 may be used to explain the secretion of GO into the surroundings i.t.o the GO driving force without knowledge of the cell wall characteristics.

6.6 Conclusions

A novel method to quantify the morphology of *Penicillium* sp. CBS 120262 using analySIS® was developed successfully using manual and semi-automatic procedures. The measurements from 50 individual hyphae were reproducible and provided statistically representative data for analysis. Using this method, the morphological trends were determined during batch cultivation of *Penicillium* sp. under conditions of mycelial growth in the absence of clumping. The N_t, L_e and L_t indices increased during the active growth phase while the L_{ghu} index decreased and the L_d index remained constant. The morphology of *A.niger* NRRL-3 was quantified using different morphological indices.

A modified two-film mass transfer theory, with GO concentration gradient as the driving force for secretion, was used to describe the transport of GO from the intracellular region to the external environment. This cell-based mass transfer analysis of experimental data to provide understanding of the changing relative location of GO provides new insights. As the GO accumulated intracellularly, the concentration gradient between its intracellular and extracellular location increased providing an increased driving force for GO secretion, and hence an increased specific rate of secretion. During the stationary

phase, the specific rate of production decreased while the specific rate of secretion remained constant. This translated into the product becoming increasingly extracellular during the stationary phase. The extracellular location of GO is important for the simplification of the downstream enzyme recovery, purification and enzyme yield of the downstream process. The limiting rate of enzyme transport may compromise attaining maximised extracellular location of GO, while this restricted rate may increase the concentration driving force. Optimising the extracellular location is well recognised as key in improved product recovery through downstream processing. This study provides insight into protein secretion in fungi as well as the limiting steps involved in its secretion, using a novel GO enzyme.

Chapter 7 Conclusions and Recommendations

The objective of this study was to investigate enzyme location in a fungal system and its impact on downstream processing for enzyme recovery. The influence of changing process conditions, such as micro-organism used, growth phase and using different pH control agents on enzyme location and fungal morphology was studied. The production of the enzyme glucose oxidase (GO) from *Aspergillus niger* NRRL-3 (*A. niger*) and *Penicillium* sp. CBS 120262 (*Penicillium* sp.) was studied and used as a model system. The outcomes obtained in this study may inform the development of other enzyme and microbial processes.

GO was produced in batch cultivations of *A. niger* and *Penicillium* sp. and achieved similar specific growth rates of 0.15 h^{-1} and 0.16 h^{-1} respectively. In both these systems GO was a growth associated product and was modelled using Luedeking-Piret equation. While glucose induces GO production, it was efficiently metabolised to GA (85 % for *A. niger* and 76% for *Penicillium* sp.). A direct relationship between the amount of GA produced and the amount of base needed to neutralise GA was established. *Penicillium* sp. supported higher biomass (2.20 g l^{-1} vs. 1.56 g l^{-1}), higher total volumetric GO concentration (8.1 U ml^{-1} vs. 4.7 U ml^{-1}) and higher specific GO (3598 U g^{-1} vs. 2838 U g^{-1}) on reaching stationary phase than *A. niger*. Although *A. niger* runs have shorter cultivation times (25 h vs. 45h) it had equivalent biomass (0.04 g l^{-1} h^{-1}) and total GO productivity (0.19 U $l^{-1}h^{-1}$) compared to *Penicillium* sp. while the extracellular GO productivity from *Penicillium* was double than that of *A. niger* at 0.08 U $l^{-1}h^{-1}$. The overall specific GO activity in *Penicillium* sp. was 1.2-fold greater than that in *A. niger*. This indicated that *Penicillium* sp. showed a better productivity of GO activity than *A. niger*, since the specific growth rates of the two organisms were the same. Further, the maximum cell concentration was enhanced in the *Penicillium* culture, resulting in a greater volumetric GO activity. These observations, and the coincident occurrence of the maximal specific GO activity, maximal cell concentration and maximal extracellular location, makes *Penicillium* sp. CBS 120262 a preferred choice over *A. niger* NRRL-3 for GO production and was used to study the effect of changing the pH control from NaOH to $Ca(OH)_2$ on the production of GO. Using $Ca(OH)_2$ as pH control agent the production of GO from *Penicillium* sp. was favourably influenced with a 2.4- and 2.5- fold increase in GO and biomass productivity as well as a higher supernatant GO content.

Addressing the first hypothesis posed in Section 2.11, GO was found in multiple locations in *A. niger* and *Penicillium* sp. in the extracellular, slime mucilage, cell wall and membrane fragments and cytoplasm

fractions. In both *A. niger* and *Penicillium* sp. the ratio of the GO activity in each fraction varied as a function of micro-organism, growth phase and growth conditions and is an important link to product formation and recovery optimisation. The results showed that as the cultures moved from active growth to the stationary phase, more enzyme was secreted from the cytoplasm. In *Penicillium* sp. this resulted in an increase in GO activity in the extracellular fluid. In *A. niger* cultures, however, the concurrent increased GO entrapment reduced the fraction of GO activity in the extracellular fluid. GO from *A. niger* was trapped predominantly in the cell wall. In *Penicillium* sp. the entrapment of GO in the cell wall was partially overcome in the stationary phase and was largely overcome when $Ca(OH)_2$ was used to control the suspension pH during cultivation instead of NaOH, resulting in an increased Ca concentration in solution. Since the distribution of activity varied with growth phase, the GO recovered depended on the time at which the culture was harvested.

Table 7.1 GO location in *Penicillium* sp. CBS120262 and *A. niger* NRRL-3 cultures in terms of growth phase and micro-organism used

Micro-organism	*Penicillium* sp. CBS120262		*Aspergillusniger* NRRL-3		*Penicillium* sp. CBS120262	
% GO in fraction	Mid-exponential (27 h)	Stationary (45 h)	Mid-exponential (15.5 h)	Stationary (25 h)	NaOH Stationary (45 h)	$Ca(OH)_2$ Stationary (45 h)
Extracellular fluid	30	59	46	38	59	93
Slime mucilage	17	9	12	16	9	1
Cell wall and membrane fragments	18	10	26	34	10	3
Cytoplasm fraction	35	22	16	12	22	3

In accordance with Hypothesis 2, the GO activity recovered at the end of the process depends not only on the organism, growth phase and time of harvest, but also on the purification programme used. The mixed location of GO in the fungal cultures limits its recovery in that there is a play off between the number of purification steps required and increased theoretical yield. The result will also depend on the step yield employed in the purification process. The results from the study demonstrated the relative benefit of achieving extracellular location in production vs. the downstream process recovery after enzyme recovery, purification and enzyme yield of the downstream process, this study illustrated the limiting effect of enzyme transport, which is governed by the concentration driving force, in attaining maximised extracellular location of GO.

To address the role of morphology on the location of the GO enzyme, a novel method to quantify the morphology of *Penicillium* sp. CBS 120262 using analySIS® was developed successfully using manual and semi-automatic procedures. The measurements from 50 individual hyphae were reproducible and provided statistically representative data for analysis. Using this method, the morphological trends were determined during batch cultivation of *Penicillium* sp. and the N_t, L_e and L_t indices increased during the active growth phase while the L_{ghu} index decreased and the L_d index remained constant. The morphology of *A.niger* NRRL-3 was quantified using different morphological indices, such as roughness and compactness. During growth the morphological indices for the $Ca(OH)_2$-controlled culture showed marked differences from those obtained for the NaOH-controlled culture with higher values for the morphological indices except for a lower L_{ghu} index which indicated that the hyphae were more branched in the presence of calcium. At the end of the *Penicillium* sp. cultivation controlled with $Ca(OH)_2$, there were 19 tips per hyphal body compared to the 8 tips per hyphal body for NaOH-controlled culture. With the predominantly extracellular location of GO (93%) and the increased hyphal tips, GO secretion was improved when $Ca(OH)_2$ was used as pH control agent.

Fick's law of diffusion with GO concentration gradient (ΔC) as the driving force for secretion, was used to describe the transport of GO from the intracellular region to the external environment. As the GO accumulated intracellularly, the concentration gradient between its intracellular and extracellular location increased providing an increased driving force for GO secretion, and hence an increased specific rate of secretion. During the stationary phase, the specific rate of production decreased while the specific rate of secretion remained constant. This translated into the product becoming increasingly extracellular during the stationary phase. Results indicated that as GO was produced, when $Ca(OH)_2$ was used as pH control agent, it was secreted into the external medium. In comparison, there was a delay in GO secretion for the NaOH-controlled culture. In accordance with Hypothesis 3, using ΔC, the transport of GO from the cell associated region to the extracellular region was defined in terms of an overall volumetric GO transport coefficient ($k_s a$) calculated from a generalised transport

$$Rate\ of\ transport = \frac{dC_{GO,E}}{dt} = k_s\, a\left(\Delta C\right)$$

where: k_s = the solid phase mass transfer coefficient representing the inverse of the resistance provided by the solid barrier (i.e. cell wall and slime layer).

a = the hyphal area per unit volume across which the transfer takes place.

The coefficient $k_s a$ represented the overall resistance of GO transport from the cell associated region through the cell wall and slime layer to the extracellular region and was evaluated graphically as 0.185 ± 0.020 h^{-1} for NaOH and 0.154 ± 0.005 h^{-1} for $Ca(OH)_2$. This result might be used on a macro-scale to provide new insight into the secretion of GO into the surroundings i.t.o the GO driving force without knowledge of the cell wall characteristics.

Results illustrated that with an increase in biomass concentration the apparent viscosity increased and therefore has an effect on the process but the same could not be shown for morphology. The relationship between fungal morphology and culture rheology did not show the dominant effect. Since the biomass concentration and resultant apparent viscosity of *A. niger* and *Penicillium*sp were low, these did not influence the production of GO. The *Penicillium* culture with its sparsely branched mycelia was 1.5–fold more viscous than *A. niger* with its highly branched mycelia arranged in a pellet morphology. The culture rheology of *Penicillium* sp. may be expected to become detrimental to GO production due to mass transfer limitations on increasing the biomass concentration and apparent viscosity. Conversely intra-pellet mass transfer limtations may influence GO production in *A.niger*.

Using GO as a model system it was shown that there was a relationship between (i) enzyme location, micro-organism used, growth and growth conditions, (ii) enzyme location and DSP to recover and purify the enzyme, (iii) location, growth rate and morphology, (iv) morphology, secretion and transport of GO. The relationship between (i) morphology and culture rheology, and (ii) culture rheology and GO production was not as dominant as expected.

From the outcomes of this study is recommended that fed-batch experiments are performed for *Penicillium* sp. CBS 120262 in order to maximize biomass concentration, thereby increasing the total GO activity. It is recommended that a variable volume approach should be considered to maintain a constant specific growth rate in the reactor. It is also recommended that NH_4OH should be used as the pH control agent in fed-batch cultivations (Korz*et al*., 1995; Kim *et al*., 2004; Haack *et al*., 2006) to act as an additional N-source. Owing to the link between enzyme location, growth phase and growth conditions, such a study should be preceded by duplicate batch experiments using NH_4OH as pH control agent should be carried out and the results obtained compared to results obtained on using $Ca(OH)_2$as pH control agent in terms of GO production, GO location, morphology, enzyme secretion and culture rheology to enable optimal production and secretion conditions to be selected.

The study has demonstrated clearly the inter-relatedness of enzyme production, location and recovery by downstream processing. This illustrates the value of assessing distributed enzyme location and undertaking combined optimisation of the production and recovery stages of the bioprocess, as opposed to the sequential optimisation typically reported.

References

Adams H.L., Thomas C.R. (1988), "The use of image analysis for morphological measurements on filamentous micro-organisms", *Biotechnology and Bioengineering*, **32**, 708 – 712.

Aiba S., Humphrey A.E., Millis N.F. (1965), "The Characteristics of Biological Material", In: *Biochemical Engineering*, Academic Press, New York, 17 – 40.

Allen D.G., Robinson C.W., (1990), "Measurement of rheological properties of filamentous fermentation broths", *Chemical Engineering Science*, **45**(1), 37 – 48.

Amanullah A., Jüsten P., Davies A., Paul G.C., Nienow A.W., Thomas C.R. (2000), "Agitation induced mycelial fragmentation of *Aspergillus oryzae* and *Penicillium chrysogenum*", *Biochemical Engineering Journal*, **5**, 109 – 114.

Amanullah A., Christensen L.H., Hansen K., Nienow A.W., Thomas C.R. (2002), "Dependence of morphology on agitation intensity in fed-batch cultures of *Aspergillus oryzae* and its implications for recombinant protein production", *Biotechnology and Bioengineering*, **77** (7), 817 – 826.

Aragon S., Hahn D.K. (2006), "Precise boundary element computation of protein transport properties: diffusion tensors, specific volume, and hydration", *Biophysical Journal*, **91**, 1591 – 1603.

Archer D.B., Pederby J.F., (1997), "The molecular biology of secreted enzyme production by fungi", *Critical Reviews in Biotechnology*, **17** (4), 273 – 306.

Archer D.B. (2000), "Filamentous fungi as microbial cell factories for food use", *Current Opinion in Biotechnology*, **11** (5), 478 – 483.

Armstrong J.K., Wenby R.B., Meiselman H.J., Fisher T.C. (2004), "The hydrodynamic radii of macromolecules and their effect on red blood cell aggregation", *Biophysical Journal*, **87**, 4259 – 4270.

Asenjo, J. A., Ventom, A. M., Huang, R.-B., Andrews, B. A. (1993), Selective release of recombinant protein particles (VLPs) from yeast using a pure lytic glucanase enzyme. *Bio Technology*, **11**, 214 - 217.

Atkinson and Lester (1974), "Appendix II: Free solution kinetics of glucose oxidase" In *Biochemical Engineering and Biotechnology Handbook*, 574-578.

Atkinson B., and Mavituna, F., (1991) "Flow behaviour of fermentation fluids", In: *Biochemical Engineering and Biotechnology Handbook*, 2nd ed., Stockton Press, New York, 670 – 696.

Balasundaram B., Harrison S., Bracewell D.G. (2009), "Advances in product release strategies and impact on bioprocess design", *Trends in Biotechnology*, **27** (8), 477 – 485.

Belmar-Beiny M.T. and Thomas C.R. (1991), "Morphology and clavulanic acid production of *Streptomyces clavuligerus*: Effect of stirrer speed in batch fermentations", *Biotechnology and Bioengineering*, **37**, 456 – 462.

Berovic M., Koloini T., Olsvik E.S., Kristiansen B., (1993), "Rheological and morphological properties of submerged citric acid fermentation broth in stirred-tank and bubble column reactors", *The Chemical Engineering Journal*, **53**, B35 – B40.

Blom R.H., Pfeifer V.F., Moyer A.J., Traufler D.H., Conway H.F. (1952), "Sodium gluconate production fermentation with *Aspergillus niger*", *Industrial and Engineering Chem*istry, **44**, 435 – 440.

Braun S., Vecht-Lifshitz S.E. (1991), "Mycelial morphology and metabolite production", *Trends in Biotechnology*, **9**, 63 – 68.

Bucke C. (1983) Glucose transforming enzymes. In: Fogarty WM (ed) *Microbial enzymes and biotechnology*. Applied Science Publishers, London, pp 111 – 123.

Caldwell I.Y., Trinci A.P.J. (1973), 'The growth unit of the mould *Geotrichum candidum*", *Archives Mikrobiology*, **88**, 1 – 10.

Casadevall A., Nosanchuk J.D., Williamson P., Rodrigues M.L. (2009), "Vesicular transport across the fungal cell wall", *Trends in Microbiology*, **17**(4), 158 – 162.

Casas López J.L., Sánchez Pérez J.A., Fernández Sevilla J.M., Rodríguez Porcel E.M., Christi Y., (2005), "Pellet morphology, culture rheology and lovastin production in cultures of *Aspergillus terreus*", *Journal of Biotechnology*, **116**, 61 – 77.

Chang P.L.Y., Trevithick J.R. (1970), "Biochemical and histochemical localization of invertase in *Neurospora crassa* during conidial germination and hyphal growth", *Journal of Bacteriology*, **102**, 423 – 429.

Chang P.L.Y., Trevithick J.R. (1974), "How important is secretion of exoenzymes through apical cell walls of fungi?" *Archives of Microbiology*, **101**: 281-293.

Charles M. (1978), "Technical aspects of the rheological properties of microbial cultures" In: *Advances in Biochemical Engineering: Mass transfer in Biotechnology*, Ghose T.K., Fiechler A., Blakebrough N. (ed), Springer-Verlag, New York, 1 – 62.

Childs R.E., Bardsley W.G. (1975), "The steady-state kinetics of peroxidise with 2,2'-Azino-di-(3-rthylbenzthiazoline-6-sulphonic acid) as chromogen, *Biochemical Journal*, **145**, 93 – 103.

Ciucu A., Patroescu C. (1984), "Fast spectrophotometric method of determining the activity of glucose oxidase", *Analytical Letters*, **17**, 1417 – 1427.

Clark D.C. (1962), "Submerged citric acid fermentation of ferrocyanide-treated beet molasses: Morphology of pellets of *Aspergillus niger*", *Canadian Journal of Microbiology*, **8**, 133 -136.

Clarke K.G., Williams P.C., Smit M.S., Harrison S.T.L. (2006) "Enhancement and repression of the volumetric oxygen transfer coefficient through hydrocarbon addition and its influence on oxygen transfer rate in stirred tank bioreactors", *Biochemical Engineering Journal*, **28**, 237 – 242.

Conesa A., Punt P.J., Van Luijk N., Van den Hondel C.A.M.J.J. (2001), "The secretion pathway in filamentous fungi: A Biotechnological view", *Fungal Genetics and Biology*, **33**, 155 – 171.

Cox P.W., Thomas C.R. (1992), "Classification and measurement of fungal pellets by automated image analysis", *Biotechnology and Bioengineering*, **39**, 945 – 952.

CRC Handbook of Chemistry and Physics, (1978), West R.C. (ed), 58th edition, CRC Press Inc., Florida.

Danneel H-J., Rössner E., Zeeck A., Giffhorn F. (1993), "Purification and characterization of a pyranose oxidase from the basisiomycete *Peniophora gigantean* and chemical analyses of its reaction products", *European Journal of Biochemistry*, **214**, 795 – 802.

De Nobel J.G., Dijkers C., Hooijberg E., Klis F.M. (1989),"Increased cell wall porosity in *Saccharomyces cerevisiae* after treatment with dithiothreitol or EDTA", *Journal of General Microbiology*, **135**, 2077 – 2084.

De Nobel J.G., Klis F.M., Priem J., Munnik T., Van den Ende H. (1990a), "An assay of relative cell wall porosity in *Saccharomyces cerevisiae*, *Kluyveromyces lactis* and *Schizosaccharomyces pombe*", *Yeast*, **6**, 483- 490.

De Nobel J.G., Klis F.M., Priem J., Munnik T., Van den Ende H. (1990b), "The glucanase-soluble mannoproteins limit cell wall porosity in *Saccharomyces cerevisiae*", *Yeast*, **6**, 491- 499.

De Nobel J.G., Barnett J.A. (1991), "Passage of molecules through yeast cell walls: A brief essay-Review", *Yeast*, **7**, 313 – 323.

De Nobel J.G., Klis F.M., Ram A., Van Unen H., Priem J., Munnik T., Van den Ende H. (1991), "Cyclic variations in the permeability of the cell wall of *Saccharomyces cerevisiae*", *Yeast*, **7**, 589-598.

Deshpande N., Wilkins M.R., Packer N., Nevalainen H. (2008), "Protein glycosylation pathways in filamentous fungi", *Glycobiology*, **18** (8), 626 – 637.

Döppner T., Hartmeier W. (1984), "Glucose oxidation by modified mould mycelium", *Starch*, **36** (8), 283 – 287.

Doran P.M. (1999), *Bioprocess Engineering Principles*, Academic Press, London.

Edwards A.G., Ho C.S., (1988), "Effects of carbon dioxide on *Penicillium chrysogenum*: an autoradiographic study", *Biotechnology and Bioengineering*, **32**, 1 – 7.

El-Enshasy H. (1998), "Optimization of Glucose Oxidase production by recombinant *Aspergillus niger",* PhD dissertation, Technische Universität Carolo-Wilhelmina, Braunschweig.

Fatile I.A., (1985), "Rheological characteristics of suspensions of *Aspergillus niger*: correlation of rheological parameters with microbial concentration and shape of the mycelial aggregates", *Applied Microbiology and Biotechnology*, **21**, 60 – 64.

Fiedurek J., Rogalski J., Ilczuk Z., Leonowicz A. (1986), "Screening and mutagenis of molds for improvement of glucose oxidase production", *Enzyme and Microbial Technology*, **8**, 734 – 736.

Fiedurek J. and Gromada A. (1997), "Screening and mutagenesis of molds for improvement of the simultaneous production of catalase and glucose oxidase", *Enzyme and Microbial Technology*, **20**, 344-347.

Fiedurek J. (1998), "Effect of osmotic stress on glucose oxidase production and secretion by *Aspergillus niger*", *Journal of Basic Microbiology*, **2**, 107 – 112.

Fiedurek J., Gromada A. (2000), "Production of catalase and glucose oxidase by *Aspergillus niger* using unconventional oxygenation of culture." *Journal of Applied Microbiology*, **89**, 85-89.

Fontaine T., Simenel C., Dubreucq G., Adam O., Delepierre M., Lemoine J., Vorgias C.E., Diaquin M., Latge J-P. (2000), "Molecular organization of the alkali-insoluble fraction of *Aspergillus fumigatus* cell wall", *The Journal of Biological Chemistry*, **275** (36), 27594 – 27607.

Galbraith J.C., Smith J.E., (1969), "Filamentous growth of *Aspergillus niger* in submerged shake culture", *Transactions of the British Mycological Society*, **52**, 237 – 246.

Gervais P., Martinez de Maranon I. (1995), "Effect of the kinetics of temperature variation on *Saccharomyces cerevisiae* viability and permeability", *Biochimica et Biophysica Acta*, **1235**, 52 – 56.

"Glucose oxidase (GOx) E.C.1.1.3.4", Date accessed: 2006-10-23, http://chem.ch.huji.ac.il/~eugeniik?glucose_oxidase.htm.

Gordon C.L., Khalaj V., Ram A.F.J., Archer D.B., Brookman J.L., Trinci A.P.J., Jeenes D.J., Doonan J.H., Wells B., Punt P.J., Van den Hondel C.A.M.J.J., Robson G.D. (2000), "Glucoamylase::green fluorescent protein fusions to monitor protein secretion in *Aspergillus niger*", *Microbiology*, **146**, 415 – 426.

Gouka R.J., Punt P.J., Van den Hondel C.A.M.J.J. (1997), "Efficient production of secreted proteins by *Aspergillus*: progress, limitations and prospects", *Applied Microbiology and Biotechnology*, **47**, 1 – 11.

Goudar C.T., Strevett K.A., Shah S.N., (1999), "Influence of microbial concentration on the rheology of non-Newtonian fermentation broths", *Applied Microbiology and Biotechnology*, **51**, 310 – 315.

Gray P.P and Tribe D.E. (1979), "The commercial production of microbial enzymes: Part 2. Production processes", *Food technology in Australia*, **31**(6), 254-260.

Grimm L.H., Kelly S., Krull R., Hempel D.C. (2005), "Morphology and productivity of filamentous fungi", *Applied Microbiology and Biotechnology*, **69**, 375 – 384.

Gromada A., Fiedurek J. (1996), "Influence of medium components and metabolic inhibitors on glucose oxidase production by *Aspergillus niger* mycelium, *Acta Microbiologica Polonica*, **45**(1), 37 – 43.

Haack M.B., Olsson L., Hansen K., Lantz A.E. (2006), "Change in hyphal morphology of *Aspergillus oryzae* during fed-batch cultivation", *Applied Microbiology and Biotechnology*, **70**, 482 – 487.

Harlow E., Lane D. (1988), *Antibodies: A laboratory manual*, Cold Spring harbour Laboratory Press, Cold Spring Harbor, New York.

Harrison S.T. (1991), "Bacterial cell disruption: a key unit operation in the recovery of intracellular products", *Biotechnology Advances*, **9(2)**, 217 – 240.

Harrison STL (2011), "Cell disruption", In: Moo-Young and Webb (eds) *Comprehensive biotechnology*, 2nd ed, Vol 2, Chapter 44, Elsevier, Oxford, 619 – 640.

Hatzinikolaou D.G., Macris B.J. (1995), "Factors regulating production of glucose oxidase by *Aspergillus niger*". *Enzyme and Microbial Technology* **17**, 530 – 534.

Hatzinikolaou D.G., Hansen O.C., Macris B.J., Tingey A., Kekos D., Goodenough P., Stougaard P. (1996), "A new glucose oxidase from *Aspergillus niger*: characterization and regulation studies of enzyme and gene", *Applied Microbiology and Biotechnology*, **46**, 371 – 381.

Hellmuth K., Pluschkell S., Jung J-K, Ruttkowski E., Rinas U. (1995), "Optimization of glucose oxidase production by *Aspergillus niger* using genetic- and process-engineering techniques". *Applied Microbiology and Biotechnology*, **43**, 978-984.

Hendle J., Hecht H-J, Kalisz H. M., Schmid R.D., Schomburg D. (1992), "Crystallization and preliminary X-ray diffraction studies of a deglycosylated glucose oxidase from *Penicillium amagasakiense*", *Journal of Molecular Biology*, **223**, 1167 – 1169.

Heydarian S.M., Ison A.P., Shamlou P.A., (1999), "Rheology of filamentous microorganisms in submerged culture", In: Encyclopedia of Bioprocess Technology – Fermentation, Biocatalysis and Bioseparation, Flickinger M.C. and Drew S.W (eds), John Wiley and Sons, New York, Vol 5, 2278 – 2289.

Hong S.Y., Choi S.K., Lee Y.H., Pek U.H., Jung J.K. (1998), "Overproduction and high level secretion of glucose oxidase in *Saccharomyces cerevisiae*", *Korean Journal of Applied Microbiology and Biotechnology*, **26**, 68 -75.

Jackson S.L., Heath I.B. (1993), "Roles of calcium ions in hyphal tip growth", *Microbiological Reviews*, **57**(2), 367 – 382.

Johansen C.L., Coolen L., Hunik J.H. (1998), "Influence of morphology on product formation in *Aspergillus awamori* during submerged fermentations", *Biotechnology Progress*, **14**, 233 – 240.

Johnson K.H.S. (1995), "Glucose oxidase induction and the modelling of gluconic acid production using *Aspergillus niger"*, MSc dissertation, Department of Chemical Engineering, University of Cape Town, South Africa.

Kapat A., Jung J.K., Park Y.H., Hong S.Y., Choi H.K. (1998), "Effect of agitation and aeration on the production of extracellular glucose oxidase from a recombinant *Saccharomyces cerevisiae*", *Bioprocess Engineering*, **18**, 347 – 351.

Kapat A., Jung J.K., Park Y.H. (2000), "Effects of continuous feeding of galactose on the production of recombinant glucose oxidase using *Saccharomyces cerevisiae*", *Bioprocess Engineering*, **23**, 37 – 40.

Kapat A., Jung J-K., Park Y-H. (2001), "Enhancement of glucose oxidase production in batch cultivation of recombinant *Saccharomyces cerevisiae*: optimization of oxygen transfer condition", *Journal of Applied Microbiology*, **90**, 216-222.

Kalisz H.M., Hendle J., Schmid R.D. (1990), "Purification of the glycoprotein glucose oxidase from *Penicillium amagasakiense* by high-performance liquid chromatography", *Journal of Chromatography*, **521**, 245 – 250.

Keilin D., Hartree E.F. (1948), "The use of glucose oxidase (notatin) for the determination of glucose in biological material and the study of glucose-producing systems in manomeric methods", *Biochemistry Journal*, **42**, 221-229.

Kim J.H., Lebeault, J.M., Ruess M., (1983), "Comparative study on rheological properties of mycelial broth in filamentous and pelleted forms", *European Journal of Microbiology and Biotechnology*, **18**, 11 -16.

Kim B.S, Lee S.Y., Chang Y.K., Chang H.N. (2004), "High cell density fed-batch cultivation of *Escherichia coli* using exponential feeding combined with pH-stat", *Bioprocess and Biosystems Engineering*, **26**, 147 – 150.

Kisser M., Kubicek C.P., Rohr M. (1980), "Influence of manganese on morphology and cell wall composition of *Aspergillus niger* during citric acid fermentation". *Archives of Microbiology*, **128**, 26-33.

Klis F.M. (1994), "Review: Cell wall assembly in yeast", *Yeast*, **10**, 851 – 869.

Klis F.M., Mol P., Hellingwerf K., Brul S. (2002), "Dynamics of cell wall structure in *Saccharomyces cerevisiae*", *FEMS Microbiology Review*, **26**, 239 – 256.

Klis F.M., Boorsma A., De Groot P.W.J. (2006), "Cell wall construction in *Saccharomyces cerevisiae*", *Yeast*, **23**, 185-202.

Kobayashi T., Van Dedem G., Moo-Young M. (1973), "Oxygen transfer into mycelial pellets", *Biotechnology and Bioengineering*, **15**, 27 – 45.

Kona RP., Qureshi N., Pai JS (2001) Production of glucose oxidase using *Aspergillus niger* and corn steep liquor, *Bioresource Technology*, **78**, 123-126.

Korz D.J.,Rinas U., Hellmuth K., Sanders E.A., Deckwer W.D. (1995), "Simple fed-batch technique for high cell density cultivation of *Escherichia coli*", *Journal of Biotechnology*, **39**, 59 – 65.

Kröger S., Setford S.J., Turner P.F. (1998), "Electrochemical assay method for the rapid determination of oxidase enzyme activities", *Biotechnology Techniques*, **12**(2), 123 – 127.

Kusai K., Sekuzu I., Hagihara B., Okunuki K., Yamauchi S., Nakai M. (1960) "Crystallization of glucose oxidase from *Penicillium amagasakiense*". *Biochimica et Biophysica Acta*, **40**, 555 – 557.

Leammli U.K. (1970), "Cleavage of structural proteins during the assembly of the head of bacteriophage T4", *Nature*, **227**, 680 – 685.

Lejeune R., Baron G.V. (1998), "Modeling the exponential growth of filamentous fungi during batch cultivation", *Biotechnology and Bioengineering*, **60**(2), 169 – 179.

Li T-H, Chen T-L. (1994), "Enhancement of glucose oxidase fermentation by addition of hydrocarbons", *Journal of Fermentation and Bioengineering*, **78**(4), 298 – 303.

Liu J-Z, Yang H-Y, Weng L-P, Ji L-N. (1999) "Synthesis of glucose oxidase and catalase by *Aspergillus niger* in resting cell culture system". *Letters in Applied Microbiology*, **29**, 337-341.

Liu J-Z, Huang Y-Y, Liu J, Weng L-P, Ji L-N. (2001), "Effects of metal ions on simultaneous production of glucose oxidase and catalase by *Aspergillus niger*", *Letters in Applied Microbiology*, **32**, 16 – 19.

Lloyd J.B., Whelan W.J. (1969), "An improved method for enzymic determination of glucose in the presence of maltose", *Analytical Biochemistry*, **30**, 467 – 470.

Lockwood L.B. (1975), In: The filamentous Fungi, Vol.I, *Industrial Mycology*, Ch. 8, Ed. Smith J.E., Berry D.R., Ardold E., London, 140-145.

Lu T., Peng X., Yang H., Ji L. (1996), "The production of glucose oxidase using the waste myceliums of *Aspergillus niger* and the effects of metal ions on the activity of glucose oxidase", *Enzyme and Microbial Technology*, **19**, 339-342.

MacKenzie D.A., Jeenes D.J., Belshaw N.J., Archer D.B. (1993), "Regulation of secreted protein production by filamentous fungi: recent developments and perspectives", *Journal of General Microbiology*, **139**, 2295 – 2307.

Manchanda A.C., Jogdand V.V., Karanth N.G. (1982), "Studies on fermentation-broth rheology of a Penicillium strain with cellulose as substrate", *Journal of Chemical Technology and Biotechnology*, **32**, 660- 665.

Margaritis A., Zajic J.E. (1978), "Mixing, mass transfer and scale-up of polysaccharide fermentations", *Biotechnology and Bioengineering*, **10**, 939 - 1001.

Markwell J., Frakes L.G., Brott E.C., Osterman J., Wagner F.W. (1989), "*Aspergillus niger* mutants with increased glucose oxidase production", *Applied Microbiology and Biotechnology*, **30**, 166 – 169.

McIntyre M., McNeil B., (1997), "Dissolved carbon dioxide effects on morphology, growth, and citrate production in *Aspergillus niger* A60", *Enzyme and Microbial Technology*, **20**(2), 135 – 142.

McIntyre M., Müller C., Dynesen J., Nielsen J. (2001), "Metabolic engineering of the morphology of *Aspergillus*", Advances *in Biochemical Engineering and Biotechnology*, **73**, 103 – 128.

Messing R.A. (1974), "Simultaneously immobilized glucose oxidase and catalase in controlled-pore titania", *Biotechnology and Bioengineering*, **16**, 879 - 908.

Metz B., Kossen N.W.F. (1977), "The growth of molds in the form of pellets - a literature review", *Biotechnology and Bioengineering*, **19**, 781 – 799.

Metz B., Kossen N.W.F., Van Suijdam J.C., (1979), "The rheology of mould suspensions" *Advances in Biochemical Engineering*, **11**, 103 – 156.

Metz B., De Bruin E.W., Van Suijdam J.C. (1981), "Method for quantitative representation of the morphology of molds", *Biotechnology and Bioengineering*, **23**, 149 – 162.

Metzner A.B. Otto R.E., (1957)," Agitation of non-Newtonian fluids", *American Institute of Chemical Engineers*, **3**(1), 3 – 10.

Middelberg A.P.J. (1995), "Process-scale disruption of microorganisms", *Biotechnology Advances*, **13**, 491 – 551.

Miles E.A., Trinci A.P.J. (1983), "Effect of pH and temperature on morphology of batch and chemostat cultures of *Penicillium chrysogenum*", *Transactions of the British Mycological Society*, **81**, 193 – 200.

Miller G.L. (1959), "Use of dinitro salicyclic acid reagent for determination of reducing sugar", *Analytical Chemistry*, **31**, 426 – 428.

Mirón J., González M.P., Vázquez J.A., Pastrana L., Murado M.A. (2004), "A mathematical model for glucose oxidase kinetics, including inhibitory, deactivant and diffusional effects, and their interactions", *Enzyme and Micobial Technology*, **34**, 513 – 522.

Mischak H., Kubicek C.P., Rohr M. (1985), "Formation and location of glucose oxidase in citric acid producing mycelia of *Aspergillus niger*", *Applied Microbiology and Biotechnology*, **21**, 27-31.

Miura Y., Tsuchiya K., Tsusho H., Miyamoto K. (1970), "Kinetic studies of gluconic acid fermentation using *Aspergillus niger*", *Journal of Fermentation Technology*, **48**, 795- 803.

Moo-Young M. (1985), "Comprehensive Biotechnology: The principles, applications and regulations of biotechnology in industry, agriculture and medicine", Pergamon Press, Oxford, **3**, 681 – 699.

Morrison K.B., Righelato R.C. (1974), "The relationship between the hyphal branching, specific growth rate and colony radial growth rate in *Penicillium chrysogenum*", *Journal of General Microbiology*, **81**, 517 – 520.

Mukataka S., Kataoka H., Takahashi J., (1980), "Effects of vessel size and rheological properties of suspensions on the distribution of circulation times in stirred vessels", *Journal of Fermentation Technology*, **58**(2), 155 – 161.

Muller C., McIntyre M., Hansen K., Nielsen J. (2002), "Metabolic engineering of the morphology of *Aspergillus oryzae* by altering chitin synthesis", Applied Environmental Biotechnology, **68(4)**, 1827 – 1836.

Nakamatsu T., Akamatsu T., Miyajima R. (1975), "Microbial production of glucose oxidase". *Agricultural and Biological Chemistry*, **39** (9), 1803 – 1811.

Nevalainen K.M.H., Téo V.S.J., Bergquist P.L. (2005), "Heterologous protein expression in filamentous fungi", *Trends in Biotechnology*, **23**(9), 468 – 474.

Nielsen J. (1992), "Modelling the growth of filamentous fungi", *Advances in Biochemical Engineering and Biotechnology*, **46**, 187 – 223.

Nielsen J. (1993), "A simple morphologically structured model describing the growth of filamentous microorganisms", *Biotechnology and Bioengineering*, **41**, 715 – 727.

Nielsen J., Villadsen J. (1994), "Morphologically structured models", In*: Bioreaction Engineering Principles*, 1st ed., Plenum Press, New York, p 249 – 259.

Nielsen J. (1996), "Modelling the morphology of filamentous microorganisms", *Trends in Biotechnology*, **14**, 438 – 443.

Nomenclature Committee of the International Union of Biochemistry (NC-IUB), (1979), "Units of enzyme activity", *European Journal of Biochemistry*, **97**, 319 – 320.

Olsvik E., Tucker K.G., Thomas C.R., Kristiansen B., (1993), "Correlation of *Aspergillus niger* broth rheological properties with biomass concentration and the shape of mycelial aggregates", *Biotechnology and Bioengineering*, **42**, 1046 – 1052.

Olsvik E.S., Kristiansen B., (1992), "On-line rheological measurements and control in fungal fermentations", *Biotechnology and Bioengineering*, **40**, 375 – 387.

Olsvik E., Kristiansen B., (1994), "Rheology of filamentous fermentations", *Biotechnology Advances*, **12**, 1 -39.

Ostergaard L.H., Olsen H.S. (2010), "Industrial applications of fungal enzymes", In: *Industrial Applications, The Mycota X*, 2nd ed, Hofrichter M., (ed), Springer-Verlag, Berlin, Chapter 13, 269 – 290.

Pace G.W., (1980), "Rheology of mycelial fermentation broths", In: *Fungal Biotechnology*, Smith J.E, Berry D.R., Kristiansen B., (ed), Academic Press, London, 95 – 110.

Packer H.L., Thomas C.R. (1990), "Morphological measurements on filamentous microorganisms by fully automatic image analysis", *Biotechnology and Bioengineering*, **35**, 870 – 881.

Papagianni M., Mattey M., Kristiansen B. (1999), "The influence of glucose concentration on citric acid production and morphology of *Aspergillus niger* in batch and glucostat culture", *Enzyme and Microbial Technology*, **25**, 710 – 717.

Papagianni M., Moo-Young M. (2002), "Protease secretion in glucoamylase producer *Aspergillus niger* cultures: fungal morphology and inoculum effects", *Process Biochemistry*, **37**, 1271 – 1278.

Papagianni M. (2004), "Fungal morphology and metabolite production in submerged mycelial processes", *Biotechnology Advances*, **22**, 189 – 259.

Paul G.C., Kent C.A., Thomas C.R. (1994), "Hyphal vacuolation and fragmentation in *Penicillium chrysogenum*", *Biotechnology and Bioengineering*, **44**, 655 – 660.

Pazouki M., Panda T. (2000), "Understanding the morphology of fungi", *Bioprocess Engineering*, **22**, 127 – 143.

Pazur J.H., Kleppe K., Ball E. (1963), "The glycoprotein nature of some fungal carbohydrates", *Archives of Biochemistry and Biophysics*, **103**, 515 – 516.

Pazur J.H., Kleppe K. (1964), "The oxidation of glucose and related compounds by glucose oxidase from *Aspergillus niger*", *Biochemistry*, **3**(4), 578 – 583.

Pazur J.H., Kleppe K., Cepure A. (1965), "A glycoprotein structure for glucose oxidase from *Aspergillus niger*", *Archives of Biochemistry and Biophysics*, **111**, 351 – 357.

Pazur J.H. (1966), Glucose oxidase. In: Cowolick SP, Kaplan NO (eds) *Methods in Enzymology* IX. Academic Press, New York, London, p83.

Peberdy J.F. (1994), "Protein secretion in filamentous fungi – trying to understand a highly productive black box", *Trends in Biotechnology*, **12**, 50 – 57.

Pedersen A.G., Bungaard-Nielsen M., Nielsen J., Villadsen J. (1993), "Rheological characterization of media containing *Penicillium chrysogenum*", *Biotechnology and Bioengineering*, **41**, 162 – 164.

Petersen N., Stocks S., Gernaey K.V. (2008), "Multivariate models for prediction of rheological characteristics of filamentous fermentation broth from the size distribution", *Biotechnology and Bioenegineering*, **100** (1), 61 - 71.

Petruccioli M., Fenice M., Piccioni P. (1993), "Distribution and typology of glucose oxidase activity in the genus *Penicillium*", *Letters in Applied Microbiology*, **17**, 285 – 288.

Petruccioli M., Fenice M., Piccioni P., Federici F. (1995), "Effect of stirrer speed and buffering agents on the production of glucose oxidase and catalase by *Penicillium variabile* (P16) in benchtop bioreactor". *Enzyme and Microbial Technology*, **17**, 336-339.

Petruccioli M., Piccioni P., Federici F. (1997), "Glucose oxidase overproduction by the mutant strain M-80.10 of *Penicillium variabile* in a benchtop fermenter", *Enzyme and Microbial Technology*, **21**, 458 – 462.

Petruccioli M., Federici F., Bucke C., Keshavarz T. (1999), "Enhancement of glucose oxidase production by *Penicillium variabile* P16", *Enzyme and Microbial Technology*, **24**, 397 – 401.

Pirt S.J. (1975), Principles of microbe and cell cultivation, Wiley, New York.

Pluschkell S., Hellmuth K., Rinas U. (1996), Kinetics of glucose oxidase excretion by recombinant *Aspergillus niger*", *Biotechnology and Bioengineering*, **51**, 215 – 220.

Prosser J.J. (1995), "Kinetics of filamentous growth and branching". In: Gow NAR and Gadd GM (ed) *The growing fungus*. Chapman and Hall Publishers, London, 301 -318.

Punt P.J., Van Biezen N., Conesa A., Albers A., Magnus J., Van den Hondel C. (2002), "Filamentous fungi as cell factories for heterologous protein production", *Trends in Biotechnology*, **20** (5), 200 -226.

Raba J. and Mottola H.A. (1995), "Glucose oxidase as an analytical reagent", *Critical Reviews in Analytical Chemistry*, **25**(1), 1-42.

Ramachandran S., Fontanille P., Pandey A., Larroche C. (2006), "Gluconic acid: Properties, applications and microbial production", *Food Technology and Biotechnology*, **44** (2), 185 – 195.

Rando D., Kohring G.W., Giffhorn F. (1997), "Production, purification and characterization of glucose oxidase from a newly isolated strain of *Penicillium pinophilum*", *Applied Microbiology and Biotechnology*, **48**, 34 – 40.

Reichl U., King R., Gilles E.D. (1992), "Characterization of pellet morphology during submerged growth of *Streptomyces tendae* by image analysis", *Biotechnology and Bioengineering*, **39**, 164 – 170.

Richter G. (1983), Glucose oxidase. In: Godfry T and Reiche J (eds) *Industrial Enzymology*,. The Nature Press, New York, 4: 428-437.

Righelato R.C., Trinci A.P.J., Pirt S.J. (1968), "The influence of maintenance energy and growth rate on the metabolic activity, morphology and condiation of *Penicillium chrysogenum*", *Journal of General Microbiology*, **50**, 399 – 412.

Riley G.L., Tucker K.G., Paul G.C., Thomas C.R. (2000), "Effect of biomass concentration and mycelial morphology on fermentation broth rheology", *Biotechnology and Bioengineering*, **68** (2), 160 – 172.

Rinas U., El-Enshasy H., Emmler M., Hille A., Hempel D.C., Horn H. (2005), "Model-based prediction of substrate conversion and protein synthesis and excretion in recombinant *Aspergillus niger* biopellets", *Chemical Engineering Science*, **60**, 2729 – 2739.

Robson G. (1999), "Hyphal cell biology", In: *Molecular fungal biology*, Oliver R.P., Schweizer M., (eds), Cambridge University Press, United Kingdom, 164 - 184.

Roche "Glucose oxidase", Date accessed: 2007-06-05, http://roche-applied-science.com/pack-insert/2208121a.pdf,

Roels J.A., Van den Berg J., Voncken R.M., (1974), "The rheology of mycelial broths", *Biotechnology and Bioengineering*, **16**, 181 – 208.

Rogalski J., Fiedurek J., Szczordrak J., Kapusta K., Leonowicz A. (1988), "Optimisation of glucose oxidase synthesis in submerged cultures of *Aspergillus niger* G-13 mutant.", *Enzyme and Microbial Technology*, **15**, 107-115.

Rohr, C., Kubicek J., Kominek J. (1983), Gluconic acid. In: *Biotechnology*, Vol. 3, ed. Rehm H.J. and Reed G., 456-465.

Rose A.H. (1980), Glucose oxidase, In: *Microbial enzymes and bioconversions*, Academic press, London, 173 – 225.

Rothberg A., Weegar J., Von Schalien R., Fagervik K., Rydström M, Lind K. (1999), "Optimization of an *Aspergillus niger* glucose oxidase production process", *Bioprocess Engineering*, **21**, 307 – 312.

Schröder M. (2008), "Engineering eukaryotic protein factories", *Biotechnology Letter*, **30**, 187 – 196.

Schuster E., Dunn-Coleman N., Frisvad J.C., Van Dijck P.W.M. (2002), "On the safety of *Aspergillus niger* – a review", *Applied Microbiology and Biotechnology*, **59**, 426 – 435.

Scott D. (1953), "Glucose conversion in preparation of albumen solids by glucose oxidase-catalse system", *Journal of Agricultural and Food Chemistry*, **1**(11), 727 – 730.

Shaeiwitz J.A., Blair J.B., Ruaan, R-C. (1989), "Evidence that yeast cell wall debris can separate proteins by ion-exchange during cell lysis", *Biotechnology and Bioengineering*, **34**, 137 – 140.

Shen A.L., Porter T.D., Wilson T.E., Kasper C.B. (1989), "Structural analysis of the FMN binding domain of NADPH-cytochrome P-450 oxidoreductase by site-directed mutagenesis", *Journal of Biology and Chemistry*, **264**, 7584 – 7589.

Shoji J., Arioka M., Kitamoto K., (2008), "Dissecting cellular components of the secretory pathway in filamentous fungi: insights into their application for protein production", *Biotechnology Letters*, **30**, 7 – 14.

Simpson C. (2005), "Isolation, purification and characterization of a novel glucose oxidase from *Penicillium canescens* tT42", MSc dissertation, Rhodes University, South Africa.

Simpson C., Jordaan J., Gardiner N.S., Whiteley C. (2007), "Isolation, purification and characterization of a novel glucose oxidase from *Penicillium* sp. CBS 120262 optimally active at neutral pH", *Protein Expression and Purification*, **51**, 260 – 266.

Steel R., Lentz C.P., Martin S.M. (1954), "A standard inoculum for citric acid production in submerged culture", *Canadian Journal of Microbiology*, **1**, 150 -157.

Swoboda B.E.P., Massey V. (1965), "Purification and properties of the glucose oxidase from *Aspergillus niger*", *Journal of Biological Chemistry*, **240** (5), 2209 – 2215.

Torralba S., Raudaskoski M., Pedregosa A.M., Laborda F. (1998), "Effect of cytochalasin A on apical growth, actin cytoskeleton organization and enzyme secretion in *Aspergillus nidulans*", *Microbiology*, **144**, 45 – 53.

Traeger, M., Qazi, G.N., Onken U. and Chopra, C.L. (1991), "Contribution of endo- and exocellular glucose oxidase to gluconic acid production at increased dissolved oxygen concentrations", *Journal of Chemical Technology and. Biotechnology*, **50**, 1-11.

Tsuge H., Natusaki O., Ohashi K. (1975), "Purification, properties, and molecular features of glucose oxidase from *Aspergillus niger*", *Journal of Biochemistry of Japan*, **78**, 835-843.

Tucker K.G., Kelly T., Delgrazia P., Thomas C.R. (1992), "Fully-automatic measurement of mycelial morphology by image analysis", *Biotechnology Progress*, **8**, 353 – 359.

Tucker K.G., Thomas C.R. (1992), "Mycelial morphology: the effect of spore inoculum level", *Biotechnology Letters*, **14**, 1071 – 1074.

Tucker K.G., Thomas C.R. (1993), "Effect of biomass concentration and morphology on the rheological parameters of *Penicillium chrysogenum* fermentation broths", *Trans IChemE* Part C, **71**, 111 – 117.

Tucker K.G. (1994), "Relationship between mycelia morphology biomass concentration and broth rheology in submerged fermentations", PhD thesis, University of Birmingham, Birmingham, UK.

Tyn M.T., Gusek T.W. (1990), "Prediction of diffusion coefficients of proteins", *Biotechnology and Bioengineering*, **35**, 327 – 338.

Underkofler L.A. (1958), "Properties and applications of the fungal enzyme glucose oxidase", *Proceedings of the International Symposium on Enzyme Chemistry*, Tokyo and Kyoto, 486 – 490.

Vainstein M.H., Pederby J.F. (1991), "Regulation of invertase in *Aspergillus nidulans*: effect of different carbon sources", *Journal of General Microbiology*, **137**, 315 – 321.

Van Dijken P.J., Veenhuis M. (1980), "Cytochemical location of glucose oxidase in peroxisomes of *Aspergillus niger*", *European Journal of Applied Microbiology and Biotechnology*, **9**, 275-283.

Van Suijdam J.C., Kossen N.W.F., Paul P.G. (1980), "An inoculum technique for the production of fungal pellets", *European Journal of Microbial Biotechnology*, **10**, 211 – 221.

Van Suijdam J.C., Metz B. (1981a), "Influence of engineering variables upon the morphology of filamentous molds", *Biotechnology and Bioengineering*, **23**, 111 –148.

Van Suijdam J.C., Metz B. (1981b), "Fungal pellet breakup as a function of shear in a fermentor", *Journal of Fermentation Technology*, **59**(4), 329 – 333.

Vishniac W., Santer M. (1975), "The Thiobacilli", *Bacteriological Reviews*, **21**(3), 195 – 213.

Wang L., Ridgway D., Gu T., Moo-Young M. (2005), "Bioprocessing strategies to improve heterologous protein production in filamentous fungal fermentations", *Biotechnology Advances*, **23**, 115 -129.

Wang X., Xu P.,Yuan Y., Liu C., Zhang D., Yang Z., Yang C., Ma C. (2006), "Modeling for gellan gum production by *Sphinogomonas paucimobilis* ATCC 31461 in a simplified medium", *Applied and Environmental Microbiology*, **72**(5), 3367 – 3374.

Warren S.J., Keshavarz-Moore E., Shamlou P.A., Lilly M.D., Thomas C.R., Dixon K. (1995), "Rheologies and morphologies of three actinomycetes in submerged culture", *Biotechnology and Bioengineering*, **45**, 80 - 85.

Wessels J.G.H. (1990), "Role of wall architecture in fungal tip growth generation", In: Heath I.B., ed., *Tip growth in plant and fungal cells*, Academic Press, San Diego, 1 – 29.

Wessels J.G.H. (1993), "Wall growth, protein excretion and morphogenesis in fungi", *New Phytologist*, **123**(3), 397 – 413.

Whitaker A., Long P.A. (1973), "Fungal pelleting", *Process Biochemistry*, **8**, 27 – 31.

Wiebe M.G. (2003), "Stable production of recombinant proteins in filamentous fungi – problems and improvements", *Mycologist*, **17**(3), 140 – 144.

Witt S., Singh M., Kalisz H.M. (1998), "Structural and kinetic properties of nonglycosylated recombinant *Penicillium amagasakiense* glucose oxidase expressed in *Escherichia coli*, *Applied & Environmental Microbiology*, **64**(4), 1405 – 1411.

Witteveen C.F.B., Van de Vondervoort P., Swart K., Visser J. (1990), "Glucose oxidase overproducing and negative mutants of *Aspergillus niger*", *Applied Microbiology and Biotechnology*, **33**, 683 – 686.

Witteveen C.F.B., Veenhuis M., Visser J. (1992), "Localization of glucose oxidase and catalyse activities in *Aspergillus niger*", *Applied and Environmental Microbiology*, **58**, 1190 – 1194.

Witteveen C.F.B., van de Vondervoort P.J.I., van den Broeck H.C., van Engelenburg F.A.C., de Graaff L.H., Hillebrand M.H.B.C., Schaap P.J., Visser J. (1993), "Induction of glucose oxidase, catalase, and lactonase in *Aspergillus niger*", *Current Genetics*, **24**, 408-416.

Wittler R., Baumgartl H., Lubbers D.W., Schugerl K. (1986), "Investigations of oxygen transfer into *Penicillium chrysogenum* pellets by microprobe measurement", *Biotechnology and Bioengineering*, **28**, 1024 –1026.

Wong C.M., Wong K.H., Chen X.D. (2008), "Glucose oxidase: natural occurrence, function, properties and industrial applications", *Applied Microbiology and Biotechnology*, **78**, 927 – 938.

Wörsten HAB, Moukha SM, Sietsma JH, Wessels JGH. (1991) "Localization of growth and secretion of proteins in *Aspergillus niger*", *Journal of General Microbiology*, **137**, 2017 – 2023.

Worthington manual, "Glucose oxidase", Date accessed: 2001-07-23, http://www.worthington-biochem.com/manual/G/GOP.html.

Yang H., King R., Reichl U., Gilles E.D. (1992), "Mathematical model for apical growth, septation, and branching of mycelial microorganisms", *Biotechnology and Bioengineering*, **39**, 49 – 58.

Zetelaki K. and Vas K. (1968), "The role of aeration and agitation in the production of glucose oxidase in submerged cultures", *Biotechnology and Bioengineering*, **10**, 45-59.

Zlotnik H., Fernandez M.P., Bowers B., Cabib E. (1984), "*Saccharomyces cerevisiae* mannoproteins form an external cell wall layer that determines wall porosity", *Journal of Bacteriology*" **159**(3), 1018 – 1026.

Znad H., Blazej M., Bales V., Markos J. (2004), "A kinetic model for gluconic acid production by *Aspergillus niger*", *Chemistry Paper*, **58**(1), 23 -28.

Znidarsic P., Pavko A. (2001), "The morphology of filamentous fungi in submerged cultivations as a bioprocess parameter", *Food technology and Biotechnology*, **39** (3), 237 – 252.

A. Assays

A.1. Cell dry weight (CDW)

1. Pre-dry 0.45 μm membrane filters placed on numbered aluminium boats in an 80°C oven for 24 hours.
2. Place dry membranes and boats into a desiccator to cool and weigh to four significant figures.
3. Note the number of the aluminium boat and place membrane on vacuum filter support.
4. Take a sample ± 20 ml and filter through the membrane under vacuum and collect the filtrate for glucose, and glucose oxidase analysis.
5. Wash the residue with distilled water and ensure no residue is left on the walls of the filter.
6. Transfer the membranes onto the aluminium boats and dry for 48 h at 80°C.
7. Place the aluminium boats in a desiccator to cool and weigh the combined boat, membrane and cell mass to four significant figures.
8. Calculate the change in dry mass and divide this by the sample volume to give the dry mass in g l^{-1}.

A.2. Reducing sugar assay

1. Standard Glucose Solution.

1.1. Dissolve 1 g glucose in 100 ml distilled water.

1.2. Prepare a dilution series in the range of 0.1 to 1.0 g l^{-1} glucose solution.

2. Dinitrosalicylic acid Reagent (DNS).

The composition of DNS is given in Table A.1.

Table A.1. Composition of Dinitrosalacyclic acid reagent (DNS)

Chemical	Amount (g)
3,5 Dinitrosalicylic acid	10.6
NaOH	19.8
Rochelle salts (Na K Tartrate)	306
Phenol	7.6
Na-metabisulphite	8.3
Distilled water	1416 ml

Dissolve the first three reagents completely in water before adding the other constituents and dissolving in turn. The phenol is melted at 50°C. The solution must be stored in a container which is protected from sunlight.

Procedure:

2.1 Into a test tube pipette 200 µl of the glucose solution and 600 µl DNS. Do in triplicate.
2.2 Boil rapidly in a water bath for exactly 5 minutes and cool on ice for five minutes.
2.3 Add 3200 µl distilled water to each test tube. Vortex to mix thoroughly.
2.4 Transfer the content of test tube to a plastic cuvette.
2.4 Measure the absorbance at 510 nm against the blank (distilled water) treated similar to the sample in steps 2.1 – 2.3.
2.5 Determine a standard glucose curve from the absorbance data of the standard glucose solutions. From this curve, determine the glucose concentrations of the samples.
2.6 For supernatant samples dilute accordingly and follow steps 2.1 – 2.4.

Figure A.1 shows the linear portion of the calibration curve between absorbance and reducing sugar concentration. The slope of the graph was obtained with a correlation coefficient, R^2 of 0.9999. The reducing sugar concentration was determined from the following equation:

Absorbance = 0.9312 * reducing sugar concentration – 0.0607
The maximum percentage coefficient of variance of the assay is less than 6%.

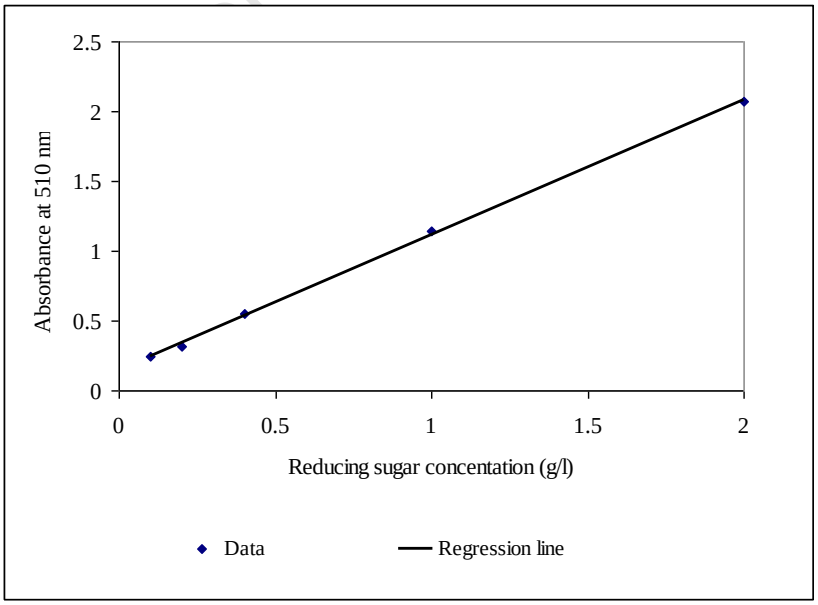

Figure A.1 Reducing sugar calibration curve

A.3. Gluconic acid determination (GA)

The assay was calibrated using a dilution series of a 10 g l^{-1} D-Gluconic acid lactone solution. Standard GA samples had an average residence time of 5.20 ± 0.14 minutes. The standard had a maximum error of 6.7% and 19% at 25 µl and 10 µl injection volumes.

Figure A.2 shows the linear portion of the calibration curve between area and GA concentration. The slope of the graph was obtained with a correlation coefficient, R^2 of 0.9995. The GA concentration in samples was determined from the following equation:

Area = 410806 * GA concentration

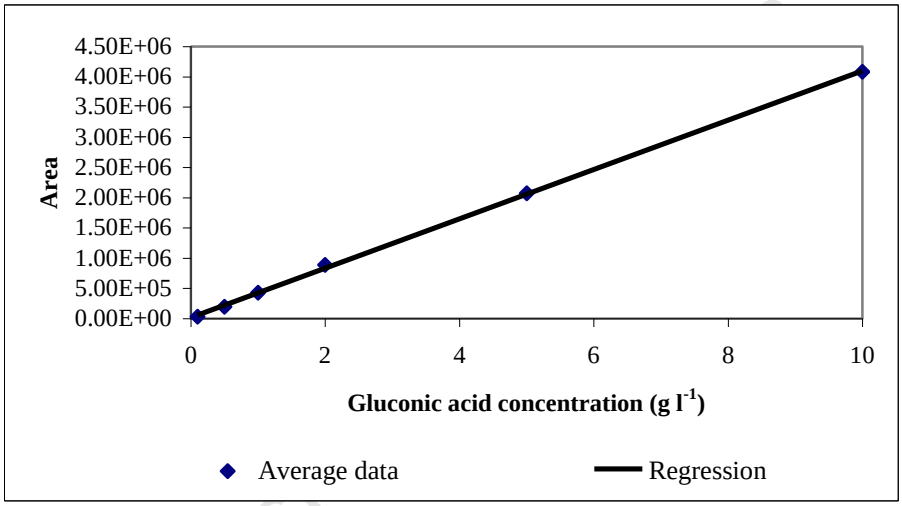

Figure A.2 Gluconic acid calibration chart

A.4. Glucose oxidase (GO) activity

The overall reaction in the *A. niger* system (Witteveen 1993) is shown in Equation A.1.

$$glucose + \frac{1}{2}O_2 \xrightarrow{GO/POD} gluconic\ acid\ (GA) \qquad A.1$$

In this study GO activity was measured by the oxygen utilisation method of Miura (1970) as modified by Johnson (1995).

A.4.1 Oxygen Utilisation Method (Modified from Johnson (1995))

GO activity was defined under the following controlled conditions (pH 5.5, glucose in excess (0.5 M), oxygen at 7.7 ppm). One unit (U) of GO activity was defined as the amount of enzyme that

catalysed the as oxidation of 1 μmole O_2 per ml per minute under the controlled conditions Johnson (1995).

Principle:

Glucose oxidase (GO) catalyses the reaction shown in Equation A.2.

$$H_2O + glucose + O_2 \xrightarrow{GO} gluconic\,acid + H_2O_2 \qquad \text{A.2}$$

The hydrogen peroxide (H_2O_2) is broken down into molecular dissolved oxygen in the presence of peroxidase (POD) as shown by Equation A.3.

$$2H_2O_2 \xrightarrow{POD} H_2O + O_2 \qquad \text{A.3}$$

In the *A. niger* system (Wittiveen 1993) the overall reaction is shown in Equation A.4.

$$glucose + \frac{1}{2}O_2 \xrightarrow{GO/POD} GA \qquad \text{A.4}$$

The oxygen consumption rate in the overall reaction under the controlled conditions refers to the equivalent glucose consumption rate and GA production rate. The μmolar glucose consumption rate per minute per ml of sample is the glucose activity.

$$GO\,activity\left[\frac{\mu mole\ glu\cos e}{ml\min}\right] = -slope\left[\frac{ppm}{s}\right] * dilution * 3.75 \qquad \text{A.5}$$

The slope was obtained from linear regression of the logged data. The slope represented the activity of the diluted sample in ppm s^{-1}. The dilution was the amount of sample (5 ml) added to the reactor volume (250 ml). Dilution = 51 (5 ml sample into 250 total volume). Prior sample dilution must also be included. The factor of 3.75 was obtained by the conversion of ppm oxygen s^{-1} to μmole glucose ml^{-1} min^{-1}.

Equipment:

- Magnetic stirrer with temperature controller
- YSI dissolved oxygen probe
- Dissolved oxygen logging computer and software

- A modified 250 ml Schott bottle with an extended arm to house the oxygen probe.
- Thermometer
- A stopper with three openings: one to house the thermometer, the other to insert the nitrogen through and one acting as a vent.
- 250 ml measuring cylinder

Chemicals:

Solution A: 0.1M KH_2PO_4 (13.7 g l^{-1})
0.5 M glucose (99.1 g l^{-1})
Solution B: 0.1M K_2HPO_4 (17.4 g l^{-1})
0.5M glucose (99.1 g l^{-1})

To prepare a 0.5 M glucose solution in a 0.1 M phosphate buffer, pH 5.5, prepare solutions A and B in a 5:1 ratio based on volume. Place solution A in a large beaker on a magnetic stirrer with a pH probe immersed in it. Add solution B slowly allowing solution B to neutralise solution A to the desired pH (5.5). A 250 ml aliquot of solution B was necessary to neutralise 4 litres of solution A to a pH of 5.5. A pH of 5.5 was chosen for maximal GO activity.

Procedure:

The experimental apparatus is shown in Figure A.3. Place the magnet in the vessel and add 250 ml buffer solution (pH 5.5) into the 250 ml modified vessel. Turn on the stirrer and heater to saturate the solution with oxygen (± 10 minutes) and to heat it up to 25°C. Blanket the headspace with nitrogen for 1 minute at a flowrate between 3 – 4 l min^{-1}. Add 5 ml of sample to the vessel and immediately start the dissolved oxygen data logging system and monitor the dissolved oxygen concentration for 250 s. Once the run is complete remove the stopper. Rinse the flask and probe in tap water and final rinse with distilled water. Reassemble and repeat. Each sample should be analysed in triplicate.

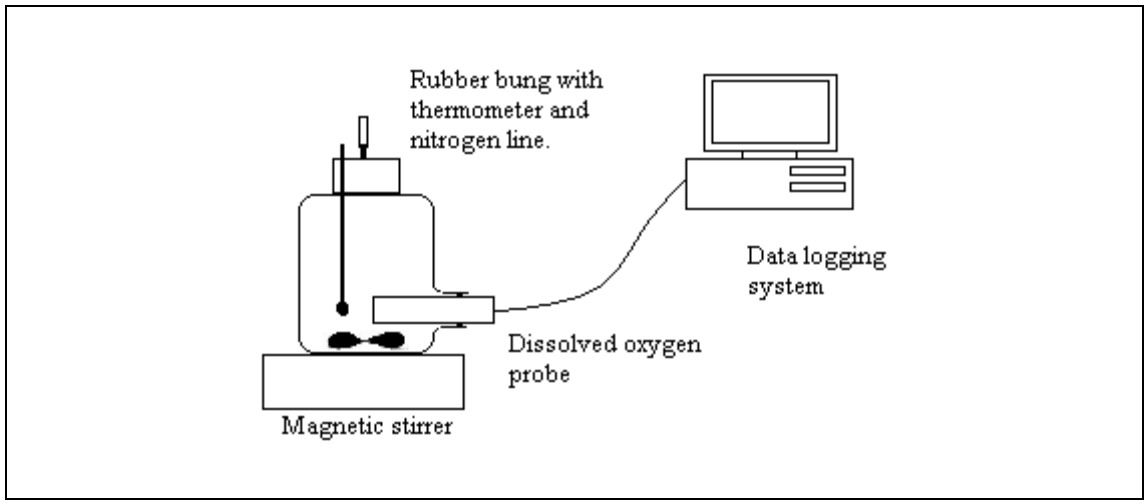

Figure A.3 Oxygen utilisation rate apparatus for GO activity determination

A.5. Immunocytochemical studies

A.5.1. SDS-polyacrylamide gel (SDS-PAGE) electrophoresis of proteins

Principle:

SDS-PAGE is the most widely used method for qualitatively analysing protein mixtures according to their molecular weights (Leammli, 1970). SDS (Sodium Dodecyl Sulfate) is a detergent that denatures proteins into their primary structure and ensures that all the proteins have a negative charge, which means that when they are placed in an electric field, will migrate towards the positive pole. Electrophoresis is the migration of charged molecules in response to an electric field. The rate of migration depends on the strength of the field, on their nett charge, size and shape. The migration of molecules occurs in a liquid medium (tank buffer), which serves as a conducting medium and which is supported by an inert semisolid gel (polyacrylamide gel) that minimizes convection currents. Typically 12% acrylamide gels are used for high molecular weight (M_w) proteins (> 50 kDa) and 20% gels for low M_w proteins (< 15 kDa). GO has a M_w of 160 kDa. Mercaptoethanol breaks the disulphide bonds and therefore GO consists of 2 x 80 kDa linear chains. In these experiments a 12% separating gel and 6.5% stacking gel were used. Electrophoresis was carried out at a constant voltage of 200 V for approximately 90 min. After electrophoresis, the gel was stained in a Coomassie Brilliant Blue R-250 solution for 30 min. Thereafter, the gel was destained in a 7% acetic acid solution overnight.

Reagents:

- 40% acrylamide 0.2% bis. Acrylamide (80 g) and bis-acrylamide (0.4 g) were dissolved in 200 ml of distilled waterand stored in a bottle wrapped in tinfoil (light sensitive).
- 1.125 M Tris-HCl, pH 8.8. Tris (27.25 g) was dissolved in 150 ml distilled water and the pH was adjusted to 8.8 with concentrated HCl and the volume was made up to 200 ml.
- 0.375 M Tris-HCl, pH 6.8. Tris (9.08 g) was dissolved in 150 ml distilled water and the pH was adjusted to 6.8 with concentrated HCl and the volume was made up to 200 ml.
- 10% SDS. SDS (1 g) was dissolved in 10 ml distilled water.
- 10% Ammonium persulphate (AMPS). AMPS (1 g) were dissolved in 10 ml distilled water.
- Sample application buffer. Add 2 ml 0.375 M Tris-HCl, pH 6.8, 2 ml 10% SDS, 2 ml glycerol, 0.5 ml 2-mercaptoethanol and make to 10 ml with distilled water.
- Tank buffer. Add glycine (30 g), Tris (6 g), SDS (2 g) and make up to 2-l with distilled water.
- Stain. Dissolve Coomassie Brilliant Blue R250 to 0.25% in 500 ml technical methanol, add 400 ml H_2O and 100 ml acetic acid.
- Destain. Add 7% acetic acid (70 ml), 25% technical ethanol (250 ml) and make to 1-l with distilled water.
- 1% agarose. Add agarose (0.50 g) to distilled water (50 ml).

For a 12% separating gel and 6.7% stacking gel use the amounts provided in Table A.2.

Table A.2 Amount of each chemical needed for 12% separating and 6.7% stacking gel

Chemical	12% Separating gel	6.7% Stacking gel
40% acryl, 0.2% bis	7.5 ml	1 ml
Buffer (Tris-HCl)	8.4 ml (pH 8.8)	2 ml (pH 6.8)
Water	8.8 ml	2.8 ml
10% SDS	250 µl	150 µl
10% AMPS	250 µl	150 µl
TEMED	25 µl	10 µl
TOTAL	25 ml	6 ml

Procedure:

To set up the apparatus for SDS-PAGE the following procedure was followed:

1. Get plates and strips and clamp them together.

2. Seal the base and sides with 1% agarose, and leave to stand for 10 min.
3. Make up 12% separating gel. Note: Add Temed last because it catalyses the polymerisation of the acrylamide and bis-acrylamide.
4. Place separating gel solution into plate, and fill to ¾ full.
5. Fill the remaining ¼ with distilled water to get a smooth meniscus of gel.
6. Prepare stacking gel. Note: Add TEMED last.
7. Discard the water that was placed in plate.
8. Add stacking gel.
9. Insert combs and wait for it to polymerise (approximately 20 min).
10. Prepare samples by aliquoting the desired lading into eppendorfs with 20 µl of application buffer. Boil the sample for 2 minutes and cool rapidly on ice for 2 minutes.
11. Remove bottom clamps from plate.
12. Get top and bottom support tanks.
13. Place plate into bottom support tank.
14. Pour tank buffer into both supports (top support to brim). Using a Hamilton syringe to eject any unpolymerised acrylamide out of the wells with tank buffer.
15. Place 20 µl of standard into comb imprints (discard the 1st and last imprint) using a Hamilton syringe.
16. Connect tank to power pack at 200 V, connect fan and leave for 90 min.
17. Collect gel and stain in Coomassie blue for 30 min.
18. Destain with 7% acetic acid overnight.

A.5.2. Generation of antisera

Rabbit polyclonal antibodies against a commercial GO (Seravac Pty (Ltd), Epping, Cape Town) were raised. The purity of the commercial enzyme was determined by running a 12% SDS polyacrylamide gel and the results indicated that the enzyme does not require further purification.

Procedure (Harlow and Lane, 1988)**:**

1. Pre-bleed the rabbit.
2. Inject once a week for 3 consecutive weeks intramuscularly with an emulsion of 500 µl of 1 mg ml^{-1} of protein, preferably in PBS with 500 µl of incomplete Freunds adjuvant (1: 9 arlacel:liquid paraffin).
3. Bleed 2 weeks later through middle ear vein. 50 µg acepromazine is administered intravenously as a sedative.

4. Boost 2 weeks later i.e. 1 month after last injection.
5. Bleed every 2 weeks thereafter. Usually 6 - 8 bleeds are sufficient.

A.5.3. Enzyme Linked ImmunoSorbent assay (ELISA)

Principle:

ELISAs are performed in 96-well plates made of PVC. The bottom of each well is coated with a protein (antigen i.e. GO) to which the antibody to be measured will bind. These antibodies are located in the clear serum and are called the primary antibodies. The serum is added to wells according to a dilution series as well as a positive and a negative control serum.

After a while the serum is removed and the weakly adherent antibodies are washed off with a series of buffer rinses. A secondary antibody solution is added to each well to detect any bound antibodies. After an incubation period, the secondary antibody solution is removed and any loosely adherent ones are washed off as before. The final step is the addition of the enzyme substrate and the production of coloured products in the wells with secondary antibodies bound. After a certain time when the enzyme reaction is complete, the entire plate is placed into a plate reader (TITRETEK MULTISCAN) and the optical density at 405 nm is determined for each well. The amount of colour produced is proportional to the amount of primary antibody bound to the proteins on the bottom of the wells.

Detection of antibody production, as well as the highest titre was determined by ELISA using commercial GO (obtained from Seravac Pty (Ltd)) as the antigen, goat anti-rabbit alkaline phosphotase conjugate as the secondary antibody and p-Nitro-phenyl phosphate (pNPP) as the substrate (Harlow and Lane, 1988).

Reagents:

- Phosphate buffered saline (PBS).
- Tris buffered saline (TBS)/TWEEN 20. [100 mM NaCl, 10 mM Tris, 0.1% TWEEN 20, pH 7.5]. NaCl (5.85 g), Tris (12.11 g), TWEEN 20 (1 ml) were dissolved in distilled water (950 ml). The pH was adjusted to 7.5 with HCl and the volume was made up to 1-l with distilled water.
- 3% BSA TBS/TWEEN

- 0.5 mM $MgCl_2$. $MgCl_2.6H_2O$ (0.01475 g) was dissolved in distilled water to a final volume of 250 ml.

Procedure (Harlow and Lane, 1988)**:**

1. Coat polysorb ELISA plate with antigen, concentrations ranging from 1 µg/µl to100 µl per well. Dilute the antigen in PBS.
2. Cover with clingwrap or aluminium foil if the antigen is light sensitive and incubate overnight at 4°C.
3. Tip excess antigen and wash 3 X with TBS TWEEN.
4. Block the wells using 3% BSA TBS TWEEN and incubate for 1 hour at room temperature.
5. Tip out excess blocking solution and wash as in step 3.
6. Add 100 µl of primary antibody. Dilution series: 10^{-2} to 10^{-8}. Use TBS/TWEEN to make your dilutions.
7. Use the first row as a blank as the machine reads as entire row at a time.
8. Incubate at room temperature for 1 hour.
9. Tip out excess antibody and wash as in step 3.
10. Add diluted secondary goat anti-rabbit alkaline phosphotase conjugate (1:1000 dilution in TBS/TWEEN).
11. Incubate at room temperature for half an hour.
12. Tip out excess and wash as in step 3.
13. Do one wash in 10% (v/v) DIETHANOLAMINE, 0.5 mM $MgCl_2$ to equilibrate.
14. Add 100 µl of substrate.
15. Stable readings can be obtained after half-hour using the 405 nm filter of the TITRETEK MULTISCAN machine in tissue culture. A positive reaction is yellow in colour.

A.5.4. Purification of serum by PEG 6000 precipitation (procedure obtained from Dr B. Price, EM Unit, UCT)

After a positive ELISA plate result the next step was to purify rabbit IgG by means of Polyethylene glycol 6000 (PEG 6000) precipitation.

Reagents:

- PEG 6000

- Borate-buffered saline, pH 8.6: 2.16 g Boric acid (H_3BO_3), 2.19 g NaCl, 0.7 g NaOH and [620 µl of a 37% (v/v) solution] HCl were dissolved in approximately 950 ml double distilled water. The pH was titrated to 8.6 with NaOH and the solution was made up to 1-l with double distilled water.
- Phosphate buffer [100 mM sodium phosphate (NaH_2PO_4), 0.02% (w/v) NaN_3, pH 7.6]. Dissolve 1.38 g NaH_2PO_4 and 0.02 g NaN_3 in 80 ml double distilled water, titrate to pH 7.6 with NaOH, made up to volume (1-l) and stored at 4°C.

Procedure:

1. Mix one volume of rabbit serum with two volumes of borate-buffered saline.
2. Add crushed PEG 6000 to the diluted serum to 14% (w/v), gently dissolve by inversion, and centrifuge (12000 g, 10 min, RT) the mixture.
3. Redissolve the pellet in the original serum volume, using phosphate buffer.
4. Add crushed PEG 6000 to 14% (w/v), dissolved, and centrifuge (12000 g, 10 min, RT) the solution.
5. Redissolve the pellet containing the rabbit IgG in half the original serum volume, using phosphate buffer containing 60% (v/v) glycerol, and stored in aliquots at –20°C.

A.5.5. Western blot

Principle:

A Western blot was performed to show that the polyclonal antibodies are specific to the specific antigen and also to show the sensitivity of the antibody to its antigen. After a positive Western blot the antibodies obtained will be used in the immunocytochemical experiments.

Reagents (obtained from Dr B. Price, EM Unit, UCT):

- Gershoni blotting buffer [25 mM Tris-HCl, 192 mM glycine, 20% (v/v) methanol, 0.01% (w/v) SDS, pH 8.3]. Tris (6.05 g), glycine (28.8 g) and SDS (2 ml of a 10% (w/v) solution) were dissolved in 1.6-l of distilled water. Methanol (400 ml) was added and the solution was stored at 4 °C without pH adjustment.

- Ponceasu S protein stain solution [0.1% (w/v) in 1% (v/v) glacial acetic acid]. Ponseau S (0.1 g) and acetic acid (1 ml) were added to a 100 ml volumetric flask and made up to volume with distilled water.
- Tris-buffered saline (TBS) [20 mM Tris-HCl, 200 mM NaCl, pH 7.4]. Tris (2.42 g) and NaCl (11.69 g) were dissolved in distilled water (950 ml). The pH was adjusted to 7.4 with HCl and the volume was made up to 1-l with distilled water.
- Blocking solution [5% (w/v) non-fat milk powder in TBS]. Non-fat milk powder (5g) was dissolved in TBS (100 ml).
- Alkaline phosphatase detection buffer [50 mM Tris-HCl, 5 mM $MgCl_2$, pH 9.5]. Tris (0.61 g) and $MgCl_2.6H_2O$ (0.10 g) were dissolved in distilled water (90 ml). The pH was adjusted to 9.5 with HCl and the volume was made up to 100 ml with distilled water.
- Alkaline phosphatase substrate solution [0.015% (w/v) BCIP, 0.03% (w/v) NBT in detection buffer]. BCIP (1.5 mg in 1 ml DMF) and NBT (3 mg) were dissolved in detection buffer (10 ml) just before use. If BCIP is a toluidine salt dissolve in DMF. If an aqueous salt just use alkaline phosphatase buffer.
- 1 M $MgCl_2$ stock solution. $MgCl_2.6H_2O$ (50.83 g) was dissolved in distilled water to a final volume of 250 ml.
- 5 M NaCl stock solution. NaCl (73.05 g) was dissolved in distilled water to a final volume of 250 ml.
- TBS/TWEEN-20. [100 mM NaCl, 10 mM Tris, 0.2% Tween 20, pH 7.5]. NaCl (5.85 g), Tris (12.11 g), and TWEEN 20 (2 ml) were dissolved in distilled water.
- (950 ml). The pH was adjusted to 7.5 with HCl and the volume was made up to 1-l with distilled water.

Procedure (From UCT Biochemistry Department, Practical Handbook):

1. After SDS-PAGE dismantle the gel from the electrophoresis unit and briefly submerge it together with Whatman 3MM filter paper and Hybond^{TM}-C nitrocellulose hybridisation transfer membrane (0.45 µm) in ice cold transfer buffer (Gershoni buffer). Note: work with gloves to prevent proteins being transferred from fingers to nitrocellulose paper. Also wet nappy liners with tranfer buffer ensuring that they are wet but not dripping. The gel is then flattened on the pre-wetted nitrocellulose paper supported on the pre-wetted Whatman 3MM paper to get rid of air bubbles. The transfer cassette consists of two carbon slabs with the anode (+, red lead) on the bottom. A wad of wet nappy liners are placed on the carbon slab and flattened. The filterpaper, nitrocellulose, and the gel are then placed on the nappy liner. The gel is then overlayed with pre-wetted Whatman filter paper

and another wad of nappy liners followed last by the other carbon block. Make sure that there are no air bubbles in this sandwich to ensure efficient transfer. Electrophoresis is allowed to proceed overnight at 20 V.

2. After electrophoresis the transfer cassette was dismantled and the nitrocellulose membrane was rinsed in distilled water and air-dried for 2 hours and then stained with Ponceau S to visualise the protein profiles and to assess the efficiency of the transfer. Use a needle on the nitrocellulose membrane to mark the position of the lanes and markers. The Ponceau S was decolourised with TBS and the membrane was air-dried then stored in a dessicator at 4°C or used in further steps. Block the nitrocellulose membrane TBS containing 2% (w/v) milk powder overnight.
3. Determine the concentration of the PEG precipitated IgG (primary antibody) by its absorbance at a wavelength of 280 nm ($\varepsilon_{280}^{1mg/m\ell} = 1.64$). The primary antibody should be probed at a concentration of 10 μg/ml.
4. Incubate the nitrocellose membrane with primary antibody in TBS containing 2% milk powder for 2 hours on a shaker.
5. Drain the TBS milk off and wash 3 times for 15 min with TBS/TWEEN.
6. Thereafter incubate the nitrocelulose membrane with the secondary antibody (1:2500 dilution) in TBS containing 2% milk powder for an hour on shaker.
7. Wash three times for 15 min each with TBS/TWEEN.
8. Wash once for 10 min with TBS/ 200 mM $MgCl_2$
9. Wash once for 5 min with TBS/ 1M NaCl.
10. Briefly rinse the nitrocellulose membrane in distilled water.
11. Briefly rinse it in alkaline phosphate buffer to equilibrate. Then add more alkaline phosphate buffer and substrate to visualise the proteins, which have bound to the antibodies as purple bands.

A.5.5. Gold labeling

A.5.5.1. Fixation

1. Fungi cells were filtered and re-suspended in fixative. They were left in fixative overnight at 4°C.

Fixative: 2% formaldehyde + 2% gluteraldehydate in PBS (Phosphate buffered saline)

2. The cells were embedded in low melting agarose at 37°C and infiltrate for 10 min. The mixture was cooled immediately thus causing the agarose to set.

3. The agarose blocks containing the fungi cells were cut into small pieces infiltrated with fixative.

A.5.5.2. Ethanol dehydration

The agarose blocks containing the fungi cells were dehydrated using different ethanol (EtOH) concentrations (i.e. 20%, 50%, 70%, 90% and 100% (v/v) EtOH). A 100% EtOH concentration was obtained by placing 96% EtOH with molecular sieves to absorb the water present in the EtOH. The dehydration series was performed at room temperature.

Procedure:

1. Add 1 ml 20% EtOH to the blocks and place on rollers to ensure good contact mixing for and hour, after ½ hour replace the 20% EtOH with fresh 20% EtOH.
2. Do the same for 50%, 70%, 90% EtOH.
3. Add 1 ml of 100% and leave for 1 hour.
4. After an hour replace with fresh 100% EtOH.
5. After an hour replace with fresh 100% EtOH and leave overnight.
6. The next morning infiltrate the blocks with 50% resin (LR White) and EtOH mixture and leave for 48 hours.
7. The next morning change to 100% resin (LR White), and after 8 hours replace with fresh 100% resin and leave overnight.
8. The next morning put the samples (plus their respective labels) into resin capsules for 24 hours at 60°C.

A.5.5.3. Gold labelling

0.25% Butvar B98 in chloroform was used to coat the copper grids (Mesh Hexagonal, G24500, Copper, 3.05 mm, Agar Scientific). Using glass knifes cut thin sections (90 to 120 nm) of the capsule containing sample specimen with an Ultramicrotome. Place these sections on the copper grids. To do the immunolabelling the following needs to be done:

Reagents:

- Blocking buffer [1% fish skin gelatine, 0.8% BSA, 20 mM glycine in TBS].
- 2 ml fish skin gelatine (stock is 45%), 0.8 g BSA, and 0.150 g glycine is made up in a 100 ml volumetric flask with TBS. Spin this at 10 000g for an hour at 4 °C.

Procedure:

1. Preincubate the grids on blocking buffer for one hour.
2. Incubate the grids in 1° antibody for 2 hours.
3. Wash 4 x 5 min with TBS/TWEEN.
4. Incubate grids with gold-antibody (5 µl in 1ml) for an hour.
5. Wash 4 x 5 min with TBS/TWEEN.
6. Wash 3 x 5 min with TBS/ 200 mM $MgCl_2$.
7. Wash 1 x 5 min with TBS/ 1 mM $NaCl_2$.
8. Wash 2 x 5 min with TBS.
9. Wash 3 x 1 min with distilled water.
10. Wash 1 x 5 min with distilled water/ 1% gluteraldehyde (25% stock, 45 µl in 1ml dH_2O).
11. Wash 5 x 1 min with distilled water.
12. Staining with heavy metals: The grids are stained with uranyl acetate for 5 minutes followed by quick distilled water washes (5 drops). The grids are then stained with Reynolds lead citrate for 5 minutes and washed with large quantity of distilled water (30 - 40 drops).
13. The grids are viewed under an electron microscope (TEM-Zeiss 109).

B.1. Distribution of glucose into individual fractions

To quantify the GO activity in the various fractions of the *A. niger* and *Penicillium* sp. cultures, the culture were separated into the fractions according to the disruption and separation techniques shown in Figure B.1. The French Press was used as the method of cell disruption, and filtration as the methods of cell separation. The GO activity was measured using the oxygen utilisation method as described in Appendix A.4.

Culture was taken (approximately 200 ml) at the end of a fermentation and divided according to Figure B.1. It is important for the calculations that the volume before and after each procedure should be noted.

A homogeneous culture was placed into a 200 ml volumetric flask and separated by vacuum filtration through a 0.45 μm Millipore filter into a liquid portion consisting of supernatant and a solid fraction consisting of whole cells. The cells were washed twice on the filter with distilled water with half the supernatant volume. The supernatant and wash water were combined for analysis of the activity in the extracellular fluid. The washed cells were resuspended in a phosphate buffer at pH 5.5, and disrupted using the French Press. The disrupted suspension was separated using filtration through a 0.45 μm Millipore filter into a liquid fraction called the cell free extract which consists of cytoplasm and slime mucilage and a solid fraction known as the cell envelope which consists of the cell and membrane wall fragments. The solid fraction (cell envelope) was resuspended in a phosphate buffer at pH 5.5 and analysed for the activity in the cell wall. Absolute ethanol was added to an aliquot of the liquid fraction (cytoplasm and slime mucilage) in a 4:1 ratio to precipitate the slime mucilage. The slime mucilage precipitate was recovered from the cytoplasm after centrifugation (5000 g, 15 min, 4°C). The activity of the cytoplasm was determined from the liquid and the precipitate was dissolved in 0.1 M NaOH to obtain the activity in the slime mucilage.

Equipment:

- Centrifuge and centrifuge tubes
- 0.45 μm 47 mm Millipore filterpaper and filter
- 25 ml, 50 ml, 100 ml and 250 ml measuring cylinders
- UCT Dissolved Oxygen/Utilisation Rate Meter
- YSI Dissolved oxygen probe (YSI 5739 Field Probe)

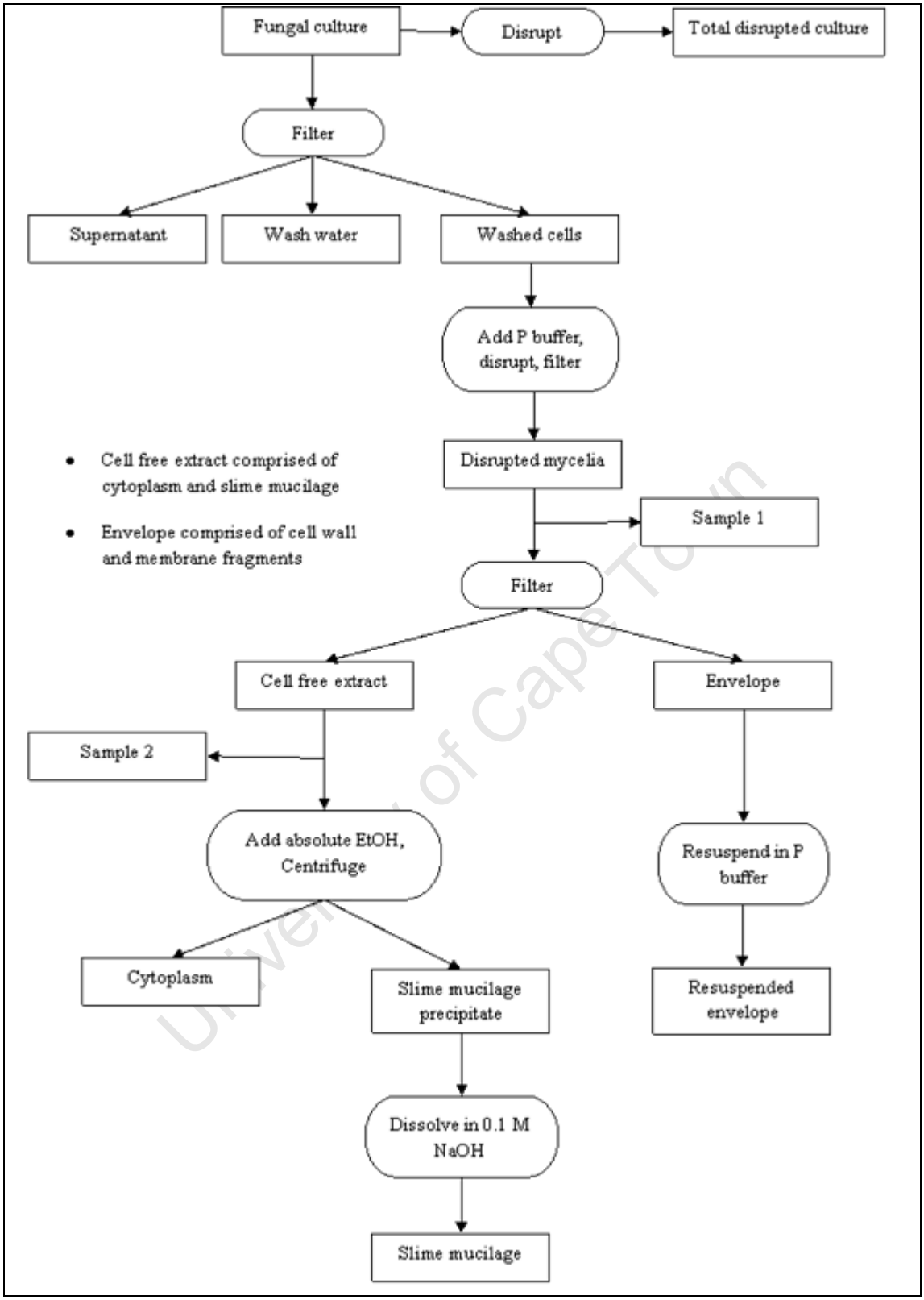

Figure B.1 Separation of GO into individual fractions.

Reagents:

- 0.1 M Potassium phosphate buffer, pH 5.5
- Absolute Ethanol
- 0.1M NaOH
- Glucose and phosphate buffer, pH 5.5

B.2. Calculations to determine the percentage GO in individual fractions

An example was given to explain the procedure.

Fermentation culture was used and separated according to Figure B.1 and as set out in Section B.1. The volumetric GO in each fraction was determined using the dissolved oxygen method. The volumes of fractions recovered as well as amount of buffer added were noted. The absolute GO activity (U) was obtained by multipying the volumetric GO activity (U ml^{-1}) by the respective volumes (Table B.1).

Table B.1 GO activity in the individual fractions and the volume recovered

Fraction	GO activity (U ml^{-1})	Volume recovered (ml)	GO activity (U)	GO activity (U) #
Supernatant (A)	1.62 ± 0.00	194	314.28	474.71
Wash water 1 (B1)	0.42 ± 0.00	110	46.20	69.78
Wash water 2 (B2)	0.32 ± 0.00	112.8	36.10	54.53
Disrupted mycelia (C)	16.35 ± 0.07	50	817.50	1234.8
Cell free extract (D)	7.22 ± 0.25	18.5	133.57	222.76
Resuspended envelope[┼] (E)	9.89 ± 0.50	16.5	163.19	271.16
Cytoplasm (F)	0.42 ± 0.005	28.4	11.93	18.16
Slime mucilage (G)	14.54 ± 0.38	1.9	27.63	41.96
Total	9.17 ± 0.41	200	1834	
Sample $*_1$	16.35 ± 0.07	30	490.5	740.88
Sample $*_2$	7.22 ± 0.25	13.5	97.47	162.55

[#] GO activity on the assumption of 100% recovery

[┼] Envelope comprised of cell wall & membrane fragments

[*] Sample means any spillage, samples taken out of the system

- Overall recovery of the separation and disintegration steps for route 1:

TOTAL = (EXTRACELLULAR FLUID + SLIME MUCILAGE + RESUSPENDEND ENVELOPE + CYTOPLASM + SAMPLES)
= ((A + B1 + B2) + G + E + F + Samples)
= (314.28 + 46.20 + 36.10 + 27.63 + 163.19 + 11.93 + 490.5 + 97.47)
= 1187.3 U

and TOTAL calculated =1834 U

Overall recovery = 1187.3/1834 = 64.7 %

- Determination of the % recovery of the solid-liquid separation steps:

Separation 1: Stage 1 Recovery

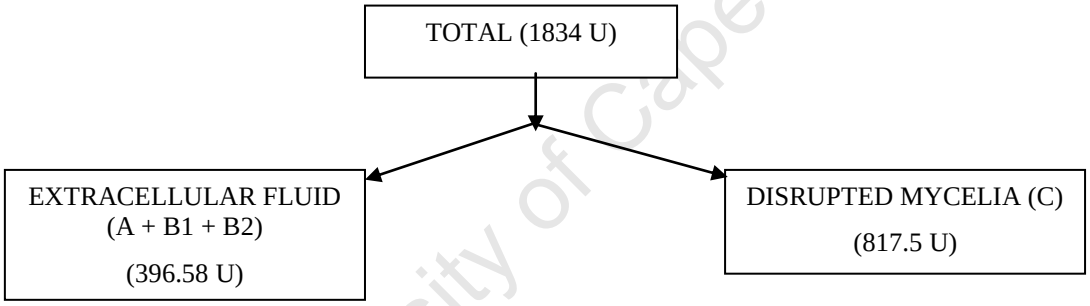

Stage 1 Recovery = (396.58 + 817.5) / 1834 = 66.2%

Separation 2: Stage 2 Recovery

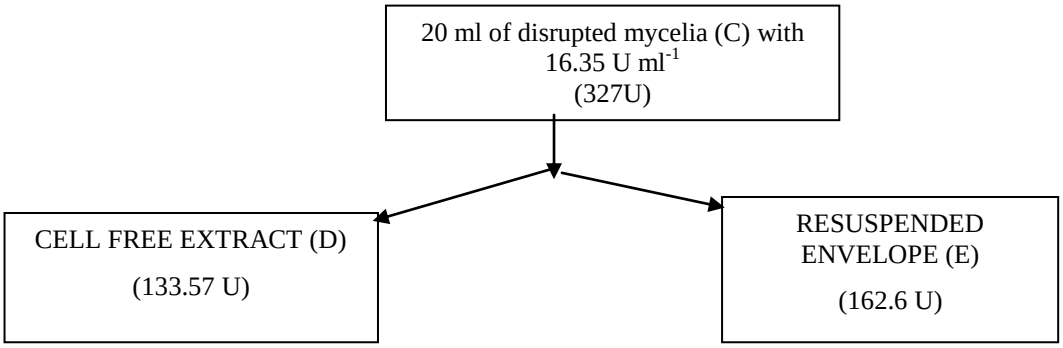

Stage 2 Recovery = (133.57 + 163.19) / 327 = 90.8%

Separation 3: Stage 3 Recovery

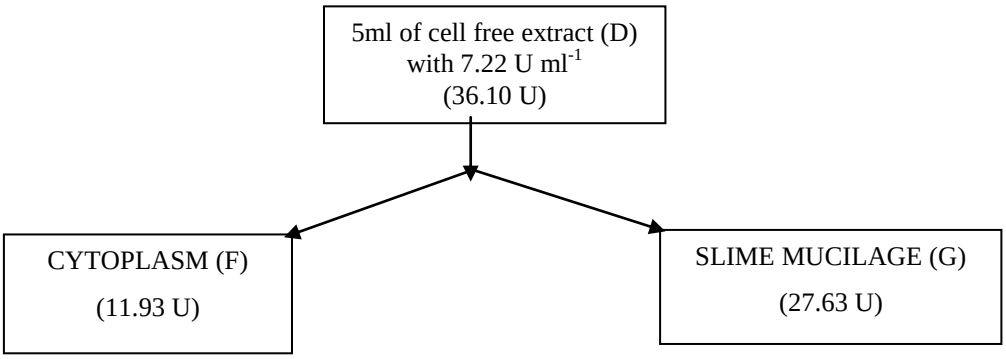

Separation 3: Stage 3 Recovery = (11.93 + 27.63)/ 36.10= 109.6%

- Determination of the absolute GO activity assuming a 100% recovery:

The new absolute activities of each fraction (last column of able B.1) the "old absolute activity" by the respective percentage stage recovery remembering that it is cumulative.

i.e. for EXTRACELLULAR FLUID (A + B1 + B2) = 396.58/ 0.662 = 599.06 U

RESUSPENDED ENVELOPE (E) = 163.19/ (0.908 x 0.662) = 271.6 U

CYTOPLASM (F) = 11.93/ (1.096 x 0.908 x 0.662) = 18.16 U

SLIME MUCILAGE (G) = 27.63/ (1.096 x 0.908 x 0.662) = 41.96 U

- Determining the % GO in each individual fraction:

% GO in EXTRACELLULAR FLUID:

EXTRACELLULAR FLUID = 599.06/ 1834 =32.7%

% GO in remaining fractions:

CYTOPLASM + SLIME MUCILAGE + RESUSPENDED ENVELOPE = 1234.8/ 1834 = 67.3%

Therefore, if the culture (TOTAL) was only separated into a liquid and a solid fraction the percentage GO in the liquid phase was 32.7% and in the disrupted "solid" fraction 67.3%. Each sample that was taken out from the stream to determine the GO activity needed to be taken into account to, i.e.

$Sample_1$ consists of (CYTOPLASM + SLIME MUCILAGE + RESUSPENDED ENVELOPE) with absolute GO activity if 100% recovery of 740.88 U.

Let RESUSPENDED ENVELOPE = x

RESUSPENDED ENVELOPE / (CYTOPLASM + SLIME MUCILAGE) = 272.16/ 222.76 = 1.22

$x + 1.22x = 740.88$

RESUSPENDED ENVELOPE = x = 333.46 U
CYTOPLASM + SLIME MUCILAGE = 407.42 U

Therefore the amount of GO in the CELL WALL fraction was:
272.16U + 333.46 U = 605.62 U

$Sample_2$ consists of (CYTOPLASM + SLIME MUCILAGE) with absolute GO activity if 100% recovery of 162.55 U plus $(CYTOPLASM + SLIME MUCILAGE)_{Sample1}$ of 407.42 U.

Let CYTOPLASM = y

CYTOPLASM/ SLIME MUCILAGE = 18.16/ 42.05 = 0.43

$y + 0.43y = 162.55 + 407.42 = 569.97$ U

CYTOPLASM = y = 398.05 U
SLIME MUCILAGE = 171.92 U

Therefore the amount of GO in the CYTOPLASM fraction was:
18.16 U + 398.05 U = 416.21 U and
in the SLIME MUCILAGE fraction: 41.96 U + 171.92 U = 213.88 U.

RESUSPENDED ENVELOPE/ (CYTOPLASM + SLIME MUCILAGE) =
605.62/ (416.21 + 213.88) = 0.96

RESUSPENDED ENVELOPE = 0.96 (CYTOPLASM + SLIME MUCILAGE)
RESUSPENDED ENVELOPE + CYTOPLASM + SLIME MUCILAGE = 67.3%
1.96 (CYTOPLASM + SLIME MUCILAGE) = 67.3%
(CYTOPLASM + SLIME MUCILAGE) = 34.3%

Therefore RESUSPENDED ENVELOPE = 34.3% = Cell wall & membrane fragments

CYTOPLASM / SLIME MUCILAGE = 416.21 / 213.97 = 1.93
CYTOPLASM = 1.93 SLIME MUCILAGE
34.3% + 1.93 SLIME MUCILAGE + SLIME MUCILAGE = 67.3%

Therefore, SLIME MUCILAGE = 11.2%
CYTOPLASM = 21.8%

Hence, the percentage GO in each individual fraction assuming a 100% recovery is:

EXTRACELLULAR FLUID	**32.7%**
SLIME MUCILAGE	**11.2%**
CELL WALL & MEMBRANE FRAGMENTS	**34.3%**
CYTOPLASM	**21.8%**

Table C.1 Summary of batch cultivation data of *Aspergillus niger* NNRL-3 and *Penicillium* sp. CBS 120262

***A. niger* runs Unmodified values**

Run C (5 M NaOH, specific gravity = 1.20)

Time	NaOH added[1]	Sample volume	Reactor volume[2]	CDW	Reducing sugar	Gluconic acid	TOTAL GO	Extracellular GO	% DO	Impeller speed	Air flowrate
h	g	ml	ml	g l^{-1}	g l^{-1}	g l^{-1}	U ml^{-1}	U ml^{-1}		rpm	l min^{-1}
0	0	19.5	5980	0.14	95	0			95	500	4.8
4	15	93	5900	0.15	91.2	2.16	0.58	0.41	86.4	500	4.8
8	90	100	5875	0.31	84.2	13.7	1.2	0.58	56.1	500	4.8
11	119	109	5865	0.45	60.8	29.1	1.91	0.65	43	500	4.8
15	197	194	5835	0.96	25	54.4	3.57	0.97	42.6	500	4.8
20	269	230	5830	2.02	9.01	89.1	6.54	1.21	54.4	500	4.8
25	33	500	5357	2.31	1.94	93.3	6.73	1.38	88.4	500	4.8

Run D (5 M NaOH, specific gravity = 1.20)

Time	NaOH added[1]	Sample volume	Reactor volume[2]	CDW	Reducing sugar	Gluconic acid	TOTAL GO	Extracellular GO	% DO	Impeller speed	Air flowrate
h	g	ml	ml	g l^{-1}	g l^{-1}	g l^{-1}	U ml^{-1}	U ml^{-1}		rpm	l min^{-1}
0	0	45	5955	0.11	98	0			96	500	4.8
4	6	86	5874	0.14	95.5	1	0.42	0.36	92.6	500	4.8
8	59	108	5815	0.29	83.1	8.6	0.75	0.44	73.8	500	4.8
12	140	134	5798	0.57	31.8	26.6	1.65	0.71	52.2	500	4.8
16	201	140	5825	0.99	11.6	52.5	2.52	0.72	53.9	500	4.8
20	220	384	5625	1.41	1.31	80.8	4.59	0.83	52	500	4.8
25	87	555	5142	1.53	0.53	92	4.22	1.12	88.2	500	4.8
30	20	60	5099	1.3	0.22	94.5	5.15	1.21	87.5	500	4.8

[1] The amount of base added is the actual amount and not the cumulative amount.

[2] The reactor volume is the volume left after base addition and sampling.

Run 1_5/9/2005 (5 M NaOH, specific gravity = 1.20)

Time h	NaOH added[1] g	Sample volume ml	Reactor volume[2] ml	CDW g l^{-1}	Reducing sugar g l^{-1}	Gluconic acid g l^{-1}	TOTAL GO U ml^{-1}	Extracellular GO U ml^{-1}	% DO	Impeller speed rpm	Air flowrate l min^{-1}
0	0	28	5972	0	82.9	0	0	0	89	300	4
22	70	100	5930	1	79.2	6.1	2.13	0.86	26	350	6
24	50	100	5872	1.6	68.5	10.5	4.47	0.98	18.3	450	6
27	190	218	5812	2.21	43.3	14.9	7.09	1.42	21.3	600	6
30	230	194	5810	2.27	28.9	65.4	8.34	1.92	29.4	600	6
34	30	73	5762	2.31	15.2	69.4	10.14	2.17	80.3	500	6
45	0	178	5584	2.61	3.2	57.6	10.24	3.57	80.6	500	6

Run 2_4/5/2004 (6.5 M NaOH, specific gravity = 1.28)

Time h	NaOH added[1] g	Sample volume ml	Reactor volume[2] ml	CDW g l^{-1}	Reducing sugar g l^{-1}	Gluconic acid g l^{-1}	TOTAL GO U ml^{-1}	Extracellular GO U ml^{-1}	% DO	Impeller speed rpm	Air flowrate l min^{-1}
0	0	0	6000	0	80.1	0	0	0	90.5	300	4
21	30	108	5915	0.32	73.6	1.9	0.56	0.44	39.3	350	6
23	0	193	5722	0.46	70.1	5	1.72	0.55	30.7	450	6
29	170	160	5695	1.37	39	25.6	6.06	1.26	22.3	550	7.5
33	190	160	5684	1.3	9.6	63.8	8.53	2.29	28	550	7.5
34.5	60	170	5561	1.89	4.9	64.2	8.88	2.74	78.6	550	7.5
45	0	212	5349	1.26	0.2	79	9.03	4.38	81.8	550	7.5

Run 3_4/4/2006 (5 M NaOH, specific gravity = 1.20)

Time h	NaOH added[1] g	Sample volume ml	Reactor volume[2] ml	CDW g l^{-1}	Reducing sugar g l^{-1}	Gluconic acid g l^{-1}	TOTAL GO U ml^{-1}	Extracellular GO U ml^{-1}	% DO	Impeller speed rpm	Air flowrate l min^{-1}
0	0	0	6000	0	80	0	0.0	0.0	100	300	6
21	27	110	5913	0.62	68.9	4.7	1.5	0.7	16.8	400	6
24	161	100	5947	1.31	50.5	20.2	3.4	1.1	2.8	650	7
26	190	232	5873	1.52	25.7	42.3	6.5	1.8	0.2	650	7
28.5	152	90	5910	1.61	5.6	61	7.2	2.4	1.5	650	7
31	1	200	5711	1.74	0.4	63.1	8.2	3.2	0	650	7
34	0	164	5547	2.05	0.3	59.9	8.4	3.9	0	650	7
45	0	240	5307	2.8	0.3	61.3	8.5	4.2	0	650	7

[1] The amount of base added is the actual amount and not the cumulative amount.

[2] The reactor volume is the volume left after base addition and sampling.

Run 1_4/5/2005 (25% $Ca(OH)_2$, specific gravity = 1.164), pH 6.5

Time	$Ca(OH)_2$ added[1]	Sample volume	Reactor volume[2]	CDW	Reducing sugar	Gluconic acid	TOTAL GO	Extracellular GO	% DO	Impeller speed	Air flowrate
h	g	ml	ml	g l^{-1}	g l^{-1}	g l^{-1}	U ml^{-1}	U ml^{-1}		rpm	l min^{-1}
0	0	0	6000	0	81.7	0	0	0	95	300	4
20	40	95	5939	0.43	75.4	14.4	0.87	0.51	64.4	400	6
24	70	83	5917	0.61	62.9	22.3	2.61	0.81	26.8	500	6
27	70	81	5890	0.95	41.4	39.6	7.27	1.26	25.9	650	6
31.5	250	82	6028	1.74	14.8	69.6	14.24	3.22	82	600	6
40	10	86	5951	3.51	6.29	77.6	15.4	3.94	63.2	600	6
45	0	91	5860	4.68	3.12	67.6	19.5	9.28	58.4	600	6

Run 2_5/8/2004 (25% $Ca(OH)_2$, specific gravity = 1.164), pH 6.5

Time	$Ca(OH)_2$ added[1]	Sample volume	Reactor volume[2]	CDW	Reducing sugar	Gluconic acid	TOTAL GO	Extracellular GO	% DO	Impeller speed	Air flowrate
h	g	ml	ml	g l^{-1}	g l^{-1}	g l^{-1}	U ml^{-1}	U ml^{-1}		rpm	l min^{-1}
0	0	0	6000	0	80.5	0	0.0	0.0	87.5	300	6
24	40	124	5910	0.44	79	6.73	0.6	0.4	27.9	500	6
30	180	244	5821	0.94	43.5	46.6	2.8	1.1	18.9	600	6
42	260	248	5796	8.3	10.7	61.6	13.1	6.7	48.4	600	6
46	0	174	5622	4.6	5.54	63.9	17.7	9.9	70.3	600	6

[1] The amount of base added is the actual amount and not the cumulative amount.

[2] The reactor volume is the volume left after base addition and sampling.

Glucose

	Time	$Glucose_{measured}$	Reactor volume	Base added	Sample taken	$Glucose_{taken\ out}$	$Glucose_{remaining\ in\ reactor}$	$Glucose_{used}$	$Glucose_{corrected}$
	h	g/l	ml	ml	ml	g	g	g	g/l
initial	0	100	6000	0	0	0.0	600	0	100
after base addition	4	98.5	6022	22			593	7	
after sampling		98.5	5929		93	9.2	584		97.3
after base addition	8	70.4	6010	82			423	161	
after sampling		70.4	5910		100	7.0	416		69.3
after base addition	12	42.6	6023	113			257	160	
after sampling		42.6	5914		109	4.6	252		42.0
after base addition	17	7.50	6140	226			46	206	
after sampling		7.50	5946		194	1.5	45		7.4
after base addition	20	0.12	6058	113			1	44	
after sampling		0.12	5828		230	0.0	1		0
after base addition	25	0.01	5834	6			0	1	
after sampling		0.01	5334		500	0.0	0		0
	Total			560	1226	22.3		577.6	

Glucose balance: $? Glucose_{taken\ out} + Glucose_{remaining\ in\ reactor\ at\ t\ =\ 25h} + ? Glucose_{used} = Glucose_{initial}$

Cell dry weight (CDW)

	Time	$CDW_{measured}$	Reactor volume	Base added	Sample taken	$Cells_{taken\ out}$	$Cells_{remaining\ in\ reactor}$		$CDW_{corrected}$
	h	g/l	ml	ml	ml	g	g		g/l
	0	0	6000	0	0	0	0		0
after base addition	4	0.12	6022	22					
after sampling		0.12	5929		93	0.01	0.70		0.12
after base addition	8	0.61	6010	82					
after sampling		0.61	5910		100	0.06	3.54		0.59
after base addition	12	1.03	6023	113					
after sampling		1.03	5914		109	0.11	5.98		1.00
after base addition	17	2.22	6140	226					
after sampling		2.22	5946		194	0.43	12.77		2.13
after base addition	20	2.82	6058	113					
after sampling		2.82	5828		230	0.65	15.79		2.63
after base addition	25	2.16	5834	6					
after sampling		2.16	5334		500	1.08	10.44		1.74
	Total			560	1226	2.34			

Gluconic acid (GA)

	Time	$CDW_{measured}$	Reactor volume	Base added	Sample taken	$GA_{taken\ out}$	$GA_{remaining\ in\ reactor}$		$GA_{corrected}$
	h	g/l	ml	ml	ml	g	g		g/l
	0	0	6000	0	0	0	0		0
after base addition	4	3.6	6022	22					
after sampling		3.6	5929		93	0.3	21.0		3.5
after base addition	8	16.2	6010	82					
after sampling		16.2	5910		100	1.6	94.1		15.7
after base addition	12	33.6	6023	113					
after sampling		33.6	5914		109	3.7	195.0		32.5
after base addition	17	68.5	6140	226					
after sampling		68.5	5946		194	13.3	394.0		65.7
after base addition	20	85.8	6058	113					
after sampling		85.8	5828		230	19.7	480.3		80.1
after base addition	25	86.7	5834	6					
after sampling		86.7	5334		500	43.4	419.1		69.9
	Total			560	1226	82.0			

For the volume corrections of the glucose, CDW, GA and GO concentrations (Section 3.4) the mean difference between the measured concentration (unmodified values) and the corrected concentrations (modified values) were performed using a one-tailed t-test for paired comparisons at 95% confidence interval. The null hypothesis is that there is no difference between the pairs. For n pairs:

$$t = \frac{d_{avg}}{s_d / \sqrt{n}} \qquad \text{where} \quad s_d = \sqrt{\frac{\sum \left(d_i - d_{avg}\right)^2}{n-1}}$$

where d_{avg} is the average difference between the pairs

d_i is the difference between the pairs

s_d is the standard deviation between the pairs

n is the size of the pair

Another method was used to validate the value obtained for t using t-test for non-independent samples

$$t_{obt} = \frac{d_{avg}}{\sqrt{\frac{\left(n \times \sum d_i^2\right) - \left(\sum d_i\right)^2}{n^2 (n-1)}}}$$

If the value of t obtained through the data (t_{obt}) is greater or equal than the critical t ($t_{critical}$) then the null hypothesis is significant (i.e. there is a difference between the pairs). The value for t_{crit} is obtained from the t-distribution tables where the degree of freedom (df) = n-1. The absolute value of t_{obt} is used. Here the $t_{obt} < t_{crit}$, so the null hypothesis holds (i.e. there is no difference between the measured and the modified values at 95% confidence interval).

The same statistical analysis is done for the concentrations of CDW, GA, total and extracellular GO for all cultivations. Since the statistical analysis illustrated that in some instances the null hypothesis holds and in some instances it does not it was decided to modify all the measured concentration data to their respective corrected concentrations to ensure uniformity.

Standard error of the means (SEM) is calculated using the standard deviation of a sample (σ) and the number of samples (n):

$$SEM = \frac{\sigma}{\sqrt{n}}$$

Table E.1 Summary of the corrected values of the data for batch cultivations of *Aspergillus niger* NRRL-3 and *Penicillium* sp. CBS 120262

***A. niger* runs**

Run C		NaOH	Corrected values		
Time	Glucose	CDW	GA	Total GO	Extracellular GO
h	g l^{-1}	g l^{-1}	g l^{-1}	U ml^{-1}	U ml^{-1}
0	94.69	0.139	0.0		
4	89.68	0.145	2.1	0.56	0.40
8	82.45	0.30	13.2	1.16	0.56
11	59.43	0.43	27.9	1.83	0.62
15	24.31	0.90	51.1	3.36	0.91
20	8.75	1.89	83.2	6.10	1.13
25	1.73	1.87	75.6	5.45	1.12

Run D		NaOH	Corrected values		
Time	Glucose	CDW	GA	Total GO	Extracellular GO
h	g l^{-1}	g l^{-1}	g l^{-1}	U ml^{-1}	U ml^{-1}
0	98	0.11	0.0		
4	93.49	0.14	1.0	0.41	0.35
8	80.54	0.28	8.2	0.71	0.42
12	30.73	0.54	25.1	1.56	0.67
16	11.26	0.94	49.7	2.39	0.68
20	1.23	1.23	70.6	4.01	0.72
25	0.47	1.22	73.4	3.37	0.89
30	0.20	1.20	87.0	4.74	1.11

***Penicillium* runs**

Run 5/9/2005 (Run1)		NaOH	Corrected values		
Time	Glucose	CDW	GA	Total GO	Extracellular GO
h	g l^{-1}	g l^{-1}	g l^{-1}	U ml^{-1}	U ml^{-1}
0	82.5	0	0.0	0	0
22	78.3	0.97	5.9	2.07	0.83
24	67.1	1.54	10.1	4.30	0.94
27	41.9	2.06	13.9	6.61	1.32
30	28.0	2.12	61.2	7.81	1.80
34	14.6	2.19	65.8	9.61	2.05
45	3.0	2.35	51.9	9.23	3.21

Run 4/5/2004 (Run 2)		NaOH	Corrected values		
Time	Glucose	CDW	GA	Total GO	Extracellular GO
h	g l^{-1}	g l^{-1}	g l^{-1}	U ml^{-1}	U ml^{-1}
0	80.1	0	0.0	0	0
21	72.6	0.31	1.8	0.54	0.43
23	66.9	0.42	4.6	1.59	0.51
29	37.0	1.26	23.6	5.59	1.16
33	9.1	1.20	58.7	7.85	2.11
34.5	4.5	1.70	57.7	7.98	2.46
45	0.2	2.00	67.6	7.73	3.75

Run 4/4/2006 (Run 3)		NaOH	Corrected values		
Time	**Glucose**	**CDW**	**GA**	**Total GO**	**Extracellular GO**
h	**g l^{-1}**	**g l^{-1}**	**g l^{-1}**	**U ml^{-1}**	**U ml^{-1}**
0	80.0	0.0	0.0	0	0.0
21	67.9	0.6	5.9	1.42	0.6
24	50.1	1.3	24.2	3.27	1.1
26	25.2	1.4	47.0	6.13	1.7
28.5	5.5	1.6	70.8	7.01	2.3
31	0.4	1.6	69.4	7.56	2.9
34	0.3	1.8	64.2	7.56	3.5
45	0.3	2.4	62.1	7.20	3.5

Run 4/5/2005 (Run1)		$Ca(OH)_2$	Corrected values		
Time	**Glucose**	**CDW**	**GA**	**Total GO**	**Extracellular GO**
h	**g l^{-1}**	**g l^{-1}**	**g l^{-1}**	**U ml^{-1}**	**U ml^{-1}**
0	81.7	0	0.0	0	0
20	74.6	0.42	14.0	0.85	0.50
24	62.0	0.59	21.7	2.54	0.79
27	40.6	0.92	38.3	7.05	1.22
31.5	14.9	1.72	69.0	10.11	2.20
40	6.2	3.43	75.9	15.05	5.40
45	3.0	4.50	65.0	18.75	8.92

Run 5/8/2004 (Run 2)		$Ca(OH)_2$	Corrected values		
Time	**Glucose**	**CDW**	**GA**	**Total GO**	**Extracellular GO**
h	**g l^{-1}**	**g l^{-1}**	**g l^{-1}**	**U ml^{-1}**	**U ml^{-1}**
0	80.1	0	0.0	0	0
24	77.8	0.42	6.5	0.54	0.41
30	42.2	0.87	43.3	2.56	0.99
42	10.3	7.68	57.0	12.15	6.22
46	5.2	4.18	58.0	16.10	9.02

A. niger (Run G) 30/04/2004

Sample	Time	CDW	Spindle used	Shear rate range	Shear stress range	Model	Equation	Parameters			infinite shear viscosity	R^2
	h	[g l^{-1}]		[s^{-1}]	[Pa]			a	b	p	η_∞ [mPas]	
t3	10	0.746	Z2	176.3-504	0.414-2.54	Ostwald	$y = a x^b$	9.14E-05	1.6579			0.98756
						Bigham	$y = a + bx$	-0.74677	0.0066		0.0065998	0.99804
						Herschel-Bulkley	$y = a + bx^p$	-1.4297	4.36E-02	0.72256		0.99911
						Casson	$y^{1/p} = a + bx^{1/p}$	-0.73245	0.10553	2	0.011137	0.99344
t4	13	1.28	Z2	212.2-504.1	0.713-2.59	Ostwald	$y = a x^b$	3.68E-04	1.4253			0.99912
						Bigham	$y = a + bx$	-0.5792	0.006177		0.0061765	0.99912
						Herschel-Bulkley	$y = a + bx^p$	-0.53049	5.17E-03	1.0263		0.99921
						Casson	$y^{1/p} = a + bx^{1/p}$	-0.50548	0.09399	2	0.0088341	0.99943
t5	25	1.58	Z2	212.2-504.0	0.806-2.72	Ostwald	$y = a x^b$	6.67E-04	1.3354			0.99925
						Bigham	$y = a + bx$	-0.48953	0.006219		0.0062189	0.99879
						Herschel-Bulkley	$y = a + bx^p$	-0.24719	0.002356	1.1448		0.99923
						Casson	$y^{1/p} = a + bx^{1/p}$	-0.41156	0.091227	2	0.0083223	0.99924
t6	30	1.7	Z2	212.2-504.0	0.842-2.91	Ostwald	$y = a x^b$	4.16E-04	1.426			0.9985
						Bigham	$y = a + bx$	-0.64435	0.00697		0.0069699	0.99847
						Herschel-Bulkley	$y = a + bx^p$	-0.2205	1.35E-03	1.2468		0.99891
						Casson	$y^{1/p} = a + bx^{1/p}$	-0.53337	0.099869	2	0.0099738	0.99895
t7	32	1.42	Z2	212.2-504.0	0.775-2.8	Ostwald	$y = a x^b$	3.28E-04	1.4588			0.99727
						Bigham	$y = a + bx$	-0.68241	0.00687		0.0068703	0.99951
						Herschel-Bulkley	$y = a + bx^p$	-0.93239	0.014116	0.8944		0.99954
						Casson	$y^{1/p} = a + bx^{1/p}$	-0.57041	0.10031	2	0.010062	0.99875
sample 1		0.967	Z2	226-504	0.831-2.82	Ostwald	$y = a x^b$	3.11E-04	1.4653			0.99929
						Bigham	$y = a + bx$	-0.70179	0.006846		0.0068455	0.99883
						Herschel-Bulkley	$y = a + bx^p$	-0.37147	0.002063	1.1785		0.9994
						Casson	$y^{1/p} = a + bx^{1/p}$	-0.581	0.10033	2	0.010067	0.99944
sample 2		2.08	Z2	212.2-504	0.865-3.02	Ostwald	$y = a x^b$	3.37E-04	1.4668			0.99867
						Bigham	$y = a + bx$	-0.73128	0.007386		0.0073858	0.99969
						Herschel-Bulkley	$y = a + bx^p$	-0.384	0.002208	1.1806		0.99976
						Casson	$y^{1/p} = a + bx^{1/p}$	-0.59526	0.10428	2	0.010875	0.99969
sample 3		4.36	Z2	212.2-504	1.24-3.7	Ostwald	$y = a x^b$	1.05E-03	1.313			0.99962
						Bigham	$y = a + bx$	-0.6153	0.008403		0.0084027	0.99844
						Herschel-Bulkley	$y = a + bx^p$	0.20446	4.00E-04	1.4611		0.99951
						Casson	$y^{1/p} = a + bx^{1/p}$	-0.4454	0.10514	2	0.011055	0.99931
sample 4		8.2	Z2	212.2-504	3.7-6.63	Ostwald	$y = a x^b$	3.44E-01	0.47598			0.99984
						Bigham	$y = a + bx$	2.5566	0.008511		0.0085105	0.99484
						Herschel-Bulkley	$y = a + bx^p$	-0.44861	4.69E-01	0.43616		0.99989
						Casson	$y^{1/p} = a + bx^{1/p}$	1.1621	0.063965	2	0.0040915	0.99832
sample 5		11.32	Z2	146.5-504	6.71-11.3	Ostwald	$y = a x^b$	7.50E-01	0.4381			0.99928
						Bigham	$y = a + bx$	4.8432	0.013764		0.013764	0.99539
						Herschel-Bulkley	$y = a + bx^p$	1.4115	3.88E-01	0.52335		0.99929
						Casson	$y^{1/p} = a + bx^{1/p}$	1.6551	0.078099	2	0.0060995	0.99845
sample 6		14.01	Z2	146.5-504	11-18.8	Ostwald	$y = a x^b$	1.14E+00	0.44561			0.99611
						Bigham	$y = a + bx$	7.5911	0.022352		0.022352	0.99981
						Herschel-Bulkley	$y = a + bx^p$	7.4257	2.67E-02	0.97334		0.99983
						Casson	$y^{1/p} = a + bx^{1/p}$	2.0583	0.10034	2	0.010067	0.99905

A. niger **22/3/2006**

Sample	Time	CDW	Spindle used	Shear rate range	Shear stress range	Model	Equation	Parameters			infinite shear viscosity	R^2
	h	[g l^{-1}]		[s^{-1}]	[Pa]			a	b	p	η_∞ [mPas]	
t6	25	1.7	Z2	209.8-496	0.893-2.83	Ostwald	$y = a x^b$	7.96E-04	1.318			0.99959
						Bigham	$y = a + bx$	-0.4906	0.006591		0.0065912	0.99944
						Herschel-Bulkley	$y = a + bx^p$	-0.30061	3.27E-03	1.1045		0.99969
						Casson	$y^{1/p} = a + bx^{1/p}$	-0.40127	0.093288	2	0.0087026	0.99972
t7	30	2.1	Z2	209.8-496	0.818-2.71	Ostwald	$y = a x^b$	6.07E-04	1.3556			0.9993
						Bigham	$y = a + bx$	-0.52427	0.006444		0.0064439	0.99965
						Herschel-Bulkley	$y = a + bx^p$	-0.48348	5.58E-03	1.0213		0.99969
						Casson	$y^{1/p} = a + bx^{1/p}$	-0.43916	0.09357	2	0.0087553	0.99972
super	30	0	dgap	190.6-496	0.227-0.566	Ostwald	$y = a x^b$	1.68E-03	0.93655			0.99949
						Bigham	$y = a + bx$	0.021923	0.001092		0.001092	0.99958
						Herschel-Bulkley	$y = a + bx^p$	0.00657	1.48E-03	0.95453		0.99952
						Casson	$y^{1/p} = a + bx^{1/p}$	0.037712	0.03198	2	0.0010227	0.99955
super	30	0	Z2	209.8-496	0.817-2.79	Ostwald	$y = a x^b$	4.43E-04	1.4088			0.99983
						Bigham	$y = a + bx$	-0.57451	0.006568		0.0065683	0.99759
						Herschel-Bulkley	$y = a + bx^p$	0.01608	3.99E-04	1.4249		0.99984
						Casson	$y^{1/p} = a + bx^{1/p}$	-0.4935	0.096357	2		0.99914
t8	48	1.8	Z2	209.8-496	0.89-3.07	Ostwald	$y = a x^b$	4.05E-04	1.4406			0.99985
						Bigham	$y = a + bx$	-0.68618	0.007404		0.0074042	0.99879
						Herschel-Bulkley	$y = a + bx^p$	-0.10944	7.40E-04	1.348		0.99995
						Casson	$y^{1/p} = a + bx^{1/p}$	-0.56023	0.10346	2	0.010705	0.99982
sample1		1.5	Z2	230.8-496	0.98-2.89	Ostwald	$y = a x^b$	4.82E-04	1.4028			0.99961
						Bigham	$y = a + bx$	-0.65915	0.007064		0.0070635	0.99972
						Herschel-Bulkley	$y = a + bx^p$	-0.35437	2.49E-03	1.1549		0.99995
						Casson	$y^{1/p} = a + bx^{1/p}$	-0.52272	0.099653	2	0.0099308	0.99994
sample2		2.7	Z2	230.8-496	1.09-3.12	Ostwald	$y = a x^b$	5.23E-04	1.4052			0.99869
						Bigham	$y = a + bx$	-0.7305	0.00779		0.0077899	0.99966
						Herschel-Bulkley	$y = a + bx^p$	-0.40241	2.83E-03	1.1503		0.99958
						Casson	$y^{1/p} = a + bx^{1/p}$	-0.55193	0.10474	2	0.010971	0.9995
sample 3		5	Z2	50-230.8	0.742-1.79	Ostwald	$y = a x^b$	0.074604	0.57821			0.99764
						Bigham	$y = a + bx$	0.45478	0.005873		0.0058727	0.99929
						Herschel-Bulkley	$y = a + bx^p$	0.38028	1.10E-02	0.8916		0.99966
						Casson	$y^{1/p} = a + bx^{1/p}$	0.44182	0.05856	2	0.0034293	0.99951
sample 4		5.6	Z2	50-279.5	0.953-2.44	Ostwald	$y = a x^b$	0.11104	0.54197			0.99644
						Bigham	$y = a + bx$	0.65044	0.006564		0.0065643	0.99945
						Herschel-Bulkley	$y = a + bx^p$	0.55072	1.31E-02	0.88306		0.99984
						Casson	$y^{1/p} = a + bx^{1/p}$	0.55122	0.06006	2	0.0036071	0.99949
sample 5		7.8	Z2	60.5-450.8	2.21-5.06	Ostwald	$y = a x^b$	0.31496	0.46454			0.99824
						Bigham	$y = a + bx$	1.7376	0.009021		0.0090207	0.99541
						Herschel-Bulkley	$y = a + bx^p$	1.0575	6.79E-02	0.68618		0.99985
						Casson	$y^{1/p} = a + bx^{1/p}$	0.97392	0.065598	2	0.004303	0.99961

Combined rheology for *A. niger*

CDW	Spindle used	Shear rate	Shear stress range			Parameters			infinite shear viscosity	
[g l^{-1}]		[s^{-1}]	[Pa]	Model	Equation	a	b	p	η_∞ [mPas]	R^2
1.5	Z2	230.8-496	0.98-2.89	Ostwald	$y = a\,x^b$	4.82E-04	1.4028			0.99961
				Bigham	$y = a + bx$	-0.65915	0.007064		0.0070635	0.99972
				Herschel-B	$y = a + bx^f$	-0.35437	2.49E-03	1.1549		0.99995
				Casson	$y^{1/p} = a + b$	-0.52272	0.099653	2	0.0099308	0.99994
1.8	Z2	209.8-496	0.89-3.07	Ostwald	$y = a\,x^b$	4.05E-04	1.4406			0.99985
				Bigham	$y = a + bx$	-0.68618	0.007404		0.0074042	0.99879
				Herschel-B	$y = a + bx^f$	-0.10944	7.40E-04	1.348		0.99995
				Casson	$y^{1/p} = a + b$	-0.56023	0.10346	2	0.010705	0.99982
2.1	Z2	209.8-496	0.818-2.71	Ostwald	$y = a\,x^b$	6.07E-04	1.3556			0.9993
				Bigham	$y = a + bx$	-0.52427	0.006444		0.0064439	0.99965
				Herschel-B	$y = a + bx^f$	-0.48348	5.58E-03	1.0213		0.99969
				Casson	$y^{1/p} = a + b$	-0.43916	0.09357	2	0.0087553	0.99972
2.7	Z2	230.8-496	1.09-3.12	Ostwald	$y = a\,x^b$	5.23E-04	1.4052			0.99869
				Bigham	$y = a + bx$	-0.7305	0.00779		0.0077899	0.99966
				Herschel-B	$y = a + bx^f$	-0.40241	2.83E-03	1.1503		0.99958
				Casson	$y^{1/p} = a + b$	-0.55193	0.10474	2	0.010971	0.9995
5	Z2	50-230.8	0.742-1.79	Ostwald	$y = a\,x^b$	0.074604	0.57821			0.99764
				Bigham	$y = a + bx$	0.45478	0.005873		0.0058727	0.99929
				Herschel-B	$y = a + bx^f$	0.38028	1.10E-02	0.8916		0.99966
				Casson	$y^{1/p} = a + b$	0.44182	0.05856	2	0.0034293	0.99951
5.6	Z2	50-279.5	0.953-2.44	Ostwald	$y = a\,x^b$	0.11104	0.54197			0.99644
				Bigham	$y = a + bx$	0.65044	0.006564		0.0065643	0.99945
				Herschel-B	$y = a + bx^f$	0.55072	1.31E-02	0.88306		0.99984
				Casson	$y^{1/p} = a + b$	0.55122	0.06006	2	0.0036071	0.99949
7.8	Z2	60.5-450.8	2.21-5.06	Ostwald	$y = a\,x^b$	0.31496	0.46454			0.99824
				Bigham	$y = a + bx$	1.7376	0.009021		0.0090207	0.99541
				Herschel-B	$y = a + bx^f$	1.0575	6.79E-02	0.68618		0.99985
				Casson	$y^{1/p} = a + b$	0.97392	0.065598	2	0.004303	0.99961
8.2	Z2	212.2-504	3.7-6.63	Ostwald	$y = a\,x^b$	3.44E-01	0.47598			0.99984
				Bigham	$y = a + bx$	2.5566	0.008511		0.0085105	0.99484
				Herschel-B	$y = a + bx^f$	-0.44861	4.69E-01	0.43616		0.99989
				Casson	$y^{1/p} = a + b$	1.1621	0.063965	2	0.0040915	0.99832
11.32	Z2	146.5-504	6.71-11.3	Ostwald	$y = a\,x^b$	7.50E-01	0.4381			0.99928
				Bigham	$y = a + bx$	4.8432	0.013764		0.013764	0.99539
				Herschel-B	$y = a + bx^f$	1.4115	3.88E-01	0.52335		0.99929
				Casson	$y^{1/p} = a + b$	1.6551	0.078099	2	0.0060995	0.99845
14.01	Z2	146.5-504	11-18.8	Ostwald	$y = a\,x^b$	1.14E+00	0.44561			0.99611
				Bigham	$y = a + bx$	7.5911	0.022352		0.022352	0.99981
				Herschel-B	$y = a + bx^f$	7.4257	2.67E-02	0.97334		0.99983
				Casson	$y^{1/p} = a + b$	2.0583	0.10034	2	0.010067	0.99905